UNIVERSITY OF Southampton

FACULTY OF MEDICINE

Centre for Human Development, Stem Cells and Regeneration

Role of microRNAs in the Hypoxic Regulation of Human Embryonic Stem Cells

by

Sophia Petra Sander

Thesis for the degree of Doctor of Philosophy

September 2016

"Der große Reichtum unseres Lebens, das sind die kleinen Sonnenstrahlen, die jeden Tag auf unseren Weg fallen."

Hans Christian Andersen

"Phantasie ist wichtiger als Wissen,

denn Wissen ist begrenzt."

Albert Einstein

UNIVERSITY OF SOUTHAMPTON

ABSTRACT

FACULTY OF MEDICINE

Centre for Human Development, Stem Cells and Regeneration

Thesis for the degree of Doctor of Philosophy

ROLE OF MICRORNAS IN THE HYPOXIC REGULATION OF HUMAN EMBRYONIC STEM CELLS

Sophia Petra Sander

Human embryonic stem cells (hESCs) derived from the inner cell mass of the blastocyst, are pluripotent, capable of indefinite self-renewal and have the capacity to differentiate into all cells of the three germ layers. Thus, hESCs hold great potential for a wide range of applications such as regenerative medicine and drug development. However, improved propagation and use of hESCs in medical applications requires a better knowledge of the underlying mechanisms that regulate hESC pluripotency.

Hypoxia (5% oxygen) has been shown to be beneficial for maintaining pluripotent stem cells. Hypoxia inducible factors are crucial for this process, being stabilised under low oxygen conditions and promoting the expression of several pluripotency associated genes. However, microRNAs (miRNAs) as multi-purpose gene regulators might also have an important role in regulating these processes. Currently, little is known about specific miRNAs that may regulate pluripotency in hESCs in response to changes in environmental oxygen. Thus, this thesis aims to determine the involvement of miRNAs in the hypoxic regulation of hESCs.

Using miRNA arrays, differentially expressed miRNAs were found in hESCs cultured at 5% oxygen compared to those maintained at atmospheric, 20% oxygen. Validation of the arrays using RT-qPCR showed that hESCs cultured at 5% oxygen displayed increased levels of the hypoxamir miR-210 and decreased levels of miR-122-5p and miR-223-3p. Using bioinformatic analysis miR-122-5p and miR-223-3p were found to target the NANOG 3'UTR.

Using synthetic pre-miRs to transiently up-regulate either miR-122-5p or miR-223-3p in hESCs cultured at 5% oxygen significantly reduced NANOG protein expression. Dual-Luciferase-Reporter Assays and site-directed mutagenesis confirmed the location of a novel binding-site for miR-223-3p in the NANOG 3'UTR. The data presented in this thesis show that miRNA-223-3p directly regulates NANOG expression and that miRNAs have a physiological role in regulating the response of hESCs to environmental oxygen.

I. Table of Contents

ABSTRACT I
I. Table of Contents III
II. Table of Figures VII
III. List of Tables XIII
IV. Declaration of Authorship XVII
V. Acknowledgements XIX
VI. Abbreviations XXI
Chapter 1 Introduction 1
1.1 Stem Cells 3
1.1.1 Types of Potency 3
1.1.2 Pluripotent stem cells 4
1.1.3 Embryonic stem cells 6
1.1.4 Induced pluripotent stem cells (iPSCs) 7
1.1.5 Derivation of hESCs 8
1.1.6 States of pluripotent stem cells: naïve and primed mESCs and hESCs 9
1.1.7 Culture conditions for hESCs 11
1.1.8 Pluripotency Factors and Markers 13
1.1.9 Control and Regulation of Pluripotency 16
1.1.10 Differentiation of hESCs 23
1.2 Effect of environmental oxygen on hESCs 26
1.2.1 Oxygen concentration in pre-implantation embryos and hESC culture 26
1.2.2 The hypoxic response regulated by hypoxia inducible factors 28
1.3 Energy metabolism of hESCs 32
1.4 Role of microRNAs as multipurpose regulators 34
1.4.1 Overview of miRNAs 34
1.4.2 The biogenesis and mechanism of miRNAs 35
1.4.3 Mechanisms of how miRNA mediate inhibition/degradation of protein translation 38
1.4.4 Role of miRNAs in ESCs 40
1.4.5 The hypoxic regulation of miRNAs 43
1.5 Hypothesis with Aims and Objectives 45
1.5.1 Hypothesis 45
1.5.2 Aims & Objectives 45
Chapter 2 Materials and Methods 47
2.1 Cell culture 49

2.1.1 Derivation of mouse embryonic fibroblasts....49
2.1.2 Culture of mouse embryonic fibroblasts (MEFs)....51
2.1.3 Preparation of γ-irradiated MEFs for conditioned media or for culture of hESCs....51
2.1.4 Culture of hESCs....53
2.1.5 Preparation of Matrigel coated plates for feeder-free culture of hESCs....54
2.1.6 Culture of hESCs on Matrigel coated plates....54
2.1.7 Transfection of Shef3 hESCs with synthetic pre-miR miRNA precursor molecules (pre-miRs) or synthetic anti-miR miRNA inhibitors (anti-miRs) 54
2.2 Gene Expression Analysis....56
2.2.1 RNA isolation....56
2.2.2 Reverse Transcription of RNA using oligo-dT primer....56
2.2.3 Genomic contamination check....57
2.2.4 Reverse Transcription of RNA using random hexamer primer....57
2.2.5 Real Time quantitative PCR (RT-qPCR) Analysis....58
2.3 Protein Analysis....61
2.3.1 Immunocytochemistry....61
2.3.2 Protein extraction....62
2.3.3 Protein quantification....62
2.3.4 Sodium dodecyl sulfate – polyacrylamide gel electrophoresis (SDS-PAGE)....63
2.3.5 Western Blotting....64
2.3.6 Development of Western blots by film....65
2.4 Statistical Analysis....65
Chapter 3 Expression of miRNAs in hESCs....67
3.1 Introduction to Arrays and Bioinformatics on miRNAs in hESCs....69
3.1.1 MiRNAs in the Hypoxic Regulation of hESC....69
3.1.2 Prediction of miRNA Targets....70
3.1.3 Rational of miRNA Arrays and Target-Mining....71
3.1.4 Study Aims....72
3.2 Materials and Methods....73
3.2.1 TaqMan MicroRNA Array....73
3.2.2 In silico data analysis....74
3.2.3 Reverse transcription of RNA using specific stem-loop primers and RT-qPCR 75
3.3 Results....77
3.3.1 Characterisation of hESCs....77

3.3.2 Array analysis of miRNAs in hESCs cultured at either 5% or 20% oxygen 95
3.3.3 Bioinformatic Analysis - miRNA target mining 106
3.3.4 Validation of miRNAs 120
3.4 Discussion 125
3.4.1 Expression of pluripotency markers 125
3.4.2 Array analysis of miRNAs with bioinformatics 125
3.4.3 Validation of miRNA arrays of hESCs cultured under hypoxic conditions 128
Chapter 4 Modulation of miRNA expression in hESCs 131
4.1 Introduction 133
4.1.1 Study Aims 135
4.2 Materials and Methods 137
4.3 Results 139
4.3.1 Morphology of Shef3 hESC colonies transfected with pre-miRs 139
4.3.2 Effect of pre-miR-122-5p or pre-miR-223-3p on the mRNA expression of OCT4, SOX2 and NANOG in hESCs 140
4.3.3 Effect of pre-miR-122-5p and pre-miR-223-3p on the protein expression of OCT4, SOX2, NANOG and PKM2 146
4.4 Discussion 155
4.4.1 Effect of modulating miRNA expression in hESCs 156
4.4.2 Possible role of miR-122-5p in energy metabolism 159
Chapter 5 Evaluation of miR-122-5p and miR-223-3p binding sites in the NANOG 3'UTR 161
5.1 Introduction to evaluate miR-122-5p and miR-223-3p binding sites in the NANOG 3'UTR 163
5.1.1 Rational of miR-122-5p/miR-223-3p targeting the NANOG 3'UTR 163
5.1.2 Prediction of exact miRNA target sites 164
5.1.3 Study Aims 166
5.2 Material and Methods 167
5.2.1 Cloning Methods 167
5.2.2 Dual-Luciferase Assay 185
5.2.3 Proliferation assay using Ki67 187
5.3 Results 189
5.3.1 Dual-Luciferase-Assay analysis of miR-122-5p and miR-223-3p in NANOG 3'UTR189
5.3.2 Functional Analysis of down-stream effects of the miR-223-3p binding site in the NANOG 3'UTR of hESCs 216
5.4 Discussion 227

5.4.1 Challenges in miRNA-mRNA binding predictions 227
5.4.2 Functional impact of miR-223-3p in hESCs 230
Chapter 6 General Discussion and Future Work 233
6.1 General Discussion 235
6.2 Future Work 240
VII. Apendices 243
Appendix A Supplementary Data 243
Appendix B Supplementary Methods 245
B.1 QIAprep Spin Miniprep Kit 245
B.2 Qiagen Gel Extraction Kit 245
B.3 QIAgen Plasmid Maxiprep Kit 246
VIII. List of References 247

II. Table of Figures

Figure 1: Schematic representation of types of stem cells 5
Figure 2: Expression of cell- surface markers and transcription factors in hESCs and mESCs 15
Figure 3: Control of stem cell pluripotency in mice 17
Figure 4: Auto-feedback loop of OCT4, SOX2 and NANOG 18
Figure 5: Example of Wnt/β-catenin signalling in hESCs fate (adapted from Dalton, 2013) 20
Figure 6: Simplified schematic representation of the major signalling pathways involved in regulation of pluripotency in hESCs 22
Figure 7: Degradation or stabilisation of the HIFα subunit 30
Figure 8: miRNA biogenesis 36
Figure 9: Conventional miRNA targeting showing canonical site types 39
Figure 10: 1.5% Agarose gel showing typical products of uncontaminated samples from primary un-irradiated MEF culture using the Mycoplasma PCR Detection Kit (Intronbio) 50
Figure 11: Schematics of hESC culture 53
Figure 12: Typical BSA standard curve used to calculate the concentration of protein in samples (OD=optical density) 62
Figure 13: Expression of pluripotency markers in Shef3 hESCs at 5% oxygen 78
Figure 14: Characterisation of Shef3 hESCs at 5% oxygen 79
Figure 15: Expression of pluripotency and differentiation marker in Shef3 hESCs at 5% oxygen 80
Figure 16: Characterisation of TRA-1-60 and SSEA-1 expression in Shef3 hESCs at 5% oxygen 81
Figure 17: Expression of pluripotency markers in Shef3 hESCs at 20% oxygen 82
Figure 18: Characterisation of Shef3 hESCs at 20% oxygen 83
Figure 19: Expression of pluripotency and differentiation marker in Shef3 hESCs at 20% oxygen 84
Figure 20: Characterisation of TRA-1-60 and SSEA-1 expression in Shef3 hESCs at 20% oxygen 85
Figure 21: Expression of pluripotency markers in Hues7 hESCs at 5% oxygen 86
Figure 22: Characterisation of pluripotency markers in Hues7 hESCs at 5% oxygen 87
Figure 23: Expression of pluripotency and differentiation marker in Hues7 hESCs at 5% oxygen 88

Figure 24: Characterisation of TRA-1-60 and SSEA-1 expression in Hues7 hESCs at 5% oxygen 89
Figure 25: Expression of pluripotency markers in Hues7 hESCs at 20% oxygen 90
Figure 26: Characterisation of pluripotency markers in Hues7 hESCs at 20% oxygen 91
Figure 27: Expression of pluripotency and differentiation marker in Hues7 hESCs at 20% oxygen 92
Figure 28: Characterisation of TRA-1-60 and SSEA-1 in Hues7 hESCs at 20% oxygen 93
Figure 29: Relative NANOG protein expression in Shef3 hESCs cultured at either 20% or 5% oxygen 94
Figure 30: Shef3 hESC colonies for RNA collection 95
Figure 31: Absolute variation of miRNA expression data in hESCs cultured at either 5% or 20% oxygen 96
Figure 32: Normalised miRNA expression data in hESCs cultured at either 5% or 20% oxygen concentration 98
Figure 33: Number of differential expressed miRNAs across each of the array-sets . 100
Figure 34: Heat-map, expression of the consistently up- and down-regulated miRNAs in hESCs across 3 array sets under hypoxia compared to normoxia (A, B, C) 105
Figure 35: Percentage of concurrently either up- or down-regulated miRNAs predicted to target HIF isoforms in hESCs in hypoxia compared to normoxia between the 3 array-sets..... 108
Figure 36: Down-regulated miRNAs in hESCs under hypoxia that target HIF isoforms supported by at least two array sets..... 111
Figure 37: Predicted consequential pairing between target regions and miR-122-5p 113
Figure 38: Predicted consequential pairing of the target region of miR-223-3p 115
Figure 39: Heat-map, expression of validated miRNAs (ddCt) in hESCs under hypoxia compared to normoxia in each array (A, B and C)..... 120
Figure 40: Relative miRNA-expression of miR-223-3p (A) and miR-122-5p (B) at 5% oxygen compared to 20% oxygen in Shef3 or Hues7 hESCs..... 121
Figure 41: Relative miRNA-expression of miR-210 (A) and miR-135a (B) at 5% oxygen compared to 20% oxygen in Shef3 or Hues7 hESCs 122
Figure 42: Relative miRNA-expression of miR-29a at 5% oxygen compared to 20% oxygen in Shef3 or Hues7 hESCs..... 123
Figure 43: Stem-loop structure of miR-122 (adapted from miRBase) 137
Figure 44: Stem-loop structure of miR-223 (adapted from miRBase) 137
Figure 45: Pre-miRNA transfected Shef3 colonies 139

Figure 46: Representative cDNA samples which were free of genomic contamination 140
Figure 47: miR-122-5p and miR-223-3p do not affect OCT4 mRNA expression levels in Shef3 hESCs. 143
Figure 48: miR-122-5p and miR-223-3p do not affect SOX2 mRNA expression levels in Shef3 hESCs. 144
Figure 49: miR-122-5p and miR-223-3p do not affect NANOG mRNA expression levels in Shef3 hESCs. 145
Figure 50: Effect of either pre-miR-122-5p or pre-miR-223-3p transfection on OCT4 protein expression in Shef3 hESCs 147
Figure 51: Effect of either pre-miR-122-5p or pre-miR-223-3p transfection on SOX2 protein expression in Shef3 hESCs cultured at 5% oxygen..... 149
Figure 52: Transfection of either pre-miR-122-5p or pre-miR-223-3p reduces NANOG protein expression levels in Shef3 hESCs 151
Figure 53: Transfection of either pre-miR-122-5p or pre-miR-223-3p has no effect on PKM2 protein levels in Shef3 hESCs..... 153
Figure 54: Effect of either pre-miR-122-5p or pre-miR-223-3p on HIF2A protein expression 154
Figure 55: Schematic representation of miRNA-mRNA interaction with a GU wobble165
Figure 56: Schematics of Cloning strategy:..... 168
Figure 57: pCR2.1-TOPO vector..... 169
Figure 58: pRL-TK vector..... 170
Figure 59: pcDNA3.1(-) vector 171
Figure 60: pGL2-Control vector map (Promega) 172
Figure 61: Part of NANOG 3'UTR sequence..... 175
Figure 62: miR-122-5p sequence..... 175
Figure 63: miR-223-3p sequence..... 176
Figure 64: Schematic of site-directed mutagenesis of miR-122-5p binding site in NANOG 3'UTR at position 306 181
Figure 65: Schematics of site-directed mutagenesis of miR-223-3p binding site in NANOG 3'UTR at position 18 181
Figure 66: Schematic representation of the mutated pRL-TK vectors 183
Figure 67: Schematics of applying the Dual-Luciferase transfection cocktail..... 185
Figure 68: Predicted and annotated miRNA binding sites of miR-122-2p (red) and miR-223-3p (black) in the NANOG 3'UTR (highlighted binding positions were predicted by SegalLab). 190

Figure 69: miR-223-3p binding site for position 39 (and 40) in the NANOG 3'UTR as predicted by SegalLab 190
Figure 70: miR-223-3p binding site for position 18 in the NANOG 3'UTR 191
Figure 71: miR-122-5p binding sites in the the first 500bp of the NANOG 3'UTR as predicted by SegalLab 193
Figure 72: PCR amplified NANOG 3'UTR region 194
Figure 73: PCR amplified miR-122-5p and miR-223-3p 195
Figure 74: EcoRI digested TOPO-NANOG 3'UTR clones 196
Figure 75: Sequence result from TOPO-NANOG 3'UTR clone 10 198
Figure 76: EcoRI digested TOPO-miR-122-5p clones 199
Figure 77: EcoRI digested TOPO-miR-223-3p clones 199
Figure 78: Sequence result from TOPO-miR-122-5p clone 3 200
Figure 79: Sequence result from TOPO-miR-223-3p clone 6 201
Figure 80: Vector digest of TOPO-NANOG and pRL-TK-vector with XbaI and NotI 202
Figure 81: XbaI and NotI digested pRL-TK-NANOG 3'UTR clones 203
Figure 82: Vector digest of TOPO-miR-122-5p with XbaI and HindIII HF 204
Figure 83: Vector digest of TOPO-miR-223-3p and pcDNA3.1(-)-vector with XbaI and HindIII HF 205
Figure 84: XbaI and HindIII HF digested pcDNA3.1(-)-miR-122-5p clones 206
Figure 85: XbaI and HindIII HF digested pcDNA3.1(-)-miR-223-3p clones 207
Figure 86: XhoI/BamHI digest of pRLTK-3'UTR NANOG miR-122-5p or miR-223-3p binding site mutant clones 208
Figure 87: Sequence result from pRL-TK-NANOG 3'UTR with mutated miR-122-5p binding site 210
Figure 88: Sequence result from pRL-TK-NANOG 3'UTR with mutated miR-223-3p binding site 211
Figure 89: miR-122-5p has no miRNA binding site in the first ~500bp of the NANOG 3'UTR 213
Figure 90: miR-223-3p targets NANOG 3'UTR 215
Figure 91: Relative Brachyury mRNA expression levels when either Shef3 or Hues7 hESCs were transfected with 200nM pre-miR-223-3p and cultured at 5% oxygen for 48h. 217
Figure 92: Relative CDK6 mRNA expression levels when either Shef3 or Hues7 hESCs were transfected with 200nM pre-miR-223-3p and cultured at 5% oxygen for 48h. 218
Figure 93: Cell count of Ki67 positive stained hESC nuclei using Cellprofiler 221

Figure 94: Ki67 expression in hESCs cultured at 5% oxygen and transfected with pre-miRs for 48h 223
Figure 95: Ki67 expression in hESCs cultured at 5% oxygen and transfected with anti-miRs for 48h 225
Figure 96: Schematic representation of miR-223-3p regulating NANOG expression in hESCs 237

III. List of Tables

Table 1: Two specific hESC miRNA clusters 41
Table 2: Mature miRNAs produced by the miR-290 cluster in mESCs 42
Table 3: Composition of MEF medium 49
Table 4: Composition of hESC culture medium 52
Table 5: List of synthetic pre-miRs and anti-miRs (Ambion, Applied Biosystems) 55
Table 6: PCR reagents for genomic contamination check 57
Table 7: Reverse Transcription of RNA using random hexamer primers 58
Table 8: Reagents for RT-qPCR in 384-well plates 58
Table 9: Details for TaqMan probes used in RT-qPCR reactions for mRNA expression levels 59
Table 10: Composition of antibody-solutions for ICC 61
Table 11: List of primary and secondary antibodies used for ICC with appropriate dilutions 61
Table 12: Chemicals used for SDS-gels 63
Table 13: 5x Running Buffer for SDS-gel electrophoresis 63
Table 14: Transfer buffer for Western blotting 64
Table 15: Primary Antibodies for Western blotting 64
Table 16: Secondary Antibodies for Western blotting 65
Table 17: Megaplex reverse transcription conditions 73
Table 18: Details for TaqMan primers used for the reverse transcription and probes used for RT-PCR for the measurement of miRNA expression levels .. 75
Table 19: Reverse transcription conditions using Applied Biosystems reagents for specific Stem-loop primers 76
Table 20: Absolute expression values of positive control genes and negative arthropod miRNA in hESCs of three independent array-sets 97
Table 21: Differentially expressed miRNAs in hESCs cultured at either 5% or 20% oxygen 99
Table 22: List of down-regulated miRNAs expressed in hESCs cultured at 5% oxygen compared to 20% oxygen. MiRNAs down-regulated in at least two of the array sets are depicted. 101
Table 23 : List of up-regulated miRNAs expressed in hESCs cultured at 5% oxygen compared to 20% oxygen. MiRNAs up-regulated in at least two of the array sets are depicted. 103

Table 24: Number of hits of miRNAs targeting HIF isoforms and HIF1AN which are either down- or up-regulated under hypoxia compared to normoxia in hESCs, using TargetScan as mRNA/miRNA target database 109
Table 25: List of down-regulated miRNAs targeting HIFs and FIH under hypoxia compared to normoxia in hESCs with the addition of the target-frequency along the 3'UTR. (Double underlined are miRNAs predicted to simultaneously target HIFs and FIH.) 110
Table 26: Biological predicted targets of miR-24-3p using TargetScan (Lewis, Burge and Bartel, 2005; Grimson *et al.*, 2007) 112
Table 27: Biological targets of miR-122-5p and miR-223-3p using TargetScan (Lewis, Burge and Bartel, 2005; Grimson *et al.*, 2007) 114
Table 28: Top10 targets for HIF2A, NANOG, SOX2 and OCT4 using the Segal lab predictions on all down-regulated miRNAs that were common between at least two array sets, showing how many target sites one miRNA had and a summed up ddG as "score" (number in front of the miRNA refers to position in Table 22) 116
Table 29: Segal Lab prediction outcome for HIF2A (EPAS1) targeted by miR-223-3p with a cut off at ddG=-5 (number in front of the miRNA refers to position in Table 22) 117
Table 30: Segal Lab prediction outcome for HIF2A (EPAS1) targeted by miR-122-5p with a cut off at ddG=-5 (number in front of the miRNA refers to position in Table 22) 117
Table 31: SegalLab prediction outcome for NANOG targeted by miR-122-5p with a cut off at ddG=-5 118
Table 32: SegalLab prediction outcome for SOX2 targeted by miR-122-5p with a cut off at ddG=-5 119
Table 33: Segal Lab prediction outcome for NANOG targeted by miR-223-3p with a cut off at ddG=-5 119
Table 34: Standard deviation across samples for mRNA expression level of HKGs UBC and β-ACTIN using oligo-dT, or random hexamers to reverse transcribe RNA into cDNA 141
Table 35: Primer and their sequences with highlighted restriction enzyme sites synthesised by Eurofins Genomics 174
Table 36: PCR reaction for the amplification of NANOG 3'UTR, miR-122-5p and miR-223-3p 175
Table 37: Topo-Plasmid digestion for NANOG 3'UTR or miR-122-5p or miR-223-3p insert using EcoRI: 177

Table 38: Vectors with their desired restriction enzyme conditions 178
Table 39: Ligation conditions for final vector constructs 179
Table 40: Restriction Enzyme Digest for constructs in their final vector pRLTK or pcDNA3.1(-) 180
Table 41: Parameters for QuikChange site-directed mutagenesis 180
Table 42: Site-directed Mutagenesis PCR reaction 182
Table 43: Dual-Luciferase transfection cocktail for each well of a 24-well-plate: 185
Table 44: List of miRNAs targeting KLF4 which are down-regulated under hypoxia compared to normoxia in hESCs 243

IV. Declaration of Authorship

I, Sophia Petra Sander declare that this thesis entitled

Role of microRNAs in the Hypoxic Regulation of Human Embryonic Stem Cells

and the work presented in it are my own and has been generated by me as the result of my own original research.

I confirm that:

1. This work was done wholly or mainly while in candidature for a research degree at this University;
2. Where any part of this thesis has previously been submitted for a degree or any other qualification at this University or any other institution, this has been clearly stated;
3. Where I have consulted the published work of others, this is always clearly attributed;
4. Where I have quoted from the work of others, the source is always given. With the exception of such quotations, this thesis is entirely my own work;
5. I have acknowledged all main sources of help;
6. Where the thesis is based on work done by myself jointly with others, I have made clear exactly what was done by others and what I have contributed myself;
7. None of this work has been published before submission.

Signed: .....

Date: .....

V. Acknowledgements

There are quite a number of people whom I'd like to thank for their support whilst carrying out my four year PhD here in Southampton, UK.

First of all I'd like to thank my funding organisations; The Gerald Kerkut Charitable Trust and the Society for Reproduction and Fertility. The Gerald Kerkut Trust hosted twice yearly symposiums, which were always well catered and perhaps more importantly provided an opportunity to present my research and to meet the trustees as well as other students funded by them. I also attended two excellent conferences organised by the SRF where I presented my research to a broad audience.

My supervisor Dr Franchesca Houghton for guidance throughout my PhD. You were always encouraging me in seeing the sunny side of my data where I could hardly see past the clouds of miRNA data and yet another Western blot that had failed. Also, a big thank you for proofing and editing my writing over the years, I'm very grateful for the considerable time you spent doing this.

My supervisor Dr Tilman Sanchez-Elsner for his ideas and support. You taught me many techniques without which I'd have not been able to write that dreaded third Chapter. I also met many helpful and friendly people in your lab. Dankeschön und muchos gracias.

I'd also like to say thank you to our lab-manager Kate Perry, you always had an open ear and shared all the many weekends we had to come in to look after the cells. Thanks for getting me started in the lab and your friendship. I wish you good luck and happiness.

Within the FDH lab I'd also like to thank the old and new members, Raffaella Petruzzelli, David Christensen, Irina Fesenko, Lauren Javons and Sophie Arthur. Your support and cake baking prowess generated a friendly and pleasant working environment.

A big thank you is also going to my friends, to the old ones back from school and university times that came to visit me but especially to my friends here. You were always up for countless lunches, coffees, chats and laughs (sometimes beers or mulled wine too, not at lunch time though). I'm very grateful to have spent these last four years with you and hope we can stay in touch.

Zu guter Letzt möchte ich mich bei meiner Familie bedanken. Ohne eure Unterstützung und Zuspruch wären diese letzten vier Jahre um einiges härter gewesen. Oma, ich danke dir dass wir so viel Zeit miteinander verbringen konnten vor deinem 90. Geburtstag und dass du uns alle zusammengebracht hast und wir so eine fröhliche Zeit miteinander verbringen konnten. Mutti und Vati, ich danke euch für eure Unterstützung und dass ihr

immer an mich geglaubt habt, oft mit einer Selbstverständlichkeit die ich nicht verstehen wollte oder konnte. Markus, ohne dich und deine SIM Karten Tricks wäre ich bedeutend weniger „connected“ gewesen mit der ganzen Familie. Sabine, ich erinnere mich noch wie du mit mir Hausaufgaben gemacht hast als ich noch in die Grundschule ging, jetzt ist hoffentlich das Ende der lehrreichen Jahre erreicht; ich danke dir für deine guten Gespräche und deinen Rat. Pia, du hast mir zweimal riesig tolle Osterpakete geschickt mit lauter guten Sachen aus der Heimat und Stephan hatte immer ein Sonderlos parat. Theres, du hast mich insgesamt zweimal besucht, beides Mal schwanger und bei deinem zweiten Besuch hatten wir eine tolle Zeit zusammen mit Tom und Tabea in Somerset. Ich habe mich sehr gefreut, dass ihr es alle geschafft habt mich zu besuchen. Die letzten Jahre waren nicht immer einfach, so weit weg von euch zu sein, vor allem von den Kleinen; Moritz, Marie, Elisa, Valeria, Tabea und Theo. Ihr seid jetzt alle gar nicht mehr so klein. Ich habe irre viel verpasst. Auch wenn ich oft kein Land gesehen habe, ihr habt immer an mich geglaubt. Ich bin stolz, dass ich so eine tolle Familie habe.

Finally, I can’t thank enough My Love without whom this PhD would have been a much harder experience, especially the end of it. Your invaluable support in listening to me, giving me advice, cycling to our Winchester, cooking delicious left over surprises, making teas and coffees and just being always there for me no matter where you were. I’m so lucky and very grateful to have met you during my PhD. Thank you for being My Love!

VI. Abbreviations

ADP	Adenosine diphosphate
AGO	Argonaute-subfamily
AKT	Ak=mouse strain, t=thymoma
ATP	Adenosine triphosphate
bp	Basepair
bFGF	Fibroblast growth factor b
BMP	Bone morphogenetic protein
BSA	Bovine serum albumin
CBP	Creb-binding protein
CDC25A	M-phase inducer phosphotase (cell divisin cycle 25 homolog A)
CDK	Cyclin dependend kinase
Cdkn	Cyclin-dependend kinase inhibitor
cDNA	Complementary desoxyribonucleic acid
CDS	Coding sequence
CDX2	Homeobox protein CDX-2
circ RNA	Circular RNA
c-Myc	Multifunctional, nuclear phosphoprotein
Ct (dCt or ΔCt)	Treshold cycle (delta Ct)
Cq	Quantification cycle
DAPI	4', 6-diamidino-2-phenylindole
DEPC	Diethylpyrocarbonate
Dgcr8	Microprocessor complex subunit DGCR8 (Pasha); DiGeorge syndrome critical region gene 8
DMEM	Dulbecco’s modified Eagle's minimal essential medium
DMSO	Dimethyl sulphoxide
DNAse	Desoxyribonuclease
dNTPs	Desoxynucleotide triphosphate
DTT	Dithiothreitol
EB	Embryoid bodies
ECC	Embryonic carcinoma cell
ECL	Electrochemiluminescence
EDTA	Ethylenediaminetetraacetate
EGC	Embronic germ cell
Eomes	Eomesodermin
EPAS1	Gene that encodes for HIF2A
EpiSC	Epiblast stem cell
ERK	Extracellular-signal regulated kinase
ESC	Embryonic Stem Cell
FACS	Fluorescent activated cell sorting
FAM	Fluorescein amidite
FBS	Fetal bovine serum
FGF	Fibroblast growth factor
FIH	Factor inhibiting HIF
FITC	Fluorescein isothiocyanate
FoxD3	Forkhead protein
gDNA	Genomic desoxyribonucleic acid
G	Gray, absorption of one joule of radiation energy per kg of matter

GAPDH	Glyceraldehye 3-phosphate dehydrogenase
Gata	Transcription factor gata
GLUT	Glucose transporter
GSK	Glycogen synthase kinase
h	Human or hours
HAND1	Heart-and neural crest derivatives-expressed protein 1
H_2O_2	Hydrogen peroxide
HDAC	Histone deacetylase
HIF	Hypoxia inducible factor
HKG	House-keeping gene
HMG	High mobility group
HRP	Horse radish peroxidase
HRE	Hypoxia response element
hsa	miRNA of human origin
HTH	Helix turn helix
ICC	Immunocytochemistry
ICM	Inner cell mass
ID	Inhibitor of differentiation
IGF	Insulin-like growth factor
IPAS	Inhibitory PAS domain
iPSC	induced pluripotent stem cell
IQR	Inter quartile range
IVF	*in vitro* fertilisation
kDa	kilo Dalton
Ki67	Proliferation-related Ki67 antigen
KLF4	Kruppel-like factor 4
KO	Knock-out
KRT7	Keratin gene
LDHA	Lactate dehydrogenase A
LIF	Leukaemia inhibitor factor
LIN	RNA-binding protein
m	Mouse/mice
MAPK	Mitogen-activated protein kinases
MEF	Mouse embryonic fibroblast
MEK	Mitogen-activated protein kinase kinase
miRNA/miR	microRNA
MIXL1	Homeobox transcription factor of the Mix/Bix family
mRNA	Messenger RNA
MSRT	Multiscripe reverse transcriptase
mTOR	Mechanistic target of rapamycin
NANOG	Homeobox transcription factor Nanog
NEB	New England Biolabs (UK)
NR2F2	Orphan nuclear receptor
ns	Not significant
nt	Nucleotides
NTC	Non-template control
OAZ	Ornithine decarboxylase antizyme
OCT4	POU class 5 homeobox 1 transcription factor
ORF	Open reading frame

OTX2	Homeobox protein OTX
PABP	Polyadenylation binding protein
PAGE	Polyacrylamide gel electrophoresis
PAX	Family of genes involved in early development
PBS	Phosphate buffered saline
PBST	Phosphate buffered saline with Tween
PCR	Polymerase chain reaction
PDH	Pyruvate dehydrogenase
PDK1	Pyruvate dehydrogenase kinase-1
PGC	Primordial germ cell
PHD	Prolyl-hydroxylase domain
PITA	Probability of Interaction by Target Accessibility
PI3K	Phosphatidylinositol-3-kinase
PKM	Pyruvate kinase isoenzyme/ Pyruvate kinase muscle isoenyzme
POU	PIT/OCT/UNC
pre-miRNA	Precursor micro RNA
pri-miRNA	Primary microRNA
PSC	Pluripotent stem cells
p300/CBP	p300/ Creb-binding protein -associated factor
RanGTP	Ras-related nuclear protein Guanosine-5'-triphosphate
RIPA	Radio-immuno-precipitation assay
RISC	RNA induced silencing complex
RNA	Ribonucleic acid
RNAse	Ribonuclease
ROS	Reactive oxygen species
rpm	Rounds per minute
RT	Reverse transcriptase
qPCR	Quantitative polymerase chain reaction
SC	Stem cell
SDS	Sodium dodecyl sulphate
SEM	Standard error of the mean
siRNA	Small interfering RNA
SMAD	SMA-small body size, MAD-mothers against decapentaplegic
SNAIL	Zinc finger protein SNAI1
SOX2	SRY (sex determining region Y)-box 2
SPS	Seed-pairing stability
SSEA	Stage-specific embryonic antigen
Stat	Signal transducers and activators of transcription
STDEV	Standard deviation
TA	Target-site abundance
TAE	Tris base, acetic acid and EDTA
TBX6	T-box protein
TEMED	N,N,N,N,-tetramethylethylenediamine
TF	Transcription factor
TFAP2A	Transcription factor AP-2 alpha
TGF	Transforming growth factor
TLDA	TaqMan quantitative real-time PCR Low Density Array
TRA	Trafalgar-antigen
UBC	Ubiquitin C

UTR	Untranslated region
V	Volts
VHL	Von Hippel-Lindau tumour suppressor protein
VPA	Valproic acid
WNT	Wingless-related integration site
ZIC1	Zinc finger of the cerebellum protein family
2i	Two inhibitor

Chapter 1

Introduction

1.1 Stem Cells

Stem cells are unspecialised cells that are capable of indefinite proliferation and they are able to differentiate into more specialised cells (Till and McCulloch, 1961; Becker, McCulloch and Till, 1963; Till, McCulloch and Siminovitch, 1963).

The term “Stammzelle” (German for stem cell) was mentioned as early as 1868 by Ernst Haeckel, when he called the fertilised egg a stem cell (Haeckel, 1868). In the English language the term “stem cell” was first mentioned by Wilson (Wilson, 1896). However, it was not until the early 1960s when the foundations of stem cell science were established and researchers proved the existence of stem cells in mouse bone marrow on the basis of hematopoietic stem cells (Till and McCulloch, 1961; Becker, McCulloch and Till, 1963; Till, McCulloch and Siminovitch, 1963).

1.1.1 Types of Potency

Stem cells are classified based on their developmental potential/ potency. Only a fertilized egg (zygote) is totipotent, thus giving rise to a complete organism by having the ability to develop into embryonic and extra-embryonic cell types (Figure 1) (Schöler, 2004; Mitalipov and Wolf, 2009; Condic, 2014). Thus, pluripotent cells such as embryonic stem cells (ESCs) have the capability to develop into all cells of the three germ layers but pluripotent stem cells are not capable of producing derivates of trophectoderm and/or primitive endoderm (Figure 1). Multipotent cells, for instance mesenchymal stem cells are able to differentiate into multiple cell types such as bone, cartilage, muscle and fat cells. An oligopotent cell can develop into few cell types, such as myeloid or lymphoid stem cells. If a cell is only capable of developing into one type of cell then it is unipotent, for instance spermatogonia.

1.1.2 Pluripotent stem cells

ESCs are derived from the ICM of the blastocyst, the final stage of pre-implantation development. In humans, the blastocyst develops 5-6 days after fertilisation of the oocyte (zygote) and consists of an outer layer of trophectoderm cells and the inner cell mass (ICM). The trophectoderm gives rise to extra-embryonic tissues and the ICM gives rise to the embryo proper. As ESCs self-renew and can also give rise to all cells of the three germ layers they are pluripotent (Figure 1).

Embryonic carcinoma cells (ECCs) are also able to give rise to cells of all three germ layers, endoderm, ectoderm and mesoderm and are pluripotent. ECCs are derived from teratocarcinomas arising from transformed germ cells and are generally considered to be the malignant counterpart of ESCs (Figure 1) (Andrews, 1998). In contrast to ESCs, ECCs are aneuploid (Pera, Reubinoff and Trounson, 2000).

Primordial germ cells (PGCs) have been demonstrated to differentiate into cells of all three germ layers and are pluripotent (Shamblott *et al.*, 1998). In vivo, hPGCs are present in the embryonic and foetal gonad and develop into the egg or sperm (Figure 1) (Jørgensen *et al.*, 1995). Furthermore, PGCs tend to display a more stable karyotype compared to ECCs (Shamblott *et al.*, 1998)

Embryonic germ cells (EGCs) are derived from primordial germ cells (PGCs), can give rise to all three germ layers and are also pluripotent (Figure 1) (Matsui *et al.*, 1991; Resnick *et al.*, 1992). Although EGCs are considered to be the parallel of ESCs, they are difficult to derive and maintain undifferentiated in culture which is in contrast to ESCs (Onyango *et al.*, 2002; Turnpenny *et al.*, 2003, 2006; Liu *et al.*, 2004).

PGCs, ECCs and EGCs are pluripotent but how distinct they are from ESCs has not yet been resolved.

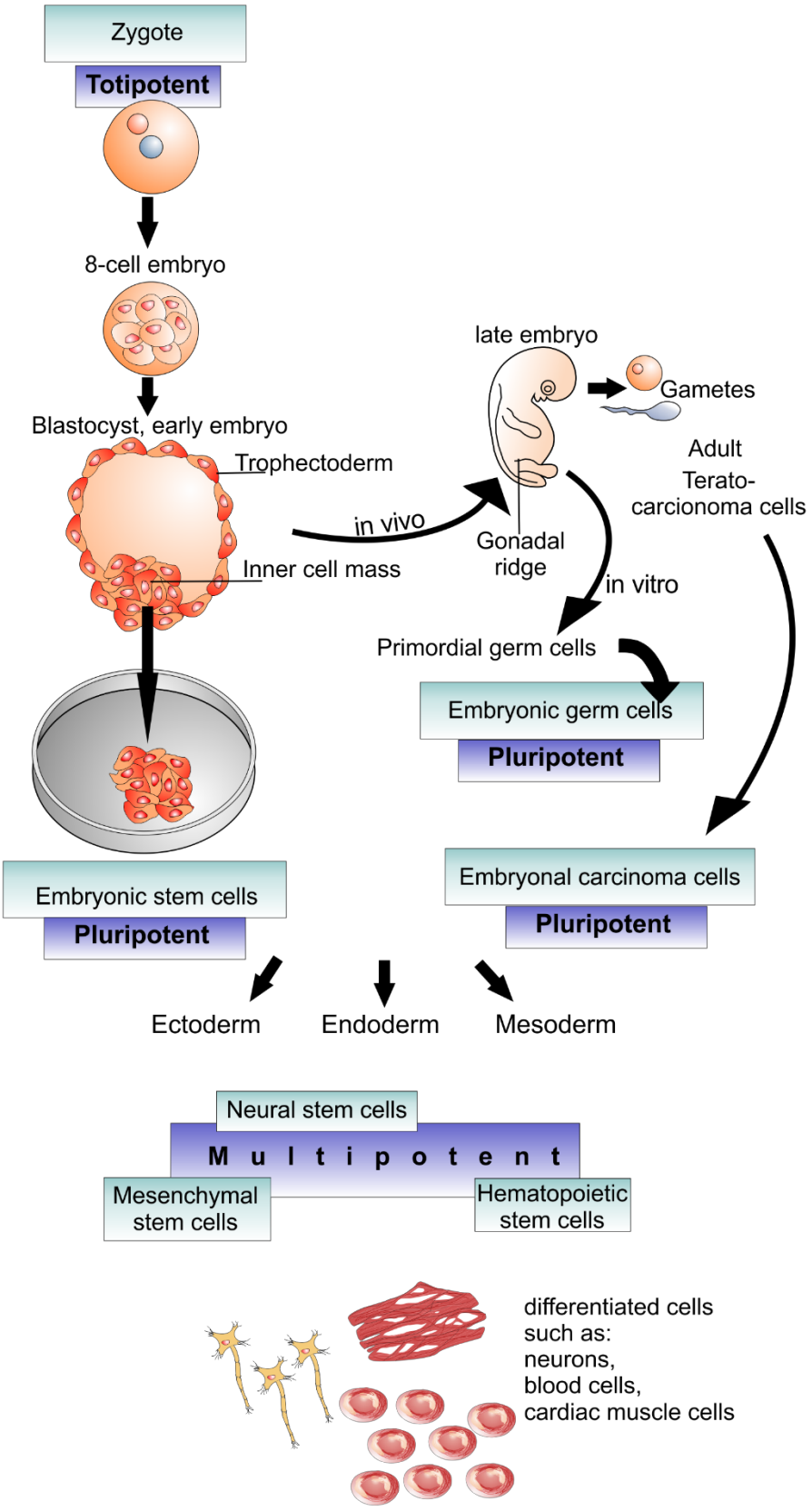

Figure 1: Schematic representation of types of stem cells

The schematics shows the derivation of embryonic stem cells, embryonic germ cells, primordial germ cells and embryonic carcinoma cells, which are all able to give rise to all three germ layers that are ectoderm, endoderm and mesoderm and thus are pluripotent.

1.1.3 Embryonic stem cells

The first embryonic stem cells (ESCs) were derived from mouse embryos in 1981 (Evans and Kaufman, 1981), and 17 years later, human ESCs were first derived from the inner cell mass (ICM) of the blastocyst and successfully maintained in culture (Figure 1) (Thomson *et al.*, 1998). ESCs can proliferate in an undifferentiated state and are capable of indefinite self-renewal while maintaining their potential to give rise to cells of all three embryonic germ layers (Figure 1) (Evans and Kaufman, 1981; Thomson *et al.*, 1998; Pera, Reubinoff and Trounson, 2000), thus they are said to be pluripotent. Despite ethical controversies, the latter characteristic means they hold the potential for a limitless source of every cell type in the body (Reubinoff *et al.*, 2000) making human ESCs (hESCs) enormously attractive for applications in drug testing and regenerative medicine such as transplantation therapy. Such developments would require safe propagation of wholly pluripotent and undifferentiated hESCs in culture, necessitating an in depth understanding of the underlying mechanisms which regulate pluripotency and how to efficiently direct differentiation into specific cell types.

1.1.3.1 Characteristics of ESCs

ESCs possess the following characteristics (Evans and Kaufman, 1981; Martin, 1981; Thomson *et al.*, 1998):

- Derived from the ICM of the blastocyst
- Stable diploid karyotype
- High nuclear to cytoplasm ratio
- Indefinite self-renewal, which means they can continuously proliferate in an undifferentiated manner.
- High telomerase activity
- Express characteristic surface markers and transcription factors
- Are pluripotent, i.e. have the potential to give rise to all cell types of all three germ layers

hESCs are capable of infinite and undifferentiated proliferation (Thomson *et al.*, 1998), so called indefinite self-renewal (Avery, Inniss and Moore, 2006), which means that after every cell division the daughter cells will have exactly the same characteristics as their parent cell (symmetrical division) without any signs of senescence. hESCs are therefore immortal through high telomerase activity, which preserves the length of the telomere at the chromosome ends and is important in replicative life-span (Harley, 1991; Harley *et al.*, 1992; Thomson *et al.*, 1998). The advantage of using ESCs over adult stem cells is that isolated adult stem cells are not capable of long term self-renewal *in vitro* (Wang *et al.*, 2005). Additonally adult stem cells are difficult to maintain and expand

undifferentiated in culture (Trounson, 2006). Furthermore, adult stem cells have not been isolated and fully characterised for all tissues. Adult stem cells are also a very rare cell population in mature tissue; they are limited in their developmental potential and can only develop into cells of their tissue of origin.

Morphology is a distinguishing feature for the identification of human and non-human primate ESCs: they have a uniform undifferentiated appearance with a high nuclear to cytoplasmic ratio, as well as a normal hESC karyotype of 46 chromosomes (46, XX or 46, XY) (Thomson *et al.*, 1998). Alkaline phosphatase expression is associated with pluripotency, and there are also several well-established markers used to identify pluripotent ESCs, such as the transcription factors (TFs) SOX2, OCT4 (encoded by *POU5F1*) and NANOG as well as cell surface markers such as TRA-1-81 and TRA-1-60, glycoproteins that are attached to transmembrane proteins. Expression of SOX2, OCT4 and NANOG is essential for pluripotency while suppressing genes which lead to differentiation – for this reason they are known as “core pluripotency factors” (Nichols *et al.*, 1998; Avilion *et al.*, 2003; Chambers *et al.*, 2003a; Mitsui *et al.*, 2003; Young, 2011). Some markers, such as NANOG are immediately down-regulated upon differentiation (Hyslop *et al.*, 2005), and SSEA1 is a marker of early differentiation in hESCs (Reubinoff *et al.*, 2000; Avilion *et al.*, 2003; Chambers *et al.*, 2003a; Boyer *et al.*, 2005) that is typically not expressed in hESCs.

Since ESCs are derived from the ICM, they are not able to develop into extra-embryonic tissue such as the placenta, which is largely derived from the trophectoderm (Thomson *et al.*, 1998; Smith, 2001). This means that ESCs are pluripotent, rather totipotent.

1.1.4 Induced pluripotent stem cells (iPSCs)

In 2006, Takahashi and Yamanaka demonstrated that fully committed and specialised cells such as mice fibroblast cells could be re-programmed into ESC-like cells by using a retroviral vector which introduced the ectopic expression of four transcription factors, OCT4, SOX2, KLF4 and c-MYC (Takahashi and Yamanaka, 2006). One year later, the generation of iPSCs from human fibroblasts was accomplished (Takahashi *et al.*, 2007). Pluripotent stem cells are enormously important for studying early development and differentiation and hold great potential for regenerative medicine, thus iPSCs overcome the ethical controversy which exists for hESCs and more importantly iPSCs seem to be the ideal patient specific medicine. However, iPSCs are generated with the introduction of a retrovirus which cannot be used in therapeutic applications. Newer studies try to overcome the retroviral introduction by using other non-integrative viruses such as adenovirus (Stadtfeld *et al.*, 2008; Zhou and Freed, 2009) or a RNA virus such as Sendai

virus (Fusaki *et al.*, 2009; Seki *et al.*, 2010). Remarkably, although only validated in fibroblasts, a non-viral method such as the transfection of synthetic modified mRNA was able to re-programme human fibroblast much more efficiently with a 4.4% success rate compared to the usually obtained 0.0001-1% success rates when viruses were used (Warren *et al.*, 2010). Many more methods have been developed for generating iPSCs, for example miRNA transfections (Anokye-Danso *et al.*, 2011a; Miyoshi *et al.*, 2011; Subramanyam *et al.*, 2011). However, still more efforts are needed for generating iPSCs to achieve higher efficiencies and a greater quality of cells (no heterogeneity of obtained cells, less genomic mutations and loss of their epigenetic memory). This is most likely to be achieved by developing a better understanding of how pluripotency is regulated.

1.1.5 Derivation of hESCs

hESCs are obtained from surplus embryos donated with informed consent by patients undergoing *in vitro* fertilisation (IVF). Embryos from IVF will then be *in vitro* cultured to the blastocyst stage. The derivation of hESCs can be performed by either immunosurgery or blastocyst outgrowth. In the blastocyst outgrowth method, the blastocyst hatches from the zona pellucida and the cells of the ICM grow out from the blastocyst where they can then be isolated and cultured. In the immunosurgery method, the zona pellucida is dissolved with acid tyrodes (Chen and Melton, 2007) or digested with a pronase enzyme (Solter and Knowles, 1975; Reubinoff *et al.*, 2000). Anti-human serum antibodies bind to the trophectoderm followed by complement lysis to lyse the trophectoderm cells (Chen and Melton, 2007). Which are removed by mechanical disaggregation resulting in an isolated ICM. The isolated ICM can then be expanded in culture to produce a new ESC line.

Another way of obtaining a hESC line is by clonal expansion of a single cell, different to the method used by Thomson (1998) who selected and expanded an ICM. An advantage of using cell lines originated by clonal expansion is that each individual cell has the same developmental potential that can give rise to cells of all three embryonic germ layers (Amit *et al.*, 2000).

1.1.6 States of pluripotent stem cells: naïve and primed mESCs and hESCs

New insights into pluripotent stem cells have evolved since the origin of ESCs became more intensively studied and post-implantation epiblast stem cells (EpiSCs) were derived and characterised (Brons *et al.*, 2007). At the blastocyst stage two lineages are distinguishable, the ICM and the trophectoderm. The ICM develops into the epiblast and hypoblast, while the trophectoderm mainly contributes to extraembryonic tissue such as the placenta. The first ESCs from post-implantation mouse embryos were derived under culture conditions usually used for the derivation of ESCs from human blastocysts with activin and a fibroblast growth factor (Fgf2)-supplemented culture media (Thomson *et al.*, 1998; Brons *et al.*, 2007; Tesar *et al.*, 2007; Nichols and Smith, 2009a). EpiSCs cannot be cultured from single cells and comprise a limited capacity to form chimerism. However, EpiSCs have many characteristics in common with pluripotent hESCs. They share gene expression patterns and signalling responses, which may suggest that hESCs are in a later developmental stage than mESCs derived from blastocysts (Brons *et al.*, 2007; Tesar *et al.*, 2007; Nichols and Smith, 2009b, 2011). It therefore seems that pluripotency exists in two stages, naïve and primed. The naïve stage encompasses the ICM of pre-implantation embryos such as mESCs, whereas primed stem cells include post-implantation epiblast-derived cell types such as mEpiSCs and hESCs. This may indicate that ESCs from epiblast cells are already prone to a primordial germ cell (PGC) fate (Brook and Gardner, 1997). The ICM develops into the epiblast and hypoblast, which in the mouse embryo can be distinguished by Nanog expression for the epiblast and Gata6 and Gata4 expression for the hypoblast (Chambers *et al.*, 2003a). Another feature used as a marker of successful formation of naïve ESCs is the reactivation of the inactive X chromosome in female cells (Silva *et al.*, 2008). Female mESCs usually have two active X chromosomes whereas mEpiSCs and hESCs underwent already one X chromosome inactivation (Lengner *et al.*, 2010). Naïve ESCs have thus far mainly been obtained in mice with the addition of leukaemia inhibitor factor (LIF) and with the two inhibitor (2i) culture conditions by adding Mitogen-activated protein kinase kinase (MEK), an Extracellular-signal regulated kinase (ERK) -inhibiting signalling kinase, and glycogen synthase kinase 3 (GSK3) inhibitor (Ying *et al.*, 2008). Those naïve ESCs were able to undergo single cell passage with the morphology of mounded colonies, had an active X chromosome and were able to contribute to germline chimeras (Ware *et al.*, 2014). Only recently have researchers shown that it is possible to derive human naïve ESCs without ActivinA and transgenes in 2i culture (Gafni *et al.*, 2013; Ware *et al.*, 2014). These naïve hESCs seem to be more comparable to mESCs and have an increased ability to form expanded endoderm, which had not previously been reported for hESCs (Ware *et al.*, 2014). Although mESCs and hESCs differ, it is still unclear how comparable the mESC

and the hESCs state need to be to maintain naïve pluripotency as their gene regulatory network is not 100% conserved. For example, hESCs with induced expression of KLF2 and NANOG were highly similar to mESCs and different to normal hESCs (Takashima *et al.*, 2014; Theunissen *et al.*, 2014). However, when hESCs where derived from embryos under more physiological, low oxygen concentration in the absence of FGF and other serum factors but with LIF and 2i that usually inhibit GSK3 and Mitogen-activated protein kinase (MAPK)/ERK signalling the expression of naïve pluripotency markers such as hypomethylation, KLF4, TFCP2L1, TBX3, KLF17 and NANOG was observed (Guo *et al.*, 2016). Further investigations are necessary to describe the earliest developmental state of pluripotent hESCs and to understand the underlying mechanisms of pluripotency, naïve and primed as well as how culture conditions influence these states.

1.1.7 Culture conditions for hESCs

In vitro, hESCs are notoriously difficult to culture and to maintain pluripotent as they require many factors and properties to ensure cell attachment, cell survival and undifferentiated proliferation. hESCs typically grow in colonies rather single cells thus interacting through cell-cell-contact. However, hESCs have the propensity to spontaneously differentiate in inadequate culture conditions (Reubinoff *et al.*, 2000) or display poor survival when they are dissociated into single cells (Peerani *et al.*, 2009). Thus much effort has been made to improve culture conditions for maintaining hESCs in an undifferentiated and pluripotent stem cell state. The conditions for long-term culture of hESCs usually involve animal products in both the derivation process and the subsequent culture environment such as feeder layers and cell medium. Although the use of animal products is less problematic in basic research, these animal products need to be ultimately replaced to avoid xeno-contamination for any type of clinical applications.

1.1.7.1 Culture on feeder layers

The ICM is often derived on feeder layers that provide support. Typically, cells such as mitotically inactivated mouse embryonic fibroblasts (MEF) are used as feeder cells for the maintenance of the hESCs (Thomson *et al.*, 1998; Reubinoff *et al.*, 2000). Except basic fibroblast growth factor (bFGF) which is only secreted by human feeder layers (Eiselleova *et al.*, 2008), both human and MEF feeders release important soluble factors that are beneficial for the long-term culture and maintenance of hESCs such as Activin A, transforming growth factor beta 1 (TGFβ1) and bone morphogenetic protein (BMP4) (Amit *et al.*, 2004; Beattie *et al.*, 2005; Eiselleova *et al.*, 2008). However, culturing cells with MEFs may expose hESCs to mouse retroviruses, and culturing along with other animal products such as serum in growth media is a difficulty when it comes to clinical translation. Other improvements in hESC culturing methods include animal-free feeder layers such as human neonatal foreskin fibroblasts with knock-out serum replacements (xeno-free), supplemented with human recombinant fibroblast growth factor (Amit *et al.*, 2003; Ellerström, Strehl and Moya, 2006; Ilic *et al.*, 2012) and Activin A (Eiselleova *et al.*, 2008). Human foreskin fibroblast feeders overcome the risk of zoonosis and were able to support maintenance and prolonged culture of pluripotent hESCs (Amit *et al.*, 2003).

1.1.7.2 Feeder-free culture

Culturing hESCs in the absence of direct feeder cells can be performed using a protein matrix to support the cells such as Matrigel (Xu *et al.*, 2001). Matrigel is a routinely used

feeder-free matrix in combination with MEF-conditioned media and showed next to laminin to be one of the best matrices for long-term culture of hESCs compared to fibronectin or collagen IV (Xu *et al.*, 2001). However, Matrigel is a gelatinous protein mixture that is derived from mouse sarcoma cells (Kleinman and Martin, 2005) and hESCs still require feeding with MEF-conditioned media and thus does not overcome the requirement for animal free co-culture (Xu *et al.*, 2001). Other matrices are recombinant fibronectin (Amit *et al.*, 2004; Amit and Itskovitz-Eldor, 2006; Tsutsui *et al.*, 2011), vitronectin (Braam *et al.*, 2008) or laminin (Miyazaki *et al.*, 2008; Tsutsui *et al.*, 2011) and thus also provide a feeder free culture system for hESCs. More recently, a polysaccharide/extra cellular matrix combination such as heparin-catechol and collagen type-1 has shown to support long-term culture and maintenance of hESCs (M. Lee *et al.*, 2016).

1.1.7.3 Culture media

Although it has been shown that mESCs can be maintained feeder-free by adding a factor called LIF, which activates the transcription factor Stat3 and inhibits differentiation (Dani *et al.*, 1998; Niwa *et al.*, 1998; Niwa, Miyazaki and Smith, 2000), LIF has no effect on hESCs (Thomson *et al.*, 1998; Reubinoff *et al.*, 2000). The addition of FGF2, Activin A and TGFβ1 into the culture medium has been shown to support hESC culture in an undifferentiated state under feeder-free conditions (Beattie *et al.*, 2005; Amit and Itskovitz-Eldor, 2006). Furthermore, defined, feeder-independent and serum-free medium such as mTeSR are now available, demonstrating that hESCs cultured on Matrigel with mTeSR maintained all their stem cell characteristics (Ludwig and Thomson, 2007; Lannon *et al.*, 2008). The major challenge in developing an optimal and defined medium for hESCs culture is that the signalling pathways associated with hESC maintenance are not yet fully understood. However, feeder-free culture systems will enhance safety and efficiency of ESCs towards translational research and regenerative medicine.

1.1.8 Pluripotency Factors and Markers

OCT4, SOX2 and NANOG are the “core transcription factors“, which play important roles in the early development of an embryo and are responsible for the maintenance of undifferentiated ESCs in cell culture (Nichols *et al.*, 1998; Avilion *et al.*, 2003; Chambers *et al.*, 2003a; Boyer *et al.*, 2005; Loh *et al.*, 2006). Thus showing that OCT4 together with Sox2 (Ambrosetti *et al.*, 2000) and NANOG (Chambers *et al.*, 2003b) are required for pluripotency.

OCT4, octamer-binding transcription factor 4 (also known as OCT3/4), is a protein encoded by the human gene *POU5F1* (POU domain, class5, transcription factor 1) that belongs to the to the subfamily of homeobox genes, the PIT/OCT/UNC (POU) family. The octamer DNA sequence is an 8 bp motif 5’-ATTTGCAT-3’ (Petryniak *et al.*, 1989). The POU-specific domain is a N-terminal bipartite DNA-binding domain with four alpha-helices forming a helix-turn-helix (HTH) structure (Sturm, Das and Herr, 1988) and is connected with a non-conserved linker to the C-terminus POU-homeodomain (Sturm and Herr, 1988; Sturm, Das and Herr, 1988). Both domains can bind DNA together, if they are not connected by the linker (Klemm and Pabo, 1996).

OCT4 is an essential TF for the formation of pluripotent cells in the mammalian embryo (Schöler *et al.*, 1990; Nichols *et al.*, 1998). One of the first discoveries of the relationship between the early development of an embryo and OCT4 was made 1990, when it was demonstrated by in situ hybridisation on northern blots that Oct4 mRNA was present in the mouse zygote, morula and blastocyst but not in differentiated cells (Rosner *et al.*, 1990). Additionally, Oct4-deficient mice embryos were differentiating into trophoblast (Nichols *et al.*, 1998). Thus showing that the expression of OCT4 is restricted to the early embryo and important for pluripotency in cells of the ICM (Yeom *et al.*, 1991; Nichols *et al.*, 1998). However, the level of OCT4 expression can vary and plays an important role as it has been shown that the amount of *Oct4* expression is correlated with ability to sustain self-renewal in mESCs, since an increase of more than 50% in *Oct4* expression leads to differentiation into primitive endoderm and mesoderm and a reduction of more than 50% caused loss of pluripotency and trophoectodermal dedifferentiation (Rosner *et al.*, 1990; Schöler *et al.*, 1990; Niwa, Miyazaki and Smith, 2000). More recently it was shown, that pluripotency is regulated by defined levels of Oct4 expression that were controlling cell state transitions resulting into differentiation towards all three germ layers upon Oct4 overexpression (Radzisheuskaya *et al.*, 2013). Thus in mESCs Oct4 seems to play two important but opposing roles, regulating pluripotency and self-renewal and initiating differentiation.

The importance of OCT4 can be further demonstrated in the progression of creating iPSCs. Originally, OCT4, SOX2, KLF4 (Kruppel-like factor 4) and c-MYC were required for iPSC generation (Maherali *et al.*, 2007; Okita, Ichisaka and Yamanaka, 2007; Wernig *et al.*, 2007). Then two factors OCT4 and KLF4 (Kim *et al.*, 2008) were used and by 2009 iPSC could be generated using only OCT4 (Kim *et al.*, 2009).

NANOG is a transcription factor that also has a homeodomain for DNA binding, and was discovered much later than OCT4. Homeodomains at NANOG are highly conserved, with the murine *Nanog* homeodomain showing 94% identity to rat and 87% to human (Chambers *et al.*, 2003a). A B2 element was found in the 3'UTR of the *Nanog* mRNA (Chambers *et al.*, 2003a) and since it was known that B2 elements are greatly expressed in embryonic cells (Ryskov *et al.*, 1983), the B2 element was considered to play a role in *Nanog* gene expression. Chambers et al. (2003) were the first to relate pluripotency with *Nanog* expression, by observing *Nanog* mRNA in ESCs, PGCs that will become EGCs and ECCs. Expression studies throughout the early development of mouse embryos revealed very similar expression patterns as described for *OCT4* with the difference, that at the stage of epiblast formation *Nanog* mRNA was not detectable in the primitive endoderm (Chambers *et al.*, 2003a). Nanog showed also different levels of expression in mESCs, thus expressing GATA6, an early endodermal marker, when NANOG was lowly expressed (Singh *et al.*, 2007). When *Nanog*-deficient mice were examined, it revealed that the epiblast could not be generated from the ICM, and that ESCs lost their pluripotent state by differentiating into the extraembryonic endoderm lineage (Mitsui *et al.*, 2003). Another report shows that the fluctuating levels of NANOG expression could be important in balancing differentiation and pluripotency in mESCs (MacArthur *et al.*, 2012). This confirms once more that these markers successfully distinguish pluripotency and are not expressed upon tissue differentiation. However, in the progress of inducing pluripotent stem cells, Nanog was surprisingly dispensable (Takahashi and Yamanaka, 2006) which demonstrates that the underlying mechanisms of pluripotency are still not completely understood.

SOX2 belongs to a family of transcription factors containing a high mobility group (HMG) box, a DNA-binding motif that facilitates DNA looping for chromatin remodelling and transcriptional activation (Bowles, Schepers and Koopman, 2000; Nelson and Cox, 2000). As one of the target genes of OCT4, SOX2 contains an OCT4-binding octamer element to facilitate interaction of its HMG domain with the POU domain of OCT4 (Ambrosetti *et al.*, 1997, 2000). SOX2 is one of the most studied SOX proteins and plays a very important role in mammalian early development (Rizzino, 2009). Hence, inactivated Sox2 leads to mouse embryonic lethality (Avilion *et al.*, 2003). SOX2

expression plays an important role in both hESCs and mESCs and is reduced upon differentiation (Chew *et al.*, 2005). Similar to OCT4 knock-out, SOX2 knock-out results also in differentiation towards trophectoderm (Chew *et al.*, 2005).

Aside from OCT4, SOX2 and NANOG, there are also surface antigens that are valuable markers for characterising undifferentiated hESCs. The Trafalgar-antigens (TRA), such as TRA-1-81 and TRA-1-60 – both sialylated keratin sulphate proteoglycans (Badcock *et al.*, 1999) – are expressed in hESCs and monkey ESCs (Pera, Reubinoff and Trounson, 2000). In hESCs, stage-specific embryonic antigens (SSEA) such as SSEA3 and SSEA4 are expressed but SSEA1 is not expressed (Henderson, Draper and Baillie, 2002). hESCs and mESCs share many characteristics but differ in their expression of cell surface pluripotency makers. Both express OCT4, SOX2 and NANOG, whereas SSEA3, SSEA4, TRA-1-60 and TRA-1-81 show expression only in hESCs, and SSEA1 only in mESCs (Figure 2). In fact, expression of SSEA1 in hESCs indicates early differentiation (Reubinoff *et al.*, 2000; Avilion *et al.*, 2003; Chambers *et al.*, 2003a; Boyer *et al.*, 2005).

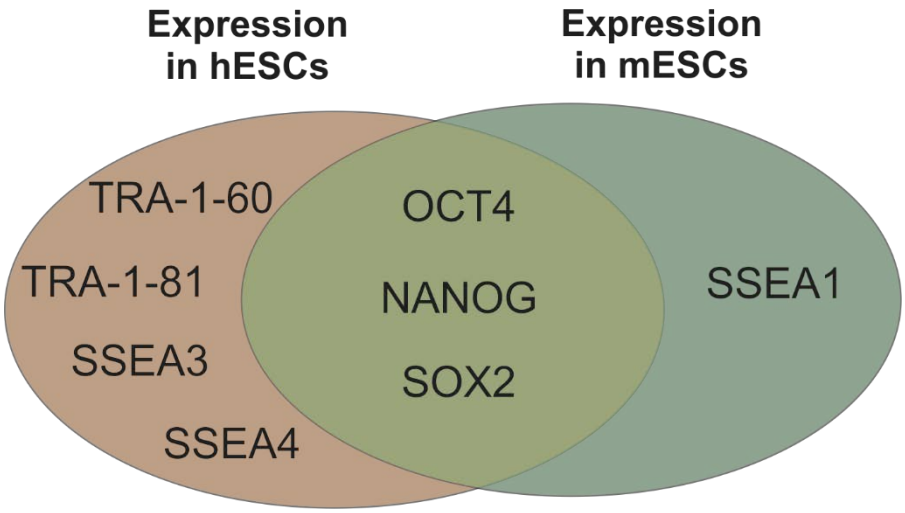

Figure 2: Expression of cell- surface markers and transcription factors in hESCs and mESCs

The antigens OCT4, SOX2 and NANOG are expressed by both hESCs and mESCs. The antigens TRA-1-60, TRA-1-81, SSEA3 and SSEA4 are only expressed by hESCs and SSEA1 is only expressed by mESCs.

1.1.9 Control and Regulation of Pluripotency

OCT4 can form heterodimers with SOX2. In mice, these Oct4/Sox2 heterodimers have been shown, both *in vitro* and *in vivo*, to bind to an important regulatory region of the *Nanog* promoter (Kuroda *et al.*, 2005; Rodda *et al.*, 2005). This Oct4/Sox2 motif is a necessary requirement for pluripotency (Kuroda *et al.*, 2005). However, investigations in the regulatory network revealed that the expression of *Nanog* was unaltered in *Oct4*-deficient mice (Chambers *et al.*, 2003a). This suggests that *Nanog* is not necessarily dependent on *Oct4* expression, but where *Oct4* would lead to differentiation, *Nanog* seems to be beneficial for pluripotency, even at high expression levels (Rosner *et al.*, 1990; Schöler *et al.*, 1990; Niwa, Miyazaki and Smith, 2000).

Along with Oct4 and FoxD3, which are both important pluripotency factors in mice (Hanna *et al.*, 2002; Pan *et al.*, 2006), Nanog is also part of a negative feedback loop controlling stem cell pluripotency and self-renewal (Figure 3). These three TFs interact in a complex manner: Oct4 and FoxD3 generally promote Nanog expression, but if Oct4 expression is elevated then Oct4 can also repress both itself and Nanog. If Oct4 is overexpressed, Nanog also starts a negative auto-feedback loop to limit its own expression. This feedback loop involves activation of Oct4 through Nanog and FoxD3 (Pan *et al.*, 2006). The importance of fluctuations in Nanog expression levels for controlling ESC identity and fate at the single-cell level has been previously described (MacArthur *et al.*, 2012). This work analysed feedback loops in pluripotency, where Oct4, Sox2 and Nanog contributed to two thirds of 28 identified feedback loops (MacArthur *et al.*, 2012). Interestingly, Nanog plays a more central role in the regulatory network, as its loss destroys two thirds of identified feedback loops (Chambers *et al.*, 2007; MacArthur *et al.*, 2012). In mice, Oct4, Sox2 and Nanog are also able to bind to their own promoters, which creates additional auto-feedback loops to regulate themselves to promote ESC identity (Loh *et al.*, 2006).

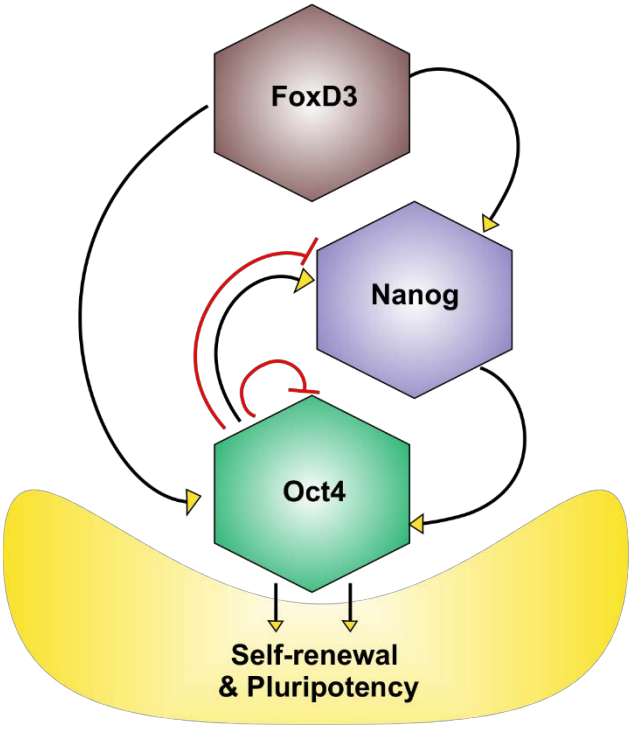

Figure 3: Control of stem cell pluripotency in mice

Oct4 is positively regulated by FoxD3 and Nanog while Oct4 is able to regulate itself and Nanog negatively. FoxD3 can elevate Nanog, which in turn elevates Oct4 expression. (Adapted from Pan et al. (2006)).

In humans, the three TFs OCT4, SOX2 and NANOG all interact together to promote or repress genes responsible for stem cell characteristics and differentiation (Figure 4) (Boyer *et al.*, 2005). These three TFs also overlap in their target genes. Approximately half of the genes bound to OCT4 are the same bound by SOX2, and more than 90% of the promoter regions of both are also bound by NANOG (Boyer *et al.*, 2005). In hESCs, over 300 genes are concurrently bound by OCT4, SOX2 and NANOG (Boyer *et al.*, 2005).

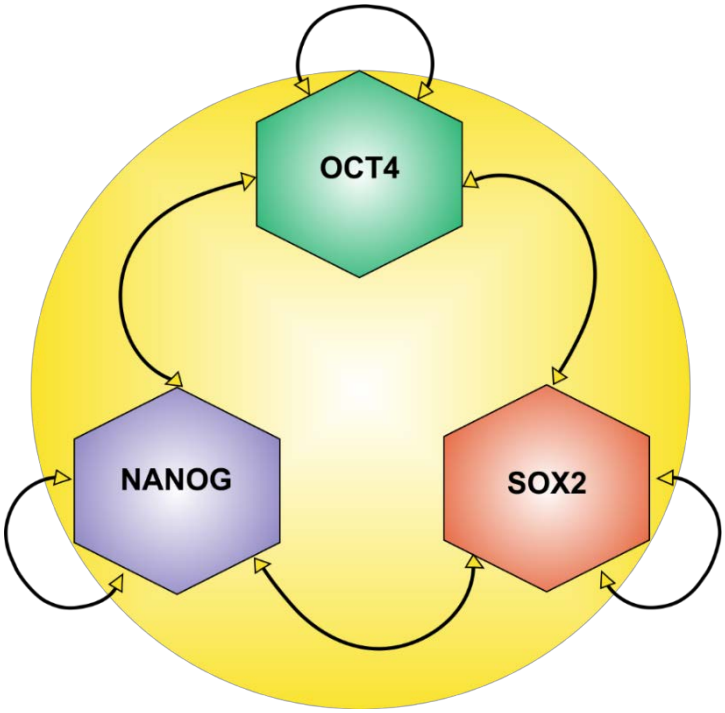

Figure 4: Auto-feedback loop of OCT4, SOX2 and NANOG
The TF OCT4, SOX2 and NANOG build the core regulatory network maintaining the stemness of ESCs while regulating their own expression as well as the expression of the other two TFs. (Adapted from Chan et al. (2011))

All these findings suggest that the “core transcription-factors” of pluripotency work in a complex network together, co-regulating gene expression networks to maintain ESC properties. Indeed, when the protein network of Nanog in mice was investigated, numerous physically associated proteins that are important in the maintenance of ESCs were identified (Wang *et al.*, 2006).

The ESC transcriptome contains a huge number of genes for signal transduction and regulation. About 150,000 expressed sequence tags (ESTs) were analysed from hESCs and differentiated subpopulations, revealing 532 up- and 140 down-regulated genes in undifferentiated hESCs (Brandenberger *et al.*, 2004). The investigation of those

identified ESTs showed that all FGF receptors expressed by hESCs are up-regulated in undifferentiated hESCs (Brandenberger *et al.*, 2004; Wray, Kalkan and Smith, 2010). Other identified differentially expressed genes that encode for ligand-receptors are transforming growth factor (*TGF*)/bone morphogenetic protein (*BMP*) as well as the Nodal and Wingless type (WNT) signalling pathways (Brandenberger *et al.*, 2004; Sato *et al.*, 2004)

1.1.9.1 WNT signalling in ESCs

The WNT pathway is initiated by the binding of the WNT protein to the Frizzled receptor, leading to the inhibition of glycogen-synthase kinase-3 (GSK3). The inhibition of GSK3 leads to β-catenin release that is then transported into the nucleus and initiate the expression of genes such as *OCT4*, *SOX2* and *NANOG*, thus showing that an active WNT pathway maintains pluripotency of both mESCs and hESCs (Sato *et al.*, 2004). However, there are conflicting reports about the consequence of the WNT pathway and more recent advances suggest that the initiation of the WNT pathway with its effector β-catenin leads to differentiation (Figure 5) (Tang *et al.*, 2002; Ding *et al.*, 2003; Bone *et al.*, 2011; Davidson *et al.*, 2012; Singh, Reynolds, *et al.*, 2012). GSK3 is also important in regulating pluripotency but the mechanism of action is yet to be fully understood thus making it difficult to judge if GSK3 is promoting or supressing the WNT pathway. GSK3 inhibition enhanced self-renewal in mESC and in hESCs low levels of GSK3 were shown to stabilise c-myc –a key regulator of PCS maintenance (Doble, 2003; Doble *et al.*, 2007; Dalton, 2013). Other reports suggest that low levels of GSK3 are activating the WNT pathway and hPSCs start differentiating (Trompouki *et al.*, 2011; Singh, Reynolds, *et al.*, 2012). The WNT pathway is acting through β-catenin release which in turn is interacting with SMAD2/3 and, in contrast to the TGF-β pathway this interaction is promoting differentiation (Figure 6) (Singh, Reynolds, *et al.*, 2012).

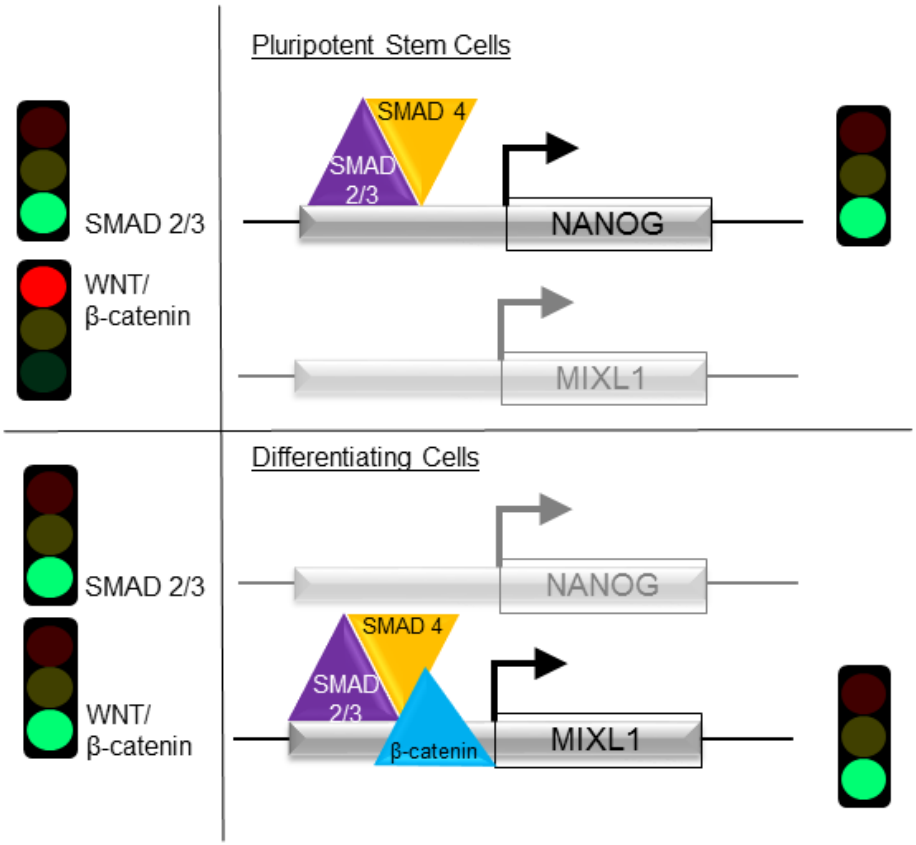

Figure 5: Example of Wnt/β-catenin signalling in hESCs fate (adapted from Dalton, 2013)

SMAD2/3 usually activate pluripotency target genes such as NANOG in the absence of Wnt/β-catenin signalling and therefore maintain pluripotency. Once the WNT effector β-catenin is activated through Wnt signalling it can bind SMAD2/3 and SMAD4 which then lead to the initiation of transcription of genes involved in mesoderm differentiation such as MIXL1.

1.1.9.2 TGF-β signalling in ESCs

The TGF-β family comprises many proteins such as TGF-β itself, BMPs, activins and nodal (Attisano *et al.*, 2002). Interestingly, MEF-conditioned medium frequently used to culture hESCs contains ActivinA (Beattie *et al.*, 2005; Xiao, Yuan and Sharkis, 2006) whereas other media contain either ActivinA or other proteins of the TGF-β family to promote hESC maintenance (Ludwig, Bergendahl, *et al.*, 2006). Pluripotency is promoted through the interaction between TGF-β and SMAD2/3 with NANOG for example as a well-studied target (Xu *et al.*, 2008; Vallier *et al.*, 2009; Yu *et al.*, 2011). SMAD2/3 binding together with Activin and NANOG has also shown to promote pluripotency (Bertero *et al.*, 2015). The opposing roles of SMAD2/3 between the TGF-β and WNT signalling pathways are not completely understood but another factor, SMAD4 (a co-activating binding factor), might compete with the binding to SMAD2/3 to initiate

differentiation (Ying *et al.*, 2003; Dalton, 2013; Tsankov *et al.*, 2015). SMAD4 is also binding to SMAD1/5/8 or SMAD1/5/9 induced by BMP4 to then promote differentiation (Figure 6) (Ying *et al.*, 2003; Dalton, 2013; Tsankov *et al.*, 2015).

1.1.9.3 Signalling of PI3K in ESCs

The opposing functions of SMAD2/3 in maintaining pluripotency or promoting differentiation have been suggested to depend on Phosphatidylinositol-3-kinase (PI3K) expression levels: high PI3K levels attenuate SMAD2/3 phosphorylation and promote pluripotency whereas low PI3K levels cause an increase in SMAD2/3 phosphorylation which supports differentiation (Teo *et al.*, 2011; Singh, Reynolds, *et al.*, 2012). In mESCs and probably in hESCs, PI3K itself is activated through insulin or IGF through which PI3K is enabled to signal through AKT. AKT acts to inhibit GSK3 that in turn stabalises c-myc but AKT stimulates also the mTOR pathway but the influence of the mTOR pathway towards pluripotency are currently unknown (Figure 6) (Doble, 2003; Cartwright *et al.*, 2005; Doble *et al.*, 2007; Ohtsuka and Dalton, 2008; Singh, Bechard, *et al.*, 2012; Dalton, 2013).

1.1.9.4 FGF2 signalling in ESCs

It is unclear if FGF2 signalling is negligible as reports have shown that hESCs can be maintained without FGF2 (Singh, Reynolds, *et al.*, 2012). However, the FGF2 signalling pathway seems to be concentration dependent. High levels of FGF2 signal through PI3K, where AKT inhibits ERK (Singh, Reynolds, *et al.*, 2012). In contrast, low levels of FGF2 activate the MAPK pathway and thus activate MEK and ERK (Singh, Reynolds, *et al.*, 2012). Low levels of MEK and ERK are important for the maintenance of pluripotency whilst elevated ERK might cause differentiation (Figure 6) (Singh, Reynolds, *et al.*, 2012; Dalton, 2013).

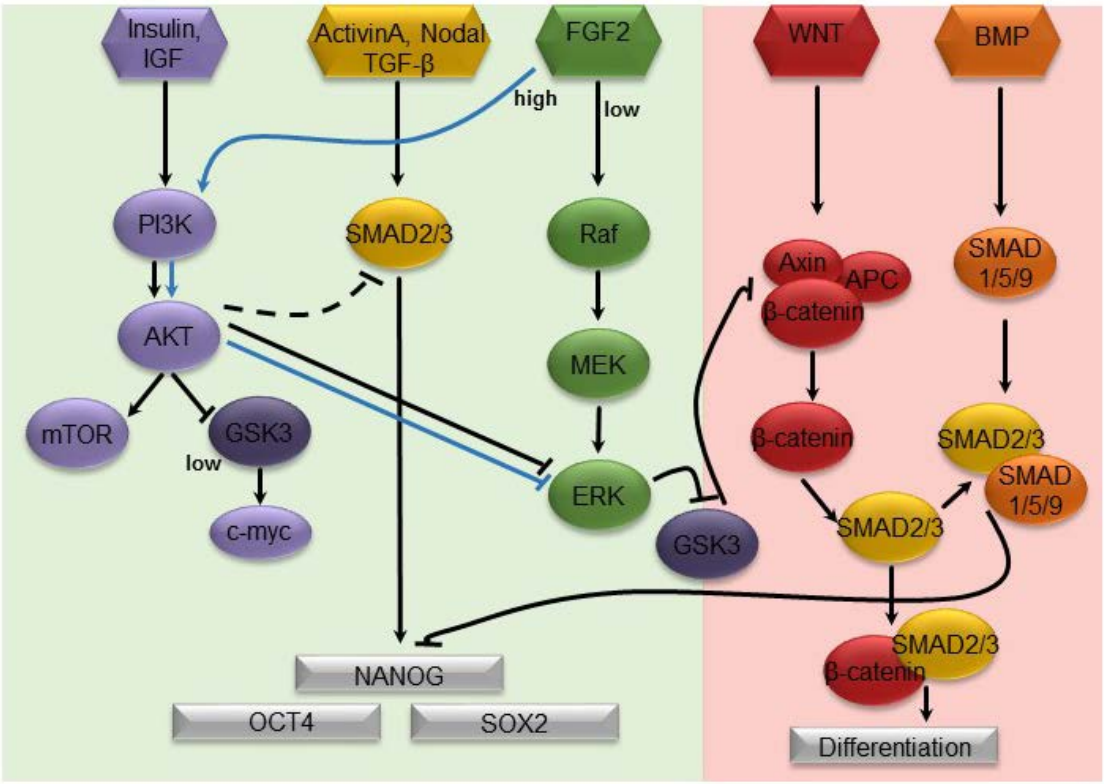

Figure 6: Simplified schematic representation of the major signalling pathways involved in regulation of pluripotency in hESCs

Communication and interaction between PI3K, TGF-β, FGF2, WNT and BMP pathways.

1.1.10 Differentiation of hESCs

The differentiation capacity of hESCs can be demonstrated *in vivo* if injected into mice, where they form teratomas and benign tumours, and develop into cells of all three germ-layers (Thomson *et al.*, 1998). Should ESCs or transformed derivates maintain their pluripotent state after transplantation, there is a risk that these cells could form dangerous teratocarcinomas. It is therefore important to gain an in depth understanding of the underlying mechanisms of pluripotency, which can be used to direct differentiation of hESCs into specific cell types in a controlled manner.

Highly pluripotent hESC populations would be required to efficiently direct the differentiation into mature cell types of all three germ layers. However, it is not yet well understood how ESCs maintain their pluripotency. Due to the propensity of hESCs to spontaneously differentiate in culture it remains challenging to preserve wholly pluripotent populations of cells.

Spontaneous differentiation is a common unwanted feature of hESC culture and therefore it is important to refine culture conditions to supress differentiation and maintain hESCs as pluripotent cell populations. Nevertheless, studying hESC differentiation and how they might be influenced by certain treatments and culture conditions provides insights into the mechanisms regulating pluripotency/loss of pluripotency. This may help to further improve hESC culture conditions.

Once hESCs commit towards differentiation, they can develop into any cell type of the three germ layers; endoderm, mesoderm and ectoderm. Typically demonstrated in the formation of embryoid bodies (EBs), which are 3D spheroids that comprise distinct markers specific to each of the three germ layers such as ζ-globin for mesoderm, the neuronal marker neurofilament-68Kd for ectoderm and α-fetoprotein for endoderm development (Keller, 1995; Itskovitz-Eldor *et al.*, 2000; Xu *et al.*, 2002; Segev *et al.*, 2004). Itskovitz-Eldor et al. (2000) were the first to show the developmental potential in hESCs using EB rather than the formation of teratomas by demonstrating the gene expression of hematopoietic cells, myocardial cells, neuronal cells and endodermal cells within EBs (Itskovitz-Eldor *et al.*, 2000).

Pluripotent hESCs have a shortened G1 cell cycle phase for maintaining pluripotency and a high rate of proliferation (White and Dalton, 2005; Becker *et al.*, 2006; Kapinas *et al.*, 2013). If the G1 phase is prolonged, hESCs will lose their pluripotent state and start differentiating (Filipczyk *et al.*, 2007; Calder *et al.*, 2012). The earliest differentiation to occur following G1 extension progresses through endodermal and mesodermal

differentiation followed by neuroectodermal commitment in a later stage of G1 (Sela *et al.*, 2012; Pauklin and Vallier, 2013).

Contrary, all pluripotency factors are constitutively supressing differentiation but their overexpression directs ESCs towards lineage commitment (Reviewed by Young 2011; Jaenisch & Young 2008; Silva & Smith 2008). In hESCs each pluripotency factor OCT4, SOX2 or NANOG represses mainly embryonic cell fates and since their interaction towards differentiation is uncoupled each of them can control specific cell fates (Z. Wang *et al.*, 2012a). NANOG for example, was shown to be involved in preventing hESCs to differentiate into extraembryonic lineages such as endoderm and trophectoderm (Hyslop *et al.*, 2005) and other studies showed that Activin/Nodal are positively regulating NANOG expression blocking neuroectodermal lineage commitment by FGF signalling and therefore maintaining pluripotency (Xu *et al.*, 2008; Vallier *et al.*, 2009; Greber *et al.*, 2010; Z. Wang *et al.*, 2012a). However, if NANOG is overexpressed hESCs start differentiating into the mesendodermal lineage (Teo *et al.*, 2011; Yu *et al.*, 2011). As NANOG but also SOX2 and OCT4 are able to regulate the expression of Eomesodermin (Eomes), a T-box transcription factor of definitive endoderm, Eomes is subsequently up-regulated and interacts with SMAD2/3 causing hESCs to differentiate towards definitive endoderm (Teo *et al.*, 2011).

Additionally, there are several factors highly enriched at lineage “super-enhancers” (Tsankov *et al.*, 2015). Enhancers usually increase the probability of gene transcription and super-enhancers are multiple enhancers that interact with numerous transcription factors and proteins to control gene expression. Hence, the core transcription factors of pluripotency not only bind to hESC super-enhancers they also bind to specific lineage super-enhancers (Tsankov *et al.*, 2015). For example, Gata4 and SMAD1 in mesoderm and OTX2 is important in neuronal regulation in ectoderm enhancers (Vernay, 2005; Tsankov *et al.*, 2015). Eomes, Brachyury, SOX2, OCT4, NANOG and OTX2 are also found at mesendoderm enhancers (Tsankov *et al.*, 2015).

Over recent years deeper insights into the transition from pluripotent stem cells to differentiated cells have been made. Thus it is emerging that hESCs and mESCs are differentially organised as the expression of OCT4, SOX2 and NANOG seem to have different requirements in the maintenance of pluripotency in both, hESCs and mESCs (Boyer *et al.*, 2005; Ivanova *et al.*, 2006; Brons *et al.*, 2007; Tesar *et al.*, 2007; Kunarso *et al.*, 2010; Z. Wang *et al.*, 2012a). For example, despite the sequence homology between mice and human when the binding profiles/locations of OCT4 and NANOG between mESCs and hESC were compared only 5% homology was found (Kunarso *et al.*, 2010). This shows that mESCs and hESCs are not entirely conserved in their

regulatory networks which underpins the importance of studies in the relevant species as well as it demonstrates the plasticity of the core transcription network of ESCs (Kunarso *et al.*, 2010).

Differentiation studies of ESCs show that specific markers are expressed upon lineage commitment and are beneficial for examining the stem cell state. For example, high expression of OCT4 without BMP4 in hESCs allows self-renewal but also promotes differentiation to mesoderm. In contrast, low OCT4 levels without BMP4 promote differentiation to neuroectoderm (marker expression such as PAX6 and ZIC1) but with BMP4 promote differentiation to extra-embryonic ectoderm (marker expression such as CDX2, HAND1, GATA3, TFAP2A, KRT7) and primitive endoderm (markers such as SOX7, GATA6, GATA4) (Z. Wang *et al.*, 2012b). In the same study, only SOX2 seemed to be non-essential for self-renwal due to compensation with SOX3, however when both were depleted differentiation towards mesoderm and definitive endoderm was observed (Z. Wang *et al.*, 2012a).

Brachyury– a T-box transcription factor - is one of the most frequently used and earliest differentiation markers of mesodermal/endodermal differentiation in ESCs as both germ layers are derived from the primitive streak (Murry and Keller, 2008; Papaioannou, 2014). Recently, in hESCs Brachyury has been shown to be essential for mesodermal lineage commitment while interacting with BMP4 and SMAD1 but Brachyury is not essential for endodermal cell lineages (Faial *et al.*, 2015). Strikingly, Brachyury seems to have some kind of interaction with OCT4 in respect of co-regulating genes which they both have in common as underpinned by Chip-seq data (Spitz and Furlong, 2012; Voss and Hager, 2013; Tsankov *et al.*, 2015). This is perhaps not too surprising as OCT4 was shown to have lineage specifying roles outside the regulation of pluripotency (Loh and Lim, 2011; Thomson *et al.*, 2011; Z. Wang *et al.*, 2012a)

1.2 Effect of environmental oxygen on hESCs

Oxygen is one of the most essential molecules for nearly every living creature and one of the most abundant elements on our planet. Under standard conditions two oxygen atoms bind to form a gas, dioxygen (O_2), which typically comprises 20.8% of the air (Cook and Lauer, 1968).

Increased oxygen levels can be toxic to many tissues thus leads to cell and DNA damage because of the accumulation of reactive oxygen species (ROS) (Guérin, Mouatassim and Ménézo, 2001). ROS are reactive molecules such as oxygen ions (O_2^-), peroxides (H_2O) and hydroxyl radicals (OH^-), which occur as part of normal oxygen metabolism. ROS generation can also occur in the process of energy conversion, such as adenosine triphosphate (ATP) production. Multiple antioxidant enzymes are present in oocytes, embryos and oviducts to protect the embryo against ROS (Guérin, Mouatassim and Ménézo, 2001). A correlation has been observed between higher concentrations of ROS and increased apoptosis (Yang *et al.*, 1998), suggesting that environmental culture conditions (including oxygen levels) during IVF and embryo transfer should aim to mimic the *in vivo* conditions as closely as possible. Moreover, decreased levels of ROS have been observed in mESCs when cultured under 5% compared to 20% oxygen (Goto *et al.*, 1993), suggesting that reducing the atmospheric oxygen level during ESC culture might be beneficial.

1.2.1 Oxygen concentration in pre-implantation embryos and hESC culture

Mammalian tissues differ in their oxygen levels and requirements. The oxygen concentration in *in vivo* adult tissues is much lower than atmospheric levels, for example, tissues such as brain, eye and bone marrow reside in between 0.5% to 7% oxygen. Bone marrow (Chow *et al.*, 2001) and renal papilla in the kidney (Oliver *et al.*, 2004) both have stem cell populations which reside in low oxygen concentrations.

hESCs are commonly cultured and were mostly derived under atmospheric oxygen levels (Thomson *et al.*, 1998; Pera, Reubinoff and Trounson, 2000; Cowan *et al.*, 2004), termed “normoxia”. Maintaining cells *in vitro* under atmospheric air is certainly more convenient, however these culture conditions result in oxygen concentrations much greater than those *in vivo*. *In vivo*, rhesus monkey, hamster, mouse, rabbit and human pre-implantation embryos develop in very low oxygen concentrations ranging from 1.5% to 8.7% oxygen (Auerbach and Brinster, 1968; Fischer and Bavister, 1993; Dumoulin *et al.*, 1999). Studies using low oxygen concentrations (1-10% oxygen) showed improved embryo development from mammals such as mice, cattle, sheep, rabbits and hamsters

(Auerbach and Brinster, 1968; Mitchell and Yochim, 1968; Fischer and Bavister, 1993). *In vitro* culture at a reduced oxygen concentration was also found to improve pre-implantation development of the human embryo (Dumoulin *et al.*, 1999). Strikingly, the global pattern of gene expression of mouse embryos cultured at 5% than at 20% oxygen was observed to be more similar to in vivo embryos (Rinaudo *et al.*, 2006). In addition, a study that compared the effect of 5% and 20% oxygen concentration on the development of IVF embryos in a sibling oocyte study showed higher implantation, pregnancy and live birth rates as well as better quality embryos when 5% oxygen was used during embryo incubation (Kasterstein *et al.*, 2013).

But what are the consequences of lower oxygen conditions on ESCs in culture? hESCs do not appear to grow differently in hypoxia compared to normoxia, but strikingly, they grow with fewer spontaneous cell differentiations in hypoxic conditions (Ezashi, Das and Roberts, 2005).

The beneficial effects of culturing hESCs under low oxygen levels are: less indication of morphological differentiation of hESC colonies, better maintenance of hESC colonies in the pluripotent state (which necessitates less passaging) and a higher rate of EB formation with better attachment (Ezashi, Das and Roberts, 2005). hESCs cultured under hypoxia compared to normoxia contain also less spontaneous cell differentiation (Ezashi, Das and Roberts, 2005). Furthermore, an increase of stem cell markers such as OCT4, SOX2 and NANOG (Forristal *et al.*, 2010) is observed when cultured in hypoxia, as well as an increased cell proliferation, less spontaneous cell differentiation (Ezashi, Das and Roberts, 2005; Westfall *et al.*, 2008; Forristal *et al.*, 2010) and decreased chromosomal aberrations (Forsyth *et al.*, 2006). Continuous culture of hESCs under hypoxic conditions also enhances self-renewal (Westfall *et al.*, 2008; Zachar *et al.*, 2010). The first hESC line to be derived under a low oxygen concentration was in 2010 (Lengner *et al.*, 2010). Strikingly, hESCs are able to display two different developmental stages, naïve and primed pluripotency. These two stages can greatly vary according to their culture conditions. Thus, these low oxygen-derived hESCs prevented the precocious X chromosome inactivation (Lengner *et al.*, 2010). Thus showing a more immature state at 5% oxygen concentration than derived under atmospheric oxygen concentration and therefore displaying “more” pluripotent characteristics. The low oxygen concentration is possibly enhancing a more euchromatic state as the gene responsible for X chromosome inactivation (XIST) is highly methylated and therefore not expressed (Sun, Deaton and Lee, 2006; Lengner *et al.*, 2010). Culture under 5% oxygen also maintains OCT4, SOX2 and NANOG in a euchromatic state while under atmospheric conditions a heterochromatic state is maintained (Petruzzelli *et al.*, 2014).

These are all features of improved stemness, suggesting that culturing hESCs under reduced oxygen concentration is beneficial. Indeed, ESCs from mouse blastocysts that were derived in physiological oxygen concentrations showed increased proliferation, suggesting a reduction in oxidative stress (Wang, Thirumangalathu and Loeken, 2006). Similar results were revealed for iPSCs, where an improved stemness and cell quality were reported when cultured under a low oxygen concentration (Guo *et al.*, 2013). Despite these beneficial effects of culturing hESCs at low oxygen levels controversy remains since it was reported in 2009 that culturing hESCs at 5% oxygen does not show any beneficial effect as assessed by morphology, apoptosis and gene expression profiles (H.-F. Chen *et al.*, 2009). Chen et al. (2009) did not observe statistically significant differences between cells cultured at the two different oxygen levels based on gene expression investigations for pluripotency markers and differentiation genes such as OCT4 and NANOG or DESMIN and NESTIN respectively, but nevertheless concluded that the colonies appeared better under hypoxia. So far little is known about why a hypoxic environment might be better for hESCs culture. However, hypoxia most closely mimics the natural *in vivo* environment of ESCs, and it is important that *in vitro* conditions are as close as possible to their physiological environment in order to prevent oxidative stress. To overcome contradictory findings and improve hESCs culture *in vitro* further investigations are necessary.

1.2.2 The hypoxic response regulated by hypoxia inducible factors

Hypoxia inducible factors (HIFs) are transcription factors that are regulated by cellular oxygen concentration. In hypoxia, HIFs are stabilised, allowing them to bind to hypoxia-response elements (HRE) and further regulate the expression of over 200 genes (Semenza, 2004; Smith, Robbins and Ratcliffe, 2008).

The first HIF to be discovered was HIF-1, found in mammalian cells cultured under hypoxia (Semenza and Wang, 1992). HIF1 is thought to be a master regulator of oxygen homeostasis (Iyer *et al.*, 1998), having a role in the regulation of erythropoiesis, angiogenesis and glycolysis (Jiang *et al.*, 1997; Semenza, 2004). Two other HIFs have been identified to date: HIF2A (*EPAS1*), a protein similar to HIF1A but not expressed in all cell types (Park *et al.*, 2003) and HIF3A (*IPAS,* inhibitory Per/Arnt/Sim domain) (Gu *et al.*, 1998). Little is known about HIF3A but it is thought to bind to and negatively regulate HIF1A (Makino *et al.*, 2001, 2002).

Under normoxic conditions, the oxygen sensitive HIF-1α subunit becomes hydroxylated via the prolyl hydroxylase domain (PHD), which is dependent upon iron and oxygen. Hydroxylated HIF-1α then binds to the von Hippel-Lindau tumour suppressor protein (VHL) and the whole complex is ubiquitinated and degraded by the proteasome. Under hypoxia, HIF-1α is not hydroxylated and can bind to the constitutively expressed HIF-1β subunit in the nucleus and form heterodimers (Kallio *et al.*, 1998). The same mechanism applies to HIF-2α, which is also able to bind to HIF-1β (Tian, McKnight and Russell, 1997). These HIFα/HIFβ heterodimers are additionally bound by P300/creb-binding domain (CBP) which then leads to transcriptional activation of HIF target genes by binding to the hypoxia response element (HRE) of oxygen sensitive genes (Figure 7) (Wang *et al.*, 1995; Smith, Robbins and Ratcliffe, 2008).

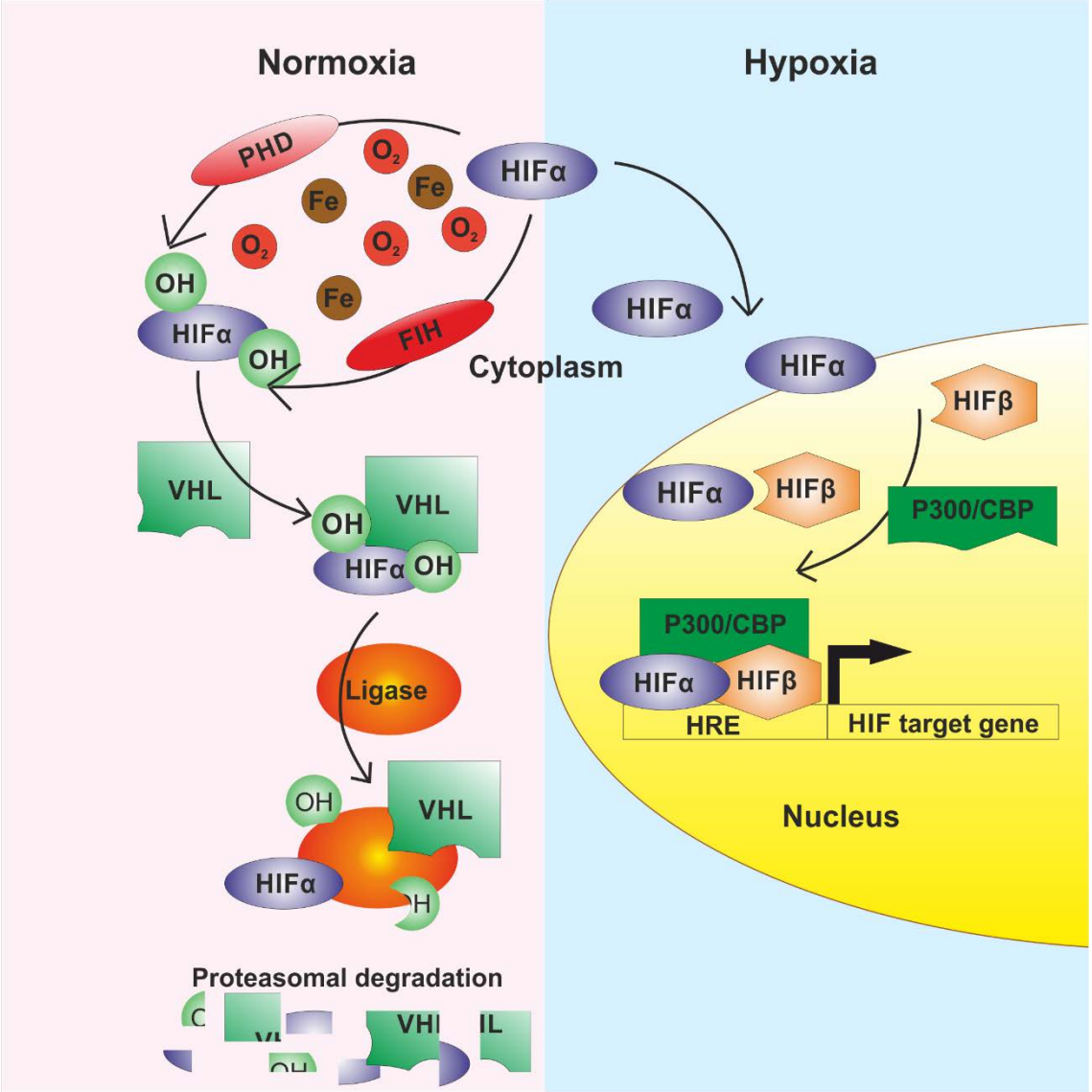

Figure 7: Degradation or stabilisation of the HIFα subunit

Under normoxia HIFα becomes hydroxylated via the prolyl hydroxylase domain (PHD) or factor inhibiting HIF (FIH) which are dependent upon iron and oxygen. The hydroxylated HIF1α binds to the von Hippel-Lindau tumour suppressor protein (VHL) and is then ubiquitinated by ubiquitin ligase and degraded by the proteasome. In contrast, when oxygen is limited, HIFα cannot be hydroxylated, is stabilized and translocates to the nucleus where it binds to the HIFβ subunit and the transcriptional co-activator P300/ creb-binding domain (CBP). The resulting complex can then interact with the hypoxia response element, initiating the transcription of HIF target genes.

Additonally, a negative regulator of HIF1α was identified, the factor inhibiting HIF1 (FIH1 or HIF1AN) (Mahon, Hirota and Semenza, 2001). HIF1AN is able to interact with HIF1α and with the VHL, therefore both interactions are negatively regulating the expression of HIF1A also in an oxygen-dependent manner (Mahon, Hirota and Semenza, 2001). When oxygen is available, HIF1AN is able to hydroxylate the C-terminal activation domain of HIF1A repressing the interaction of HIF1A with co-activators such as CBP (Lando *et al.*, 2002).

The impact of HIFs on pluripotency regulation in hESCs cultured under hypoxic conditions was examined by Forristal *et al.* (2010). HIF1A is degraded in hESCs cultured under hypoxia after approximately 48h whereas HIF2A is stabilised under long-term culture and translocates from the cytoplasm to the nucleus (Forristal *et al.*, 2010). HIF3A was found to regulate HIF1A and HIF2A but it is HIF2A that is mainly involved in regulating hESC pluripotency and proliferation in hypoxia (Forristal *et al.*, 2010).

HIF2A (EPAS1) and HIF3A were significantly up-regulated in haematopoietic stem cells under hypoxic compared to normoxic conditions (Takubo *et al.*, 2010). It has also been shown that these factors play a key role in maintaining and regulating hESC pluripotency and proliferation (Forristal *et al.*, 2010). Indeed, HIFs induce a hESC-like transcriptional program in several cancer cell lines under hypoxia (Mathieu *et al.*, 2011). HIF2α also increases the expression of stem cell markers such as SOX2, NANOG and OCT4 in hESCs (Covello *et al.*, 2006; Forristal *et al.*, 2010) by binding directly to the HREs in the proximal promotors of these genes (Petruzzelli *et al.*, 2014). This further supports physiological low oxygen concentrations in culture systems of hESCs. However, the exact mechanisms regulating HIF expression to support hESCs pluripotency under hypoxia remain to be elucidated.

1.3 Energy metabolism of hESCs

After demonstrating that HIFs play a key role in maintaining and regulating hESC pluripotency and proliferation (Forristal *et al.*, 2010), perhaps it is not surprising that HIF1A has several target genes important for glucose uptake and glycolysis (Hu *et al.*, 2003). Further investigations revealed that metabolism plays a fundamental role in human pre-implantation embryos in regulating their phenotype and developmental potential (Houghton *et al.*, 2002).

Metabolism is essential for Adenosine triphosphate (ATP) production and can be generated through oxidative phosphorylation or glycolysis. In glycolysis, ATP is generated through the conversion of glucose to pyruvate. Many stem cell types such as hESCs and iPSC produce their energy through anaerobic glycolysis (Prigione *et al.*, 2010; Folmes *et al.*, 2011; Varum *et al.*, 2011; Zhang *et al.*, 2011; Zhou *et al.*, 2012). *In vivo*, stem cells usually reside in areas of low oxygen concentration making glycolysis an evolutionary adaption for energy production (reviewed by Mohyeldin et al. 2010 and Uckac et al. 2014). Additionally, glycolysis has been suggested to minimise the accumulation of ROS which might further promote stemness (Jang and Sharkis, 2007). This is supported by the ICM of mice blastocyst being completely glycolytic, compared to the differentiated trophectoderm where just 55% of the glucose consumed could be accounted for by lactate production (Hewitson and Leese, 1993). The trophectoderm also has a higher proportion of mitochondria with a higher consumption of oxygen compared to the ICM (Houghton, 2006). Thus showing that the ICM is metabolically quiescent whereas the trophectoderm is metabolically active.

That hESCs rely mainly on glycolysis is further supported by their immature mitochondria limiting the amount of oxygen consumed (Sathananthan and Trounson, 2000; Varum *et al.*, 2009; Forristal *et al.*, 2013). hESCs cultured at 5% oxygen take up significantly more glucose, less pyruvate and produce more lactate compared to those maintained at 20% oxygen (Forristal *et al.*, 2013). The higher rate of glycolysis at low oxygen concentration seems to be regulated by GLUT3, an important glucose transporter which is involved in regulating OCT4 expression (Christensen, Calder and Houghton, 2015). It has also been suggested that the expression of high levels of hexokinase II and an inactive pyruvate dehydrogenase (PDH) complex could be a mechanism through which hPSCs maintain a high level of glycolysis (Varum *et al.*, 2011).

The glucose up-take of cells is also regulated through pyruvate kinases, also known as pyruvate kinase muscle isoenyzmes (PKM), which are glycolytic enzymes that catalyse the final step of glycolysis, where phosphoenolpyruvate and adenosine-diphosphate

(ADP) are converted to pyruvate and adenosine-triphosphate (ATP). PKM exists in two different splice forms, PKM1 and PKM2, with alternative terminal exons. PKM1 consists of exons 1-9 and PKM2 consists of exons 1-8 & 10 (Noguchi, Inoue and Tanaka, 1986). According to Gupta and Bamezai (2010), PKM2 possesses multi-functional roles in a variety of pathways (Gupta and Bamezai, 2010). Interestingly, in the generation of iPSCs up-regulated HIF1A expression using small molecules caused elevated PKM2 expression levels thus resulting in increased glycolysis (Prigione *et al.*, 2014). PKM2 was also observed to have a greater expression in hESCs cultured at 5% compared to those maintained at 20% oxygen concentration (Christensen, Calder and Houghton, 2015). OCT4 and PKM2 are known to interact, and the transcriptional activity of OCT4 is positively regulated by PKM2 as investigated in human cervical cancer cells (HeLa) and monkey fibroblast-like cells (COS7), suggesting PKM2 functions not only as an enzyme, but also as a transcription factor (J. Lee *et al.*, 2008). Recent investigations also suggest a transcriptional role for PKM2 in regulating OCT4 in hESCs cultured under low oxygen concentrations and thus supporting the hypoxic culture of hESCs (Christensen, Calder and Houghton, 2015). This study showed that PKM2 displays a nuclear localisation and therefore is likely to be acting as transcription factor rather being involved in glycolysis which is located in the cytoplasm (Christensen, Calder and Houghton, 2015). In summary, these studies demonstrate the importance of understanding the interplay between metabolism and hESC maintenance and thus augments the knowledge of how pluripotency is regulated.

.

1.4 Role of microRNAs as multipurpose regulators

1.4.1 Overview of miRNAs

MicroRNAs (miRNAs) are small endogenous (20-25 nucleotides (nt) of length) non-coding single stranded RNAs (Pasquinelli and Ruvkun, 2002) that are multipurpose regulators of gene expression, exerting their effects in several processes such as development, proliferation, haematopoiesis, apoptosis and stem cell regulation (Lee, Feinbaum and Ambros, 1993; Houbaviy, Murray and Sharp, 2003). hESCs, as earlier described, have the potential to develop into any cell type of the human body. A complex network of gene regulation is required to maintain hESC pluripotency but also to supress and activate very specific gene sets to become one of each of the 200 different cell types in the human body. In fact, all cells of the human body have the exact same genetic information thus miRNAs play an important role in fine tuning the differential expression of genes in every different cell type. The existence of stem cell-specific miRNAs was first described in 2003, where miRNAs identified in undifferentiated and differentiated mESCs were found to be important for the regulation of pluripotency (Houbaviy, Murray and Sharp, 2003).

Since mature miRNAs are very short in length and they only need to bind with a 6-8 nt long seed sequence, they can potentially bind to hundreds of mRNAs to prevent their translation. Investigating and identifying these small regulatory molecules will advance the understanding of how hESCs pluripotency is regulated.

1.4.2 The biogenesis and mechanism of miRNAs

Figure 8 describes the following process of miRNA biogenesis: MiRNA genes are found in intergenic regions as well as within defined transcription units (both exons and introns), and in both orientations (sense and antisense). They are transcribed by RNA polymerase II to precursor transcripts called primary miRNAs (pri-mRNAs) (Lagos-Quintana *et al.*, 2001; Mourelatos *et al.*, 2002). Pri-miRNAs are further processed in the nucleus by Drosha and Pasha (known as the microprocessor protein complex) into the intermediate precursor miRNA (pre-miRNA) form, which has a stem-loop structure and is approximately 70 nt long. Pre-miRNAs are then translocated by the protein exportin5 into the cytoplasm. This is an active energy-dependent transport, dependent on RanGTP but sequence-independent (Bohnsack, Czaplinski and Gorlich, 2004). However, miRNAs can also be transcribed from small introns, which are called “mirtrons”. These mirtrons are not processed by the microprocessor protein complex, instead they undergo a splicing process to reach the pre-miRNA form and are then translocated into the cytoplasm in the same way by exportin5. Pre-miRNAs are further processed by Dicer (an RNase III-like enzyme) into mature miRNAs, which are only about 20-25 nt long, and are then bound by RNA-induced silencing complexes (RISCs, that contain proteins from the Argonaute-subfamily (AGOs)). The RISC complex guides one strand to the 3’ untranslated region (UTR) of the target mRNA and represses its translation (Doench, Petersen and Sharp, 2003; Zeng, Yi and Cullen, 2003).

Since the targeting occurs with just partial complementarity the mRNA target is not directly cleaved by AGO2 only, instead the AGO protein requires additional binding of a GW182 protein, a polyadenylation binding protein (PABP) and a deadenylation complex to remove the poly(A) tail which then leads to mRNA target degradation (Braun, Huntzinger and Izaurralde, 2012, 2013). If not degraded, the mRNA can be translationally repressed and stored in cytoplasmic P-bodies or re-enter the translation pathway (Bagga *et al.*, 2005).

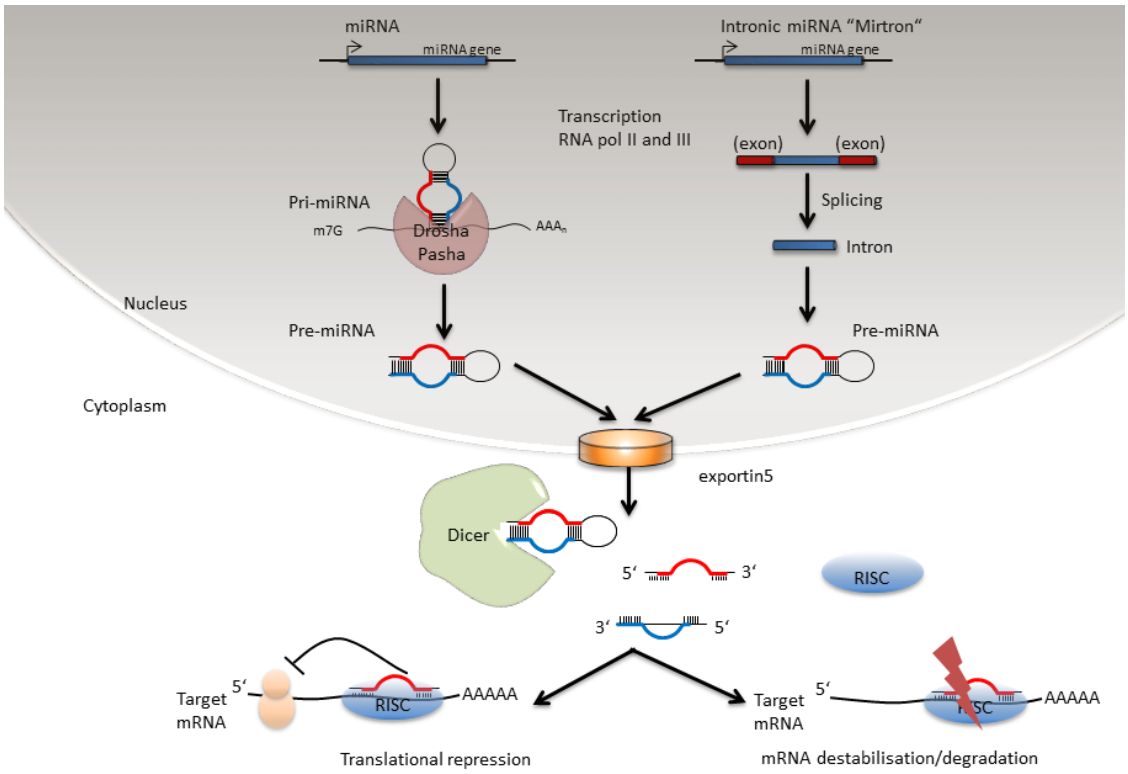

Figure 8: miRNA biogenesis

miRNAs are derived from pre-cursor transcripts (pri-miRs) or from intronic miRNA genes (mirtrons). Only pri-miRs necessitate further processing via Drosha and Pasha into pre-miRNAs whereas mirtrons are spliced into pre-miRs. These pre-miRs are transported by Ran-GTP and exportin5 into the cytoplasm where they are processed by Dicer into mature miRNAs and bound by RISC. This complex can then bind the 3'UTR of target mRNA and leads to translational repression or mRNA degradation.

Target recognition between mature miRNAs and mRNA occurs with a very short 6-8 nt sequence region called the “seed-sequence”. The seed sequence is located close to the 5’ end of the mature miRNA (Grimson *et al.*, 2007). The rest of the miRNA sequence does not require an entire binding to their target mRNA in order to have an effect. The imperfect match to their target mRNA is the reason why one miRNA can affect the expression of multiple different genes thus exerting an extremely versatile way of miRNA-mRNA modulations that requires complex algorithms to predict.

As the process of miRNA discovery has occurred, so the nomenclature to describe miRNAs has also evolved. miRNAs can now be grouped into either clusters or families. A cluster is a group of miRNAs expressed by the same primary transcript and are therefore transcriptionally co-regulated. In contrast, a family is a group of miRNAs with the same seed-region. MiRNAs with the same seed sequence will also more likely bind the same mRNA targets (Bartel, 2009; Friedman *et al.*, 2009).

1.4.3 Mechanisms of how miRNA mediate inhibition/degradation of protein translation

MiRNAs have been intensively studied over the last few years and more and more different target mechanisms have been discovered as well as target sites that are not only in the 3'UTR but also in the 5'UTR and open reading frame/coding sequence (ORF/CDS) (Tay *et al.*, 2008; Vogel *et al.*, 2010; Roberts, Lewis and Jopling, 2011). Besides, while plant miRNAs mostly target with near perfect complementarity to their target genes (Jones-Rhoades, Bartel and Bartel, 2006) animal miRNAs do not as evidenced by functional interactions with imperfect base pairing (Lewis, Burge and Bartel, 2005; Lim *et al.*, 2005).

The fact that the miRNA seed is only a short sequences of 6-8 nt should make miRNA target prediction straightforward. Unfortunately, the matching 6-8 nt can occur very frequently in the genome and the feature of pure base-pair complementarity contributes to a high rate of false-positive and false-negative miRNA-mRNA interactions (Krek *et al.*, 2005; Cloonan *et al.*, 2008; Mourelatos, 2008). For improvement in target recognition, many bioinformatic tools are available that incorporate additional factors than just sequence complementarity into their algorithms such as sequence conservation, how accessible the target site is (Kertesz *et al.*, 2007) and if additional binding outside the seed sequence occurs. Some of the current knowledge about miRNA-mRNA interaction and the challenges for target identification will be discussed.

Originally, miRNAs were thought to target only with their 5' sense-strand or guide-strand (-5p) and that the 3' anti-sense or passenger-strand (-3p) was degraded. However, recent studies found that the passenger-strand of miRNA is no longer believed to be non-functional (Stark *et al.*, 2008; Yang *et al.*, 2011; Ohanian *et al.*, 2013). Additionally, further alternative modes of microRNA interaction have been revealed such as imperfect seed-pairing. The miRNA "seed" sequence is defined from nucleotide-position 2-7 and important for target recognition (Lewis *et al.*, 2003; Lai, Tam and Rubin, 2005). The seed-sequence may be functional with only 6 but also up to 8 base pairing, that are called 6mer, 7mer and 8mer binding (Figure 9). These 6mer-8mers represent canonical site types which are further differentiated as to whether they are conserved or non-conserved across species. MiRNAs no longer require seed-pairing only, miRNAs that usually do not target their mRNA with the seed sequence to 100% are called non-canonical miRNAs. Non-canoncial binding can be extensively enhanced if they comprise additional complementarity sites towards the 3' miRNA end, also called 3'compensatory sites (Vella *et al.*, 2004; Yekta, Shih and Bartel, 2004). Notwithstanding, the current literature is

relatively controversial about the effectiveness of non-canonical sites (Brodersen and Voinnet, 2009; Loeb *et al.*, 2012; Agarwal *et al.*, 2015; Seok *et al.*, 2016).

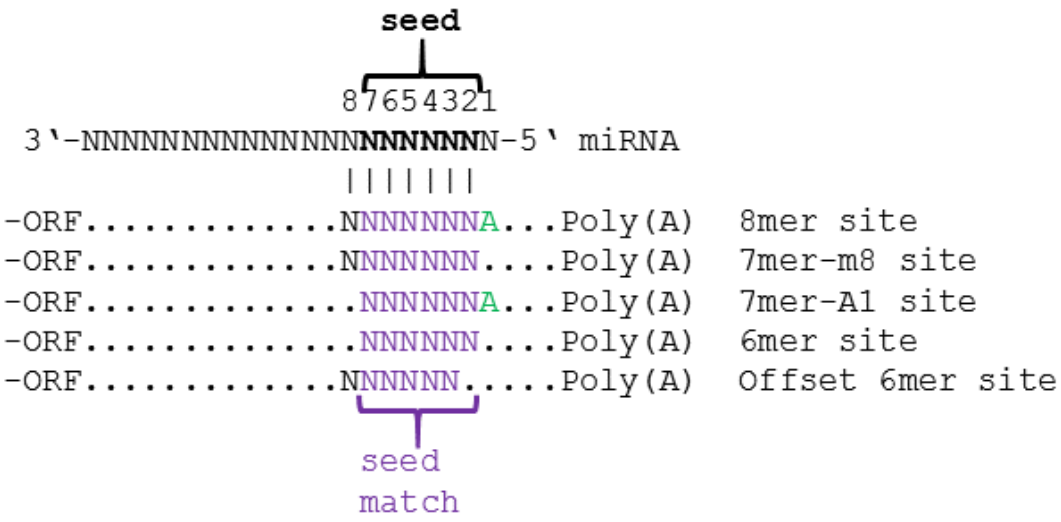

Figure 9: Conventional miRNA targeting showing canonical site types
8mer stands for seed match+A at position 1 (A1)+match at positon 8 (m8); 7mer-m8 stands for seed match +m8; 7mer-A1 stands for seed match+A1; 6mer stands for seed match 2-7; Offset 6mer stands for seed match 3-7 plus match at position 8

Furthermore, miRNA binding within the seed-sequence can have mismatches, bulges or GU wobbles (Miranda *et al.*, 2006; Kertesz *et al.*, 2007). It is possible that miRNAs do not bind with their seed sequence thus exerting functionality through binding with their central region with 11 or 12bp normal Watson-Crick base-pairing from position 4-15 or 5-15 (Shin *et al.*, 2010). All these options result in many different possibilities of binding combinations. And most prediction algorithms that include non-perfect matches lose accuracy (Grimson *et al.*, 2007). However, some of these combinations were recently studied by a group that was looking into 54 miRNA-target site-types with the outcome that miRNAs can have functional non-conventional binding sites with their target mRNA that leads to reduced protein levels (Ghosal *et al.*, 2016).

1.4.4 Role of miRNAs in ESCs

The first discovery of a pool of ESC-specific miRNAs for either maintaining stemness or for differentiating ESCs, was made in 2003 (Houbaviy, Murray and Sharp, 2003). Since then, miRNAs have been regarded to affect regulation of the pluripotent state (Houbaviy et al. 2003 and reviewed by Martinez & Gregory 2010). In depth investigations will advance our understanding of how stemness and pluripotency are regulated, and this might enable the development of safe and convenient methods for using hESCs in stem cell therapy.

The earliest studies examining the role of miRNAs in stem cell differentiation knocked out the microprocessor enzymes Dicer and Drosha with the co-factor Di George syndrome critical region gene 8 (DGCR8), an RNA-binding protein, which together are essential for canonical miRNA production. The knock-out exhibited impaired differentiation and proliferation in ESCs, suggesting a key role for miRNAs in these processes (Sinkkonen *et al.*, 2008; Wang *et al.*, 2008; Martinez and Gregory, 2010). DGCR8 studies are more specific to miRNAs, since Dicer is also involved in small interfering RNA (siRNA) pathways (Babiarz *et al.*, 2008). Indeed, further studies revealed an ESC-specific miRNA pool (Sinkkonen *et al.*, 2008; Wang *et al.*, 2008). However, since the core transcription factors SOX2, OCT4 and NANOG are able to bind to miRNA promoters, they alone can activate entire clusters of ESC-specific miRNAs (Card *et al.*, 2008; Marson *et al.*, 2008).

In terms of genomic location, miRNAs are often grouped together in clusters, suggesting that multiple miRNAs are expressed from the same primary miRNA transcript and are therefore transcriptionally co-regulated (Bartel, 2009; Friedman *et al.*, 2009). A very abundant miRNA cluster in mESCs is the miR-290 cluster (Houbaviy, Murray and Sharp, 2003; Houbaviy *et al.*, 2005; Calabrese *et al.*, 2007). The miR-290 cluster has identical or highly similar seed-sequences to the miR-17-92 cluster or miR-302 (Marson *et al.*, 2008) as well as miR-17/19, miR-106b/25, miR-106a/363, miR-302b/367, miR-15b/16 and miR-32 (Gangaraju and Lin, 2009; Wang *et al.*, 2009). These clusters cover nearly three quarters of all miRNAs expressed in undifferentiated ESCs (Marson *et al.*, 2008). Some of these miRNAs have an impact on regulating the ESC cycle for example in mESCs miR-294 and miR-295 repress the cell cycle inhibitor Cdkn1a and in hESCs miR-302a supresses a G1 regulator, Cyclin D1 (Card *et al.*, 2008; Wang *et al.*, 2008) thus promoting in both cases the typically shortened G1-S transition of ESCs (Burdon, Smith and Savatier, 2002; White and Dalton, 2005) and contributing to pluripotency (Gruber *et al.*, 2014).

miRNAs that are expressed in mESCs are mentioned here as they often have a similar genomic organisation to those miRNAs found in hESCs and many of them are conserved across mammals but especially between mouse and human. MiRNAs that are specific for hESCs are miR-302b*, -302b, -302c*, -302c, -302a*, -302a, -302d, -367, -200c, -368, -154*, -371, -372, -373* and miR-373 (Suh *et al.*, 2004). In contrast, the hESC miRNA miR-302a is also expressed in mESCs and ECCs as miR-302 (Houbaviy, Murray and Sharp, 2003; Suh *et al.*, 2004). Later it was also seen, that ECCs have very similar miRNA expression pattern to hESCs, showing several hESCs related miRNAs to be expressed at similar levels (Josephson *et al.*, 2007).

The two clusters miR-302 and miR-371 (Table 1) were shown to be the most abundant miRNAs in hESCs and also showed a high sequence homology, especially in their non-stared mature miRNAs regions. Thus these miRNAs are likely to have the same mRNA targets (Suh *et al.*, 2004). The miR-290 cluster is the mouse homolog to the human miR-302 cluster.

Table 1: Two specific hESC miRNA clusters

miR-302 cluster on Chromosome 4	miR-371 Cluster on Chromosome 19
miR-302b*, -302b, -302c*, -302c, -302a*, -302a, -302d, -367	miR-371, -372, -373*, -373

The abundant miR-290 cluster in mice produces 14 mature miRNAs (Table 2), some of which share the same seed sequence “AAGUGC“ (Houbaviy, Murray and Sharp, 2003; Houbaviy *et al.*, 2005; Landgraf *et al.*, 2007; Lüningschrör *et al.*, 2013). This is the exact same miRNA seed sequence that is also shared between the human miR-302 cluster, chromosome 19 cluster, miR-17 cluster and miR-106a cluster (Houbaviy *et al.*, 2005; Laurent *et al.*, 2008). miRNAs that share the same seed sequence are also grouped together in “families”, as they often bind to the same mRNA targets (Bartel, 2009). Later it was shown, that the miRNA family, that shares the seed sequence “AAGUGC”, also called the ESC-specific cell cycle regulating (ESCC) miRNA family is abundant in mESCs and mEpiSCs/hESCs despite their differing miRNA clusters (Kiezun *et al.*, 2012; Greve, Judson and Blelloch, 2013). mEpiSCs as well as hESCs express high levels of the miR-302-367 cluster whereas the miR-290-295 murine cluster and its homolog cluster miR-372-373 has very low expression levels (Bar *et al.*, 2008; Jouneau *et al.*, 2012). A set of miRNAs, namely miR-302b, miR-372, miR-518b, miR-520b and miR-520c can also help to determine the state of pluripotency as these miRNAs are expressed in hESCs and decline upon differentiation indicating that the highest

expression will occur in cells at the earliest pluripotent state (Ren *et al.*, 2009; Stadler *et al.*, 2010; Ware *et al.*, 2014) Other miRNAs in the miR-290 cluster have different seed sequences but are still highly expressed, whilst others are still expressed but at very low levels in mESCs (Marson *et al.*, 2008). The miR-290 cluster is conserved across many mammals, and homologues such as the miR-371 and miR-512 clusters have been identified in humans (Houbaviy *et al.*, 2005; Lichner *et al.*, 2011).

Table 2: Mature miRNAs produced by the miR-290 cluster in mESCs

Same seed sequence "AAGUGC"	Differences in their seed sequence but highly expressed	Very low expression
miR-290-3p	miR-290-5p	miR-293*
miR-291a-3p	miR-291a-5p	miR-294*
miR-291b-3p	miR-291b-5p	miR-295*
miR-292-3p	miR-292-5p	
miR-294	miR-293	
miR-295	miR-293*	
	miR-294*	
	miR-295*	

miRNAs seem to play more and more important roles in controlling differentiation and maintaining pluripotency in ESCs. There are a number of miRNAs that target *NANOG*, *SOX2* and *OCT4* and therefore repress their translation which then leads to differentiation. Those miRNAs are, for example, miR-296, miR-134 and miR-470 that target the CDS of Nanog, Sox2 and Oct4 in mESCs (Tay *et al.*, 2008). Similar observations were made with miR-200c, miR-203 and miR-183 targeting *Sox2* and *Klf4* (Wellner *et al.*, 2009). In contrast, miR-145 was reported to repress *OCT4*, *SOX2* and *KLF4* in hESCs (Xu *et al.*, 2009). Interestingly, in mESCs the three pluripotency factors OCT4, SOX2, NANOG plus TCF3 are not just targets of miRNAs in turn they can also activate the promotors of miR-290-295 and miR-302-367 (Marson *et al.*, 2008). Similar observations were made in hESCs where the expression of miR-302a is also regulated by OCT4/SOX2 which can both bind to the promotor region of miR-302a (Card *et al.*, 2008). MiR-145 has also been identified as a direct target of OCT4, SOX2 and NANOG leading to their repression in hESCs (Xu *et al.*, 2009). SMAD4, an important protein in the TGF-ß pathway promoting pluripotency that is directly targeted by miR-125 was found to initiate differentiation into the neural lineage (Boissart *et al.*, 2012). In contrast, due to differentiation and therefore down-regulation of those pluripotency genes, self-renewal becomes inhibited – miRNAs such as the miR-290 cluster are down-regulated and not detectable in adult mouse tissues (Houbaviy, Murray and Sharp, 2003). MiRNAs

like the let-7 miRNA family, are then up-regulated and therefore inhibit self-renewal. This process is usually inhibited by LIN28 in ESCs, a miRNA binding protein that binds to let-7 and prevents its maturation. LIN28 is highly expressed in both mESCs and hESCs and has been also shown to enhance the efficiency of iPSC creation from human fibroblasts (Yu *et al.*, 2007).

Another example of cell fate regulation is the orphan nuclear receptor, NR2F2 which activates neuroectoderm lineage commitment of hESCs (Lüningschrör *et al.*, 2013). In undifferentiated hESCs, NR2F2 is inhibited by OCT4 and additionally targeted by miR-302, an interaction which targets both transcriptional and post-transcriptional regulation (Lüningschrör *et al.*, 2013). OCT4, SOX2 and NANOG are positively regulating the expression of the miR-302/367 cluster from which miR-302 is generated thus creating a feedback loop with NR2F2 (Lüningschrör *et al.*, 2013). The same miR-302/367 cluster has also been shown to promote reprogramming into iPSCs (Anokye-Danso *et al.*, 2011a; Miyoshi *et al.*, 2011; S.-L. Lin *et al.*, 2011). Furthermore, the miRNAs miR-292-3p and miR-294 are important miRNAs that are only expressed in pluripotent hESCs and iPSCs as their expression decreases once cells commit towards differentiation (Zhang *et al.*, 2016).

1.4.5 The hypoxic regulation of miRNAs

hESCs were also shown to benefit from low oxygen concentrations and hypoxia has been shown to have an influence on the expression profile of miRNAs (Kulshreshtha *et al.*, 2007). These hypoxia induced miRNAs are termed hypoxamirs (Chan and Loscalzo, 2010; Loscalzo, 2010). Despite varying conditions such as cellular and physiological differences, there are several specific hypoxamirs consistently either up- or down-regulated in mammalian cells (Kulshreshtha *et al.*, 2007). Some hypoxamirs support the expression of HIFs and thus the hypoxic adaption (Loscalzo, 2010; Greer *et al.*, 2012; Semenza, 2012). For instance, miR-210 has been shown to be an important regulator in hypoxia and is consistently up-regulated under hypoxic conditions and regulated by HIFs which bind to the HRE on the proximal miR-210 promoter (Crosby *et al.*, 2009; Huang *et al.*, 2009; Z. Zhang *et al.*, 2009; Huang, Le and Giaccia, 2010). miR-210 is also repressing a HIF1A regulating enzyme, glycerol-3-phosphate dehydrogenase 1-like, thus miR-210 is indirectly stabilising HIF1A expression (Kelly *et al.*, 2011). In addition, the hypoxamir miR-210 is targeting and inhibiting proteins involved in the mitochondrial respiration which supports the shift towards glycolysis (Chan *et al.*, 2009; Favaro *et al.*, 2010). This is further supported by HIFs that are positively regulating metabolic enzymes of the glycolytic energy production such as pyruvate dehydrogenase kinase-1 (PDK1) and lactate dehydrogenase A (LDHA) and thus inhibits the pyruvate conversion for

entrance into the citric acid cycle and increases the pyruvate to lactate conversion respectively (Semenza *et al.*, 1996; Seagroves *et al.*, 2001; Kim *et al.*, 2006). A direct interaction has been observed for miR-199a and HIFα (Rane *et al.*, 2009). However, miR-199a belongs to the repressed hypoxamirs and thus rather targeting HIFα is supporting the expression of HIF regulated genes (Rane *et al.*, 2009). Additionally, several hypoxia-related miRNAs were identified in studies, thus connecting gene expression control and stress such as hypoxia (Kulshreshtha *et al.*, 2007, 2008; Camps *et al.*, 2008). Furthermore, hypoxia can either induce up- or down-regulation of miRNA-expression (as reviewed by Ivan *et al.*, 2008).

Interestingly, studies about quantitative features of miRNA mediated regulation revealed that miRNA-mRNA interactions could be classed into 3 categories. Thus miRNAs can act as a switch to inhibit their target gene expression completely, they can act as fine-tuner which would adjust the level of target gene expression or miRNAs can act as buffer to reduce fluctuations or variations of target gene expression (Bartel, 2009; Ebert and Sharp, 2012; Braillard and Malaterre, 2015). Furthermore, miRNA abundance and target site abundance are also involved in the efficacy of down-regulating target mRNA. For instance miRNAs that can target a higher number of targets will have less effect on a particular target and will more likely act as fine-tuner rather than a switch (Arvey *et al.*, 2010). It is clear that the exact mechanism through which miRNAs act is still not completely understood, and further investigations are necessary to understand their effects and impact on gene regulation.

1.5 Hypothesis with Aims and Objectives

1.5.1 Hypothesis

MiRNAs have a role in the hypoxic regulation of human embryonic stem cells.

1.5.2 Aims & Objectives

1) To investigate the differential expression of miRNAs in hESCs cultured at 5% or 20% oxygen:
    - To profile miRNA expression using TaqMan microRNA Arrays
    - To perform bioinformatics analysis to predict which genes the differentially expressed miRNAs target.
    - To validate the array results using RT-qPCR.

2) To investigate the effect of single miRNAs on the physiological regulation of hESCs:
    - To manipulate miRNA expression by transfecting hESCs with miRNA precursor molecules to up-regulate miRNA function and investigate the mRNA and protein expression of predicted targets involved in pluripotency using RT-qPCR and Western blotting.

3) To determine if the effects from overexpressing selected miRNAs (miR-122-5p and miR-223-3p) are caused by direct miRNA-mRNA interaction:
    - To investigate the locations of potential miRNA target sites for miR-122-5p and miR-223-3p in NANOG 3'UTR.
    - To perform Dual-Luciferase-Reporter Assays in HeLa cells to investigate the binding of either miR-122-5p or miR-223-3p in NANOG 3'UTR.

4) To investigate if miR-223-3p causes functional impact on hESC pluripotency:
    - To manipulate miRNA expression by transfecting hESCs with miRNA precursor molecules or miRNA mimics to up-regulate or down-regulate miRNA function respectively.
    - To investigate potential downstream targets using RT-qPCR and performing proliferation assays.

Chapter 2

Materials and Methods

2.1 Cell culture

2.1.1 Derivation of mouse embryonic fibroblasts

Mouse embryos were used to derive mouse embryonic fibroblasts in accordance with Home Office regulations and University of Southampton ethical approval (Animals (Scientific procedures) act and EU directive 2010/63). Mouse embryos (12.5 days old) were obtained from wild type mice (MF-1 or CF-1 strains). The embryos were removed from the embryonic sac, decapitated, eviscerated and approximately 9 embryos per tube washed twice in 30 ml of phosphate buffered saline (1xPBS) (without Ca^{2+} and Mg^{2+}, Invitrogen) before being minced with scalpels, collected and incubated in 15 ml Trypsin/EDTA (1x Trypsin, Invitrogen) for 15 min in a water bath at 37°C, pipetting the solution up and down every 5 min. 200 µl of DNAse (10 mg/ml stock in water, Invitrogen) and 15 ml of MEF media (Table 3) were subsequently added and incubated at 37°C until the cell mixture appeared liquid throughout, followed by centrifugation at 1000 rpm for 5 min. The supernatant was removed and cells resuspended in 15 ml of MEF medium. 5 ml of the resuspended cells were transferred into three T175 flasks (approximately 3 embryos per flask) and further 19 ml of MEF medium added per flask. The MEFs were incubated until confluent (2-3 days) in an incubator at 37°C, replacing MEF medium every 24 h. Cell samples had been collected for mycoplasma testing. Confluent cells were washed in 1xPBS, dissociated with 1xTrypsin, collected and centrifuged at 1500 rpm for 4 min. The cell pellet of one T175 flask was re-suspended in 9 ml freezing-medium (90% FBS and 10% dimethyl sulfoxide (DMSO)) for cryopreservation resulting 9 tubes of MEFs.

Table 3: Composition of MEF medium

DMEM (PAA The Cell Culture Company) supplemented with:	
10% fetal bovine serum FBS (sterile filtered)	Invitrogen
1% penicillin streptomycin (sterile filtered)	Invitrogen

2.1.1.1 Mycoplasma testing of primary MEFs

The cell and media samples taken from primary MEFs were centrifuged at 1500 rpm for 5 min and the supernatant discarded. The pellet was re-suspended in 1 ml 1xPBS, transferred into a 1.5 ml Eppendorf tube and washed twice in 1xPBS. The pellet was then re-suspended in 100 µl 1xPBS and subsequently incubated at 95°C for 10 min in a heat block, briefly vortexed and centrifuged at 13000 rpm for 2 min. 10 µl of the

supernatant was used in the Mycoplasma PCR Detection Kit (Intronbio) using following PCR cycle programme: Initialisation step at 94°C for 1 min; denaturation step at 94°C for 30 sec, annealing step at 60°C for 20 sec and extension step at 72°C for 1 min for 35 cycles followed by a final elongation step at 72°C for 5 min and final hold at 10°C. The PCR product and a 100bp ladder (New England BioLabs) were loaded onto a 1.5% agarose gel (Invitrogen) in 1xTAE buffer (40 mM Tris, 20 mM acetic acid, 1 mM EDTA Fisher BioReagents) containing 0.005% Nancy-250 (Invitrogen) and was run at 90 A for approximately 1h. The agarose gel was imaged with Syngene Bio ImagingINgenius and samples compared to the negative and positive control provided by the Mycoplasma PCR Detection Kit (Figure 10).

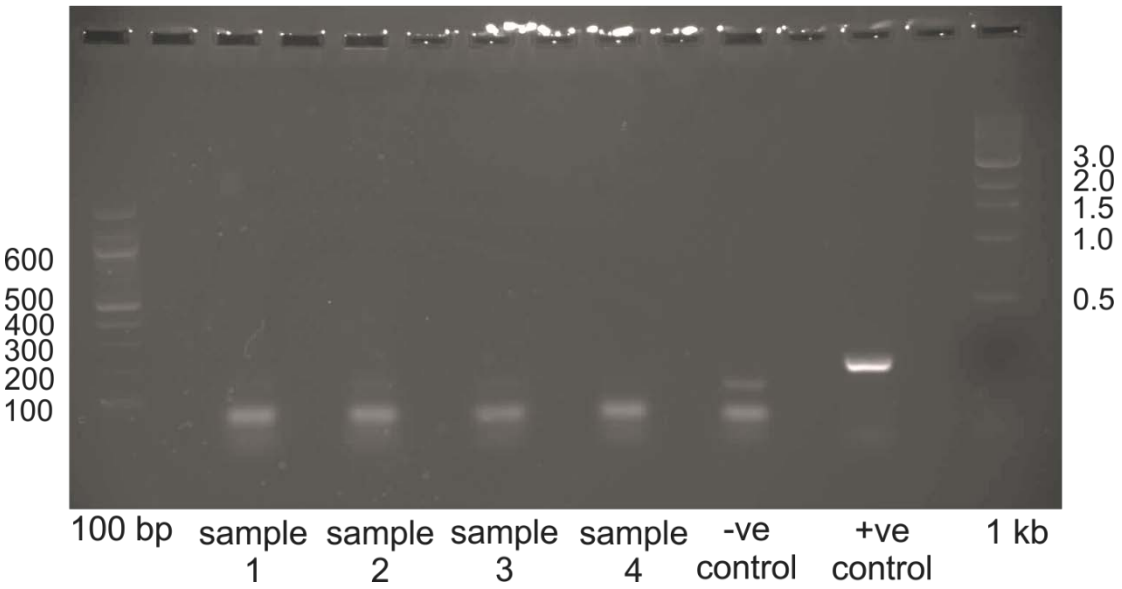

Figure 10: 1.5% Agarose gel showing typical products of uncontaminated samples from primary un-irradiated MEF culture using the Mycoplasma PCR Detection Kit (Intronbio)

2.1.2 Culture of mouse embryonic fibroblasts (MEFs)

Frozen, mycoplasma free MEFs (1 ml) were thawed and re-suspended in 10 ml pre-warmed MEF-medium, centrifuged at 1500 rpm for 4 min. The supernatant was discarded and the pellet re-suspended in 1 ml of MEF-medium and subsequently transferred into one T175 culture flask containing 20 ml MEF-medium. The cells were cultured for 2-3 days at 5% CO_2 in air at 37°C until 90% confluent. The medium was removed, cells washed in 1xPBS and dissociated with 6 ml of 1x Trypsin at 37°C for 4-5 min. Trypsin was inactivated by the addition of 6 ml MEF-medium, the dislodged cells transferred into a 50 ml tube and centrifuged at 1500 rpm for 4 min. The supernatant was discarded and the cell pellet was re-suspended in 4 ml of MEF-medium, transferring 1 ml of re-suspended cells into four T175 flasks and cultured for 2-3 days at 5% CO_2 in air at 37°C until 90% confluent. Confluent MEFs were passaged a second time in the same manner transferring the cell pellet of four flasks into 12 flasks until 90% confluent again. MEFs from 12 flasks were each washed in 1xPBS, dissociated with 6 ml of 1x Trypsin at 37°C for 4-5 min, 6 ml MEF-medium added, dislodged cells of 3 flasks combined in one tube and centrifuged at 1500 rpm for 4 min. The supernatant was discarded and all cell pellets re-suspended and combined in a total of 40 ml of MEF medium. Re-suspended cells in 50 ml tubes were then subject to γ-irradiation (50Gy (grays, SI unit for the absorption of one joule of radiation energy per kg of matter)) for 23.6 min using a Multi Rad 350 x-ray irradiator to mitotically inactivate the MEFs. The γ-irradiated MEFs were centrifuged at 1500 rpm for 4 min and the cell pellet re-suspended in 12 ml of freezing-medium (90% FBS and 10% dimethyl sulfoxide (DMSO)) for cryopreservation resulting in 12 tubes of γ-irradiated MEFs. Cells were frozen at a rate of 1°C per minute until -80°C using a container filled with isopropylalcohol (Mr. Frosty, ThermoScientific) and then transferred into liquid nitrogen.

2.1.3 Preparation of γ-irradiated MEFs for conditioned media or for culture of hESCs

γ-irradiated MEFs were used either to culture hESCs or to condition hESC medium for 24 hours prior to use.

One vial of γ-irradiated MEFs per two 6-well plates were thawed, 15 ml of MEF-medium added, centrifuged at 1500 rpm for 4 min and the cell pellet re-suspended in 12 ml of MEF-medium. 1 ml of γ-irradiated MEFs were transferred into each well of a 6-well plate. The 6-well plates were pre-coated with 0.1% gelatin for 30 min.

After 24 hours, the MEF medium was aspirated and replaced with hESCs medium to condition the medium (Table 4). After further 24 h the conditioned media was removed and used to culture hESCs under feeder free conditions.

Table 4: Composition of hESC culture medium

Knockout (KO) DMEM (Invitrogen) 410 ml supplemented with:			
Volume	Final concentration	Component	Company
75 ml	15%	Knockout serum replacement	Invitrogen
5 ml	1%	non-essential amino acids 100x	Invitrogen
5 ml	1%	penicillin streptomycin 100x	Invitrogen
5 ml	1%	glutamax 1 100x	Invitrogen
0.5 ml	50 µM	50 mM β-mercaptoethanol	Sigma
50 µl	10 ng/µl	100 ng/µl bFGF	Peprotech Ltd.
35 µl	$0.525x10^{-3}$ %	7.5% BSA	Sigma

2.1.4 Culture of hESCs

The hESC lines Shef3 and Hues7 were obtained from the University of Sheffield via the UK Stem Cell Bank, and D.Melton, Howard Hughes Medical Institute, Harvard University respectively.

Hues7 and Shef3 hESCs both have a karyotype of 46,XY and were obtained from surplus embryos donated with informed consent by a patient undergoing IVF and cultured to the blastocyst stage.

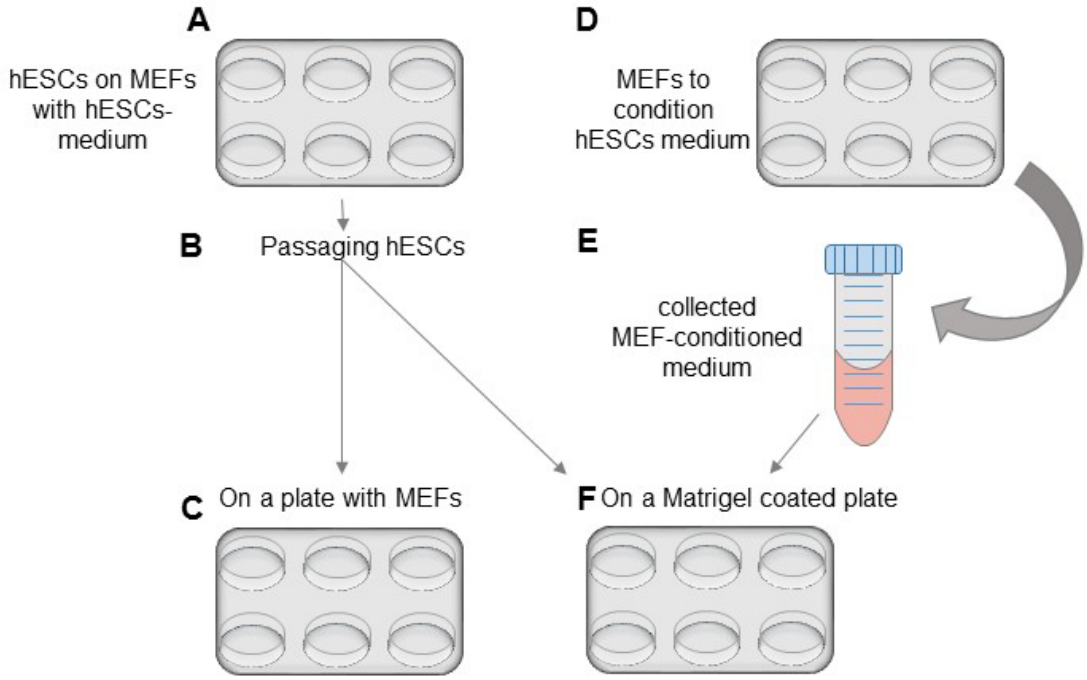

Figure 11: Schematics of hESC culture

Schematic representation of culturing and expanding hESCs: A) on mitotically inactivated MEFs, B) passaging hESCs on MEFs or F) passaging hESCs on Matrigel coated plates using D and E) MEF-conditioned medium

Hues7 and Shef3 hESCs were cultured and expanded on mitotically inactivated MEFs (Chapter 2.1.3) in 2ml of hESC culture medium (Table 2) per well of a 6-well-plate (Figure 11 A and C). The media was changed daily. For passaging, the medium was aspirated and 1 ml of collagenase type IV (Gibco) diluted to 160 U/ml in KO DMEM per well of a 6-well-plate added and incubated at 37°C for 4-5min. The collagenase was aspirated and 2 ml or 3 ml of hESC medium added for a 1:2 or 1:3 dilution respectively. Cells were mechanically lifted from the plate using a cell scraper and 1 ml of this cell suspension subsequently added to each well of mitotically inactivated MEFs in a dropwise manner (Figure 11 C). MEF medium was aspirated and 1 ml of hESC medium added prior to the transfer of hESCs. Cells were passaged every three to four days.

hESCs were cultured at either atmospheric oxygen tension (20% oxygen, denoted as normoxic) or under 5% oxygen tension and 90% nitrogen (denoted as hypoxic) at 37°C and 5% CO_2 in humidified air. Cells were cultured for at least three passages at their respective oxygen concentrations prior to use, especially for those cultured at 5% oxygen to ensure hESCs are fully adapted to this low oxygen concentration. Cells cultured at 5% oxygen were only removed for the shortest time period possible from the incubator for the purpose of passaging cells. The oxygen and CO_2 concentration of the incubators were frequently monitored using the GeoTech G100 (Gem Scientific).

2.1.5 Preparation of Matrigel coated plates for feeder-free culture of hESCs

Matrigel (BD Biosciences) was thawed and diluted to 6 mg/ml protein using KO DMEM into 400 µl aliquot. These aliquots were stored at -20°C for a maximum of 3 months. One aliquot (400 µl) was thawed overnight at 4°C and subsequently added to 5.6 ml of cold KO DMEM. 1 ml of this Matrigel solution was added to each well of a 6-well-plate and stored at 4°C overnight prior to use. Matrigel coated plates were used for up to 7 days.

2.1.6 Culture of hESCs on Matrigel coated plates

Shef3 or Hues7 hESCs were cultured feeder-free on Matrigel coated plates (Figure 11 F) with MEF-conditioned medium (Figure 11 F and E). Medium was changed daily and cells were passaged 1:2 or 1:3 every three to four days. To ensure the complete removal of y-irradiated MEFs, hESCs were cultured for a minimum of three passages on Matrigel and when cultured at 5% oxygen for at least three passages at 5% oxygen prior to experimental use.

2.1.7 Transfection of Shef3 hESCs with synthetic pre-miR miRNA precursor molecules (pre-miRs) or synthetic anti-miR miRNA inhibitors (anti-miRs)

For hESC transfection with synthetic pre-miR miRNA precursor molecules (pre-miR) or anti-miR miRNA inhibitor molecules (anti-miR) (Ambion, Applied Biosystems, Table 5), cells were routinely cultured and passaged until they reached at least their third passage on Matrigel to ensure the absence of MEFs. hESCs were also cultured for a minimum of three passages at 5% oxygen. Cells were then transfected on day one post-passage, using 1-well of a 6-well plates for RNA and 3-wells of a 6-well plate for protein collection.

Table 5: List of synthetic pre-miRs and anti-miRs (Ambion, Applied Biosystems)

Stem-loop ID	Mature miRNA ID	Catalogue no.	Assay ID	Mature miRNA sequence
hsa-miR-122	has-miR-122-5p	AM17100 for pre-miR AM 1700 for anti-miR	PM 11012 for pre-miR AM11012 for anti-miR	UGGAGUGUG ACAAUGGUG UUUG
hsa-miR-223	hsa-miR-223-3p	AM17100 for pre-miR AM17000 for anti-miR	PM 12301 for pre-miR AM12301 for anti-miR	UGUCAGUUU GUCAAAUAC CCCA
Pre-miR miRNA Precurser Negative Control #1	-	AM17110	-	-
Anti-miR miRNA inhibitor Negative Control #1	-	AM17010	-	-

On the day of transfection, the transfection cocktail was prepared in Eppendorf tubes as following: For each well of a 6-well plate, 30 µl (which gives 200nM final concentration in 1.5 ml) of the pre-miR from a 10 µM working stock solution were added to 170 µl of pre-warmed KO DMEM (37°C) in the absence of any supplements. The Eppendorf tube was briefly vortexed, 10 µl of the transfection reagent INTERFERin (Polyplus) was added and incubated for 10min at room temperature. Medium was removed from the cells and replaced with 1.3 ml of MEF-conditioned media and the transfection mix added in a dropwise manner. The medium was changed with MEF-conditioned media on day two post-passage, 24 hours post-transfection.

RNA or protein was collected from hESCs 48 h post-transfection/ day three post-passage.

2.2 Gene Expression Analysis

2.2.1 RNA isolation

RNA was isolated from Shef3 and Hues7 hESCs cultured on matrigel on day 3 post-passage using the TRIzol isolation method adapted from Invitrogen.

The medium was removed and 1 ml of TRIzol applied directly to the cells. The cells were scraped off and transferred into a screw top tube and stored at -80°C. The cell-lysate was thawed, 0.2 ml of Chloroform added, briefly vortexed and incubated for 15 min at room temperature. The sample was centrifuged at 13,000 rpm for 30 min at 4°C to allow phase separation. The upper aqueous-phase was transferred into a fresh Eppendorf tube and 0.5 ml of isopropanol and 40 µl Glycogen (5 mg/ml) added. After 15 min at room temperature, RNA was precipitated at -80°C for 30min or overnight. The sample was then centrifuged at 13,000 rpm for 30 min at 4°C and the supernatant discarded. The RNA pellet was washed in 850 µl of chilled 75% ethanol for 10 min on ice to reduce any salts and centrifuged at 13,000rpm for 15 min at 4°C. The Ethanol was removed and the pellet briefly centrifuged to remove the remaining ethanol. Finally, the RNA pellet was dried at room temperature for approximately 10 min and dissolved in 50 µl of RNAse free water containing 1 µl of RNAsin, an RNAse inhibitor. The RNA concentration was spectrophotometrically determined using NanoDrop (ThermoScientific). The samples were measured at 260 nm and 280 nm and a ratio of ~2.0 generally accepted as “pure” RNA, free of contaminants such as phenol. RNA samples were stored at -80°C.

2.2.2 Reverse Transcription of RNA using oligo-dT primer

2.2.2.1 DNAse treatment of RNA

RNA was treated with a deoxyribonuclease (DNAse) enzyme to digest any potential contaminating DNA in the sample. 1 µg total RNA (was made up in 10 µl H_2O), 1 µl 10x Reaction Buffer (Invitrogen) and 1 µl DNAse I (Amplification Grade, 1 U/µl, Invitrogen) were added and incubated for 15 min at room temperature. The reaction was stopped with the addition of 1 µl of 25 mM EDTA and incubated for 10 min at 65°C. The total reaction of 13 µl was either stored at -80°C or directly reverse transcribed.

2.2.2.2 Reverse Transcription of RNA with oligo-dT primer

3 µl DEPC H_2O and 1 µl oligo-dT primer (500 µg/µl, Promega) were added to 11 µl DNAse treated RNA, incubated for 10 min at 70°C and chilled on ice until 11 µl DEPC treated water, 8 µl of 5x Moloney Murine Leukemia Virus Reverse Transcriptase (M-MLV RT) reaction buffer, 5 µl dNTPs (10mM stock) and 1 µl M-MLV RT (200 u/ µl stock) were

added. The complete mix was then incubated for 60 min at 42°C and the resulting cDNA stored at -20°C.

2.2.3 Genomic contamination check

To determine if cDNA was contaminated with genomic DNA (gDNA) the following PCR (Table 6) was performed using intron spanning primers (Ornithine decarboxylase antizyme (OAZ1), forward primer 5'-GGCGAGGGAATAGTCAGAGG-3', reverse primer 5'-GGACTGGACGTTGAGAATCC-3'), which amplify a product of 122bp for cDNA and a product of 373 bp size if the sample is contaminated with gDNA.

Table 6: PCR reagents for genomic contamination check

Reagent	Volume (25 µl in total)
GoTaq Buffer	5.000 µl
dNTPs (10mM)	0.500 µl
Forward Primer (OAZ1)	0.500 µl
Reverse Primer (OAZ1)	0.500 µl
H_2O	17.125 µl
GoTaq Polymerase	0.375 µl
cDNA	1.000 µl

The PCR reaction for DNA amplification was incubated at 94°C for 2 min followed by 30 cycles at 94°C for 1 min, 58°C for 1 min, 72°C for 1 min. This was followed by 1 cycle at 72°C for 10 min. The PCR product and a 100bp ladder (New England BioLabs) were loaded onto a 2% agarose gel (Invitrogen) in 1xTAE buffer (Fisher BioReagents) containing 0.005% Nancy-250 (Invitrogen) and run at 80V for 1h.

2.2.4 Reverse Transcription of RNA using random hexamer primer

The use of random hexamer primers was chosen to avoid 3' bias and to provide an improved representation of the entire mRNA. Different regions of the RNA molecules are better represented if random hexamers are used when compared to oligo-dT primer.

Briefly, 200ng of total RNA plus 1 µl 10x random hexamer primer (Applied Biosystems) were used with DEPC H_2O to make a volume of total 5.1 µl. This mix was incubated for 5 min at 70°C and chilled on ice until further reagents (Table 7) were added:

Table 7: Reverse Transcription of RNA using random hexamer primers

Reagents (Promega)	Volume (10 µl in total)
5x M-MLV Reaction Buffer	2 µl
dNTPs (10 mM)	2 µl
RNAsin (40 u/ul)	0.4 µl
M-MLV Reverse Transcriptase (200 u/µl)	0.5 µl

The total mix of 10 µl was incubated for 60 min at 37°C and stored at -20°C. For subsequent use for real-time quantitative PCR (RT-qPCR), cDNA was 1/10 diluted.

The presence of any potential genomic contamination was assessed by performing the the same reaction on each RNA sample but in the absence of the reverse transcriptase. RT-qPCR was then performed on these samples together with SOX2, a probe capable of identifying genomic DNA.

2.2.5 Real Time quantitative PCR (RT-qPCR) Analysis

Reverse transcription of cDNA was either performed with oligo-dT or with random hexamers as described in chapter 2.2.2 and 2.2.4. This reverse transcribed cDNA was used to analyse the expression of protein-coding genes. RT-qPCR was then performed as described (Table 8) using the 7900 HT Fast RT-PCR System with Applied Biosystem TaqMan probes (Table 9) with following cycling parameters: 50C° for 2min, 95°C for 10min, followed by 40 cycles at 95°C for 15s and 60°C for 1min. RT-qPCR reactions are based on doubling of the PCR product with each cycle which requires 100% efficiency of the probes used. The efficiency of RT-qPCR TaqMan probes is reported to be close to 100% (with an average of 97.6%, Applied Biosystems).

Table 8: Reagents for RT-qPCR in 384-well plates

	Volume (total 5 µl)
TaqMan Universal Master Mix II	2.5 µl
RNase free water	1.25 µl
qPCR-primers (TaqMan probe)	0.25 µl
cDNA	1.0 µl

Table 9: Details for TaqMan probes used in RT-qPCR reactions for mRNA expression levels

Gene	Company	Type of Assay	Catalogue no.	Assay ID	Assay Design
NANOG	Life technologies (Applied Biosystems)	TaqMan Gene Expression	4331182	Hs02387400_g1	probe spans exons
POU5F1 POU5F1P3 POU5F1P4	Life technologies (Applied Biosystems)	TaqMan Gene Expression	4331182	Hs01895061_u1	amplicon spans exons and probe does not span exons
SOX2	Life technologies (Applied Biosystems)	TaqMan Gene Expression	4331182	Hs00602736_s1	both primers and probe map within a single exon
UBC	Life technologies (Applied Biosystems)	TaqMan Gene Expression	4331182	Hs00824723_m1	probe spans exons
ACTB	Life technologies (Applied Biosystems)	TaqMan Gene Expression	4331182	Hs99999903_m1	amplicon spans exons and probe does not span exons
CDK6	Life technologies (Applied Biosystems)	TaqMan Gene Expression	4331182	Hs01026371_m1	probe spans exon
CDC25A	Life technologies (Applied Biosystems)	TaqMan Gene Expression	4331182	Hs00947994_m1	probe spans exon

The probes used from TaqMan gene expression assays (Table 9) follow a nomenclature that can be found in the "Online Selection Guide for TaqMan Gene Expression Assays": "_g" indicates an assay that may detect genomic DNA. The assay probe and primers may also be within a single exon. "_u" indicates an assay whose amplicon spans an exon junction and the probe sits completely in one of the spanned exons. "_s" indicates an assay whose probes and primers are designed within a single exon. Such assays will, by definition, detect genomic DNA. "_m" indicates an assay whose probe spans an exon junction and will not detect genomic DNA."

The obtained data were then processed by the SDS RQ Manager. The manual C_t threshold or fluorescence detection baseline was set to 0.2 followed by calculation of the relative quantification of gene expression using the comparative Ct method ($2^{-\Delta\Delta Ct}$) (Livak and Schmittgen, 2001). This was calculated by subtracting the Ct of the treatment group from the Ct values of the control group (Equation 1) from the gene of interest (GOI) and house-keeping-gene (HKG) respectively. Next, the relative expression analysis was performed (Equation 2), where the $2^{-\Delta\Delta Ct}$ value depicts gene expression which is relative to the endogenous control group.

Equation 1

$$\boldsymbol{gene\ expression\ related\ target\ transcript\ of\ treatment\ group\ to\ control\ group}:$$

$$\mathbf{2}^{\Delta \boldsymbol{Ct}(\boldsymbol{GOI\ treated})} = \mathbf{2}^{\left(\boldsymbol{Ct}^{\boldsymbol{GOI\ control}} - \boldsymbol{Ct}^{\boldsymbol{GOI\ treated}}\right)}$$

$$\mathbf{2}^{\Delta \boldsymbol{Ct}(\boldsymbol{HKG\ treated})} = \mathbf{2}^{\left(\boldsymbol{Ct}^{\boldsymbol{HKG\ control}} - \boldsymbol{Ct}^{\boldsymbol{HKG\ treated}}\right)}$$

Equation 2

$$\boldsymbol{realtive\ gene\ expression\ levels\ to\ endogenous\ control}:$$

$$\mathbf{2}^{-\Delta\Delta \boldsymbol{Ct}} = \frac{\mathbf{2}^{\Delta \boldsymbol{Ct}(\boldsymbol{GOI\ treated})}}{\mathbf{2}^{\Delta \boldsymbol{Ct}(\boldsymbol{HKG\ treated})}}$$

2.3 Protein Analysis

2.3.1 Immunocytochemistry

Immunocytochemistry (ICC) was performed on hESCs cultured on MEFs, washed twice with PBS and fixed in 4% paraformaldehyde for 20 min at 4°C. The fixed hESCs were blocked with 3% donkey serum and where required permeabilised with 0.1% TritonX-100 for 1 h at room temperature (Table 10). The primary antibody (Table 11) was diluted in the appropriate block solution (Table 10), added to the cells and incubated overnight at 4°C in a humidified chamber. After washing three times with 1xPBS over 15 min the appropriate secondary antibody (Table 11) was diluted in the appropriate block solution and added to the cells for 2 h at room temperature in the dark and washed three times with 1xPBS over 15 min. Nuclei were labelled through DAPI, which was contained in the mounting solution (Vectashield, Vector Labs). Microscopy was performed using Zeiss microscope Observer.D1 and Observer.Z1 (Carl Zeiss MicroImaging GmbH, Jena).

Table 10: Composition of antibody-solutions for ICC

	3% serum	**Primary Antibodies**
Surface molecules	9.7ml 1xPBS 0.3ml donkey serum (AbD serotec)	SSEA-1 TRA-1-60
Intracellular	9.6ml 1xPBS 0.3ml donkey serum (AbD serotec) 0.1ml Triton X-100 (Fluka Bio Chemika)	OCT4 NANOG SOX2

Table 11: List of primary and secondary antibodies used for ICC with appropriate dilutions

Primary Antibody	**Company**	**Working dilution**	**Secondary Antibody (from Molecular Probes)**
mouse-IgG2b anti-OCT4	Santa Cruz	1:100	Anti-mouse IgG FITC 1:100
mouse- IgG-anti-NANOG	AbCam	1:250	Anti-mouse IgG FITC 1:100
rabbit-polyclonal-anti-SOX2	Millipore	1:500	Goat-anti-rabbit alexa 488 1:800
mouse-IgM-anti-TRA-1-60	Santa Cruz	1:100	Anti-mouse IgM FITC 1:200
mouse-IgM-anti-SSEA-1	Santa Cruz	1:100	Anti-mouse IgM FITC 1:200

2.3.2 Protein extraction

The protein extraction of hESCs was performed using Radio-Immuno-Precipitation-Assay (RIPA) lysis buffer (Sigma). Briefly, hESCs were cultured on Matrigel, rinsed with PBS on ice and treated with 0.1 ml RIPA lysis buffer. Cells from three wells of a 6-well-plate were detached from tissue culture plastic with a RIPA lysis buffer using a cell scraper and transferred into an Eppendorf tube on ice. The cell lysate was incubated for 20 min on ice, sonicated for 30 sec and centrifuged at for 10 min at 13,000 rpm and 4°C. The protein containing supernatant was transferred into an Eppendorf tube and stored at -80°C.

2.3.3 Protein quantification

The Bradford-Assay was used to determine protein concentration. The standard curve was performed by using a range of 0.175-1.4 mg/ml bovine serum albumin (BSA) diluted in water. The protein samples were diluted 1/20 in water. 20 µl of protein standards or samples were added to 200 µl of Bradford-Reagent in triplicate and the absorbance read at 595 nm. The readings from the standard curve were then used to estimate the unknown-protein concentration using the formula y=mx+n where “x” stands for the unknown-protein concentration (Figure 12).

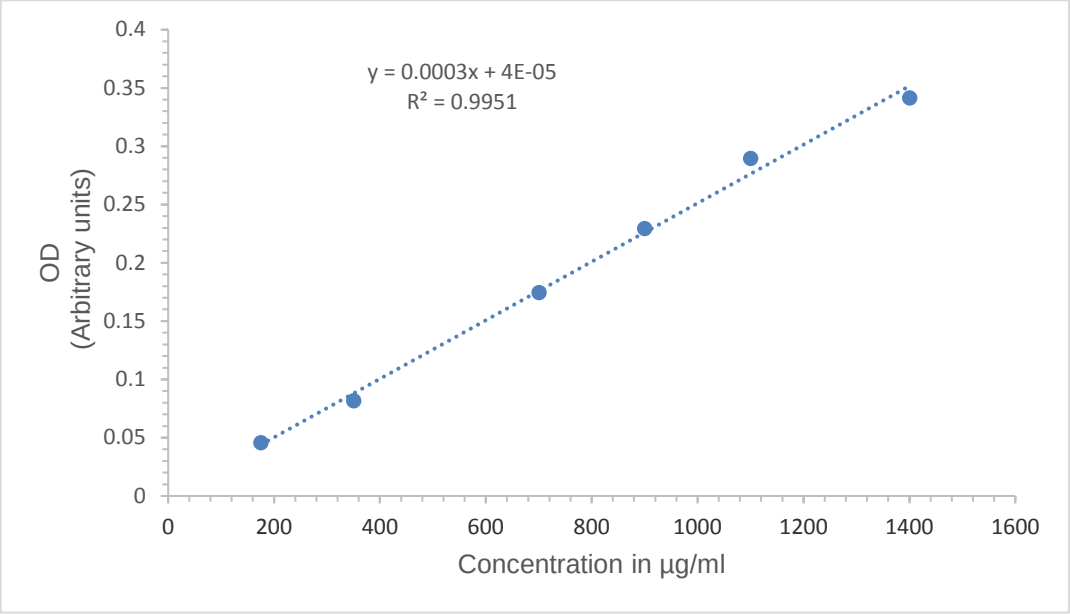

Figure 12: Typical BSA standard curve used to calculate the concentration of protein in samples (OD=optical density)

2.3.4 Sodium dodecyl sulfate – polyacrylamide gel electrophoresis (SDS-PAGE)

SDS-PAGE was performed to separate proteins according to their molecular weight. A 12% resolving gel was prepared and covered with isopropanol until polymerised followed by a layer of a 5% stacking gel (Table 12). The gels had a thickness of 0.75 mm with 10 wells in the stacking gel. Once the stacking gel was polymerised, 5 µl of the EZ-Run Pre-Stained RecProtein Ladder (Fisher), a molecular weight marker, was loaded into each SDS-Gel. The same amount of protein sample, between 50-70 µg, was loaded into each well with the addition of 7.5 µl aqueous 1M DL-Dithiothreitol (DTT) solution (Sigma), 7.5 µl of 4x NuPage LDS-sample buffer (Invitrogen) and RIPA buffer to make a total volume of 30 µl. The mix of protein, DTT, LDS-sample buffer and RIPA was then incubated at 95°C for 5 min and kept on ice until 25 µl of each sample was loaded onto the gel. Electrophoresis was performed vertically in a Bio-Rad tank for 40 to 60 min at 55 mA filled with 1x running buffer (Table 13).

Table 12: Chemicals used for SDS-gels

Reagent	Volume for 12% resolving gels	Volume for 5% stacking gels
1.5M Tris pH 8.8	2500 µl	-
1.0M Tris pH 6.8	-	695 µl
10% SDS	100 µl	50 µl
Acrylamide:N,N'-Methylenebisacrylamide 29:1 solution, 40% in H_2O (Sigma)	3000 µl	625 µl
dH_2O	5000 µl	3630 µl
10% ammonium persulphate	100 µl	50 µl
TEMED	5 µl	5 µl
Total volume	10 ml	5 ml

Table 13: 5x Running Buffer for SDS-gel electrophoresis

Reagent	**Amount or Volume**
Tris 25 mM	15.1 g
Glycine 250 mM	94 g
dH_2O	900 ml
10% SDS	50 ml
pH to 8.3, then filling up to 1000 ml with dH_2O	

2.3.5 Western Blotting

The transfer of the proteins that were separated in the SDS-Gel to a nitrocellulose membrane (Amersham Hybond-ECL) was performed by electrophoresis. The protein transfer from the SDS-Gel to the membrane was prepared in a vertical Bio-Rad blotting apparatus as following: ice, cathode, sponge, filter paper (Thermo Scientific), SDS-Gel, membrane, filter paper, sponge followed by the anode. Sponges and filter paper were incubated in freshly made transfer buffer prior to use (Table 14). The blotting apparatus was then filled with transfer buffer and run at 250 mA for 2 h.

Table 14: Transfer buffer for Western blotting

Reagent	
Glycine	2.93 g
1.5M Tris pH 8.3	32 ml
Methanol	200 ml
Filling up to 1000 ml with dH_2O	

After transfer, membranes were blocked with 5% milk in 1xPBS containing 0.1% Tween (PBST) for 1 h at room temperature, followed by incubation with a primary antibody diluted in 5% milk overnight at 4°C on a rotating platform. The membranes were then washed three times over 15 min in PBST, followed by incubation with a horseradish peroxidase labelled secondary antibody in 5% milk in TBST for 1 h at room temperature. The secondary antibody was either an anti-mouse-HRP antibody (1:100,000), anti-goat-HRP antibody (1:50,000) or an anti-rabbit-HRP antibody (1:50,000). After washing three times with PBST over 15 min the enhanced chemiluminescence (ECL) kit (Lumigen) was applied to detect protein bands. After detection of the primary antibody, a mouse anti-β-actin peroxidase conjugated antibody (1:50,000) in 5% milk in TBST was incubated for 1 h at room temperature, washed three times with PBST over 15 min and a less sensitive ECL reagents (Amersham) applied to detect β-Actin protein expression.

Table 15: Primary Antibodies for Western blotting

Primary Antibody	Raised in and isotype	Dilution	Secondary Antibody
OCT4	Mouse IgG_{2b} (Santa Cruz)	1:1,000	α-mouse HRP
SOX2	Rabbit Polyclonal (Millipore)	1:500	α-rabbit HRP
NANOG	Goat Polyclonal (R&D)	1:200	α-goat HRP
PKM2	Rabbit Polyclonal (Novus Biologicals)	1:500	α-rabbit HRP
HIF2A	Rabbit Polyclonal (Novus Biologicals)	1:250	α-rabbit HRP
β-Actin Peroxidase (conjugated)	Mouse IgG1 (Sigma)	1:50,000	-

Table 16: Secondary Antibodies for Western blotting

Secondary Antibody	Raised in and isotype	Dilution
Anti-rabbit IgG HRP	Donkey (GE Healthcare)	1:50,000
Anti-mouse IgG HRP	Sheep (GE Healthcare)	1:100,000
Anti-goat IgG HRP	Donkey (GE Healthcare)	1:50,000

2.3.6 Development of Western blots by film

The ECL treated membranes from Chapter 2.3.5 were wrapped in cling film, placed in a light excluding cassette and exposed to medical x-ray films (Kodak/Carestream). Exposure times was variable across different proteins. The film was devloped in a 1:5 dilution of GBX developer/replenisher (Sigma) in water until bands became visible, washed in water and fixed in a 1:5 dilution of GBX fixer and replenisher (Kodak) in water and washed again before drying. The developed films were then scanned and densitometry of the bands was performed with ImageJ (National Institute of Health) measuring the integrated density of bands and background. The background was subtracted from the bands of the proteins of interest and were then divided by the the values of the endogenous control β-Actin. This resulted in the relative expression of the protein of interest.

2.4 Statistical Analysis

A D'Agostino & Pearson Omnibus K2 normality test was performed on the array data to test whether the data followed a Gaussian distribution. As one set of the array data was not normally distributed, the data were analysed using a Kruskal-Wallis test. miRNA, mRNA and protein expression data were tested for normal distribution for sample-size greater than 8 and analysed using a one sample t-test comparing the treatment group to the normalised control group. Thereby "1" represents normalised data of the control group. A non-parametric test, such as a Wilcoxon Signed Rank test was used if data did not follow the normal distribution. The alpha value was set to 0.05 for all data and were considered significant different when *P≤0.05, **P≤0.01 and ***P≤0.001. Data are presented as mean ± standard error of the mean (SEM).

Chapter 3

Expression of miRNAs in hESCs

3.1 Introduction to Arrays and Bioinformatics on miRNAs in hESCs

3.1.1 MiRNAs in the Hypoxic Regulation of hESC

Culture at low oxygen tension is beneficial for hESCs maintenance because an increased expression of the pluripotency genes OCT4, SOX2 and NANOG, an increase in proliferation and reduced chromosome abnormalities were observed when compared to atmospheric oxygen concentration (Forsyth *et al.*, 2006; Wang, Thirumangalathu and Loeken, 2006; Forristal *et al.*, 2010). Thus, all these observations are showing features of increased stemness. Under low oxygen concentration, hypoxia induced factors (HIFs) are stabilised. These HIFs are master regulators of the hypoxic response as they regulated several hundreds of genes (Semenza, 2004; Smith, Robbins and Ratcliffe, 2008). Three splice-variants are known HIF1A, HIF2A and HIF3A as well as factor inhibiting HIFs (FIH) such as HIF1AN. HIF2A has been found to be the main regulator in hESCs pluripotency (Forristal *et al.*, 2010) as HIF2A binds directly to the proximal promotors of OCT4, SOX2 and NANOG under 5% oxygen (Petruzzelli *et al.*, 2014). MiRNAs are known as multipurpose regulators, usually target the mRNA at the 3'UTR and cause translational inhibition or mRNA degradation. Although miRNAs are also known to be able to target the 5'UTR or the coding sequence (Tay *et al.*, 2008; Vogel *et al.*, 2010; Roberts, Lewis and Jopling, 2011), this thesis is focusing on the more investigated 3'UTR as miRNA target. Thus miRNAs may also have a role in the hypoxic regulation of hESCs by supressing genes responsible for differentiation or by their absence promoting the expression of pluripotency genes.

In humans, the current number of annotated miRNA loci is 1,881 with 2,588 mature miRNAs that are mapped against the human genome GRCh38 (www.miRbase.org miRBase v21). Currently, there are 35,828 mature miRNAs described that are produced by 28,645 precursors in 223 species (Kozomara and Griffiths-Jones, 2014). Additionally, miRNAs can have a non-perfect complementarity to target mRNA which enables miRNAs to target hundreds of endogenous mRNAs, which massively increases the possibilities for theoretical targets (Guo, Wang and Wang, 2014). To investigate this volume of information a range of bioinformatic prediction tools were developed to provide *in silico* investigations that can be used to identify miRNA-mRNA interactions such as TargetScanHuman version 6.2 (TargetScan) or the SegalLab of Computational Biology (SegalLab). These prediction tools are based on algorithms that calculate miRNA target recognition, particularly sequence complementarity, seed region and evolutionary conservation (Brennecke *et al.*, 2005; Lewis, Burge and Bartel, 2005; Baek *et al.*, 2008).

Performing miRNA arrays will provide the first experimental insight regarding the expression profile of miRNAs in hESCs in hypoxia when compared to normoxia. The resulting data can be used with bioinformatic tools to interpret the outcome of the arrays. The prediction and evaluation of miRNAs binding to specific 3'UTRs of their target mRNA using these algorithms is the first step before biological validation can occur.

3.1.2 Prediction of miRNA Targets

TargetScan is a powerful resource for miRNA target mining. It is an *in silico* prediction tool which relies on conserved 8mer or 7mer sites aligned to the seed region of miRNA (Lewis, Burge and Bartel, 2005). Predictions are ranked by several criteria such as the calculated context+ score which includes six features such as site-type-, 3' pairing-, local AU nucleotide-, position -, target site abundance (TA) - and seed-pairing stability (SPS)-contribution (Grimson *et al.*, 2007; Garcia *et al.*, 2011). Very low context+ scores (the more negative the better) represent the most representative target. An advantage of TargetScan is that the total context+ score reflects many parameters and correlates additionally with protein down-regulation (Lewis, Burge and Bartel, 2005). A disadvantage of TargetScan is that poor seed pairings (Lewis, Burge and Bartel, 2005) also called non-canonical sites are omitted.

Another database used for miRNA-mRNA identifications is the Segal lab which takes into account the thermodynamic stability between miRNA and the 3'UTR of the target mRNA, free energy for miRNA target interactions as well as site accessibility and position of targeting in the 3'UTR for target recognition (Kertesz *et al.*, 2007; Long *et al.*, 2007; Baek *et al.*, 2008). The algorithm for target prediction used by the Segal lab is called PITA (Probability of interaction by Target Accessibility). The major difference to TargetScanHuman is the use of an energetic score (ΔΔGG) that has been manually set to "-5" as a cut-off line for the highest value for miRNA scores. This score shows the difference in the free energy release upon miRNA binding to the mRNA compared to when the nucleotides unpair. A practical advantage of using the PITA algorithm from Segal lab is the ease of using a large number of miRNA sequences simultaneously. Another advantage is that the secondary structure of the 3'UTR is taken into consideration for miRNA-mRNA interactions and parameters such as the number of minimum seed size can be adjusted more flexibly and therefore can include non-canonical sites. A drawback is that the PITA algorithms have a lower efficiency when compared to others (Kertesz *et al.*, 2007). The PITA algorithm is one of the most effective prediction tools and has been used in addition to TargetScan to predict miRNA-mRNA interactions. However, TargetScan has been used as main predictions tool since it is based on conservation criteria whereas PITA uses parameters such as free energy of

binding. Another reason for using TargetScan as main prediction tool is that it has been experimentally shown to be more precise and sensitive when compared to PITA (Alexiou *et al.*, 2009).

3.1.3 Rational of miRNA Arrays and Target-Mining

The interest of using bioinformatic analysis in particular sequence alignments between the 3'UTR and miRNAs lies in finding miRNAs that differentially regulate genes in hESCs cultured under either 5% oxygen compared to atmospheric oxygen concentrations. Since miRNAs are gene-regulators they might affect genes of interest such as *OCT4, SOX2, NANOG, HIFs* which are all known to be up-regulated at 5% oxygen (Forristal *et al.*, 2010). Additionally, low oxygen concentration was shown to increase the glycolytic rate of hESC metabolism (Forristal *et al.*, 2013). PKM2, a glycolysis rate limiting enzyme is involved in metabolic pathways (Gupta and Bamezai, 2010) and displayed an increased expression under hypoxia as well as having a role in regulating OCT4 expression (Christensen, Calder and Houghton, 2015). In particular, miRNAs which target these genes would be expected to be expressed at lower levels in hESCs cultured at 5% oxygen compared to those maintained at 20% oxygen. Thus, arrays for miRNAs together with bioinformatics can aid the investigation of differentially expressed miRNAs. This work will help to better understand the mechanisms regulating the beneficial effects of culturing hESCs under hypoxic conditions.

3.1.4 Study Aims

The aim of this Chapter is to determine which miRNAs are differentially expressed in hESCs cultured at either 5% or 20% oxygen to find miRNA regulated genes important in regulating hESC pluripotency.

Specific objectives:

- To culture and characterise hESCs in order to use for subsequent experiments performing mainly fluorescence microscopy.
- To analyse miRNA expression in hESCs cultured at either 5% or 20% oxygen tension performing TaqMan quantitative real-time PCR low density arrays for miRNAs.
- To analyse the miRNA expression profile and determine differentially expressed miRNAs using a range of software such as the SDS RQ Manager, Microsoft Excel and R.
- To determine predicted target genes involved in regulating hESC pluripotency for miRNAs down-regulated by utilising online databases and prediction algorithms such as TargetScan6.2 and SegalLab.
- To validate miRNA expression in hESCs using RT-qPCR.

3.2 Materials and Methods

3.2.1 TaqMan MicroRNA Array

The expression of 377 miRNAs plus three reference genes and one negative control was investigated in Shef3 hESCs cultured at either 5% or 20% oxygen. Therefore, TaqMan MicroRNA Array Card A version 2.0 for human miRNAs (Applied Biosystems) was performed in triplicates for each oxygen condition. Briefly, 400 ng of total extracted RNA was reverse transcribed with megaplex RT pimers (Human Pool A, Applied Biosystems) using the TETRAD PCR machine (Table 17). The reaction was incubated for 40 cycles at 16° for 2 min, 42°C for 1 min and 50°C for 1 sec. This was followed by one cycle at 85°C for 5 min.

Table 17: Megaplex reverse transcription conditions

Reagent	**µl (total 7.5 µl)**
10x RT buffer	0.8
25x dNTPs (100mM total)	0.2
Megaplex RT primers	0.8
Multiscripe Enzyme	1.5
RNAse inhibitor (Ambion) 20 U/µl	0.1
$MgCl_2$ (25mM)	0.9
RNA (400ng) + water	3.2

6 µl of the resulting cDNA with the addition of 450 µl 2x Master-Mix and 444 µl RNase free water were then loaded onto the array Card A. The run was performed by the 7900 HT Fast RT-PCR System.

The data obtained were processed by the SDS RQ Manager (Applied Biosystems). The manual Ct threshold or fluorescence detection baseline was set to 0.2 followed by calculation of the relative expression (ΔCt). This was calculated by subtracting the Ct of RNU44 from the Ct values of every miRNA (Equation 3). The relative differential expression analysis was performed using Equation 4. A negative ΔΔCt value depicts a miRNA which is higher expressed and a positive ΔΔCt value depicts a miRNA which is lower expressed in hESCs cultured under hypoxia compared to normoxia.

Equation 3:
relative expression of miRNAs

$$\textbf{relative expression}:$$
$$\Delta Ct = (Ct^{miRNA} - Ct^{RNU44})$$

Equation 4:
differential miRNA expression level

$$\textbf{differential miRNA expression levels}:$$
$$\Delta\Delta Ct = \left(\Delta Ct^{miRNA\ at\ 5\%} - \Delta Ct^{miRNA\ at\ 20\%}\right)$$

In order to select differentially expressed miRNAs, Ct values higher than 35 across the six performed arrays were discarded if all six Ct values matched this criteria. RNU44 was used as reference gene and therefore all values matching the criteria of -0.3<ΔΔCt<0.3 were set to be not differentially expressed and were not taken into consideration for further analysis.

3.2.2 In silico data analysis

The data obtained from TaqMan MicroRNA Arrays were extensively computationally analysed using Microsoft Excel as well as "R" with following criteria:

Ct values in these 3 array-datasets consisting of A5%, B5%, C5%, A20%, B20% and C20%, were discarded if all six of them were above Ct>35. Resulting in 231 expressed miRNAs out of 377 (not including reference genes). The Ct values were normalised to RNU44. Furthermore, IΔΔCt>0.3I was set for differential expression and according to equation 4 ΔΔCt>0.3 stands for down-regulated and ΔΔCt<-0.3 stands for up-regulated miRNAs in hypoxia compared to normoxia.

The online database TargetScan Human 6.2 (www.targetscan.org) was mainly used (version **6.2** (2012), newer versions are 7.0 (2015) and 7.1 (2016) but were not used for data presented in this thesis unless stated) together with the SegalLab of Computational Biology (http://genie.weizmann.ac.il/pubs/mir07/mir07_prediction.html) to obtain predicted target genes of interest. These data were obtained by sequence alignments by either searching for the genes of interest and obtaining matching miRNAs or searching for certain miRNAs and extracting potential genes of interest.

For generating the heatmaps in Figure 34 and Figure 39 the software R for statistical computing and graphics was used according to the criteria mentioned above. The function "heatmap.2" was applied with the default euclidean distance method and the default hierarchical clustering method complete linkage. Further statistical information and calculations can be found in the paper "Hierarchical Grouping to Optimize an Objective Function" (Ward, 1963).

3.2.3 Reverse transcription of RNA using specific stem-loop primers and RT-qPCR

In order to validate miRNAs, found via bioinformatics investigations, RNA samples were extracted with the TRIzol method (Chapter 2.2.1) from Shef3 and Hues7 hESCs cultured at either 5% or 20% oxygen. Briefly, specific stem-loop primer (Table 18) were used for the reverse transcription of 10 ng total RNA (Table 19). The reaction was incubated at 16°C for 30 min, 42°C for 30 min followed by 85°C for 5 min.

Table 18: Details for TaqMan primers used for the reverse transcription and probes used for RT-PCR for the measurement of miRNA expression levels

miRNA (miRBase name)	Type of Assay	Assay name (name on tube)	Assay ID (Catalogue no for all 4427975)	Mature miRNA Sequence
hsa-miR-29a-3p	TaqMan MicroRNA	hsa-miR-29a	002112	UAGCACCAUCUGAAAUCGGUUA
has-miR-122-5p	TaqMan MicroRNA	hsa-miR-122	002245	UGGAGUGUGACAAUGGUGUUUG
has-miR-223-3p	TaqMan MicroRNA	hsa-miR-223	002295	UGUCAGUUUGUCAAAUACCCCA
has-miR-135a-5p	TaqMan MicroRNA	hsa-miR-135a	000460	UAUGGCUUUUUAUUCCUAUGUGA
hsa-miR-210-3p	TaqMan MicroRNA	hsa-miR-210	000512	CUGUGCGUGUGACAGCGGCUGA
RNU44 (NR_002750)	TaqMan MicroRNA	RNU44	001094	Control miRNA Assay CCTGGATGATGATAGCAAATGCTGACTGAAACATGAAGGTCTTAATTAGACTCTAACTGACT

Table 19: Reverse transcription conditions using Applied Biosystems reagents for specific Stem-loop primers

Reagent	Total volume 8.0 µl
dNTPs (100mM total)	0.075 µl
MSRT (multiscripe reverse transcriptase)	0.5 µl
10x RT-Buffer	0.75 µl
RNase Inhibitor (Ambion) 20 U/µl	0.094 µl
RNase free water	4.081 µl
RNA (10ng/µl)	1.0 µl
Stem-loop RT primer (Table 18)	1.5 µl

RT-qPCR was performed using FAM-TaqMan-probes (Table 18) in 5 µl reactions in 384-well plates. The analysis was then performed in excel according to Equation 1 and Equation 2 (Chapter 2.2.4). All data were normalised to RNU44 and to “1” for 5% oxygen followed by statistical analysis using the Student’s t-test.

3.3 Results

3.3.1 Characterisation of hESCs

hESCs were cultured and characterised to ensure typical stem cell properties prior to use in subsequent experiments.

Hues7 and Shef3 hESC lines were both cultured at either 5% (hypoxic) or 20% (normoxic) oxygen concentration and immunocytochemistry was performed to investigate the expression of pluripotency markers. Phase contrast images showed typical stem cell properties such as clear defined colony edges, appeared to have a compact cell formation within the colonies and a cobble shaped morphology (Figure 13, 15, 17, 19, 21, 23, 25 and 27).

3.3.1.1 Expression of pluripotency and early differentiation markers in hESCs

Both, Shef3 and Hues7 hESC lines maintained at either hypoxic or normoxic conditions were positive for the nuclear stem cell markers OCT4, NANOG and SOX2 (Figure 13-14, 17-18, 21-22 and 25-26) but also the cell surface marker TRA-1-60 (Figure 15-16, 19-20, 23-24 and 27-28). A clear nuclear localisation of OCT4, NANOG and SOX2 can be seen especially at higher magnification (Figure 14, 18, 22 and 26). The presence of TRA-1-60 can also be best viewed at higher magnification which is clearly distributed across the surface of the cells (Figure 16, 20, 24 and 28).

Most colonies were not expressing the early differentiation maker SSEA-1 at all but there was sometimes a slight expression observed at the edges of colonies (Figure 19 and 23). No difference in expression of the transcription factors between the two oxygen concentrations was observed using immunocytochemistry but they were all positive for OCT4, NANOG, SOX2 and TRA-1-60 and were lacking SSEA-1 expression.

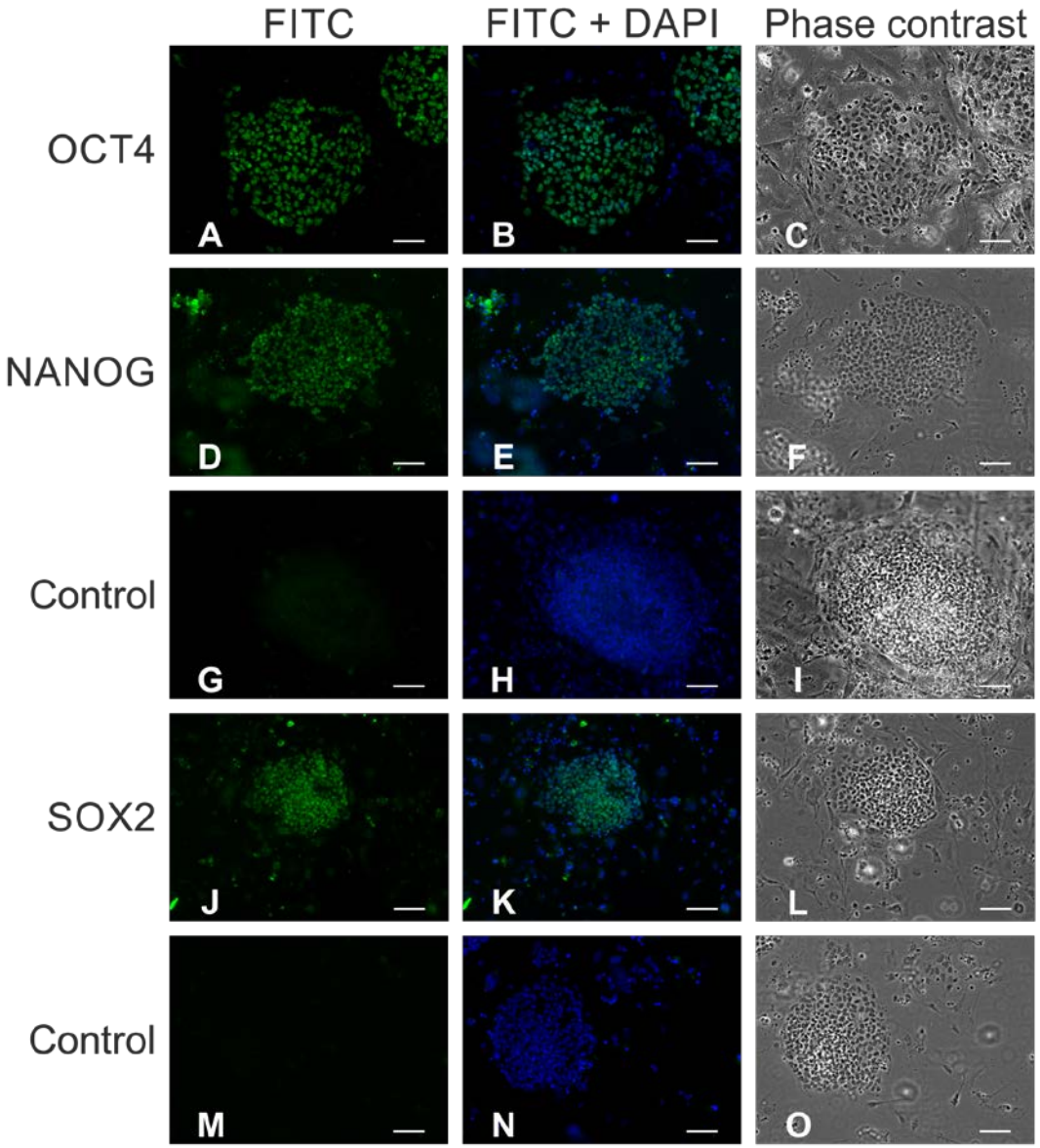

Figure 13: Expression of pluripotency markers in Shef3 hESCs at 5% oxygen

Immunocytochemistry of OCT4 (POU5F1) (green; A-B), NANOG (green; D-E) and SOX2 (green; J-K) merged with DAPI (blue; B, E, K) labelling of Shef3 hESCs cultured on MEFs under 5% oxygen on day 3 post-passage. FITC secondary antibody only = negative controls (G and M) merged with DAPI (blue, H and N). Phase contrast images of colonies (C, F, I, L, O). Scale bar = 100 μm.

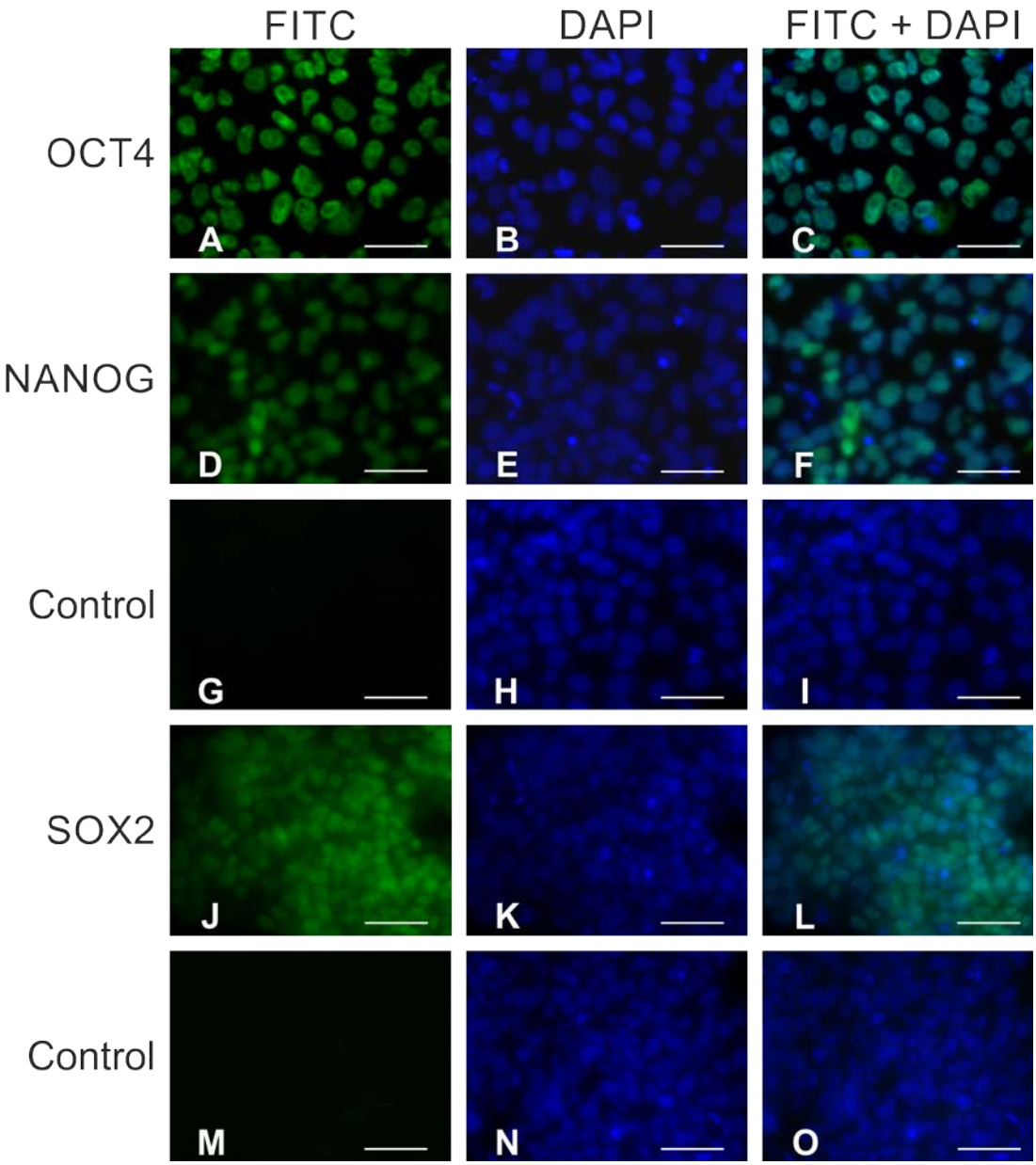

Figure 14: Characterisation of Shef3 hESCs at 5% oxygen

Immunocytochemistry of OCT4 (POU5F1) (green; A and C), NANOG (green; D and F) and SOX2 (green; J and L) merged with DAPI (blue; B-C; E-F and K-L) labelling of Shef3 hESCs cultured on MEFs under 5% oxygen on day 3 post-passage. FITC secondary antibody only = negative controls (G-M) merged with DAPI (H-I, N-O). Scale bar = 50 μm.

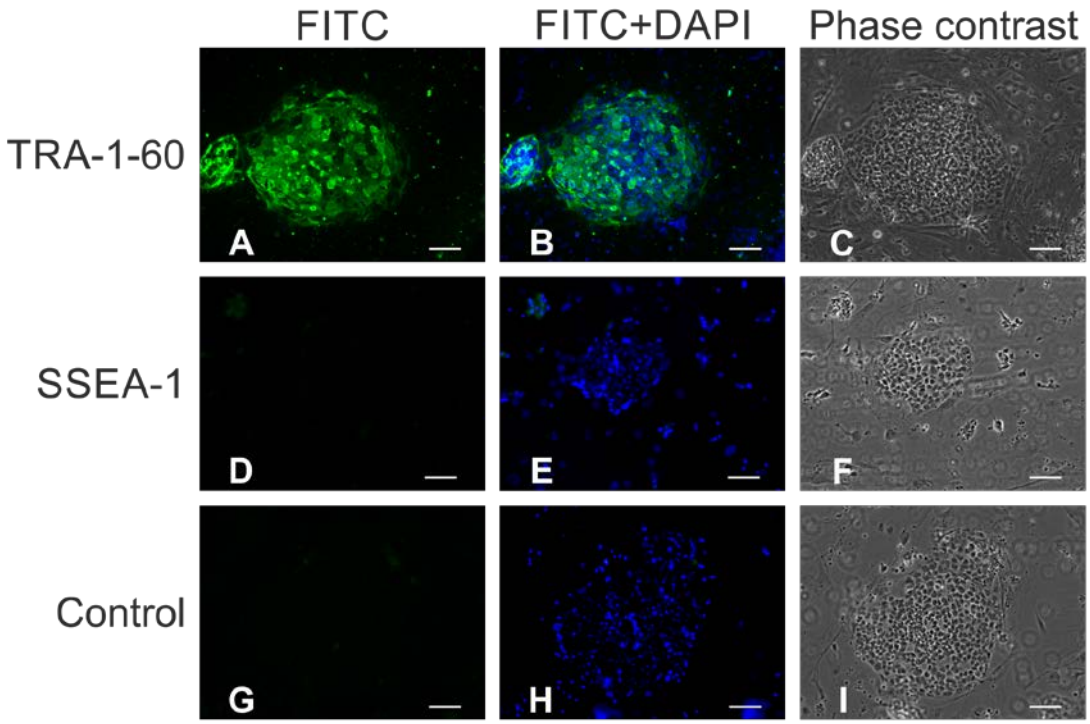

Figure 15: Expression of pluripotency and differentiation marker in Shef3 hESCs at 5% oxygen

Immunocytochemistry of pluripotency marker TRA-1-60 (green; A-B) and early differentiation marker SSEA-1 (green; D-E), merged with DAPI (blue; B and E) of Shef3 hESCs cultured on MEFs under 5% oxygen on day 3 post-passage. FITC secondary antibody only = negative controls (G, H). Phase contrast images of colonies (C, F, I). Scale bar = 100 µm.

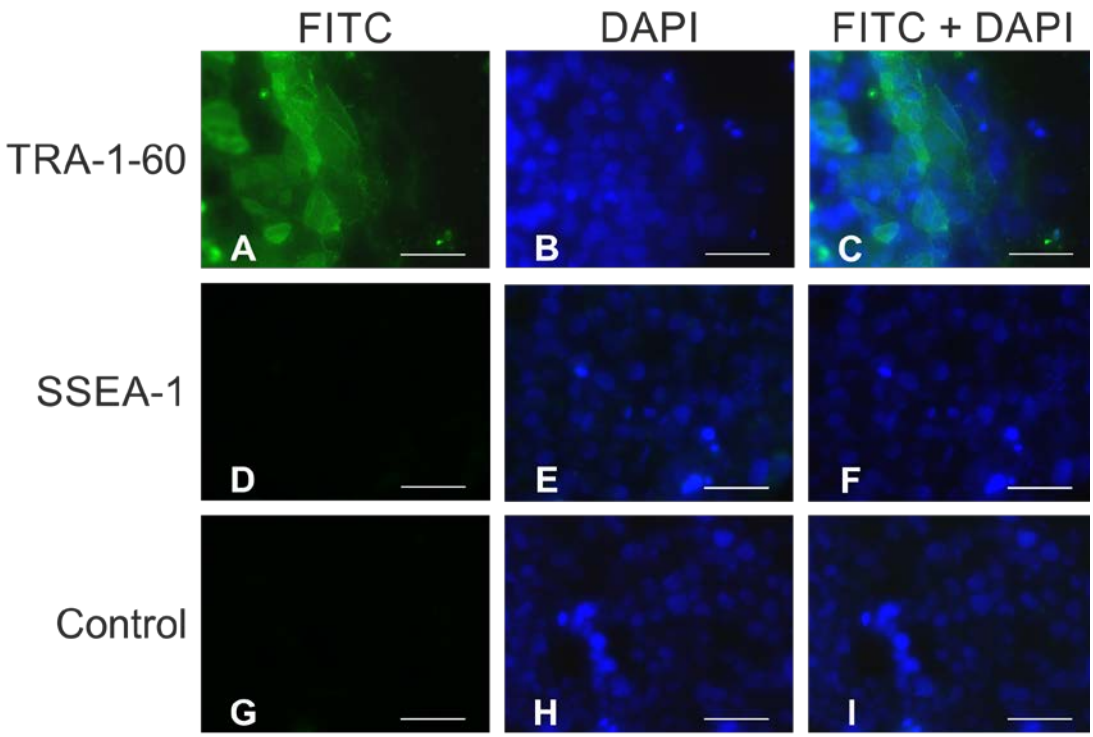

Figure 16: Characterisation of TRA-1-60 and SSEA-1 expression in Shef3 hESCs at 5% oxygen

Immunocytochemistry of pluripotency marker TRA-1-60 (green; A and C) and early differentiation marker SSEA-1 (green; D and F), DAPI (blue; B, E) and merged with DAPI (blue; C, F) of Shef3 hESCs cultured on MEFs under 5% oxygen on day 3 post-passage. FITC secondary antibody only = negative controls (G, I), DAPI (blue; H) merged with DAPI (blue; I). Scale bar = 50 µm.

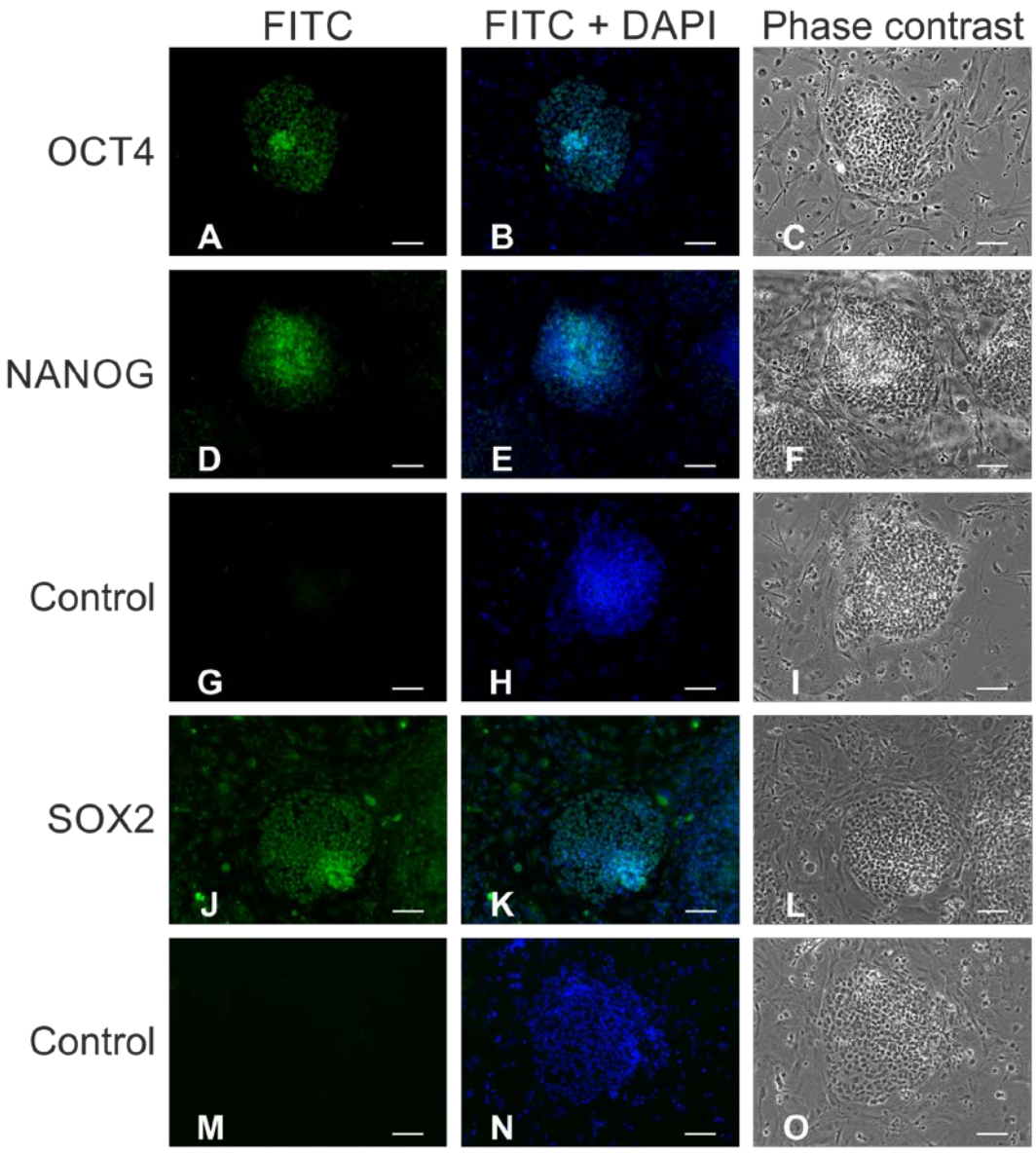

Figure 17: Expression of pluripotency markers in Shef3 hESCs at 20% oxygen

Immunocytochemistry of OCT4 (POU5F1) (green; A-B), NANOG (green; D-E) and SOX2 (green; J-K) merged with DAPI (blue; B, E, K) labelling of Shef3 hESCs cultured on MEFs under 20% oxygen on day 3 post-passage. FITC secondary antibody only = negative controls (G and M) merged with DAPI (blue, H and N). Phase contrast images of colonies (C, F, I, L, O). Scale bar = 100 μm.

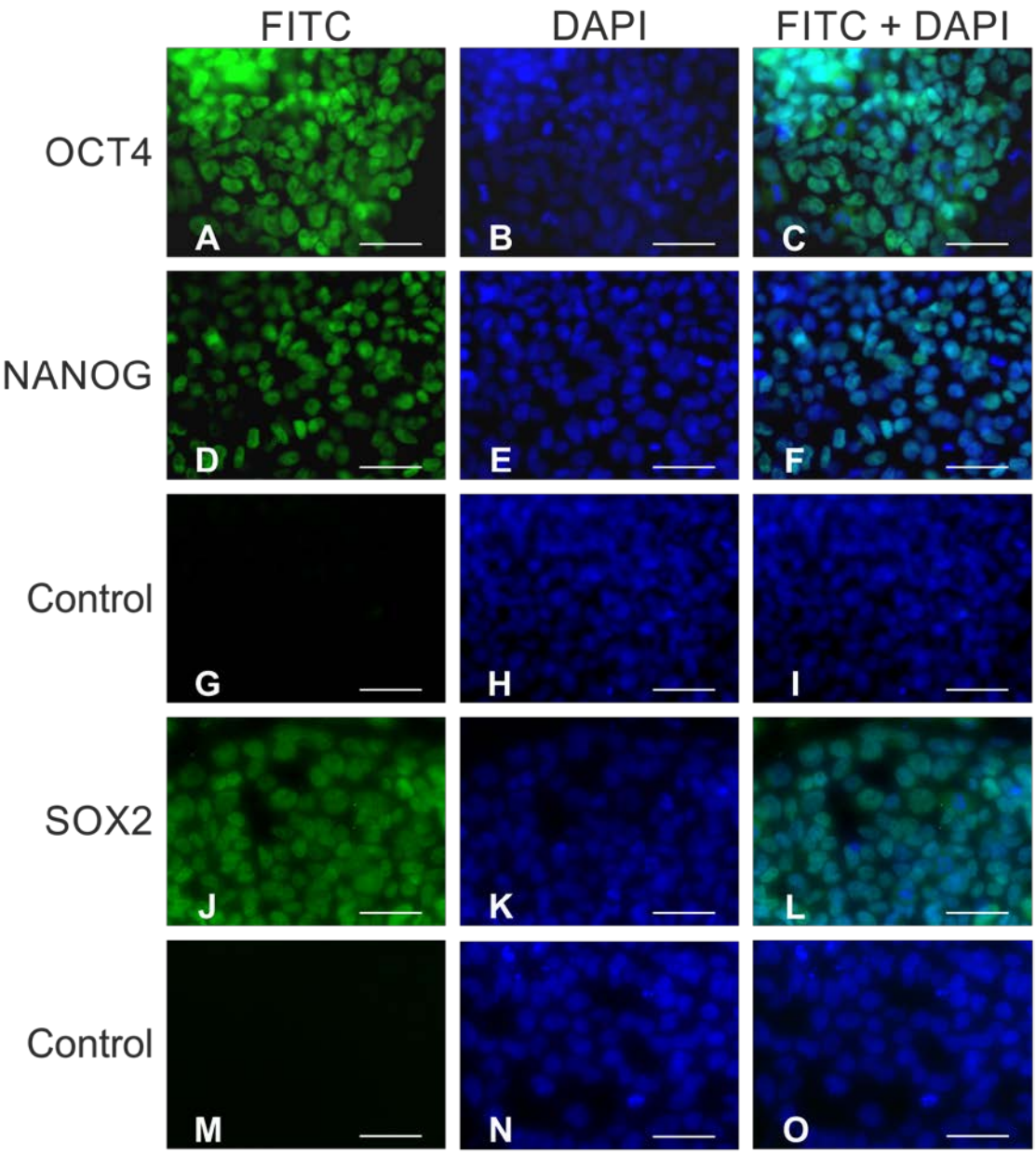

Figure 18: Characterisation of Shef3 hESCs at 20% oxygen

Immunocytochemistry of OCT4 (POU5F1) (green; A and C), NANOG (green; D and F) and SOX2 (green; J and L) merged with DAPI (blue; B, C; E, F and H, I) labelling of Shef3 hESCs cultured on MEFs under 20% oxygen on day 3 post-passage. FITC secondary antibody only = negative controls (G and I). Scale bar = 50 µm.

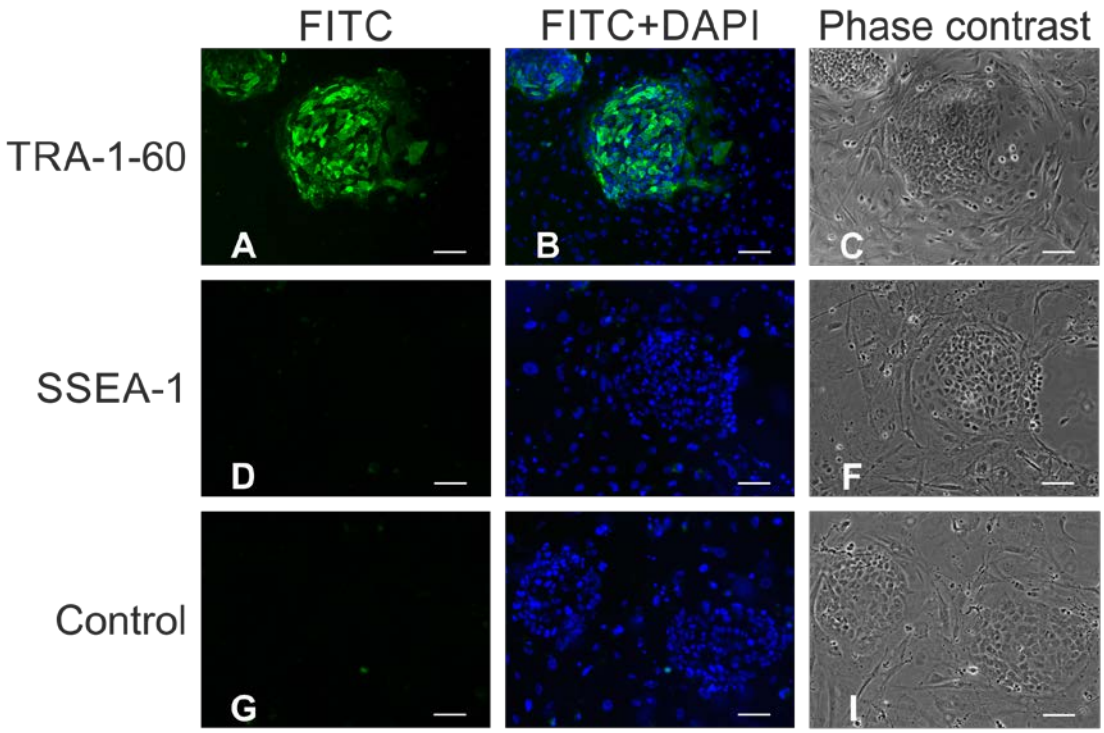

Figure 19: Expression of pluripotency and differentiation marker in Shef3 hESCs at 20% oxygen

Immunocytochemistry of pluripotency marker TRA-1-60 (green; A-B) and early differentiation marker SSEA-1 (green; D-E), merged with DAPI (blue; B and E) of Shef3 hESCs cultured on MEFs under 20% oxygen on day 3 post-passage. FITC secondary antibody only = negative controls (G, H). Phase contrast images of colonies (C, F, I). Scale bar = 100 µm.

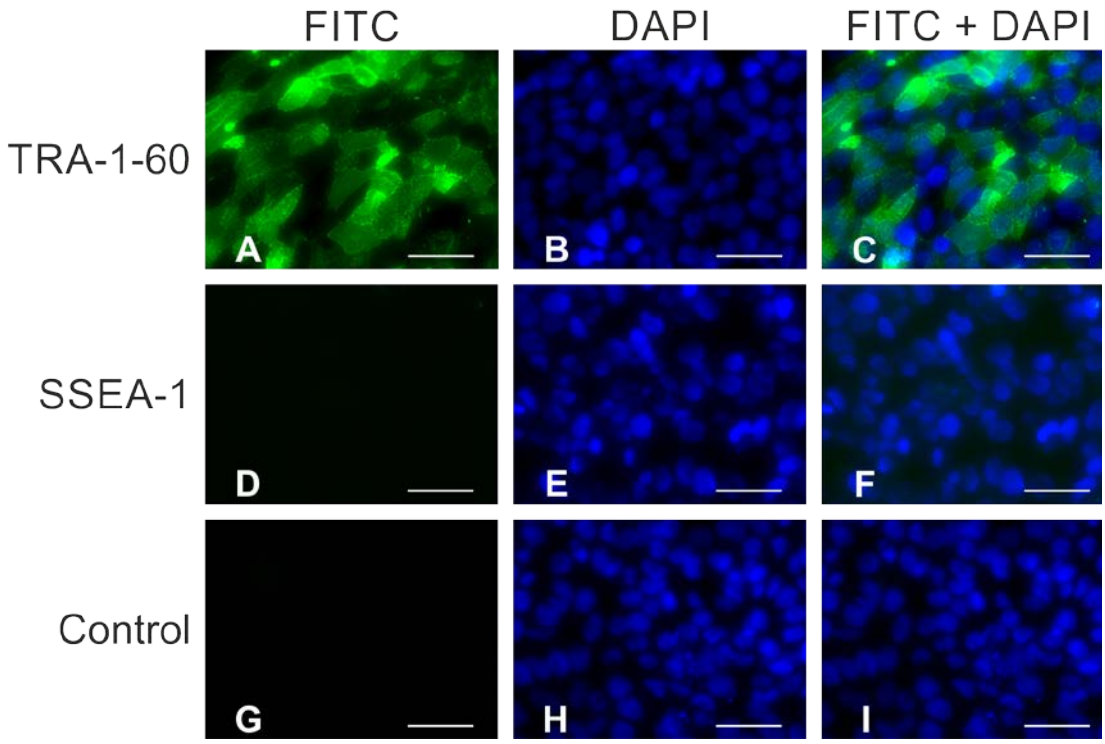

Figure 20: Characterisation of TRA-1-60 and SSEA-1 expression in Shef3 hESCs at 20% oxygen

Immunocytochemistry of pluripotency marker TRA-1-60 (green; A and C) and early differentiation marker SSEA-1 (green; D and F), DAPI (blue; B, E) and merged with DAPI (blue; C, F) of Shef3 hESCs cultured on MEFs under 20% oxygen on day 3 post-passage. FITC secondary antibody only = negative controls (G, I), DAPI (blue; H) merged with DAPI (blue; I). Scale bar = 50 µm.

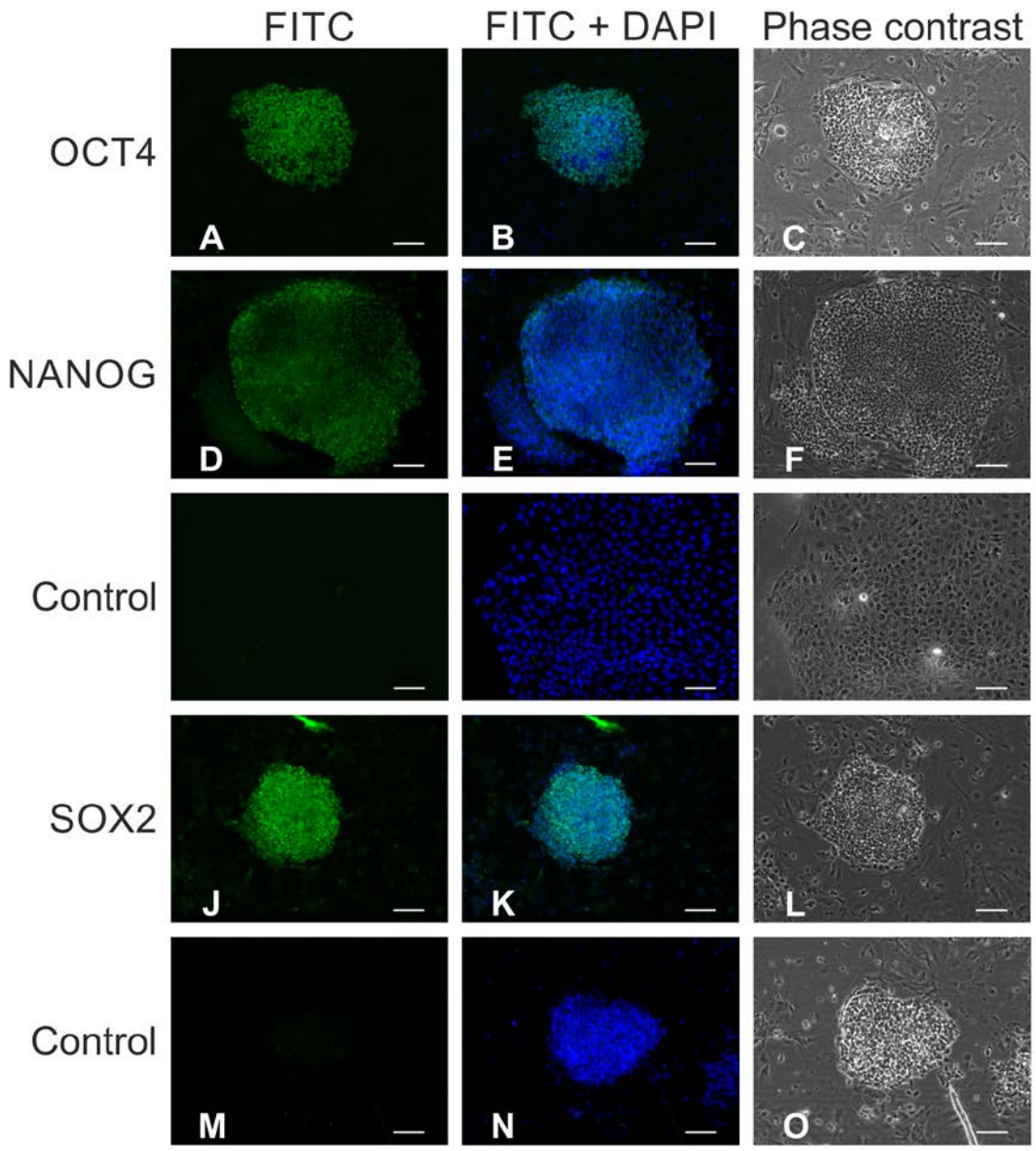

Figure 21: Expression of pluripotency markers in Hues7 hESCs at 5% oxygen

Immunocytochemistry of OCT4 (POU5F1) (green; A-B), NANOG (green; D-E) and SOX2 (green; J-K) merged with DAPI (blue; B, E, K) labelling of Hues7 hESCs cultured on MEFs under 5% oxygen on day 3 post-passage. FITC secondary antibody only = negative controls (G and M) merged with DAPI (blue, H and N). Phase contrast images of colonies (C, F, I, L, O). Scale bar = 100 µm.

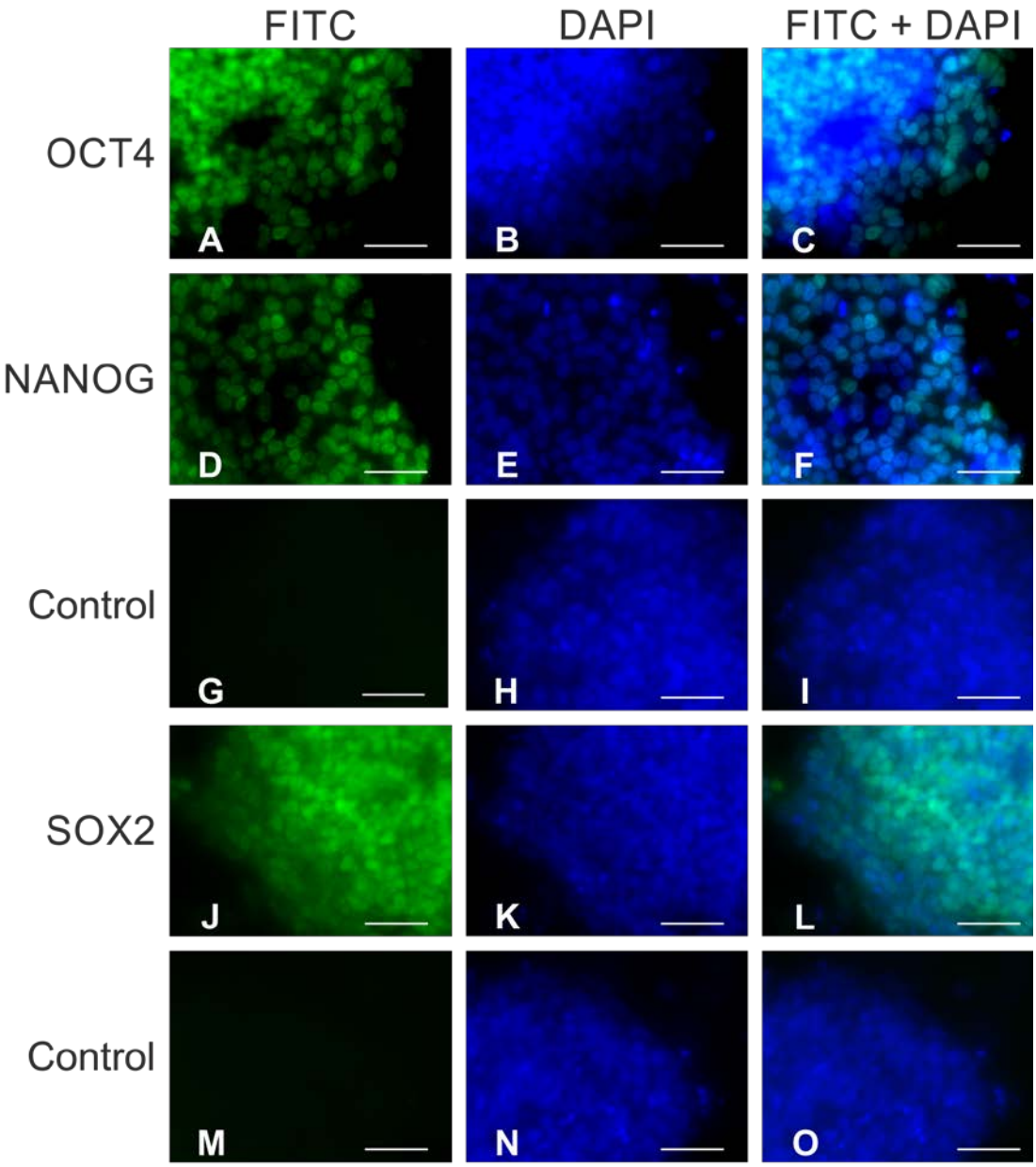

Figure 22: Characterisation of pluripotency markers in Hues7 hESCs at 5% oxygen

Immunocytochemistry of OCT4 (POU5F1) (green; A and C), NANOG (green; D and F) and SOX2 (green; J and L) merged with DAPI (blue; B-C; E-F and K-L) labelling of Hues7 hESCs cultured on MEFs under 5% oxygen on day 3 post-passage. FITC secondary antibody only = negative controls (G-M) merged with DAPI (H-I, N-O). Scale bar = 50 µm.

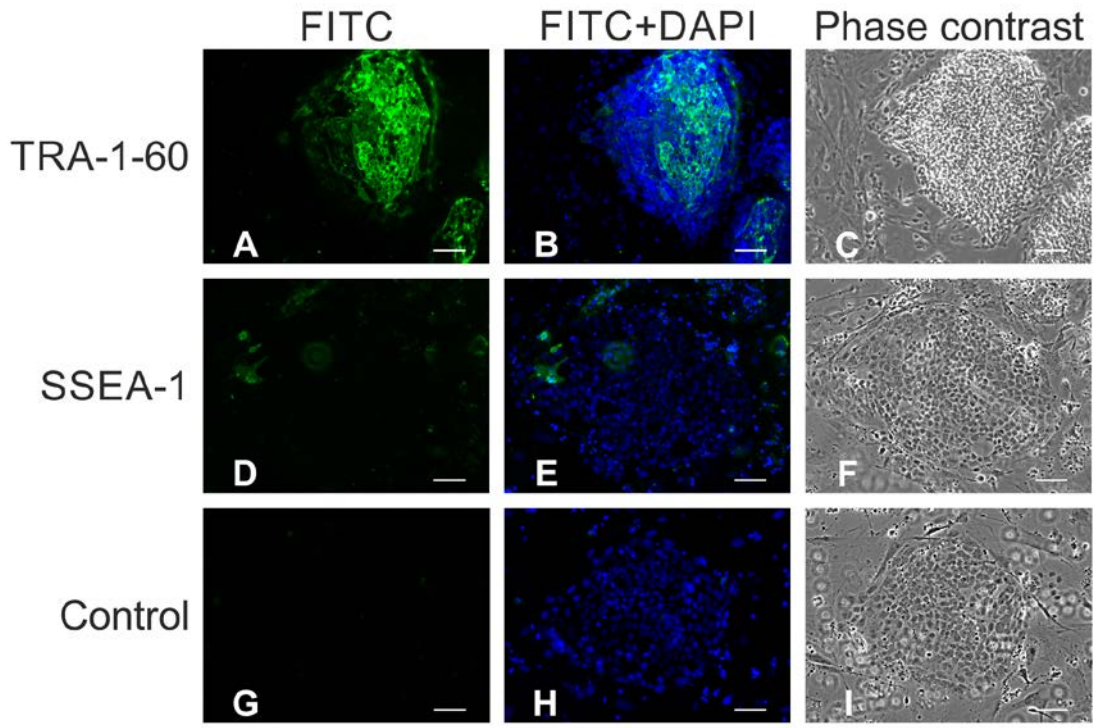

Figure 23: Expression of pluripotency and differentiation marker in Hues7 hESCs at 5% oxygen

Immunocytochemistry of pluripotency marker TRA-1-60 (green; A-B) and early differentiation marker SSEA-1 (green; D-E), merged with DAPI (blue; B and E) of Hues7 hESCs cultured on MEFs under 5% oxygen on day 3 post-passage. FITC secondary antibody only = negative controls (G, H). Phase contrast images of colonies (C, F, I). Scale bar = 100 µm.

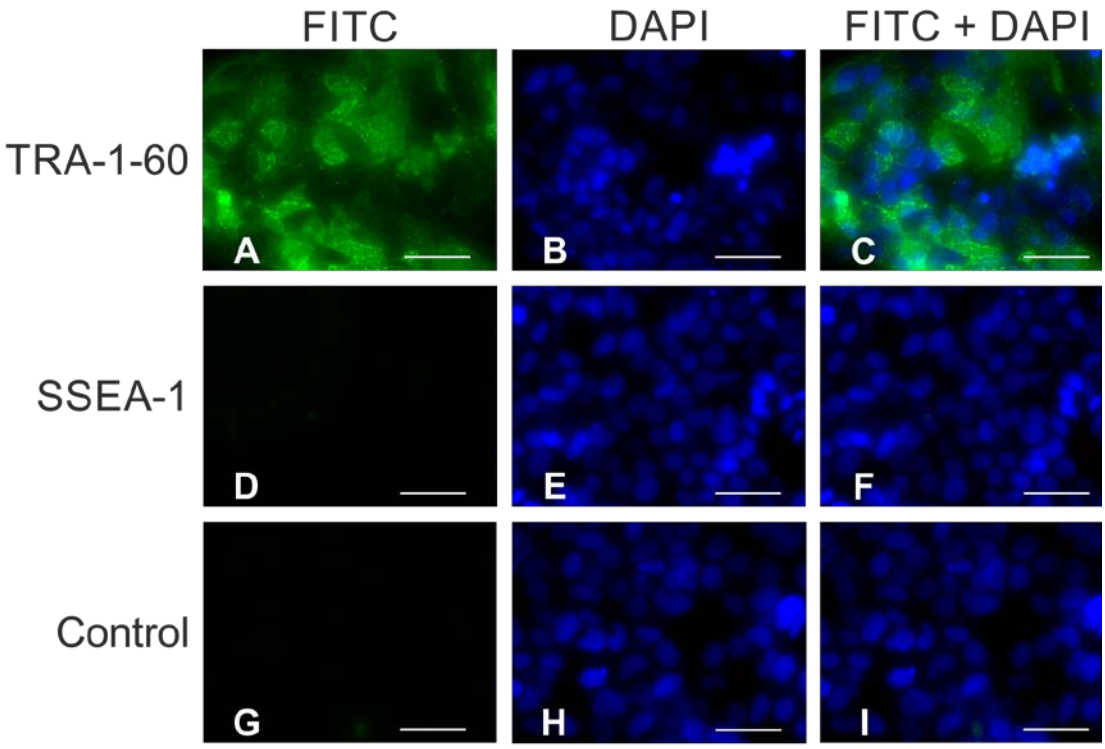

Figure 24: Characterisation of TRA-1-60 and SSEA-1 expression in Hues7 hESCs at 5% oxygen

Immunocytochemistry of pluripotency marker TRA-1-60 (green; A and C) and early differentiation marker SSEA-1 (green; D and F), DAPI (blue; B, E) and merged with DAPI (blue; C, F) of Hues7 hESCs cultured on MEFs under 5% oxygen on day 3 post-passage. FITC secondary antibody only = negative controls (G, I), DAPI (blue; H) merged with DAPI (blue; I). Scale bar = 50 μm.

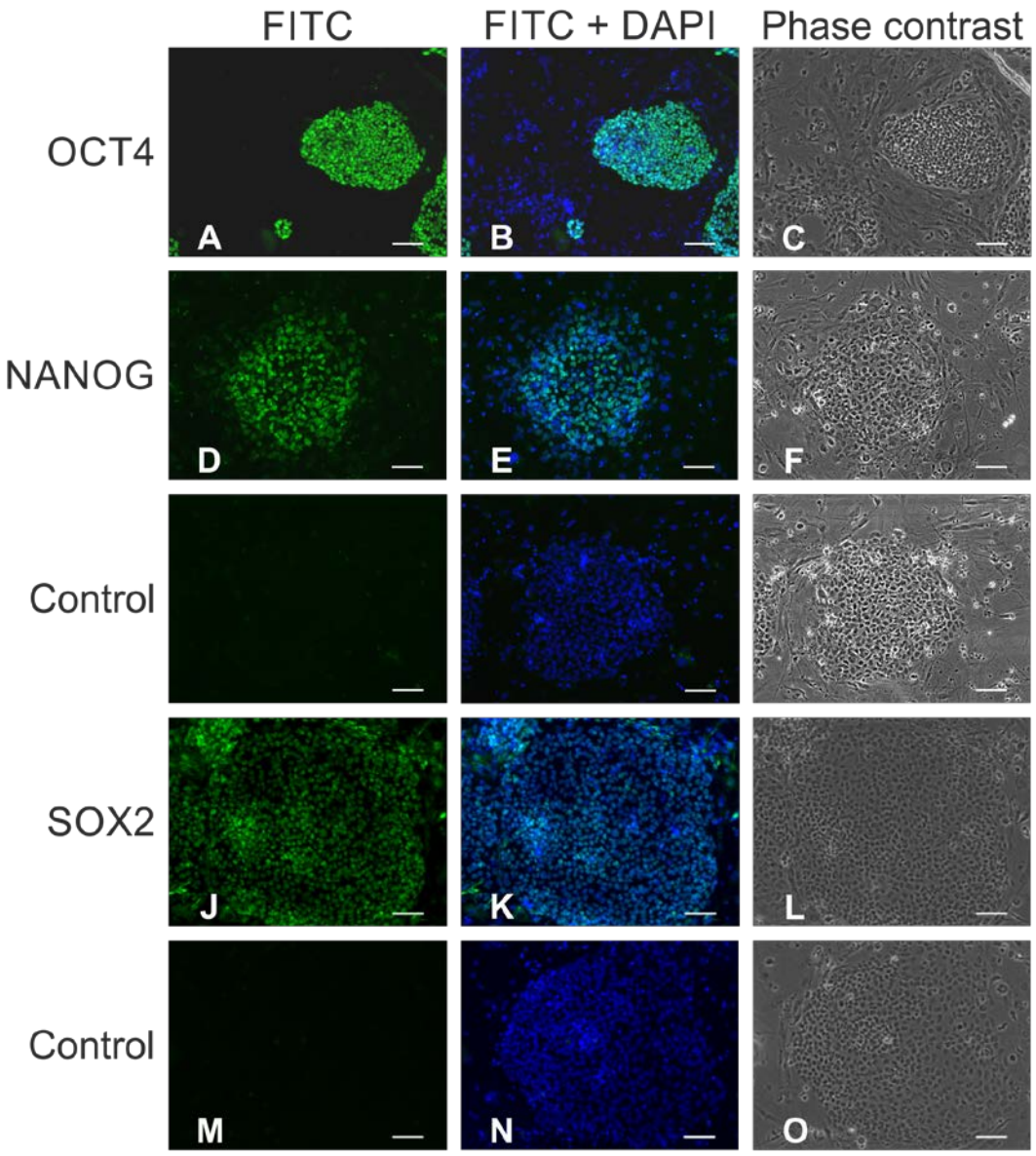

Figure 25: Expression of pluripotency markers in Hues7 hESCs at 20% oxygen

Immunocytochemistry of OCT4 (POU5F1) (green; A-B), NANOG (green; D-E) and SOX2 (green; J-K) merged with DAPI (blue; B, E, K) labelling of Hues7 hESCs cultured on MEFs under 20% oxygen on day 3 post-passage. FITC secondary antibody only = negative controls (G and M) merged with DAPI (blue, H and N). Phase contrast images of colonies (C, F, I, L, O). Scale bar = 100 μm.

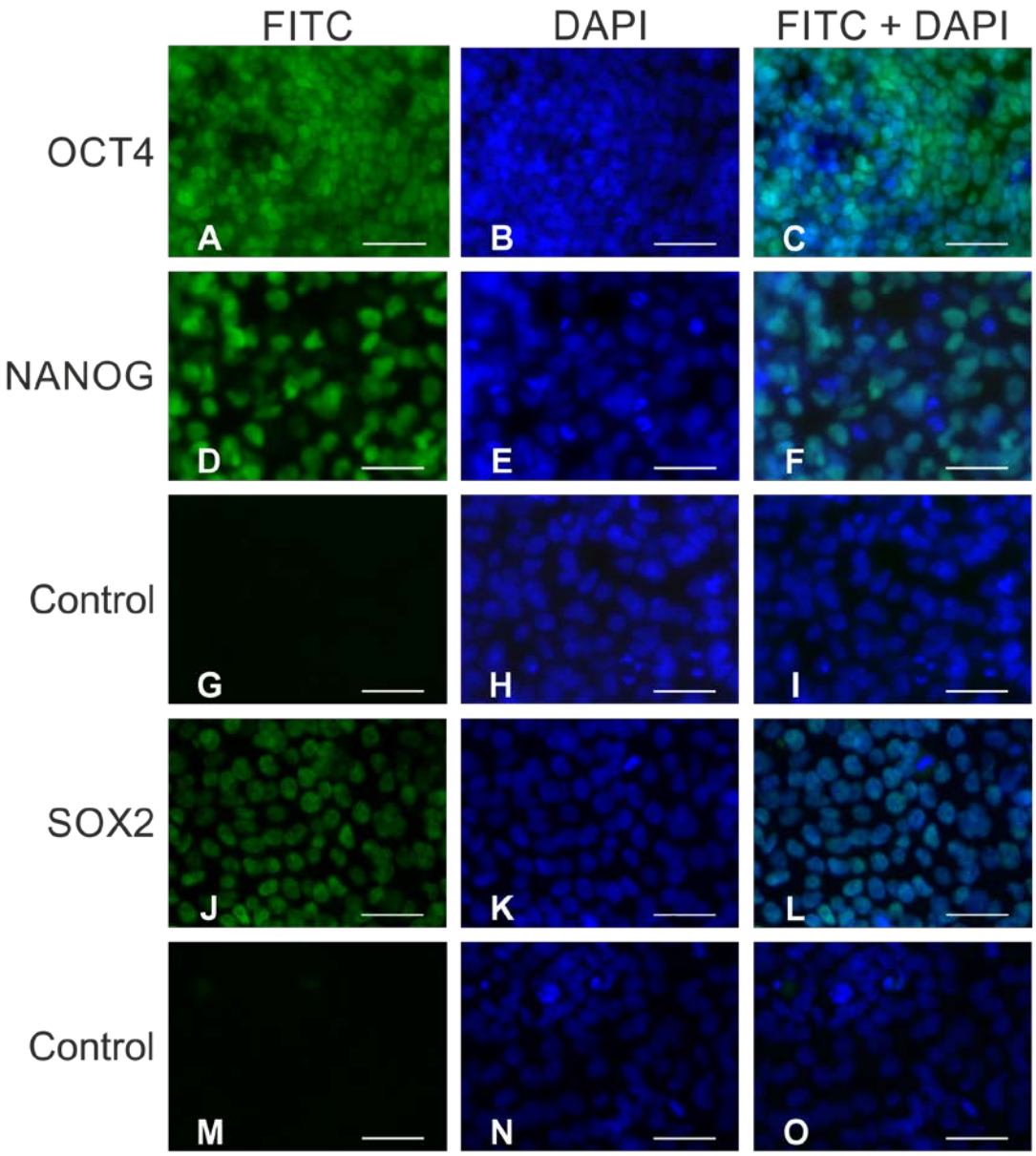

Figure 26: Characterisation of pluripotency markers in Hues7 hESCs at 20% oxygen

Immunocytochemistry of OCT4 (POU5F1) (green; A and C), NANOG (green; D and F) and SOX2 (green; J and L) merged with DAPI (blue; B, C; E, F and H, I) labelling of Hues7 hESCs cultured on MEFs under 20% oxygen on day 3 post-passage. FITC secondary antibody only = negative controls (G and I). Scale bar = 50 µm.

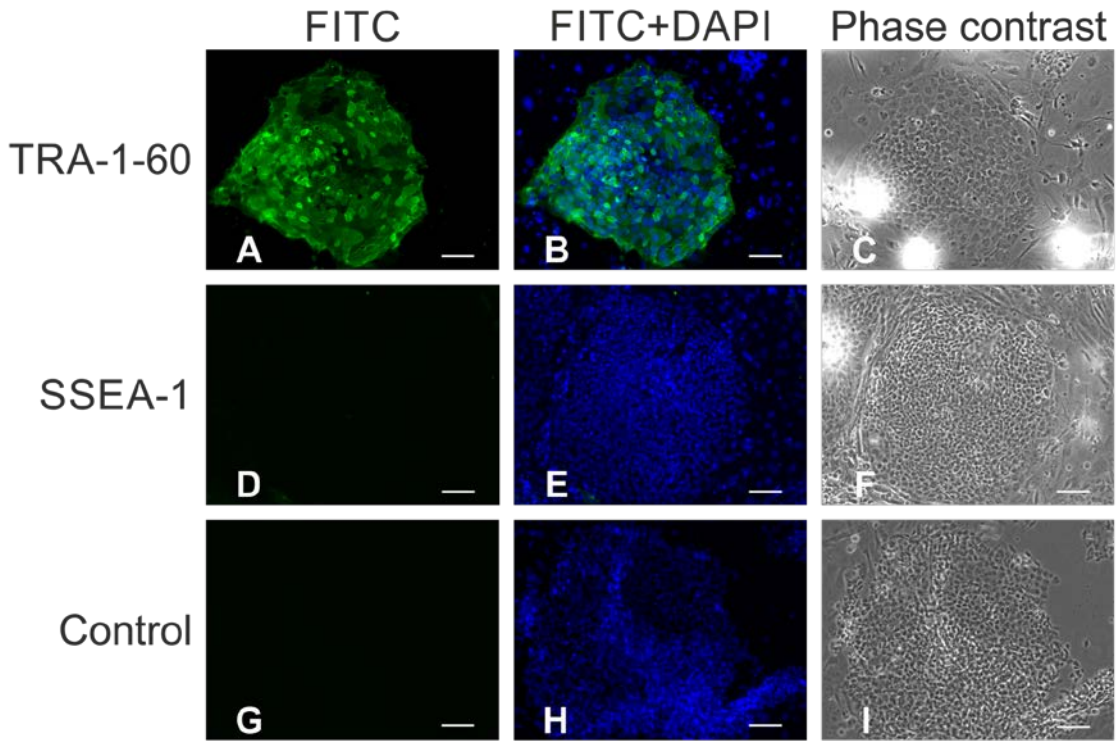

Figure 27: Expression of pluripotency and differentiation marker in Hues7 hESCs at 20% oxygen

Immunocytochemistry of pluripotency marker TRA-1-60 (green; A-B) and early differentiation marker SSEA-1 (green; D-E), merged with DAPI (blue; B and E) of Hues7 hESCs cultured on MEFs under 20% oxygen on day 3 post-passage. FITC secondary antibody only = negative controls (G, H). Phase contrast images of colonies (C, F, I). Scale bar = 100 µm.

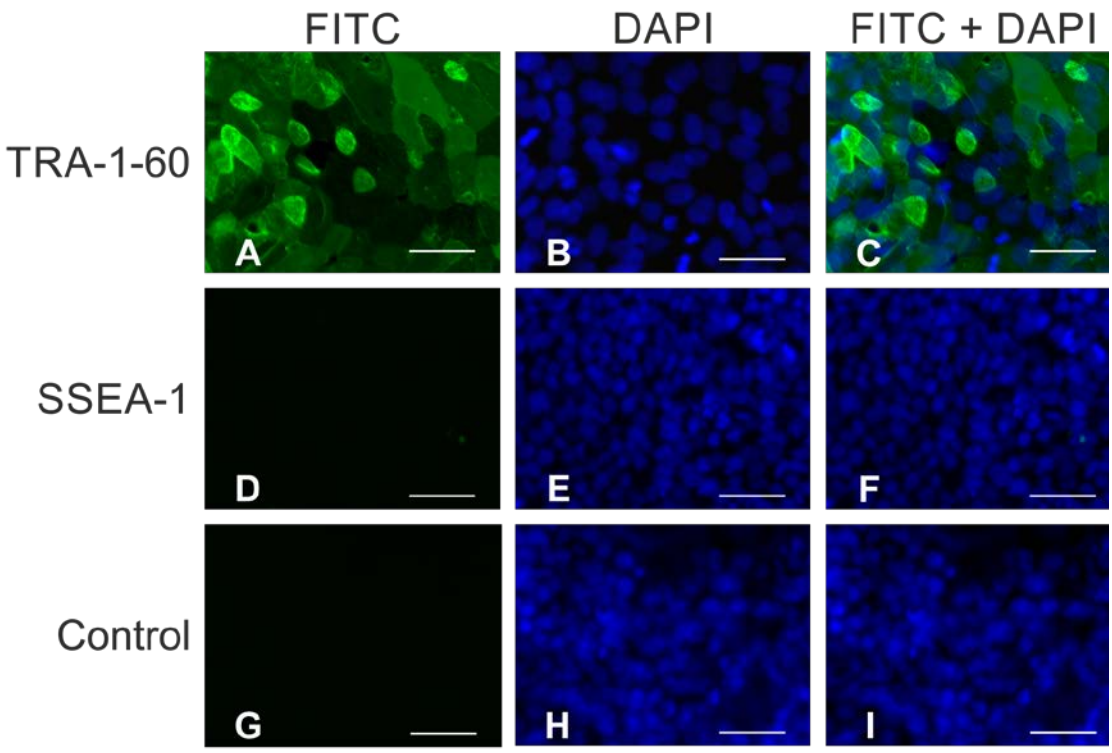

Figure 28: Characterisation of TRA-1-60 and SSEA-1 in Hues7 hESCs at 20% oxygen

Immunocytochemistry of pluripotency marker TRA-1-60 (green; A and C) and early differentiation marker SSEA-1 (green; D and F), DAPI (blue; B, E) and merged with DAPI (blue; C, F) of Hues7 hESCs cultured on MEFs under 20% oxygen on day 3 post-passage. FITC secondary antibody only = negative controls (G, I), DAPI (blue; H) merged with DAPI (blue; I). Scale bar = 50 µm.

To further confirm pluripotency in hESCs but to show quantitatively differential expression between the two oxygen concentrations, Western blots were performed for NANOG expression on Shef3 hESCs cultured at either 5% or 20% oxygen concentration. Figure 29 shows that hESCs cultured at 5% oxygen concentrations have a significant 5-fold greater NANOG protein expression than those cultured at 20% oxygen.

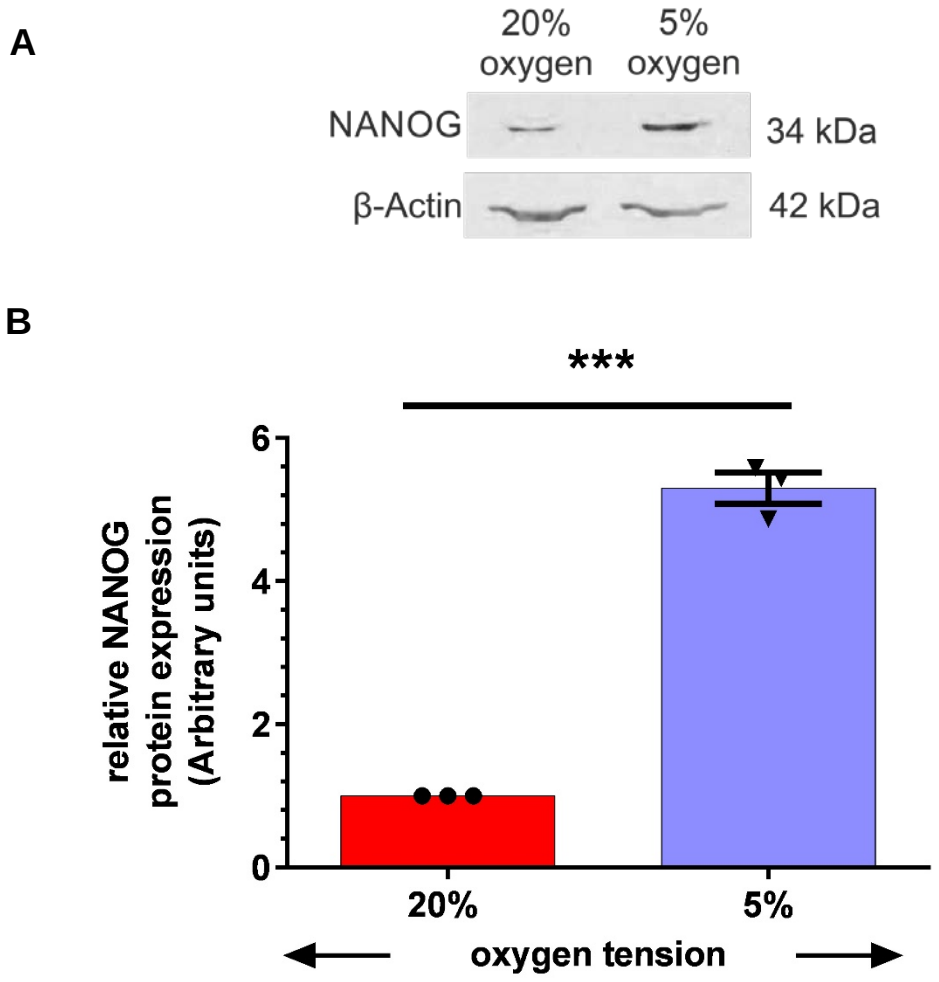

Figure 29: Relative NANOG protein expression in Shef3 hESCs cultured at either 20% or 5% oxygen

(A) Representative Western Blot of NANOG expression in hESCs cultured at either 20% or 5% oxygen

(B) Quantification of NANOG Western Blots. Data has been normalised to β-Actin and to 1 for 20% oxygen.Single points or triangles represent biological replicates and error bars represent mean ±SEM with p***≤0.001 and n=3.

3.3.2 Array analysis of miRNAs in hESCs cultured at either 5% or 20% oxygen

Shef3 hESCs were either cultured under physiological oxygen or atmospheric oxygen concentration and cells were lysed and collected for RNA isolation (see chapter 2.2.3.1). Isolated RNA was then reverse transcribed and processed as described in chapter 3.2.2.1. The phase contrast images of the Shef3 cell line reveal representative colonies cultured at either 5% or 20% oxygen tension, respectively (Figure 30). The colony surface of Shef3 hESCs cultured at 20 % oxygen tension is less smooth and they appear slightly less compact compared to those at 5% oxygen tension, therefore showing typical features of hESCs cultured at either 5% or 20% oxygen.

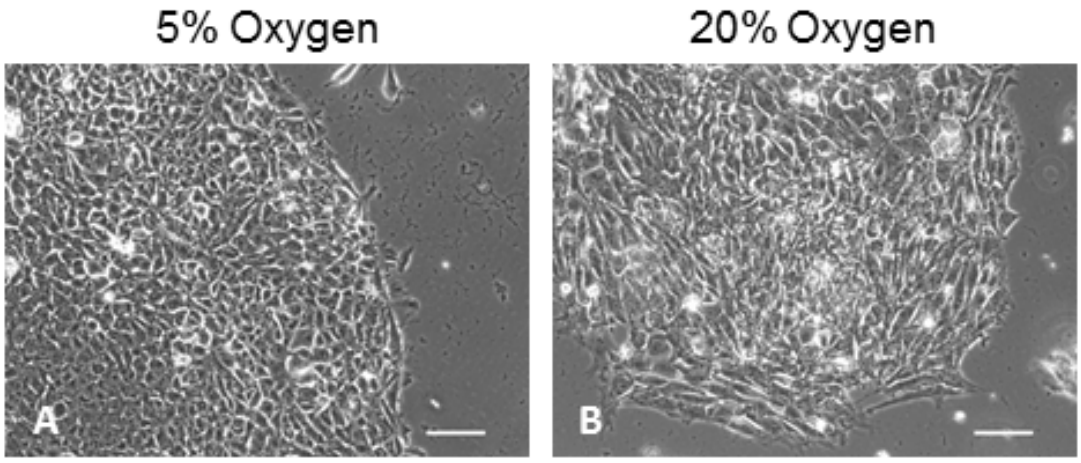

Figure 30: Shef3 hESC colonies for RNA collection
Representative phase contrast images of Shef3 hESC colonies on Matrigel coated plates cultured at either 5% or 20% oxygen for at least 3 passages. Cells were taken for RNA isolation on day 3 post-passage. Scale bar = 100 µm.

After RNA isolation and specific reverse transcription for miRNAs, TaqMan MicroRNA Arrays were performed to obtain the expression levels of 377 miRNAs and 4 controls.

To identify candidate miRNAs expressed in hESCs, three independent arrays were performed on hESCs cultured at either normoxic or hypoxic conditions. Each array consisted of 381 probes harbouring 377 human miRNAs. Three positive control genes and one negative arthropod miRNA were also included in the array. All miRNAs with a Ct value greater than 35 across all 6 arrays were deemed not to be expressed and eliminated from further analysis. This resulted in 146 miRNAs being discarded. Thus, 231 miRNAs were expressed in hESCs cultured at either 5% or 20% oxygen. To assess the absolute variation in miRNA expression between the array sets, the Ct values of the

231 expressed miRNAs were plotted in a box and whisker plot (Figure 31). Comparing each array set showed that 50% of the central miRNA expression data (depicted as box or interquartile range (IQR)) lay within very low expression values usually higher than Ct=30 and were shifted across the array sets. Therefore, variation in expression with batch number was seen to occur (Figure 31) highlighting the importance of normalising the data using a reference gene.

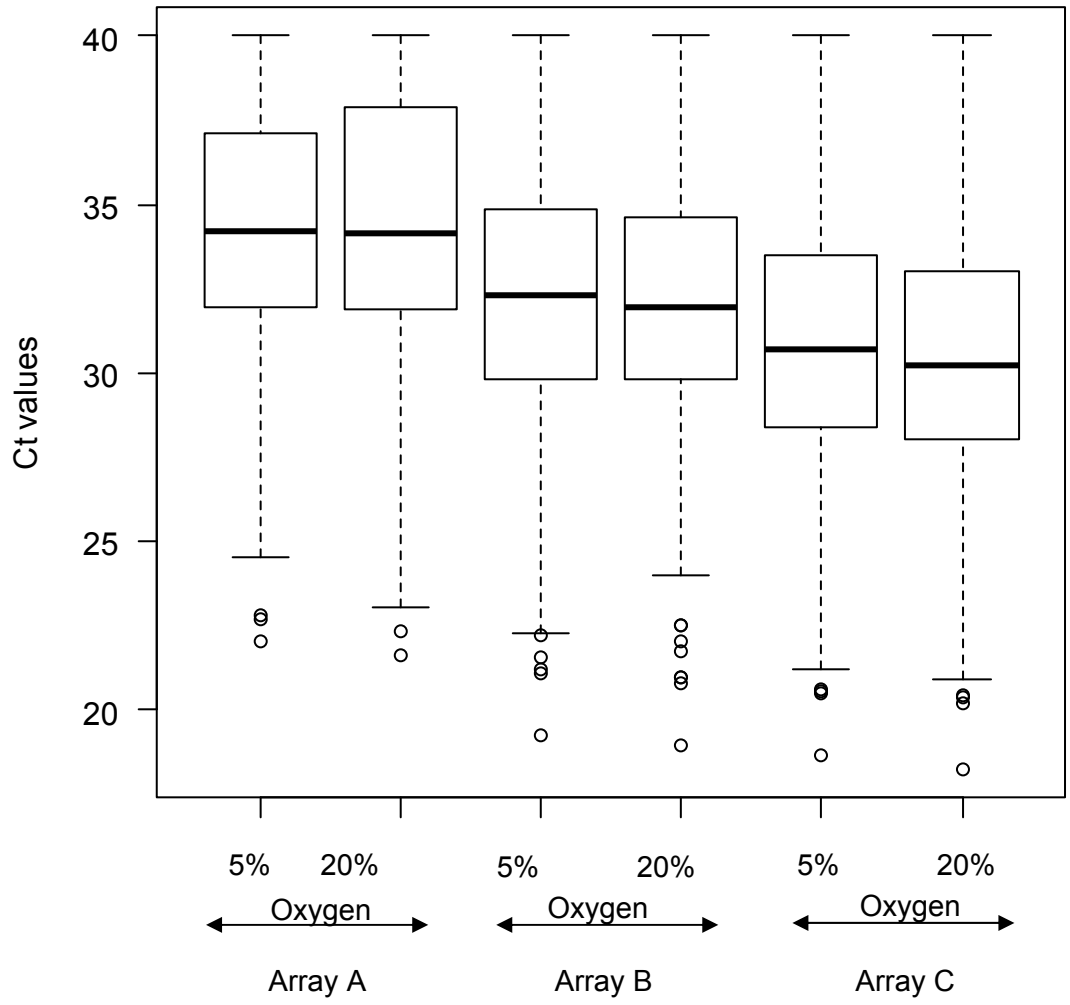

Figure 31: Absolute variation of miRNA expression data in hESCs cultured at either 5% or 20% oxygen

Box and whisker plot, showing the spread and differences of miRNA expression data across three independent array-sets (A, B, C) from hESCs cultured at either 5% or 20% oxygen. The box or interquartile range (IQR) depicts 50% of the central miRNA expression data divided by the median (bold black line). Beyond the boxes whiskers extend to a maximum of 1.5 x IQR on each side (Turkey style) and represent each 25% of the miRNA expression data. Open circles are outliers. n= 231. (This graph was produced with the help of Patrick Stumpf, Bone & Joint Research Group, University of Southampton)

The plot of the raw data (Figure 31) together with D'Agostino & Pearson Omnibus K2 normality test indicated that the data for Array A 5% and 20% (p=0.0236 and p=0.0157 respectively) were not normally distributed. Therefore, a Kruskal-Wallis test was performed on the raw data and revealed significant differences amongst the groups (Shef3 at 5% oxygen p<0.0001; Shef3 at 20% oxygen p<0.0001) which underpins the necessity of normalisation.

To compare miRNA expression between the arrays the normalisation required using an appropriate reference gene. Therefore, RNU44, MammU6 and RNU48 were each expressed at similar levels in hESCs cultured at 5% and 20% oxygen (Table 20). However, RNU44 was used to normalise the miRNA-array data since it showed the least variation between 5% and 20% oxygen of each batch with an average ΔCt of only 0.322 (Table 20) whereas the average ΔCt of RNU48 was 0.439 and MammU6 had an average ΔCt of 0.849.

Table 20: Absolute expression values of positive control genes and negative arthropod miRNA in hESCs of three independent array-sets

+ve control genes & -ve miRNA	Ct values 5%			Ct values 20%			Average ΔCt
	A	B	C	A	B	C	
RNU44	28.074	25.287	24.175	28.032	25.849	24.621	0.322
MammU6	20.929	20.015	18.358	21.043	20.792	20.015	0.84933
RNU48	24.633	23.57	21.919	24.843	23.611	22.984	0.43867
ath-miR-159a	40	40	40	40	40	40	

Normalising or calculating the ΔCt values from each miRNA with the endogenous control RNU44 and plotting them again in a box and whisker plot shows that the same miRNA-array data are now more similar across the three sets of arrays (Figure 32).

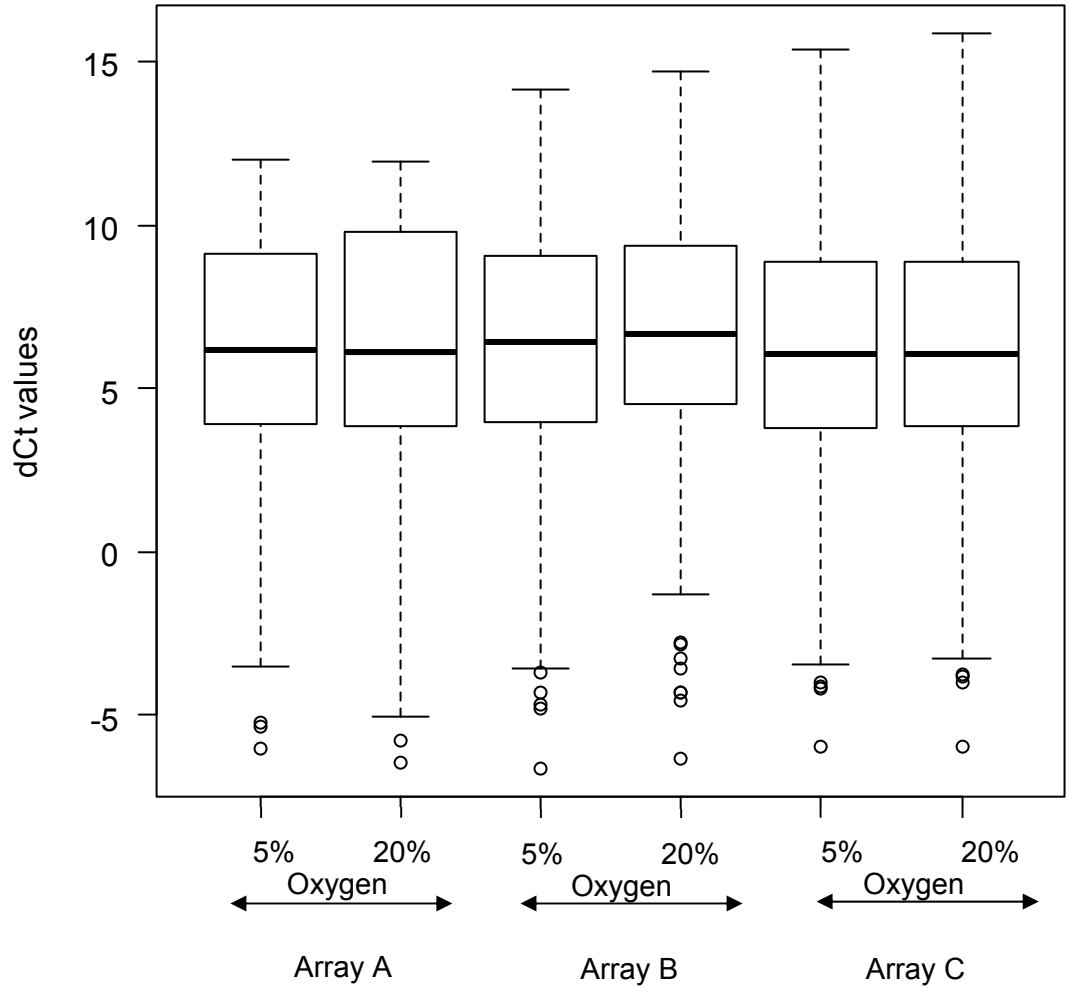

Figure 32: Normalised miRNA expression data in hESCs cultured at either 5% or 20% oxygen concentration

Box and whisker plot, showing the spread and differences of miRNA expression data across three independent array-sets (A, B, C) from hESCs cultured at either 5% or 20% oxygen. The box or interquartile range (IQR) depicts 50% of the central miRNA expression data divided by the median (bold black line). Beyond the boxes whiskers extend to a maximum of 1.5 x IQR (Turkey style) and represent each 25% of the miRNA expression data. Open circles are outliers. Data were normalised to the reference gene RNU44, n=231 (This graph was produced with the help of Patrick Stumpf, Bone & Joint Research Group, University of Southampton).

The plot of the data normalised to RNU44 and performing again a Kruskal-Wallis test demonstrated that the normalisation with the reference gene RNU44 was successful as there was no significant difference detected between the miRNA expression data of the three arrays for 5% oxygen. Further there was no significant difference detected between the miRNA expression data of the three arrays for 20% oxygen. Whiskers outside the lower and upper quartiles indicate variability though, which was expected taking into account that each miRNA was only represented once on every array card and that some miRNAs will be expressed at a higher level than the majority. Data which were not inside the 1.5 x IQR are shown as outliers and plotted individually as dots. Those outliers could be miRNAs of interest, indicating very high expression values. Differences in miRNAs which are highly expressed also mean that these miRNAs are more abundantly expressed in hESCs and could therefore play important roles in gene regulation.

To reveal miRNAs differentially expressed in hESCs in hypoxia compared to normoxia, the delta delta Ct method (ΔΔCt) was used (Chapter 3.2.1), while normalising the expression data to the endogenous control RNU44. miRNAs were assumed to be differentially expressed when the ΔΔCt values were either greater than 0.3 or smaller than -0.3. Positive or negative ΔΔCt values depict miRNAs that are either down- or up-regulated under hypoxia respectively. Therefore, Array A showed 155, array B 180 and array C 156 miRNAs which were differentially expressed in hESCs cultured under hypoxic conditions compared to those maintained at 20% oxygen (Table 21).

Table 21: Differentially expressed miRNAs in hESCs cultured at either 5% or 20% oxygen

Number of differentially expressed miRNAs in hESCs that were extracted from three independent array-sets when hypoxia was compared to normoxia, using RNU44 as reference gene.

Differentially expressed miRNAs	**Array A**	**Array B**	**Array C**
down-regulated in hypoxia	77	117	68
up-regulated in hypoxia	78	63	88
total number	155	180	156
% of the 231 miRNAs expressed	=67%	=78%	=68%

To identify miRNAs of interest, all differentially expressed miRNAs were compared between the arrays. This resulted in a number of miRNAs in hESCs which were up- or down-regulated under hypoxic conditions when compared to those cultured at 20% oxygen. 20 miRNAs were found to be consistently up – regulated and 20 miRNAs were also found to be consistently down-regulated in hESCs under hypoxia compared to normoxia across the arrays (Figure 33 and Table 22-23).

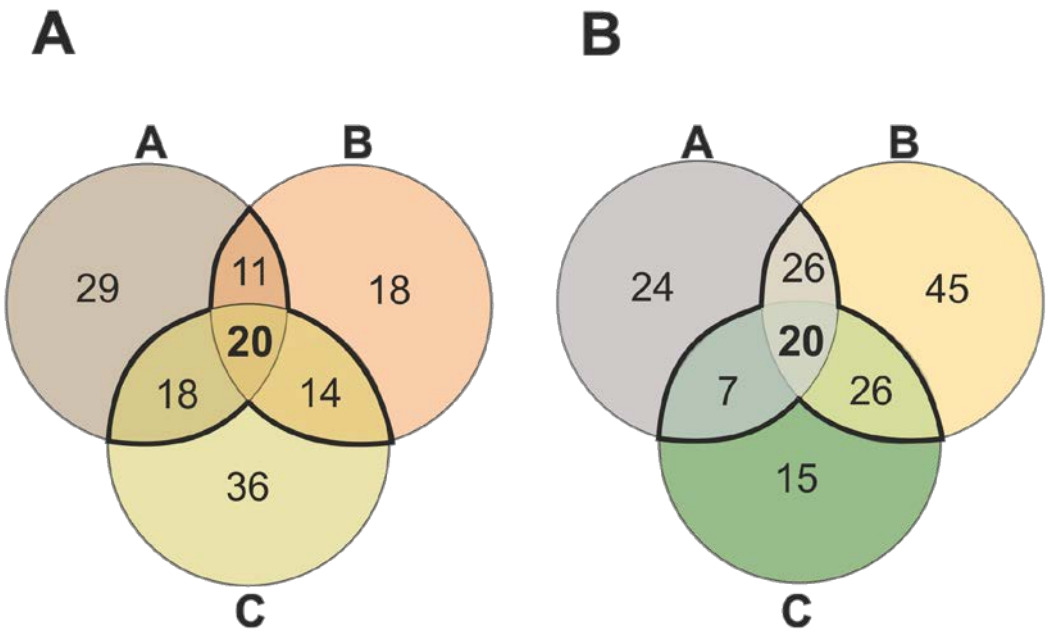

Figure 33: Number of differential expressed miRNAs across each of the array-sets

Venn-diagram, showing the number of miRNAs (A) up-regulated and (B) down-regulated in hESCs under hypoxia compared to normoxia. Three independent array-sets are depicted and normalised to RNU44. Intersecting circles depict miRNAs that are common between the array-sets.

From 231 miRNAs that were expressed across the arrays only 40 were consistently differentially expressed with 20 being up- and 20 down-regulated. This may represent variability in the hESC starting population. However, array B contained 180 differentially expressed miRNAs, almost 10% more than array A or C (Table 21). Which resulted in the greater number of 45 miRNAs down-regulated only in array B (Figure 33 B). Variability between the arrays was also seen in the number of up-regulated miRNAs (Figure 33 A), where array A contained 29 and array C 36 non-concurrently up-regulated miRNAs.

Table 22: List of down-regulated miRNAs expressed in hESCs cultured at 5% oxygen compared to 20% oxygen. MiRNAs down-regulated in at least two of the array sets are depicted.

Number according to array Card A	Array AB	Array BC	Array AC	Array ABC
8	hsa-let-7c	hsa-let-7c	hsa-let-7c	hsa-let-7c
9		hsa-let-7d		
10	hsa-let-7e	hsa-let-7e	hsa-let-7e	hsa-let-7e
16		hsa-miR-103		
21	hsa-miR-10a			
23	hsa-miR-122			
27	hsa-miR-125b	hsa-miR-125b	hsa-miR-125b	hsa-miR-125b
38	hsa-miR-133b			
46	hsa-miR-139			
53	hsa-miR-145			
54	hsa-miR-146a			
61		hsa-miR-149		
63	hsa-miR-152			
66		hsa-miR-15a		
76	hsa-miR-186			
77	hsa-miR-187			
82	hsa-miR-191			
85	hsa-miR-193a-5p	hsa-miR-193a-5p	hsa-miR-193a-5p	hsa-miR-193a-5p
89		hsa-miR-196b		
92	hsa-miR-199a			
100		hsa-miR-202		
101	hsa-miR-203	hsa-miR-203	hsa-miR-203	hsa-miR-203
107		hsa-miR-20b		
110	hsa-miR-211			
112		hsa-miR-214		
117		hsa-miR-218		
120		hsa-miR-219		
125		hsa-miR-221		
127	hsa-miR-223			
131	hsa-miR-24			
134	hsa-miR-26b			
135			hsa-miR-27a	
136			hsa-miR-27b	
139		hsa-miR-296		
144	hsa-miR-29a			
154	hsa-miR-31			
155			hsa-miR-32	
167	hsa-miR-331-5p	hsa-miR-331-5p	hsa-miR-331-5p	hsa-miR-331-5p
177	hsa-miR-345			

Number according to array Card A	Array AB	Array BC	Array AC	Array ABC
179	hsa-miR-34a	hsa-miR-34a	hsa-miR-34a	hsa-miR-34a
182		hsa-miR-362		
192		hsa-miR-373		
194	hsa-miR-374b	hsa-miR-374b	hsa-miR-374b	hsa-miR-374b
207		hsa-miR-410		
212	hsa-miR-424	hsa-miR-424	hsa-miR-424	hsa-miR-424
224	hsa-miR-452	hsa-miR-452	hsa-miR-452	hsa-miR-452
227			hsa-miR-455-3p	
228		hsa-miR-455-5p		
229	hsa-miR-483-5p			
230		hsa-miR-484		
233	hsa-miR-486-3p			
238		hsa-miR-489		
249		hsa-miR-500		
251		hsa-miR-501		
252	hsa-miR-502-3p			
268	hsa-miR-515-3p			
273	hsa-miR-517b	hsa-miR-517b	hsa-miR-517b	hsa-miR-517b
275	hsa-miR-518a			
280		hsa-miR-518d		
284	hsa-miR-519c-3p	hsa-miR-519c-3p	hsa-miR-519c-3p	hsa-miR-519c-3p
289			hsa-miR-520b	
292		hsa-miR-520f		
295	hsa-miR-522	hsa-miR-522	hsa-miR-522	hsa-miR-522
296			hsa-miR-523	
299			hsa-miR-525-5p	
301	hsa-miR-532	hsa-miR-532	hsa-miR-532	hsa-miR-532
302	hsa-miR-532-5p	hsa-miR-532-5p	hsa-miR-532-5p	hsa-miR-532-5p
308	hsa-miR-545	hsa-miR-545	hsa-miR-545	hsa-miR-545
311		hsa-miR-548b		
322	hsa-miR-574-3p	hsa-miR-574-3p	hsa-miR-574-3p	hsa-miR-574-3p
337		hsa-miR-625		
341	hsa-miR-636			
344	hsa-miR-652			
349		hsa-miR-660		
353	hsa-miR-708	hsa-miR-708	hsa-miR-708	hsa-miR-708

Number according to array Card A	Array AB	Array BC	Array AC	Array ABC
368	hsa-miR-888	hsa-miR-888	hsa-miR-888	hsa-miR-888
378	hsa-miR-96			
379	hsa-miR-98	hsa-miR-98	hsa-miR-98	hsa-miR-98
380		hsa-miR-99a		

Table 23 : List of up-regulated miRNAs expressed in hESCs cultured at 5% oxygen compared to 20% oxygen. MiRNAs up-regulated in at least two of the array sets are depicted.

Number according to array Card A	Array AB	Array BC	Array AC	Array ABC
5		has-miR-155		
12			hsa-let-7g	
14			hsa-miR-100	
15	hsa-miR-101			
31	hsa-miR-128			
32		hsa-miR-129		
37			hsa-miR-133a	
40	hsa-miR-135a	hsa-miR-135a	hsa-miR-135a	hsa-miR-135a
49			hsa-miR-141	
60			hsa-miR-148b	
67	hsa-miR-15b	hsa-miR-15b	hsa-miR-15b	hsa-miR-15b
73	hsa-miR-183	hsa-miR-183	hsa-miR-183	hsa-miR-183
74			hsa-miR-184	
75	hsa-miR-185	hsa-miR-185	hsa-miR-185	hsa-miR-185
79	hsa-miR-18a			
87	hsa-miR-194	hsa-miR-194	hsa-miR-194	hsa-miR-194
88			hsa-miR-195	
95	hsa-miR-19a			
98	hsa-miR-200b	hsa-miR-200b	hsa-miR-200b	hsa-miR-200b
99	hsa-miR-200c	hsa-miR-200c	hsa-miR-200c	hsa-miR-200c
102	hsa-miR-204			
109	hsa-miR-210	hsa-miR-210	hsa-miR-210	hsa-miR-210
111	hsa-miR-212	hsa-miR-212	hsa-miR-212	hsa-miR-212
113	hsa-miR-215	hsa-miR-215	hsa-miR-215	hsa-miR-215
128	hsa-miR-224			
132			hsa-miR-25	
138	hsa-miR-28-5p	hsa-miR-28-5p	hsa-miR-28-5p	hsa-miR-28-5p
140	hsa-miR-296-5p	hsa-miR-296-5p	hsa-miR-296-5p	hsa-miR-296-5p
148			hsa-miR-301b	
164			hsa-miR-330	

Number according to array Card A	Array AB	Array BC	Array AC	Array ABC
168			hsa-miR-335	
180	hsa-miR-34c-5p			
184			hsa-miR-363	
190			hsa-miR-371-3p	
210	hsa-miR-422a			
214	hsa-miR-429	hsa-miR-429	hsa-miR-429	hsa-miR-429
218		hsa-miR-449a		
222		hsa-miR-450b		
241		hsa-miR-491		
244		hsa-miR-494		
254		hsa-miR-503		
255			hsa-miR-504	
265		hsa-miR-512		
269	hsa-miR-515-5p	hsa-miR-515-5p	hsa-miR-515-5p	hsa-miR-515-5p
271	hsa-miR-516b	hsa-miR-516b	hsa-miR-516b	hsa-miR-516b
272	hsa-miR-517a			
277	hsa-miR-518b	hsa-miR-518b	hsa-miR-518b	hsa-miR-518b
278	hsa-miR-518c	hsa-miR-518c	hsa-miR-518c	hsa-miR-518c
282		hsa-miR-518f		
283	hsa-miR-519a	hsa-miR-519a	hsa-miR-519a	hsa-miR-519a
286	hsa-miR-519e			
293			hsa-miR-520g	
300	hsa-miR-526b			
323		hsa-miR-576		
325		hsa-miR-579		
326		hsa-miR-582		
329			hsa-miR-590-5p	
331			hsa-miR-598	
335		hsa-miR-618		
339			hsa-miR-628	
350	hsa-miR-671-3p	hsa-miR-671-3p	hsa-miR-671-3p	hsa-miR-671-3p
364	hsa-miR-885-5p	hsa-miR-885-5p	hsa-miR-885-5p	hsa-miR-885-5p
377		hsa-miR-95		

The differential expression values (ΔΔCt values) for the 20 consistently up- and down-regulated miRNAs can be found in a heatmap (Figure 34). The heatmap displays miRNAs up-regulated as negative ΔΔCt values, coded in blue and positive ΔΔCt values are labelled in red for these miRNAs down-regulated in hESCs cultured at 5% oxygen compared to 20% oxygen. As expected, the hypoxamir miR-210 was found to be one of the miRNAs up-regulated in hESCs cultured in hypoxic conditions across all three arrays and thus can be used not only as positive control but also to validate the data obtained (Table 23 and Figure 34). All miRNAs differentially expressed in at least two arrays were of potential interest and therefore used in subsequent bioinformatic analysis.

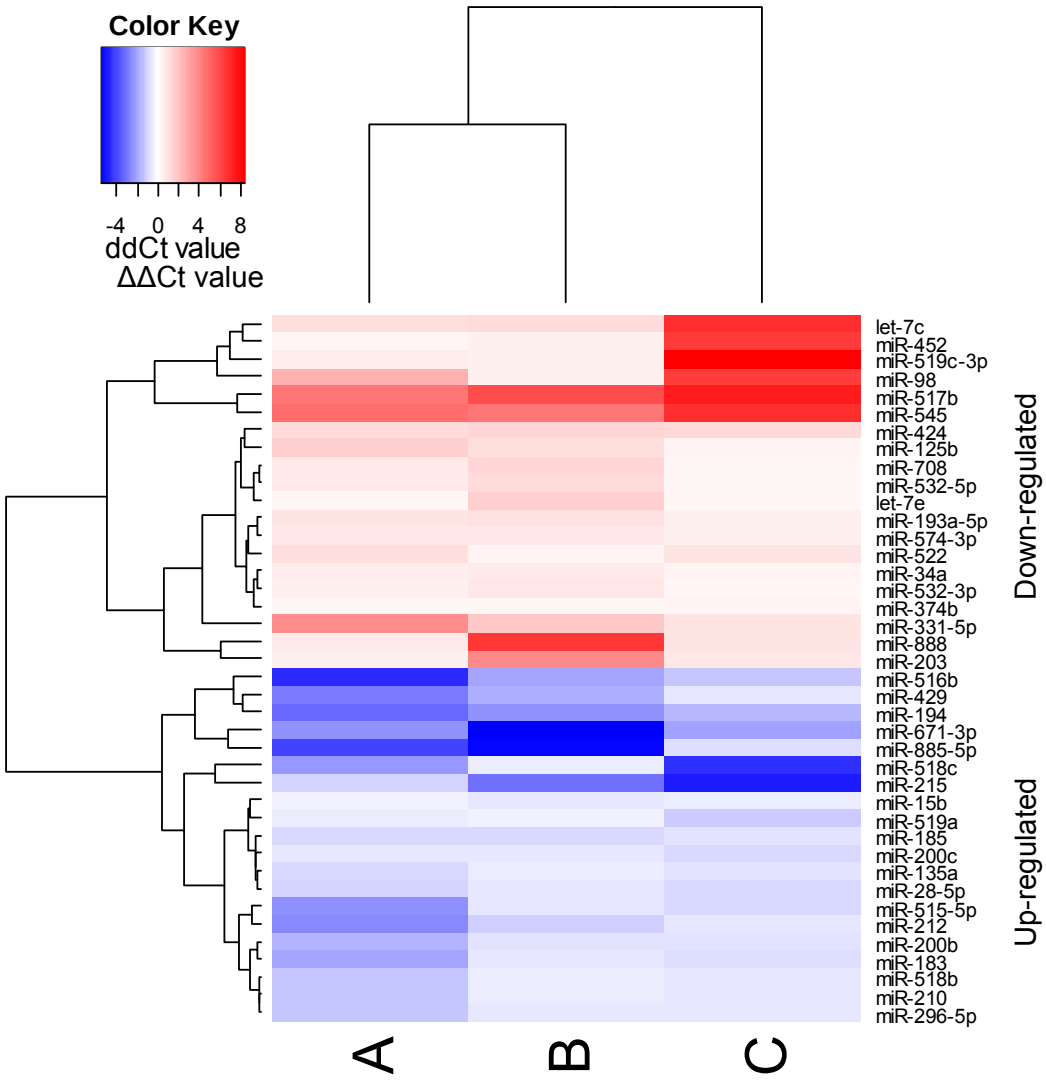

Figure 34: Heat-map, expression of the consistently up- and down-regulated miRNAs in hESCs across 3 array sets under hypoxia compared to normoxia (A, B, C)

Negative values (blue) show up-regulated and positive values (red) down-regulated miRNAs in hESCs under hypoxia compared to normoxia, using RNU44 as reference gene. Differences of less than ±0.3 in ddCt were not considered as differentially expressed and are therefore not displayed. (This graph was produced with the help of Patrick Stumpf, Bone & Joint Research Group, University of Southampton)

3.3.3 Bioinformatic Analysis - miRNA target mining

The analysis of the 3 array data sets revealed several miRNAs that were differentially expressed in hESCs under hypoxia compared to normoxia. This resulted in a comprehensive list of 40 robust differentially expressed miRNAs. These, together with miRNAs differentially expressed in at least two arrays provided a platform for bioinformatics analysis.

TargetScanHuman 6.2 (TargetScan) was mainly used as a bioinformatic database to predict and identify both, mRNA and miRNA targets of interest. Since hESCs cultured under hypoxia display increased pluripotency, an elevated glucose uptake and lactate production and an increased expression of HIFs, the genes that are involved in these processes were taken as targets of interest. Thus, miRNAs may act to regulate these genes. According to miRNA biogenesis and function, miRNAs usually target the 3'UTR of their target mRNA which generally leads to translational inhibition or degradation of their target genes. The aim was to focus on miRNAs being down-regulated in hypoxia to identify potential target genes which positively regulate pluripotency.

3.3.3.1 Target mining using TargetScan6.2

The first approach utilising TargetScan was to identify which of the differentially expressed miRNAs were predicted to target HIFs including the factor inhibiting HIF (FIH) HIF1AN. In detail, TargetScan was screened for HIF1A, HIF2A, HIF3A and HIF1AN. It was expected to identify the majority of HIFs to be targeted by down- regulated rather than up-regulated miRNAs in hypoxia compared to normoxia because HIFs are stabilised at 5% oxygen and therefore display an increased expression. The numerical data are visualised in a pie-chart (Figure 35) and further detailed in a table that gives information about how many miRNAs were either up- or down-regulated (Table 24) under hypoxia compared to normoxia.

MiRNAs can target the 3'UTR at multiple sites and thus was analysed for each of the HIFs and FIH. The pie chart depicts that out of the 16 comparisons between miRNAs either down- or up-regulated only three displayed up-regulated miRNAs as majority (Figure 35). The only instances that up-regulated miRNAs dominated over down-regulated miRNAs was found when the arrays A and C were compared for miRNAs that are predicted to target the HIF1A or HIF3A 3'UTR and for miRNAs predicted to target the HIF3A 3'UTR when all three arrays were compared (Array ABC) (Figure 35). In contrast, between all 3 arrays (Array ABC) none of the up-regulated miRNAs were predicted to target either the *HIF1A* 3'UTR or the *HIF2A* 3'UTR (Table 24 and Figure 35).

Thus, any miRNAs that are predicted to target HIF1A or HIF2A and repress the expression of these genes are already down-regulated. However, looking at the numbers of how many times each target is predicted to be bound by the differentially expressed miRNAs, HIF1AN was the most abundantly predicted target gene (Table 24). The HIF1AN 3'UTR was predicted to be targeted mainly by down-regulated miRNAs than by up-regulated miRNAs across all array comparisons (Table 24 and Figure 35). This shows that there are less miRNAs expressed at 5% than at 20% oxygen predicted to target and repress the FIH HIF1AN (Table 24 and Figure 35). Overall, the pie chart which combines multiple miRNA binding sites for each target shows that mostly miRNAs down-regulated under hypoxia were found to target HIFs when compared to those that were up-regulated under hypoxia (Table 24 and Figure 35). This shows that there are less miRNAs expressed at 5% than at 20% oxygen that could target and repress the expression of these HIFs (Figure 35).

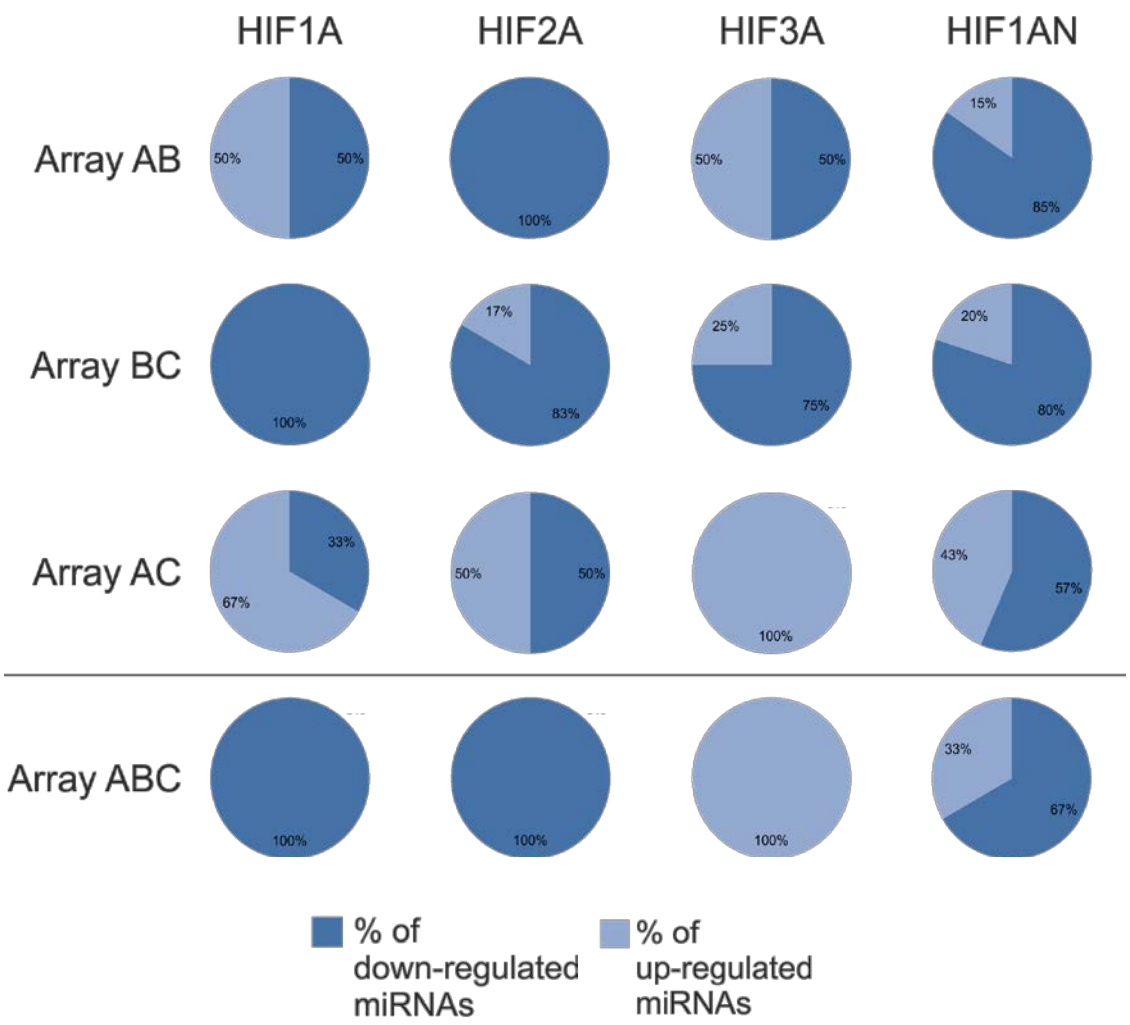

Figure 35: Percentage of concurrently either up- or down-regulated miRNAs predicted to target HIF isoforms in hESCs in hypoxia compared to normoxia between the 3 array-sets

Dark blue represents the percentage of down-regulated and light blue the percentage of up-regulated miRNAs predicted to target *HIF1A, HIF2A, HIF3A* or *HIF1AN* respectively. RNU44 was used as reference gene and TargetScan as source for predicted target genes. Multiple hits for one miRNA were allowed as well as poorly conserved hits if target was already predicted to be conserved among mammals (Lewis, Burge and Bartel, 2005; Grimson *et al.*, 2007). Absolute numbers of miRNAs predicted to target HIF isoforms can be found in Table 24 together with the exact miRNAs listen in Table 25.

Table 24: Number of hits of miRNAs targeting HIF isoforms and HIF1AN which are either down- or up-regulated under hypoxia compared to normoxia in hESCs, using TargetScan as mRNA/miRNA target database

	under hypoxia	HIF1A	HIF2A	HIF3A	HIF1AN
AB	down-regulated	1	6	4	22
	up-regulated	1	0	4	4
BC	down-regulated	2	5	9	16
	up-regulated	0	1	3	4
AC	down-regulated	1	2	0	13
	up-regulated	2	2	5	10
ABC	down-regulated	1	2	0	8
	up-regulated	0	0	3	4

The same data but this time including the information of which exact miRNAs are down-regulated and predicted to target HIF1A, HIF2A, HIF3A or HIF1AN are depicted (Table 25 and Figure 36). TargetScan was able to identify 25 different miRNAs that were down-regulated in at least two of the array sets (highlighted by double underlining in Table 25). As miRNAs target the 3'UTR at multiple sites, it was found that the number of times a particular miRNA was predicted to target *HIFs or FIH* varied between one and seven times (as depicted by the 'number x miRNA' in Table 25 and Figure 36). This demonstrates the abundance of miRNAs (Figure 36 and Table 25). For instance, miR-518d-5p was predicted to target the HIF3A 3'UTR seven times and found to be down-regulated between Array A and Array C. MiR-518d-5p is with seven binding sited the most abundant miRNA compared to the other array-comparisons (Table 25). In contrast, miR-519c-3p for instance was predicted to target the HIF1A 3'UTR only once (Table 25). However, miR-519c-3p is not only predicted to target the HIF1A 3'UTR, it is also targeting twice the HIF1AN 3'UTR and thus exerting contrasting effects (Table 25). The miRNA data mining revealed in total 5 different miRNAs predicted to simultaneously target HIFs and the FIH, these miRNAs are miR-519c-3p, -122-5p, -152-3p, -202-3p and miR-520f-3p (Table 25).

Table 25: List of down-regulated miRNAs targeting HIFs and FIH under hypoxia compared to normoxia in hESCs with the addition of the target-frequency along the 3'UTR. (Double underlined are miRNAs predicted to simultaneously target HIFs and FIH.)

	HIF1A	*HIF2A*	*HIF3A*	*HIF1AN*
ABC	1x hsa-miR-519c-3p	2x hsa-miR-374b-5p		6x hsa-miR-125b-5p 2x hsa-miR-519c-3p
AB		1x hsa-miR-223-3p 1x hsa-miR-199a-3p 2x hsa-miR-152-3p	1x hsa-miR-122-5p 2x hsa-miR-29a-3p 1x hsa-miR-515-3p	2x hsa-miR-122-5p 1x hsa-miR-152-3p 2x hsa-miR-24-3p 4x hsa-miR-31-5p 3x hsa-miR-486-3p 1x hsa-miR-636 1x hsa-miR-96-5p
BC	1x hsa-miR-20b-5p	1x hsa-miR-520f-3p 2x hsa-miR-660-5p	2x hsa-miR-202-3p 7x hsa-miR-518d-5p	1x hsa-miR-202-3p 1x hsa-miR-214-3p 3x hsa-miR-373-3p 2x hsa-miR-484 1x hsa-miR-520f-3p
AC				1x hsa-miR-455-3p 3x hsa-miR-520b 1x hsa-miR-525-5p

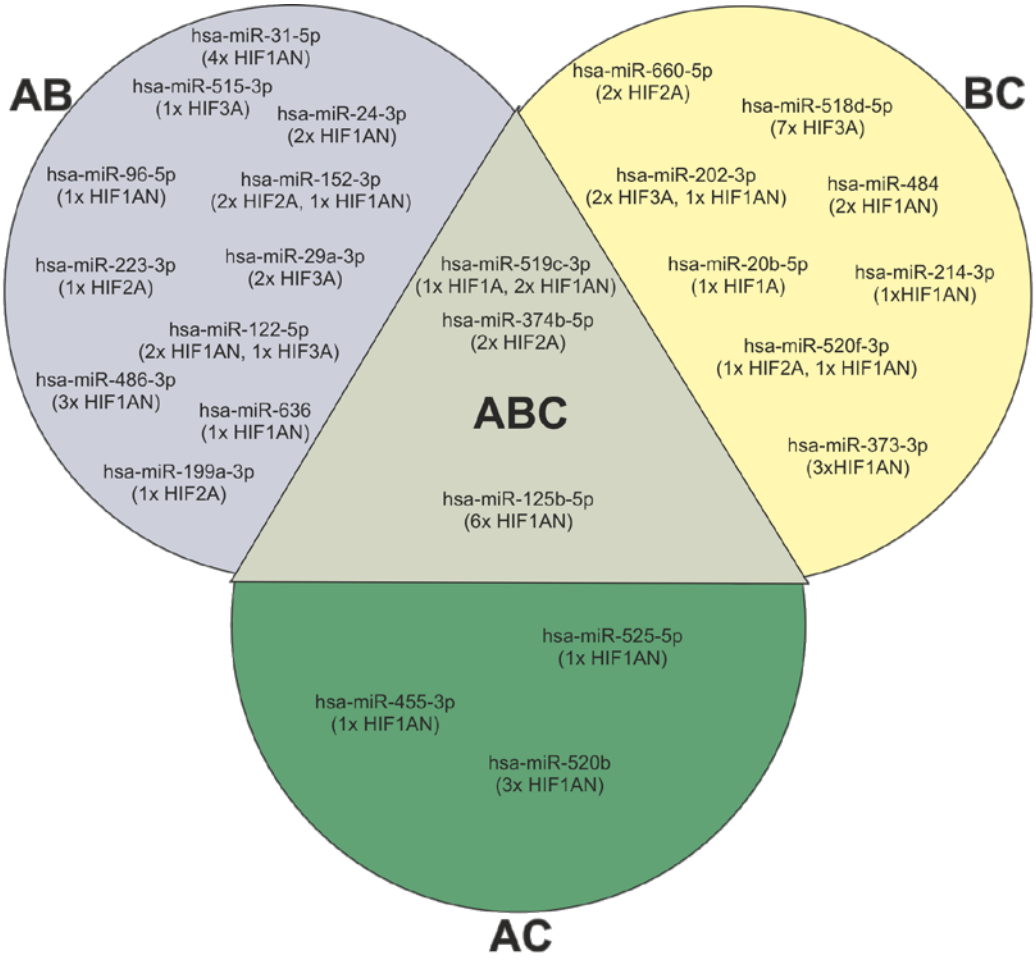

Figure 36: Down-regulated miRNAs in hESCs under hypoxia that target HIF isoforms supported by at least two array sets

Venn-Diagram, showing how many times a particular down-regulated miRNA targets HIFs in hESCs under hypoxia compared to normoxia and are common between array-sets. A, B and C represent a set of arrays. TargetScan (Lewis, Burge and Bartel, 2005; Grimson *et al.*, 2007) was used to predict HIF isoforms such as *HIF1A*, *HIF2A*, *HIF3A* and *HIF1AN*

In total, three different miRNAs, miR-519c-3p, miR-374b-5p and miR-125b-5p were robustly down-regulated under hypoxia when compared to normoxia and predicted to target HIFs in hESCs. This means that these three miRNAs will have more effect on their targets in hESCs cultured at 20% oxygen than those at 5% oxygen (Figure 36).

However, miRNAs can have multiple targets not just along a single 3'UTR but also being able to regulate different targets simultaneously. Thus they may exert joint benefits in target gene repression. Therefore, rather than focusing on miRNAs that were robustly down-regulated across the three array sets a very frequent miRNA that is only down-regulated across two array sets might also be a good candidate for further investigations.

Regardless of miRNA abundance, the strength of binding and overall complementarity to the mRNA must also be taken into consideration but especially the ability of one miRNA targeting more than only one mRNA. Therefore, taking Figure 36 as reference point further investigations with TargetScan6.2 were undertaken but did not reveal any down-regulated miRNAs predicted to target additionally *POU5F1 (OCT4)*, *SOX2*. Except for the NANOG 3'UTR, where miR-24-3p was predicted to target (Table 26). However, miR-24-3p was also predicted to have two target sites in the HIF1AN 3'UTR displaying a better total context score and aggregate P_{CT} and therefore negligible (Table 26).

Table 26: Biological predicted targets of miR-24-3p using TargetScan (Lewis, Burge and Bartel, 2005; Grimson *et al.*, 2007)

3'UTR target	miRNA	seed match	Total context+ score	Aggregate P_{CT}
NANOG	131-has-miR-24-3p	7mer-1A Poorly conserved	-0.05	<0.1
HIF1AN	131-has-miR-24-3p	7mer-m8 Conserved and 7mer-1A Poorly conserved	-0.24	0.62

However, Figure 36 was continued to be taken as a reference point, investigating further targets that might also be important for hESCs maintenance. Thus miR-122-5p was predicted to bind to four separate target genes of interest. These targets were not only *HIF3A* and *HIF1AN* (twice) but also the pyruvate kinase muscle isoenzyme (*PKM2*) (Figure 37 and Table 27). Interestingly, PKM2 was predicted to be targeted only by the miR-122/122a/1352 family of broadly conserved miRNA families amongst vertebrates. Since hESCs have an increased rate of glycolysis in hypoxia compared to normoxia, *PKM2* might also be regulated by miRNAs in hESCs. The predicted binding of miR-122-5p with the PKM2 3'UTR (Figure 37) involved an exact match of miR-122-5p positions 2 to 8 of the seed followed by an 'A'. TargetScan also assigned one of the lowest negative total context+ score of -0.33 miR-122-5p binding *PKM2* compared to *HIF1AN* with a total context+ scores of "-0.11" and ">-0.02" and *HIF3A* with "-0.26" (Table 27).These data suggest miR-122-5p with PKM2 as a possible gene of interest for further investigations.

Figure 37: Predicted consequential pairing between target regions and miR-122-5p

3'UTR sequences of target gene (top) with position relative to the start of the 3'UTR and miRNA sequence (bottom) of *HIF3A, HIF1AN* and *PKM2* for miR-122-5p using TargetScan (Lewis, Burge and Bartel, 2005; Grimson *et al.*, 2007)

Table 27: Biological targets of miR-122-5p and miR-223-3p using TargetScan (Lewis, Burge and Bartel, 2005; Grimson *et al.*, 2007)

miRNA name	seed match	predicted consequential pairing of target region and miRNA	con-text+ score	site-type contri-bution	3' pairing contri-bution	local AU contri-bution	position contri-bution	TA contri-bution	SPS contri-bution
>hsa-miR-122-5p MIMAT0000421 UGGAGUGUGACAAUGGUGUUUG	8mer conserved	Position 52-59 of HIF3A 3' UTR	-0.26	-0.247	-0.008	0.143	-0.101	0.016	-0.067
	7mer-1A conserved	Position 167-173 of HIF1AN 3' UTR	-0.11	-0.074	0.001	0.037	-0.032	0.009	-0.052
	7mer-m8 Poorly conserved	Position 3283-3289 of HIF1AN 3' UTR	>-0.02	-0.12	0.003	0.094	0.151	0.009	-0.037
	8mer conserved	Position 520-527 of PKM2 3' UTR	-0.33	-0.247	0.003	0.059	-0.09	0.016	-0.067
>hsa-miR-223-3p MIMAT0000280 UGUCAGUUUGUCAAAUACCCCA	7mer-1A conserved	Position 1951-1957 of EPAS1 3' UTR	-0.16	-0.074	-0.002	-0.011	-0.041	-0.01	-0.018

TargetScan revealed one target-site for miR-223-3p in the *HIF2A* 3'UTR with a negative total context+ score of "-0.16" together with an exact match at positions 2 to 7 of the seed followed by an 'A' (Table 27). The exact pairing of miR-223-3p with HIF2A is depicted in Figure 38.

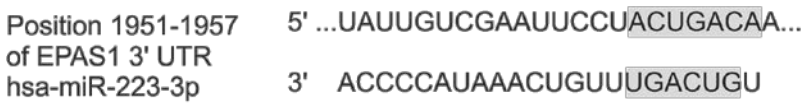

Figure 38: Predicted consequential pairing of the target region of miR-223-3p
3'UTR sequences (top) and miRNA sequence (bottom) of *EPAS1* for miR-223-3p using TargetScan (Lewis, Burge and Bartel, 2005; Grimson *et al.*, 2007)

3.3.3.2 Target mining using SegalLab

Since TargetScan was unable to detect miRNA binding sites for the important transcription factors SOX2, NANOG and OCT4 the PITA algorithm from Segal Lab was additionally used to confirm or to find further potential miRNA targets. The PITA algorithm focuses on the secondary structure of target recognition. The seed ""x:y:z" defines "seed-size : number of mismatches : number of GU wobble pairs". The 3'UTR sequence of potential target genes together with the miRNA sequence of interest was loaded into the Segal lab programme. Table 28 gives an idea of the top 10 targets for HIF2A, SOX2, NANOG and OCT4 when analysing all miRNAs that were down-regulated in at least two of the array sets. The three consistently down-regulated miRNAs (across Array ABC, Figure 36) miR-519c-3p, -374b-5p and miR-125b-5p that were predicted to target HIFs using TargetScan had no additional targets for SOX2, NANOG, OCT4 or PKM2 using either TargetScan or SegalLab (Table 28) and thus were not investigated further. However, Segal Lab confirmed HIF2A as a target for miR-223-3p and specifically revealed 41 potential sites for miR-223-3p targeting the *HIF2A* 3'UTR (Table 28). Three miR-223-3p binding sites were assigned with an energetic scores of less than "-5" suggesting they are likely to interact with the target gene (Table 29).

Table 28: Top10 targets for HIF2A, NANOG, SOX2 and OCT4 using the Segal lab predictions on all down-regulated miRNAs that were common between at least two array sets, showing how many target sites one miRNA had and a summed up ddG as "score" (number in front of the miRNA refers to position in Table 22)

HIF2A	Sites	Score	NANOG	Sites	Score	SOX2	Sites	Score	OCT4	Sites	Score
139-hsa-miR-296-3p	44	-19.36	139-hsa-miR-296-3p	13	-22.88	341-hsa-miR-636	15	-18.38	230-hsa-miR-484	3	-18.06
85-hsa-miR-193a-5p	25	-16.59	100-hsa-miR-202	24	-14.68	23-hsa-miR-122	9	-18.22	53-hsa-miR-145	5	-15.6
233-hsa-miR-486-3p	48	-16.2	85-hsa-miR-193a-5p	11	-13.57	230-hsa-miR-484	13	-17.68	38-hsa-miR-133b	3	-15.19
229-hsa-miR-483-5p	23	-15.67	10-hsa-let-7e	24	-13.53	110-hsa-miR-211	27	-16.1	61-hsa-miR-149	6	-14.66
8-hsa-let-7c	37	-14.13	16-hsa-miR-103	16	-13.01	301-hsa-miR-532-3p	15	-15.6	110-hsa-miR-211	17	-14.45
23-hsa-miR-122	32	-14.12	8-hsa-let-7c	24	-12.71	252-hsa-miR-502-3p	10	-13.89	27-hsa-miR-125b	8	-14.29
110-hsa-miR-211	26	-13.36	249-hsa-miR-500	15	-12.36	139-hsa-miR-296-3p	15	-13.85	251-hsa-miR-501-5p	11	-13.81
127-hsa-miR-223	41	-13.32	179-hsa-miR-34a	12	-12.02	53-hsa-miR-145	18	-13.77	21-hsa-miR-10a	5	-13.25
292-hsa-miR-520f	32	-12.94	131-hsa-miR-24	16	-11.76	144-hsa-miR-29a	5	-11.37	341-hsa-miR-636	4	-13.14
344-hsa-miR-652	26	-12.93	167-hsa-miR-331-5p	15	-11.63	61-hsa-miR-149	8	-11.34	177-hsa-miR-345	6	-13

Table 29: Segal Lab prediction outcome for HIF2A (EPAS1) targeted by miR-223-3p with a cut off at ddG=-5 (number in front of the miRNA refers to position in Table 22)

Gene	microRNA	Position	Seed	dGduplex	dGopen	ddG
EPAS1-001 (CCDS1825)	127-hsa-miR-223	545	8:0:1	-17.1	-3.77	-13.32
		2028	6:1:1	-10.6	-3.56	-7.03
		1827	6:1:1	-15.95	-9.4	-6.54

Strikingly, although HIF2A was not identified as a target of miR-122-5p in TargetScan, 32 potential sites were predicted for miR-122-5p targeting *HIF2A* (Table 28) and eight of them with an energetic score of less than ”-5” when Segal Lab was used (Table 30).

Table 30: Segal Lab prediction outcome for HIF2A (EPAS1) targeted by miR-122-5p with a cut off at ddG=-5 (number in front of the miRNA refers to position in Table 22)

Gene	microRNA	Position	Seed	dG duplex	dG open	ddG
EPAS1-001 (CCDS1825)	23-hsa-miR-122	52	8:1:1	-17.6	-3.93	-13.66
		96	8:1:1	-17.6	-4.94	-12.65
		52	6:0:1	-14.8	-2.73	-12.06
		56	6:1:0	-15.2	-5.31	-9.88
		265	6:1:1	-10.9	-2.7	-8.19
		96	6:1:1	-12	-4.98	-7.01
		1944	6:1:1	-15.4	-8.81	-6.58
		294	6:1:0	-12	-6.01	-5.98

Additionally, 16 sites were predicted for miR-122-5p to target NANOG and 15 were found to have an energetic score of less than ”-5” (Table 31).

Table 31: SegalLab prediction outcome for NANOG targeted by miR-122-5p with a cut off at ddG=-5

Gene	microRNA	Position	Seed	dG duplex	dG open	ddG
NANOG-001 (CCDS31736)	23-hsa-miR-122	2644	6:1:1	-16.26	-4.48	-11.77
		3238	8:1:0	-14.9	-4.22	-10.67
		1154	6:0:0	-19	-9.98	-9.01
		70	6:1:1	-9.4	-1.58	-7.81
		2287	6:1:1	-11.22	-3.75	-7.46
		2632	6:1:1	-15.5	-8.15	-7.34
		1546	6:0:1	-14.8	-7.56	-7.23
		64	6:1:1	-8.71	-1.59	-7.11
		1990	6:1:1	-11.65	-4.94	-6.7
		1983	7:1:1	-10.31	-3.81	-6.49
		325	6:1:0	-14.3	-8.35	-5.94
		61	6:1:0	-11.3	-5.37	-5.92
		56	6:1:0	-12.3	-6.76	-5.53
		2301	6:1:1	-12.1	-7.04	-5.05
		3239	8:1:0	-14.9	-4.22	-10.67

Further target predictions using SegalLab also revealed 9 potential binding sites for miR-122-5p targeting the *SOX2* 3'UTR with 6 target sites having an energetic score less than "-5" (Table 32).

Table 32: SegalLab prediction outcome for SOX2 targeted by miR-122-5p with a cut off at ddG=-5

Gene	microRNA	Position	Seed	dG duplex	dG open	ddG
SOX2-001 (CCDS3239)	23-hsa-miR-122	187	8:1:0	-19.9	-1.67	-18.22
		187	6:1:1	-13.3	-1.53	-11.76
		1068	6:0:1	-12.6	-4.08	-8.51
		829	7:1:1	-14.45	-6.55	-7.89
		821	6:1:1	-14.11	-6.48	-7.62
		106	7:1:1	-15.4	-8.23	-7.16

The Segal lab prediction algorithm showed 14 target sites of miR-223-3p targeting *NANOG* with five target sites of an energetic score of less than"-5.0" (Table 33). miR-223-3p was also found to target SOX2 13 times along the 3'UTR but none had an energetic score of less than "-5" (Data not shown).

Table 33: Segal Lab prediction outcome for NANOG targeted by miR-223-3p with a cut off at ddG=-5

Gene	microRNA	Position	Seed	dG duplex	dG open	ddG
NANOG-001 (CCDS31736)	127-hsa-miR-223	3945	6:1:1	-12.6	-5.62	-6.97
		3846	6:1:0	-12.51	-5.58	-6.92
		3840	6:1:1	-11.79	-5.13	-6.65
		843	6:1:0	-12.5	-6.56	-5.93
		2464	6:0:1	-16	-10.59	-5.4

In summary, the application of two *in silico* prediction algorithms revealed multiple genes of interest containing binding sites for targets of the identified miRNAs down-regulated in hESCs cultured at hypoxic conditions compared to atmospheric oxygen. TargetScan and Segal Lab shortened the list of comprehensible miRNAs to an experimentally approachable level. Therefore, two miRNAs were chosen for further interrogation since they appeared to target several genes involved in the hypoxic regulation of hESCs. These two miRNAs are miR-223-3p, predicted to target *HIF2A* and *NANOG* and miR-122-5p predicted to target *HIF1AN, HIF3A, PKM2, SOX2* and *NANOG*.

3.3.4 Validation of miRNAs

To further interrogate the array data and confirm differentially expressed miRNAs, RT-qPCR was performed to investigate the expression of miRNAs in hESCs cultured in hypoxia compared to those maintained at normoxic conditions. The array data showed miR-122-5p and miR-223-3p were both down-regulated in two of the array sets (A and B) under hypoxia (Figure 39).

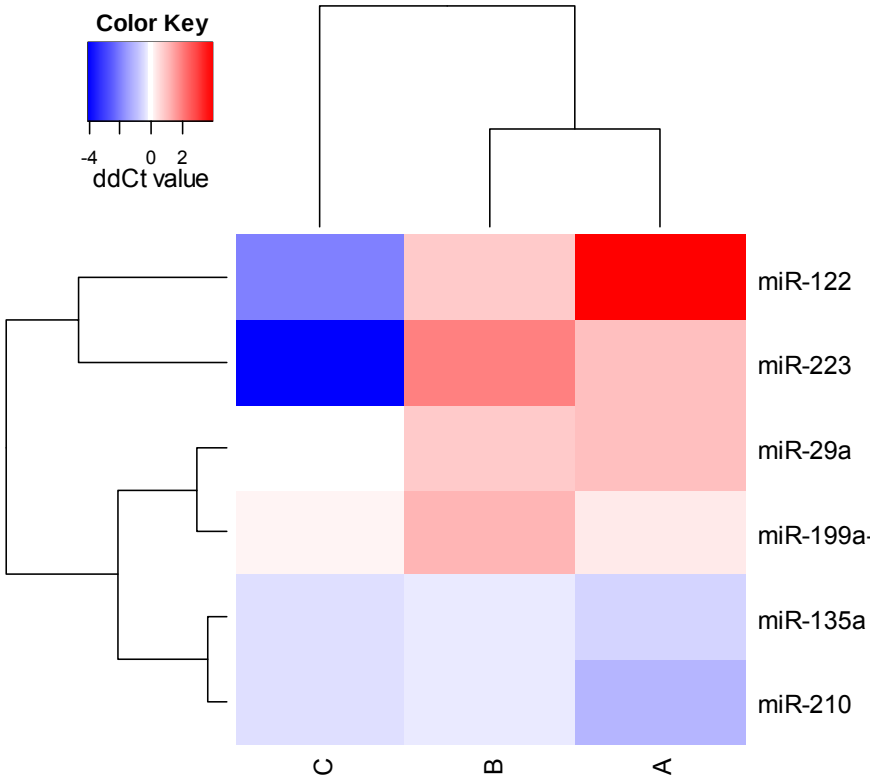

Figure 39: Heat-map, expression of validated miRNAs (ddCt) in hESCs under hypoxia compared to normoxia in each array (A, B and C)

Negative values (blue) show up-regulated and positive values (red) down-regulated miRNAs, using RNU44 as reference gene with 0.3≤ddCt≤-0.3 for differentially expressed miRNAs. (This graph was produced with the help of Patrick Stumpf, Bone & Joint Research Group, University of Southampton)

Together with the information obtained through bioinformatic analysis led to the validation of miR-122-5p and miR-223-3p in hESC lines. RT-qPCR confirmed the presence of miR-122-5p and miR-223-3p in both Shef3 and Hues7 hESCs. A significant 45% down-regulation of miR-223-3p expression was observed in both Shef3 and Hues7 hESCs when cultured at 5% oxygen compared to 20% oxygen (Figure 40 A). A more dramatic 75% down-regulation (p=0.0263) of miR-122-5p expression was observed in Shef3 hESCs cultured at 5% oxygen when compared to 20% oxygen (Figure 40 B). Hues7 hESCs cultured at 5% oxygen compared to 20% oxygen follow the same trend with an approximate reduction of 20% in miR-122-5p expression (Figure 40 B).

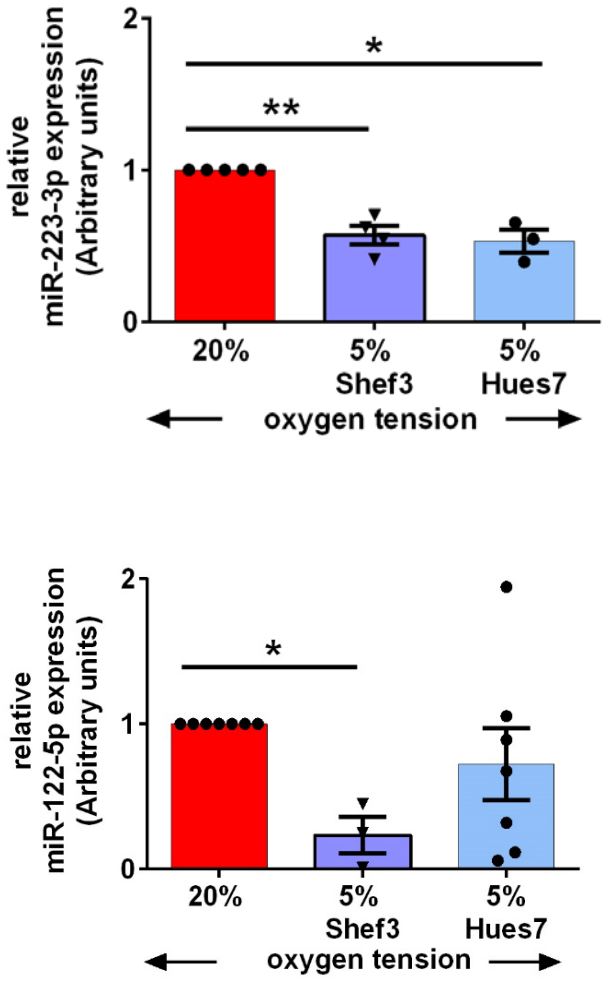

Figure 40: Relative miRNA-expression of miR-223-3p (A) and miR-122-5p (B) at 5% oxygen compared to 20% oxygen in Shef3 or Hues7 hESCs

Data were produced by RT-qPCR. All data were normalised to RNU44 and to "1" for 20% oxygen. Bars represent mean ±SEM, stars indicate significant difference to the miRNA-expression in hESCs at 20% oxygen with $p<0.05$.

Importantly, the hypoxamir miR-210 known to be up-regulated in low-oxygen concentrations was up-regulated in all 3 array data sets in hypoxia compared to normoxia. Using qPCR miR-210 was validated and found to be significantly up-regulated in the Hues7 hESC line (Figure 41 A) showing an approximate 4-fold higher expression (p=0.027) in hESCs cultured at 5% oxygen compared to 20% oxygen. The Shef3 hESCs line shows a similar trend displaying a non-significant 3-fold increase in miR-210 expression in hESCs cultured at 5% oxygen compared to 20% oxygen (Figure 41 A). Another miRNA, miR-135a (Figure 41 B) was also up-regulated across all 3 array data sets and showed a trend towards an increased expression in hESCs maintained at 5% oxygen compared to 20% oxygen in both cell lines.

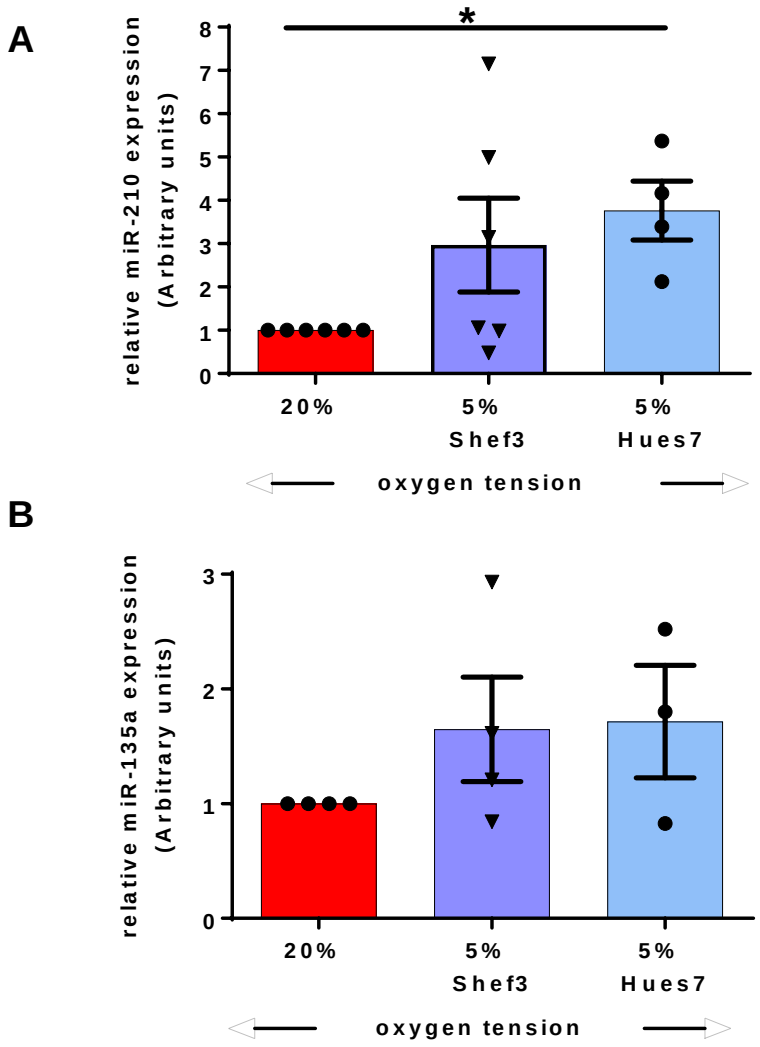

Figure 41: Relative miRNA-expression of miR-210 (A) and miR-135a (B) at 5% oxygen compared to 20% oxygen in Shef3 or Hues7 hESCs

Data were produced by RT-qPCR. All data were normalised to RNU44 and to "1" for 20% oxygen. Bars represent mean ±SEM, stars indicate significant difference to the miRNA-expression in hESCs at 20% oxygen with $p<0.05$.

miR-29a was a candidate miRNA which was investigated before the data for all three array sets were generated. miR-29a was predicted to target *KLF4* and *HIF3A* and was (after all three sets were available) down-regulated in two array data sets (Array AB) (Figure 39, KLF4 target see Appendix A Table 44). The validation showed a trend towards a 40-60% reduction in miR-29a expression in both cell lines cultured at 5% oxygen compared to those maintained at 20% oxygen (Figure 42 A). miR-199a-3p was down-regulated across two array sets (Array AB) and was predicted to target *HIF2A* (Figure 39) and therefore of interest. Unfortunately, miR-199a-3p was not able to be validated using qPCR due to an extremely low expression level in hESCs cultured at either 5% or 20% oxygen. All Ct values obtained for miR-199a-3p were greater than 35.

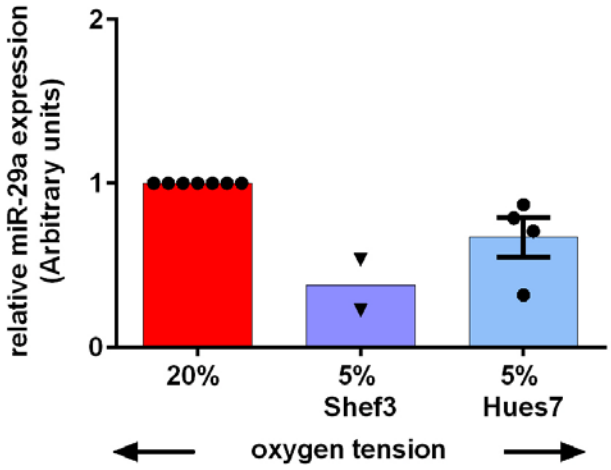

Figure 42: Relative miRNA-expression of miR-29a at 5% oxygen compared to 20% oxygen in Shef3 or Hues7 hESCs

Data were produced by RT-qPCR. All data were normalised to RNU44 and to "1" for 20% oxygen. Bars represent mean ±SEM.

3.4 Discussion

3.4.1 Expression of pluripotency markers

Pluripotency marker expression was investigated in hESCs to ensure stem cell properties and allow the use of these cells in subsequent experiments. Both hESCs lines Shef3 and Hues7 were found to express the transcription factors OCT4, SOX2 and NANOG as well as the cell surface marker TRA-1-60 but not SSEA1 at both, 5% and 20% oxygen concentration. There was no obvious difference in the expression of the pluripotency markers between hESCs cultured at 5% or 20% oxygen using immunocytochemistry which is in agreement with previously published literature (Forristal *et al.*, 2010). However, when Forristal et al.(2010) used a quantitative method such as Western blotting OCT4, SOX2 and NANOG were significantly decreased in hESCs cultured at 20% when compared to those maintained at 5% oxygen (Forristal *et al.*, 2010, 2013; Petruzzelli *et al.*, 2014). In agreement with this published work, NANOG protein expression was found to be significantly increased under hypoxic conditions. As a result, the findings confirm hESC identity allowing the cells to be used for miRNA analysis.

3.4.2 Array analysis of miRNAs with bioinformatics

The best prediction of miRNA site effectiveness is to investigate first whether or not the mRNA but also the miRNA of interest is expressed in hESCs. Thus, this thesis used miRNA arrays as a first approach to analyse and investigate miRNA expression but also differences in miRNA expression between hESCs cultured at either 5% or 20% oxygen. This cell-based method together with bioinformatics was ideal to tailor the research relatively quickly into an experimental approachable level. Additionally, it was beneficial to integrate knowledge into the bioinformatic search such as the greater expression of pluripotency markers *OCT4, SOX2* and *NANOG* and the observation of less spontaneous cell differentiation in hESCs cultured at 5% oxygen when compared to those maintained at 20% oxygen (Ezashi, Das and Roberts, 2005; Forristal *et al.*, 2010).

Research on miRNAs can be challenging since: 1) miRNAs are very short, only 22-25 nucleotides long (Ambros, 2004; Bartel, 2004), 2) only require specificity in their seed sequence which is even shorter, only 6-8 nucleotides long and additionally the seed-sequence does not need to be 100% complementarity to their target mRNA (Lewis, Burge and Bartel, 2005) and 3) miRNA family members can sometimes differ by only one nucleotide (Bartel, 2009; Friedman *et al.*, 2009). Taken together, these facts emphasise the complexity of their regulatory network. MiRNAs can target hundreds of

different genes since they only need to target with partial base complementarity. In addition, miRNAs are often tissue specific and their expression patterns can be time-dependent. Thus specialised methods to identify miRNA-mRNA interactions are required.

The aim of the first part of this study was to investigate whether miRNAs are differentially expressed in hESCs cultured at 5% oxygen compared to 20% oxygen. Therefore, three independent arrays were performed on hESCs cultured at either 5% oxygen or 20% oxygen (Figure 31 and 32) resulting in 231 miRNAs being expressed. These three independent arrays for each oxygen concentration revealed that 70-80% of the 231 expressed miRNAs were differentially expressed (Table 21). The variation in the number of down-regulated and up-regulated miRNAs between the arrays is unclear but may be due to batch to batch variations of hESCs investigated such as the state of the original hESCs cultures. A further explanation could be that the majority of miRNAs had a very low expression and therefore caused a greater variation between the arrays which is in agreement with published data using the same array platform but for rodent miRNAs (Y. Chen *et al.*, 2009). When the reproducibility of TaqMan rodent miRNA arrays was tested it was suggested that at least 4 replicates are necessary to obtain statistically valid data (Y. Chen *et al.*, 2009). With additional resources it may be possible to perform additional arrays to minimise inter-array variation though it is unclear how much variation is usually obtained using TaqMan miRNA arrays. In different cell contexts, one group used TaqMan miRNA array v1.0 for investigating bone mineral density in two different groups and found that only 156 miRNAs were expressed of 365 miRNAs investigated and were suggesting that their result are due to tissue specific expression or very low miRNA expression (Y. Wang *et al.*, 2012). Another study that used the same miRNA array platform but compared the miRNA expression profile between healthy woman and women with repeated embryo implantation defects were only able to extract 13 differentially expressed miRNAs (Revel *et al.*, 2011). However, the data obtained with the methods undertaken in this thesis provide a sensible starting point for further investigations and at this point statistical validation was not required. Despite the variation in the data from TaqMan miRNA arrays, the data represent a valuable insight into the miRNA expression profile of the hESCs studied at 5% and 20% oxygen concentration. Thus, when all three arrays for each oxygen concentration were compared there were 20 consistently down-regulated and 20 consistently up-regulated miRNAs and several differentially expressed miRNAs that were concurrently expressed in at least two of the three array sets under hypoxia. Those miRNAs were chosen for further investigation and validated with RT-qPCR to obtain statistically valid results. Interestingly, miR-210, a known hypoxamir (Chan and Loscalzo, 2010; Chan *et al.*, 2012; Bertero *et al.*, 2013; Nallamshetty, Chan

and Loscalzo, 2013) was consistently up-regulated in all three arrays. MiR-210 was also validated and significantly increased (p=0.027) in Hues7 hESCs. However, although miR-210 expression was not significantly increased in Shef3 hESCs still showed a notable trend to be up-regulated. Thus, miR-210 was used as a positive control and further increased confidence in the data. The comparison of the miRNA expression data also reveals a 20-30% fraction of miRNAs that are not differentially expressed. These miRNAs are likely those not affected by differing environmental oxygen conditions.

The most investigated mechanism of miRNA action is the targeting of the 3'UTR of mRNA preventing translation. In differentiating cells, miRNAs might target genes such as *OCT4, SOX2, NANOG, HIFs* and *PKM2* to prevent their translation. These genes are known to be important in regulating hESC maintenance (Nichols *et al.*, 1998; Avilion *et al.*, 2003; Chambers *et al.*, 2003b; Boyer *et al.*, 2005; Forristal *et al.*, 2010; Christensen, Calder and Houghton, 2015) and are therefore important to be expressed in hESCs. Conversely, miRNAs that are up-regulated in hypoxia could also exert beneficial effects on hESCs by repressing genes responsible for differentiation. However, this study focused on those miRNAs that were down-regulated in hypoxia when compared to normoxia since their low expression might preserve the stemness of hESCs or may cause beneficial effects when hESCs are cultured at 5% oxygen compared to 20% oxygen. This could be one reason why hESCs appear to be "more" pluripotent at low oxygen concentrations. Therefore, the miRNA data obtained from the three independent array sets in hESCs under hypoxia compared to normoxia were used together with *in silico* analysis to find possible interactions between genes of interest and miRNAs. These bioinformatic tools mainly involved the use of TargetScan but also the Probability of Interaction by Target Accessibility (PITA) algorithm from Segal Lab for the identification of miRNA candidates.

The search for miRNA candidates that target *HIFs* was surprisingly successful. In contrast, TargetScan did not predict any targets for the pluripotency factors. The comparison of array AC and BC showed that the majority of miRNAs predicted to target *HIF* isoforms were down-regulated under hypoxia (Figure 35) which means that these miRNAs are not degrading or inhibiting their predicted HIF isoform. This is consistent with the literature which shows that HIFs are stabilised in hypoxic culture conditions (Li *et al.*, 2006; Tanaka *et al.*, 2009; Forristal *et al.*, 2010). The fact that the majority of miRNAs that were lower expressed in cells cultured at 5% oxygen were predicted to target HIF isoforms reveals that HIF isoforms must be stabilised and therefore not targeted by those miRNAs. In turn, cells cultured at 20% oxygen concentration had higher expression levels of these miRNAs thus HIFs may be degraded not only through

hydroxylation and binding of the VHL followed by proteasomal degradation but also through miRNA repression. The cells might have developed this mechanism to save energy by not producing proteins that will be subject to degradation in an environment with a greater oxygen concentration.

Experimentally, all three array replicates for each oxygen condition have been performed in the same way but the results of each array reflect only single Ct values for each miRNA rather than more reliable average values generated out of duplicates or triplicates. In the context of HIFs, a greater miRNA variation occurred when arrays A and C were compared to arrays A and B or to B and C. It is crucial to understand that every prediction tool uses different algorithms, where characteristics of miRNA-mRNA recognition and binding follow the rules and physics pre-set or adjusted by the user. A comparison of seven different algorithms for miRNA-mRNA prediction found that TargetScan (v5.0) was best as reviewed by Witkos et al. (2011) with a precision of ~50% (Alexiou *et al.*, 2009). Although many parameters are incorporated in the final score of TargetScan, sites with poor seed pairing are not present (Witkos, Koscianska and Krzyzosiak, 2011). In other words, TargetScan does not take any sites into account for miRNAs that only bind with partial complementarity in their seed sequence and thus is likely to limit the number of targets obtained. The Segal lab 3'UTR prediction settings can potentially minimize false positives but with a risk of underestimating the true number of miRNAs. According to Segal et al. (2007), sites with a value for ddG lower than -10 are functional but depending on the miRNA expression level even higher values may still be functional (Kertesz *et al.*, 2007). Therefore the miRNAs-mRNA energetic scores were set more widely with a cut off at ddG=-5 to confirm the targets obtained by TargetScan and to find additional potential targets. However, it is important that *in silico* analysis is incorporated with *in vitro* investigations to confirm or refute miRNA-mRNA interactions.

3.4.3 Validation of miRNA arrays of hESCs cultured under hypoxic conditions

Following a thorough bioinformatics analysis of the array data, miR-122-5p and miR-223-3p were identified as potential miRNA candidates due to their predicted targets and their lower expression in at least two arrays at 5% oxygen when compared to 20% oxygen. The prediction analysis revealed that miR-122-5p target relevant hESC genes such as *PKM2, HIF3A, HIF1A, SOX2* and *NANOG* and miR-223-3p targets *HIF2A, HIF3A* and *NANOG*. These hESC important targets together with the array data led to the validation of miR-122-5p and miR-223-3p. The expression of both miRNAs was confirmed to be significantly down-regulated in hypoxia when compared to normoxia in independent

hESC samples using RT-qPCR (Figure 40). Interestingly, miR-122 expression was reported to be absent or diminished in hESCs when compared to highly specialised cells such as primary hepatocytes (Jung *et al.*, 2011). In addition, loss of miR-122 expression was found to occur with hypoxia in human hepatocellular cancer cells as a negative correlation between HIF1A and miR-122 was observed (Coulouarn *et al.*, 2009). A recent study in hepatocytes confirmed HIF1A as a miR-122 target (Csak *et al.*, 2015). It is tempting to speculate if these two observations play a similar role in hESCs that miR-122-5p should only be expressed in cells starting to specialise and that hypoxia might play a role in inhibiting the maturation of miR-122-5p. In hypoxia-induced pulmonary arterial hypertension using a mice model, miR-223 was found to be down-regulated and induced overexpression of miR-223 resulted in drastic cell changes such as the abrogation of proliferation (Zeng *et al.*, 2016). To the best of our knowledge, this is the first report of miR-122-5p and miR-223-3p being differentially regulated by environmental oxygen in hESCs.

Further validation of the array data using RT-qPCR confirmed that the hypoxamir miR-210 was significantly up-regulated in the Hues7 hESC line and displayed the same trend for the Shef3 hESCs. This finding is consistent with HeLa cervical carcinoma cells and MCF7 breast cancer cells where miR-210 expression was increased when cultured in hypoxic conditions (Crosby *et al.*, 2009). Two other miRNAs were validated based on the arrays rather on potential targets. These miRNAs were miR-135a which was one miRNA that was consistently up-regulated in all three array data sets and miR-29a which was down-regulated in Array A and Array B. Although the validation of both these miRNAs did not show a significant difference, miR-135a showed a strong trend to be up-regulated and miR-29a displayed also a trend to be down-regulated in hESCs cultured at 5% oxygen compared to 20% oxygen and thus represent the data obtained from the arrays.

The algorithms currently available are only predictive and might not capture all *bona fide* miRNA-mRNA interactions. Thus, validation using in vitro experiments are important since it has been shown that the number of up-regulated genes upon miR-122 antisense oligonucleotides (ASO) treated mice were not reflected by those predicted through *in silico* analysis (Esau *et al.*, 2006).

As well as targeting the 3'UTR, miRNAs may also bind the 5'UTR and can also promote, rather than inhibit gene expression (Jopling, Schütz and Sarnow, 2008). For example, miR-122 was found to play an important role in the replication of the hepatitis C virus (HCV) by binding 2 sites in the 5'UTR of HCV RNA resulting in the positive regulation of the viral life cycle (Jopling, Schütz and Sarnow, 2008). It is not just the 5'UTR but also

the promoter and amino acid coding region that can be targeted by miRNAs (reviewed by He & Hannon 2004). It has been already demonstrated that many miRNAs can target Oct4, Sox2 and Nanog in the coding region (Tay *et al.*, 2008). However, most databases are restricted to the 3'UTR as is the case for TargetScan. The algorithm used by Segal lab is entirely dependent on the sequence made available to the programme and therefore could analyse regions other than the 3'UTR. This further highlights the complexity of miRNA regulation. However, this study concentrated on the 3'UTR binding sites for miRNAs, which to date has been most widely studied. Using TargetScan miR-122-5p was predicted to target the 3'UTR of *PKM2, HIF3A and HIF1A*. However, using the PITA algorithm from the Segal lab miR-122-5p was further predicted to target *SOX2* and *NANOG*. Similarly, miR-223-3p was predicted to target *HIF2A* and *HIF3A* using TargetScan and *NANOG* using Segal lab. Together, these prediction tools make miR-122-5p and miR-223-3p ideal targets for regulating genes that are involved in the hypoxic response of hESCs.

In summary, the combination of accessing the miRNA expression profile in hESCs together with *in silico* analysis has been successful in validating the expression of two candidate miRNAs, miR-223-3p and miR-122-5p (Figure 40). Both these miRNAs were significantly down-regulated in Shef3 hESCs cultured at 5% oxygen compared to 20% oxygen. Additionally, confirmation of miR-210 as being a hypoxamir increased further the confidence in the data. The overall changes in miRNA expression observed from the array data were consistent with that observed using RT-qPCR. Additional experiments utilising pre-miRNAs will determine whether these validated miRNAs have a down-stream effect on targets of interest, such as *PKM2, HIF2A* and pluripotency genes (*NANOG* and *SOX2*) as was predicted by TargetScan or the Segal lab.

Chapter 4

Modulation of miRNA expression in hESCs

4.1 Introduction

The search for miRNAs that regulate the pluripotent stem cell state has been extensively studied (Suh *et al.*, 2004; Tay *et al.*, 2008; Xu *et al.*, 2009; Judson *et al.*, 2009; Melton, Judson and Blelloch, 2010; Lakshmipathy, Davila and Hart, 2011; Jouneau *et al.*, 2012; Li and He, 2012; Choi, Choi and Hwang, 2013; Huo and Zambidis, 2013; Lüningschrör *et al.*, 2013; Y. J. Lee *et al.*, 2016). A set of miRNAs has been revealed that are called embryonic stem cell cycle (ESCC) miRNAs that contribute towards pluripotency by inhibiting factors that lead to differentiation and by activating others that support pluripotency (Wang *et al.*, 2008; Melton and Blelloch, 2010). This set of ESCC miRNAs comprise the miR-290 cluster (highly expressed in mESCs) and miR-302 (highly expressed in hESCs) and were found to promote the transition of the cell cycle phases from G1 to S, hence ESCC miRNAs (Suh *et al.*, 2004; Calabrese *et al.*, 2007; Wang *et al.*, 2008). Although culture at a reduced environmental oxygen tension is beneficial for hESC maintenance (Dumoulin *et al.*, 1999; Ezashi, Das and Roberts, 2005; Forsyth *et al.*, 2006; Westfall *et al.*, 2008; Forristal *et al.*, 2010; Kasterstein *et al.*, 2013), the role played by miRNAs in regulating these effects is not known.

The previous chapter revealed that a large number (70-80%) of all expressed miRNAs investigated were found to be either up- or down-regulated in hESCs cultured under hypoxia compared to normoxia. This indicates that environmental oxygen plays a significant role not only in the direct regulation of pluripotency genes (Petruzzelli *et al.*, 2014) but also in the regulation of miRNAs. These miRNAs are able to ‘fine-tune’ or further regulate gene expression and could further explain why hESCs cultured at a more physiological (low) oxygen concentration are “more” pluripotent (Forristal *et al.*, 2010, 2013).

Bioinformatic analysis that predicts mRNA targets revealed interesting potential miRNAs that were down-regulated under hypoxia that could influence the pluripotent state of hESCs. Some of these differentially expressed miRNAs were analysed independently to validate the miRNA arrays. The arrays together with the computational predictions of miRNA-mRNA interactions revealed two miRNAs of particular interest, miR-122-5p and miR-223-3p. These miRNAs were down-regulated under hypoxia and importantly predicted to have relevant targets such as the core transcription factors for pluripotency and HIFs. In detail, miR-122-5p was predicted to target HIF3A, HIF1AN, HIF2A, SOX2, NANOG and PKM2 and miR-223-3p was predicted to target HIF2A, HIF3A and NANOG. These two miRNAs could possibly cause hESCs cultured at 20% oxygen to be “less” pluripotent, since these miRNAs are more abundant and thus may repress their target

genes at this higher oxygen concentration. In contrast, the expression of miR-122-5p and miR-223-3p are decreased in hESCs cultured under low oxygen concentrations.

Interestingly, miR-122-5p was predicted to target PKM2, an enzyme involved in the rate limiting step of glycolysis. PKM2 expression is important for the maintenance of hESCs since the rate of flux through glycolysis is increased in hESCs cultured at 5% oxygen compared to those maintained at 20% oxygen (Forristal *et al.*, 2013). Moreover, PKM2 has been shown to regulate OCT4 expression in hESCs (Christensen, Calder and Houghton, 2015). Thus, the down-regulation of miR-122 under hypoxic conditions may be beneficial for hESC maintenance.

The role of specific miRNAs can be functionally dissected and investigated by using synthetic precursor RNA molecules (pre-miRs) which should not be confused with pre-miRNAs that comprise a hairpin structure. Pre-miR transfection is a routinely used technique to increase the expression of a specific miRNA and to investigate the effect on their target mRNA/protein (Cloonan *et al.*, 2008; Martinez-Nunez *et al.*, 2009; Xu *et al.*, 2009; Louafi, Martinez-Nunez and Sanchez-Elsner, 2010; Wang *et al.*, 2010). Commercially available pre-miRs are similar to siRNA and can be transfected into hESCs as described (Chapter 2.1.7). Pre-miRs, are double-stranded RNA molecules that mimic their endogenous mature miRNA and increase the level of mature miRNAs in the cell. As the level of mature miRNAs rises, a decrease in the expression of their target mRNA is expected. Precursor negative control (pre-miR-control) have a random sequence pre-miR molecule, similar to pre-miRs but the pre-miR-control produces a random scrambled miRNA with no effect on targets. This makes the pre-miR-control an ideal negative control compared to any other small RNA fragment.

4.1.1 Study Aims

The aim of this chapter is to determine whether miR-122-5p and/or miR-223-3p regulate hESC pluripotency.

Specific objectives:

- To transfect hESCs with synthetic pre-miR-122-5p, pre-miR-223-3p or pre-miR-control and observe any potential morphological changes.
- To investigate the effect of transfecting either pre-miR-122-5p or pre-miR-223-3p in hESCs cultured at 5% on mRNA and protein expression levels of SOX2, NANOG, OCT4 and PKM2 compared to pre-miR-controls.

4.2 Materials and Methods

To investigate the effect of either miR-122-5p or miR-223-3p on hESCs, Shef3 hESCs were cultured at 5% oxygen concentration for at least three passages on Matrigel. hESCs were then transfected with the mature miRNA sequence of either pre-miR-122-5p or pre-miR-223-3p to cause an increase in the expression of their endogenous mature miRNA. Pre-miRNA transfections, were performed as described in the Method Chapter 2.1.7. The stem-loop structure as well as the mature miRNA sequences of the two miRNAs, miR-122 (Figure 43) and miR-223 (Figure 44) are depicted.

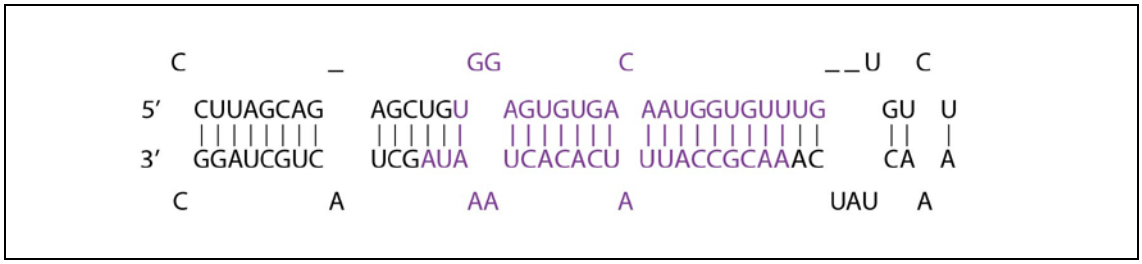

Figure 43: Stem-loop structure of miR-122 (adapted from miRBase)
Highlighted in purple is the mature miRNA sequence for miR-122-5p (top) and miR-122-3p (bottom).

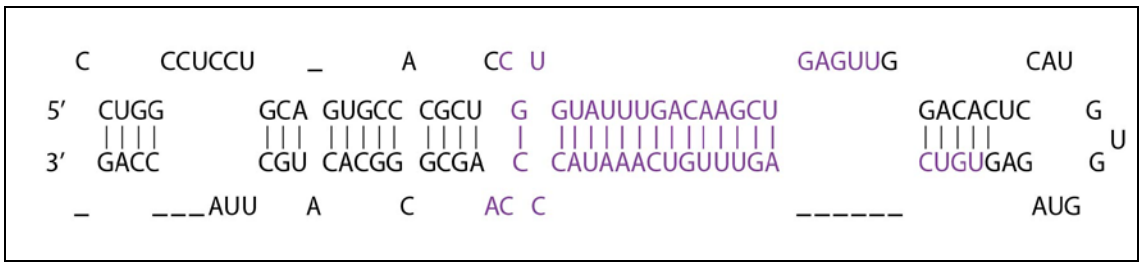

Figure 44: Stem-loop structure of miR-223 (adapted from miRBase)
Highlighted in purple is the mature miRNA sequence for miR-223-5p (top) and miR-223-3p (bottom).

Details for the methods used in this chapter are described in Chapter 2.

4.3 Results

4.3.1 Morphology of Shef3 hESC colonies transfected with pre-miRs

To determine the effect of transfecting hESCs cultured at 5% oygen with 200nM pre-miRs, cell morphology was investigated 48 h post-transfection. No overt differences in hESC morphology was observed between pre-miR-122-5p, pre-miR-223-3p, pre-miR-control and non-transfected cells (see phase contrast pictures Figure 30 and 45). This confirmed the absence of a cytotoxic response from either the transfection reagent, InterferIn, or the synthetic pre-miRs. Thus, these conditions were used in subsequent experiments.

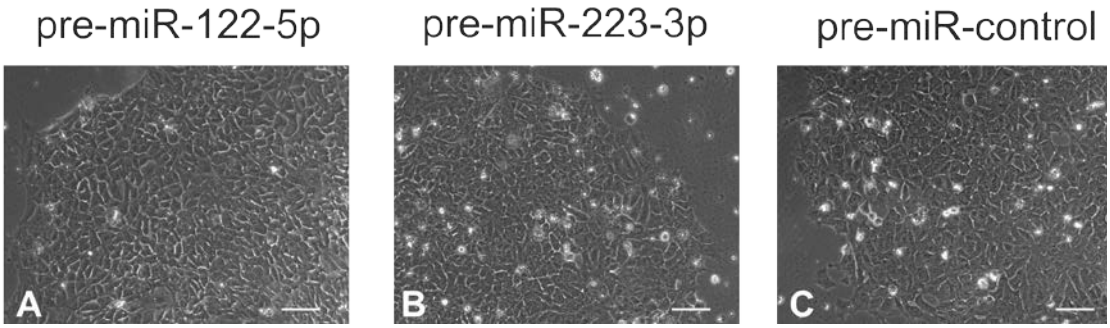

Figure 45: Pre-miRNA transfected Shef3 colonies

Representative phase contrast images of Shef3 hESCs cultured at 5% oxygen and transfected with 200nM (A) pre-miR-122-5p, (B) pre-miR-223-3p or (C) pre-miR-control. Images were taken 48h post-transfection. Scale bar = 100 µm.

4.3.2 Effect of pre-miR-122-5p or pre-miR-223-3p on the mRNA expression of OCT4, SOX2 and NANOG in hESCs

RNA from pre-miR-122-3p, pre-miR-223-3p or pre-miR-control transfected Shef3 hESC colonies cultured at 5% was collected, isolated and reverse transcribed into cDNA. To ensure that the cDNA was not contaminated with genomic DNA (gDNA) two methods were used. When cDNA was reverse transcribed using an oligo-dT primer, a PCR was performed using intron-spanning primers for OAZ1. Only samples with an amplified products of 122bp were used in subsequent experiments, since a 373bp product would have indicated genomic contamination (Figure 46). When cDNA was reverse transcribed using random hexamers, the presence of any genomic contamination was examined through RT-qPCR on samples in the absence of reverse transcriptase ("no RT control"). The RT-qPCR reaction on these control samples was performed using SOX2, a TaqMan probe that can also detect genomic DNA as this gene expression assay is designed within a single exon. This means there are no introns to interrupt the assay from detecting the gDNA. SOX2 will therefore only start amplifying a product in the control samples if gDNA is present. Genomic contamination was ruled out when the threshold cycle of the SOX2 was higher than Ct=35 out of a total of 40 cycles.

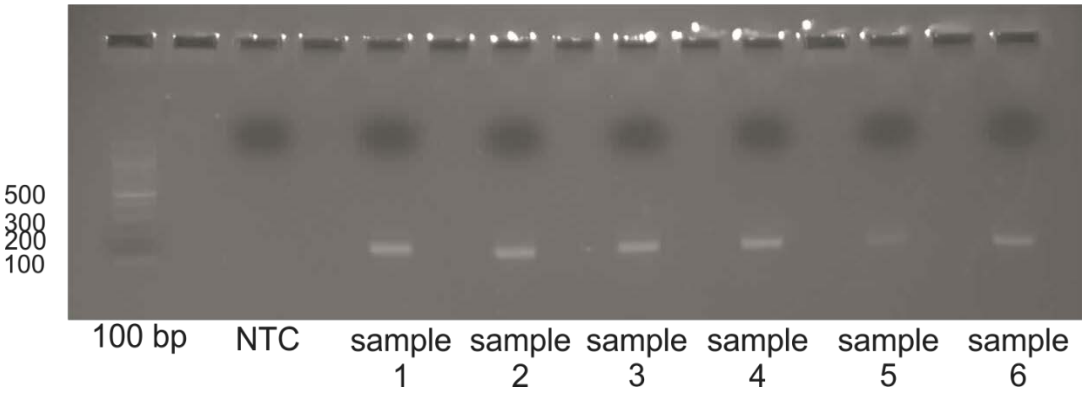

Figure 46: Representative cDNA samples which were free of genomic contamination

2% agarose gel, showing a 100bp ladder a non-template control (NTC) and PCR products of cDNA with primers against OAZ1. Amplified products of 122bp are cDNA. Genomic contamination would have been detected with amplified products of 373bp. NTC= no template control.

4.3.2.1 Identifying primers for reverse transcription of RNA

Using oligo dT in the process of reverse transcribing RNA into cDNA caused high levels of variation in the mRNA expression levels of the house keeping genes (HKG) Ubiquitin C (UBC) and β-ACTIN when compared to standard deviations of samples where random hexamers were used (Table 34). Due to the variability in HKG expression level between samples when oligo-dT were used, it was not possible to analyse the data (data not shown). However, when random hexamers were used for cDNA synthesis, the mRNA expression levels of HKGs across the samples were much closer and facilitated analysis. Since the expression levels of UBC and β-ACTIN were more stable using random hexamers, this protocol was used in subsequent experiments. Furthermore, considering the standard deviation across the samples in two different runs, UBC seemed to be the most appropriate endogenous control as depicted by lower standard deviations of STDEV=0.63 across 9 individual samples and STDEV=0.74 across 5 individual samples compared to STDEV=1.09 and STDEV=0.96 of β-Actin respectively (Table 34).

Table 34: Standard deviation across samples for mRNA expression level of HKGs UBC and β-ACTIN using oligo-dT, or random hexamers to reverse transcribe RNA into cDNA

Oligo dT used; STDEV		**Random hexamers used; STDEV**	
UBC 6 samples	0.57	UBC 9 samples	0.63
UBC 9 samples	3.34	β-ACTIN 9samples	1.09
β-ACTIN 9 samples	3.68	UBC 5 samples	0.74
UBC 6 samples	4.29	β-ACTIN 5 samples	0.96
β-ACTIN 6 samples	4.1		
UBC 2 samples	3.15		
β-ACTIN 2 samples	1.3		
UBC 6 samples	1.49		
UBC 6 samples	1.46		
UBC 6 samples	3.72		
UBC 6 samples	3.35		

4.3.2.2 OCT4, SOX2 and NANOG mRNA expression levels in Shef3 hESCs upon overexpression of miR-122-5p or miR-223-3p

Shef3 hESCs cultured at 5% oxygen were transfected with synthetic pre-miRs to overexpress either miR-122-5p or miR-223-3p. Higher miRNA expression levels can cause a decrease in their target mRNA expression if the interaction between miRNA and mRNA leads to mRNA degradation. This was investigated using RT-qPCR to analyse the mRNA expression of OCT4, SOX2 and NANOG.

Although the OCT4 mRNA expression levels for pre-miR-122-5p transfected cells appeared to be 70% greater than the control (Figure 47 A), this increase was not significantly different. When pre-miR-223-3p was transfected into hESCs there was no difference in OCT4 mRNA expression observed (Figure 47 B).

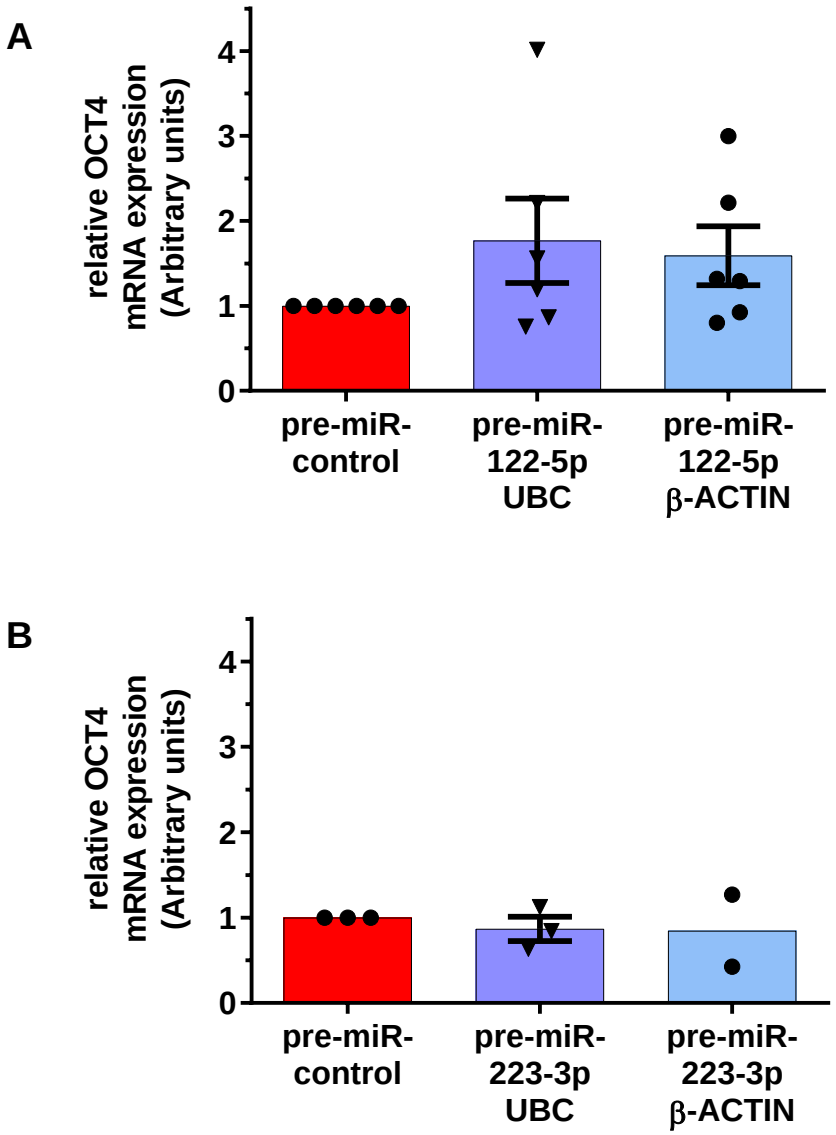

Figure 47: miR-122-5p and miR-223-3p do not affect OCT4 mRNA expression levels in Shef3 hESCs.

Relative OCT4 mRNA expression levels in Shef3 hESC cultured at 5% oxygen and transfected with 200nM (A) pre-miR-122-5p or (B) pre-miR-223-3p. Cells were collected for RNA isolation 48h post-transfection. All data have been normalised to either UBC or β-ACTIN and to 1 for the transfection control (pre-miR-control). Bars represent mean ±SEM.

The SOX2 mRNA expression levels were about 40% greater for pre-miR-122-5p (Figure 48 A) transfected cells compared to the control. These results were very similar to those observed for OCT4 mRNA (Figure 47 A) but again were not significant different to the expression of the pre-miR-control. Similarly, there was no significant difference in the expression of SOX2 in hESCs transfected with pre-miR-223-3p compared to the pre-miR-control (Figure 48 B).

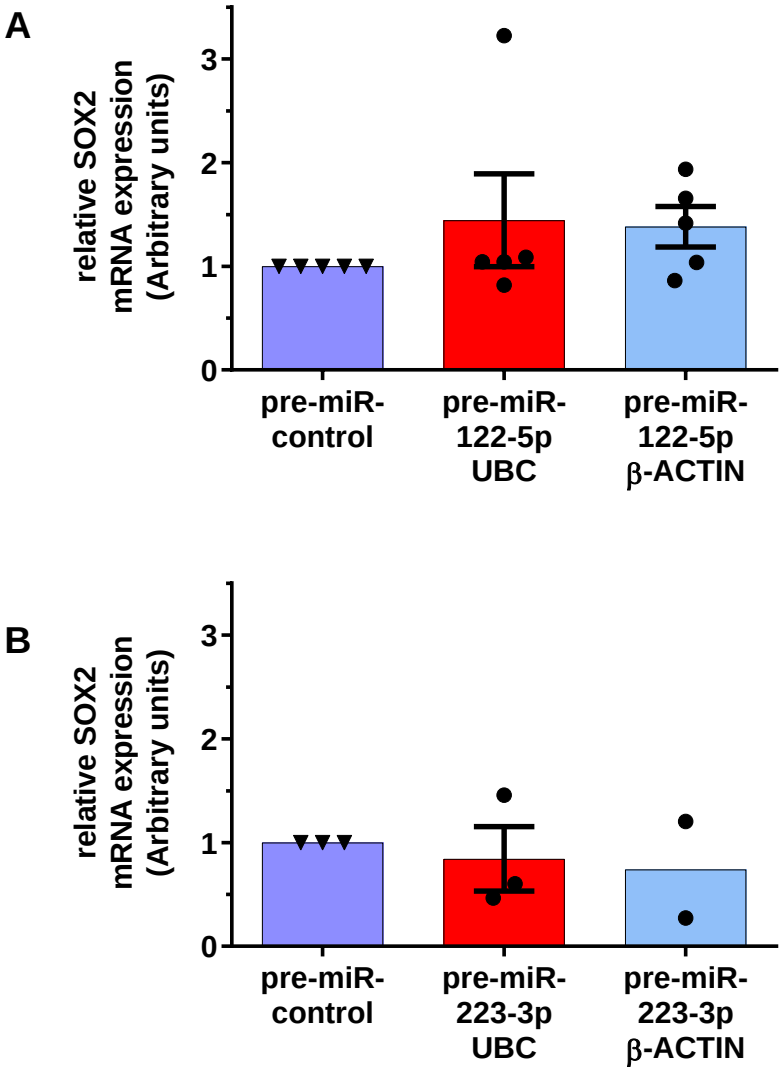

Figure 48: miR-122-5p and miR-223-3p do not affect SOX2 mRNA expression levels in Shef3 hESCs.

Relative SOX2 mRNA expression levels in Shef3 hESC cultured at 5% oxygen and transfected with 200nM (A) pre-miR-122-5p or (B) pre-miR-223-3p. Cells were collected for RNA isolation 48h post-transfection. All data have been normalised to either UBC or β-ACTIN and to 1 for the transfection control (pre-miR-control). Bars represent mean ±SEM.

The mRNA expression of NANOG displayed a trend to be 60% greater when miR-122-5p was overexpressed (Figure 49 A), though not statistically different to the pre-miR-control. Similarly, pre-miR-223-3p transfected cells displayed no difference in NANOG expression when compared to the pre-miR-control (Figure 49 B).

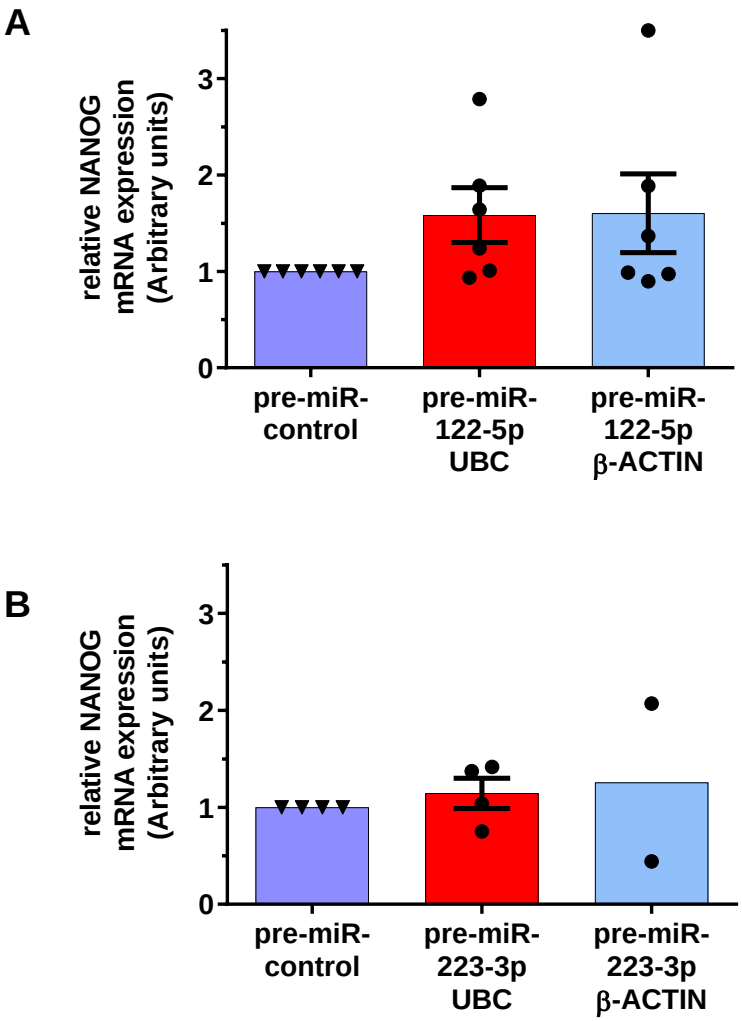

Figure 49: miR-122-5p and miR-223-3p do not affect NANOG mRNA expression levels in Shef3 hESCs.

Relative NANOG mRNA expression levels in Shef3 hESC cultured at 5% oxygen and transfected with 200nM (A) pre-miR-122-5p or (B) pre-miR-223-3p. Cells were collected for RNA isolation 48h post-transfection. All data have been normalised to either UBC or β-ACTIN and to 1 for the transfection control (pre-miR-control). Bars represent mean ±SEM.

Overall, increasing the expression level of either miR-122-5p or miR-223-3p in hESCs cultured at 5% oxygen for 48h had no effect on the mRNA expression of OCT4, SOX2 and NANOG. This suggests that miR-122-5p and miR-223-3p do not block mRNA expression in hESCs but may inhibit protein translation.

4.3.3 Effect of pre-miR-122-5p and pre-miR-223-3p on the protein expression of OCT4, SOX2, NANOG and PKM2

There were no changes detectable at the mRNA level upon increasing the expression of either miR-122-5p or miR-223-3p using pre-miR transfections (Chapter 4.3.2). mRNA data are usually a good indication of what might happen at the protein level but there are many processes involved between transcription and translation of genes which might result in very low correlations between mRNA and protein levels (Vogel and Marcotte, 2012). Furthermore, miRNAs may only block mRNA translation (Valencia-Sanchez *et al.*, 2006). Therefore, protein levels were investigated to determine whether the miRNAs were inhibiting protein translation of OCT4, SOX2, NANOG or PKM2.

The main transcription factors for pluripotency are OCT4, SOX2 and NANOG. SOX2 and NANOG as well as PKM2 were predicted to be a target of miR-122-5p and miR-223-3p was predicted to target NANOG. Therefore, Western blots were used to determine differences in protein expression between samples with increased miR-122-5p or miR-223-3p expression and compared to transfection control samples.

The data obtained indicate that OCT4 protein expression was not affected by the increased expression of miR-122-5p (Figure 50, A and C). In contrast, there was a significant, 50% reduction in OCT4 protein ($p=0.0386$) expression when pre-miR-223-3p was transfected into hESCs cultured at 5% oxygen compared to pre-miR-control (Figure 50, B and D).

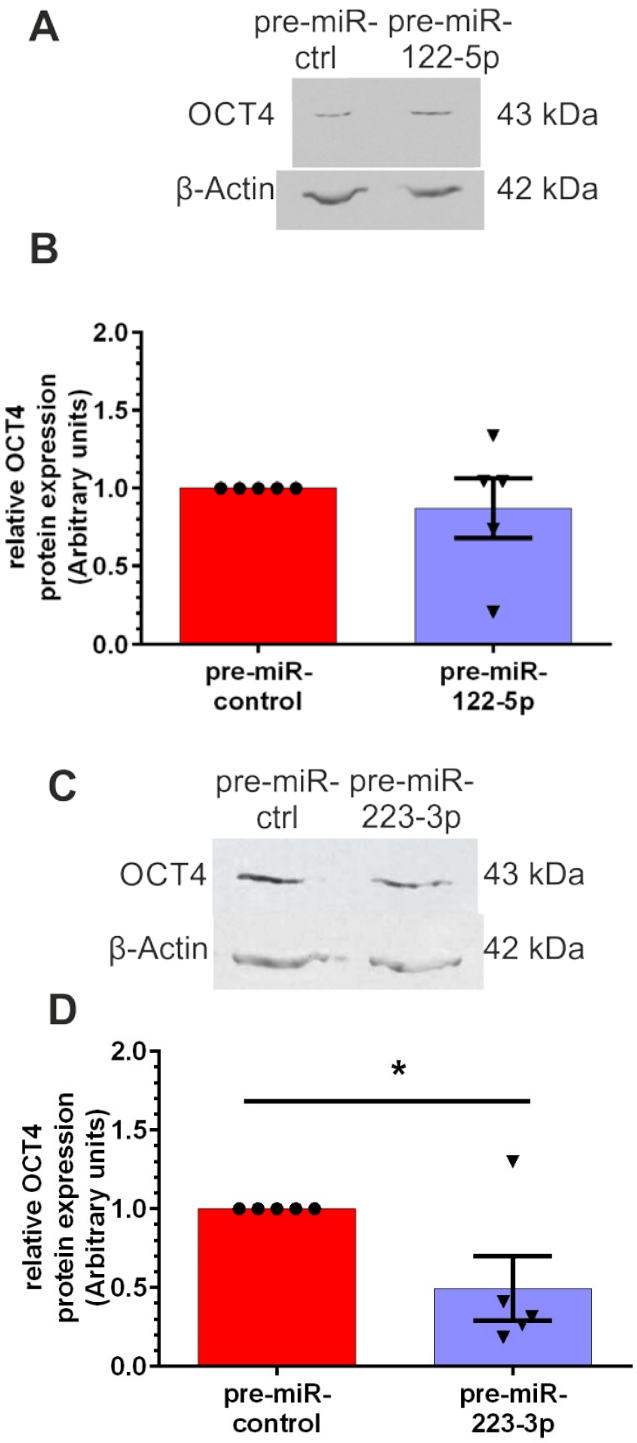

Figure 50: Effect of either pre-miR-122-5p or pre-miR-223-3p transfection on OCT4 protein expression in Shef3 hESCs

Representative OCT4 Western blot of Shef3 hESCs cultured at 5% oxygen and transfected with 200nM (A) pre-miR-122-5p or (C) pre-miR-223-3p compared to pre-miR-control. Cells were collected 48h post-transfection and protein isolated. Quantification of OCT4 expression (B and D). Protein expression was normalised to β-Actin and to 1 for pre-miR-control. Single points or triangles represent biological replicates and bars represent mean ±SEM. *P<0.05 significantly different to pre-miR-control (n=5).

Data for SOX2 indicate that hESCs cultured at 5% oxygen were affected by miR-122-5p overexpression causing a significant protein reduction. A 45% reduction in SOX2 protein expression (p=0.0289) was observed in pre-miR-122-5p treated hESCs when compared to the control (Figure 51, A and C). Although miR-223-3p overexpression was able to decrease OCT4 protein expression it did not alter SOX2 protein expression (Figure 51, B and D).

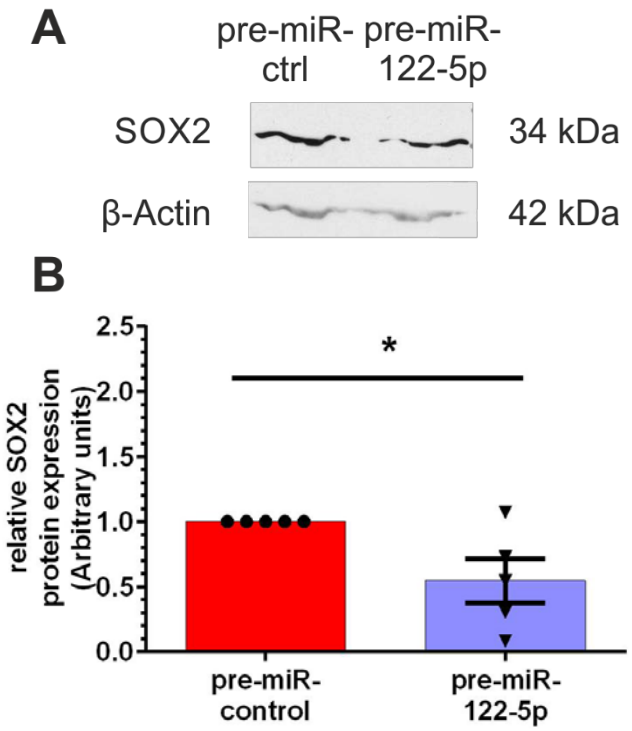

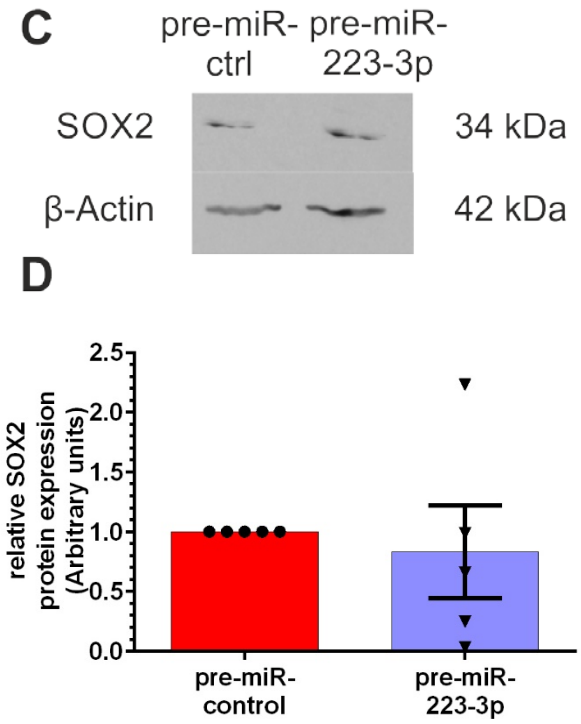

Figure 51: Effect of either pre-miR-122-5p or pre-miR-223-3p transfection on SOX2 protein expression in Shef3 hESCs cultured at 5% oxygen

Representative SOX2 Western blot of Shef3 hESCs cultured at 5% oxygen and transfected with 200nM (A) pre-miR-122-5p or (C) pre-miR-223-3p compared to pre-miR-control. Cells were collected 48h post-transfection and protein isolated. Quantification of SOX2 expression (B and D). Protein expression was normalised to β-Actin and to 1 for pre-miR-control. Single points or triangles represent biological replicates and bars represent mean ±SEM. *P<0.05 significantly different to pre-miR-control (n=5).

Intriguingly, both miRNAs miR-122-5p and miR-223-3p were predicted to target NANOG (SegalLab, see Table 31 and 33) and a significant, 50% down-regulation of NANOG protein expression was observed when either miR-122-5p (p=0.0004, Figure 52 A and C) or miR-223-3p (p=0.0003, Figure 52 B and D) was overexpressed in hESCs cultured at 5% oxygen.

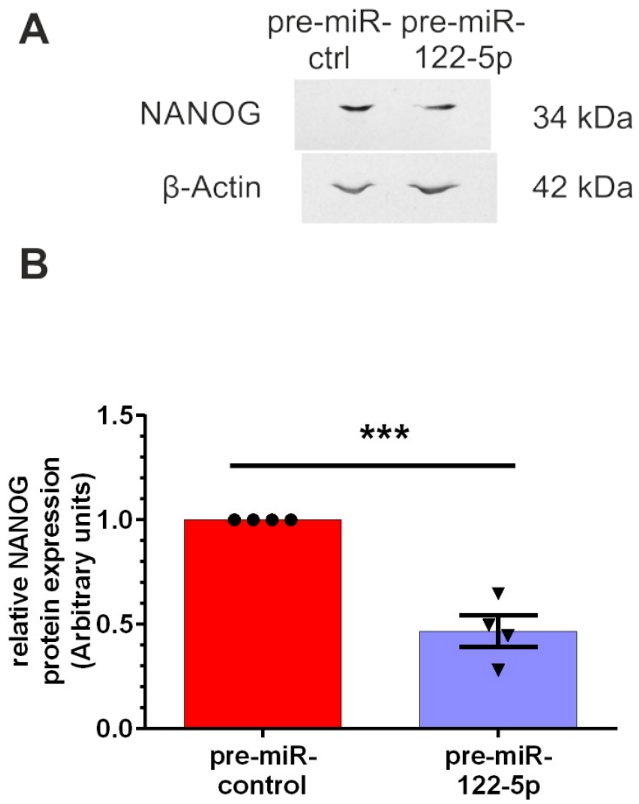

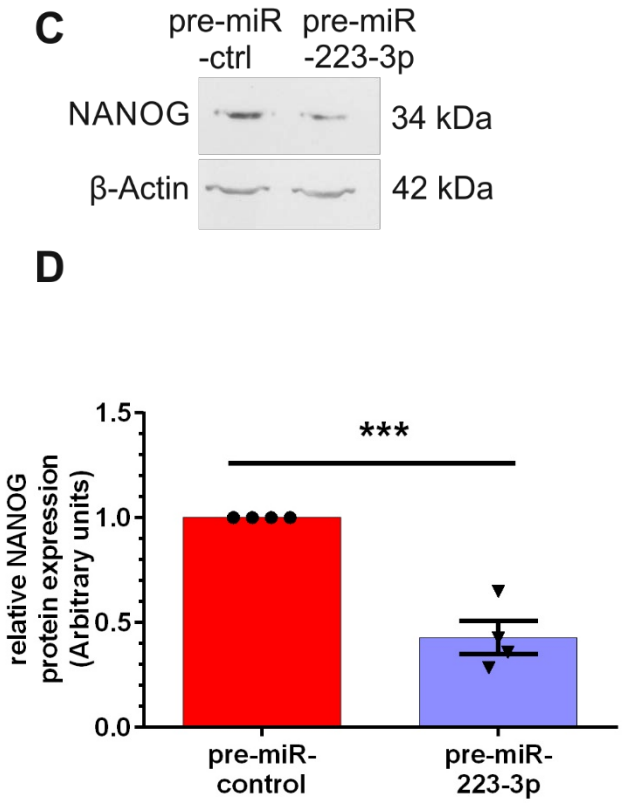

Figure 52: Transfection of either pre-miR-122-5p or pre-miR-223-3p reduces NANOG protein expression levels in Shef3 hESCs

Representative NANOG Western blot of Shef3 hESCs cultured at 5% oxygen and transfected with 200nM (A) pre-miR-122-5p or (B) pre-miR-223-3p compared to pre-miR-control. Cells were collected 48h post-transfection and protein isolated. Quantification of NANOG expression (C and D). Protein expression was normalised to β-Actin and to 1 for pre-miR-control. Single points or triangles represent biological replicates and bars represent mean ±SEM. ***P<0.001 significantly different to pre-miR-control (n=4)

PKM2 protein expression was investigated in hESCs cultured at 5% oxygen since PKM2 was a predicted target for miR-122-5p. The data show no significant differences in PKM2 expression between hESCs that were transfected with either pre-miR-122-5p or pre-miR-223-3p when compared to pre-miR-control (Figure 53).

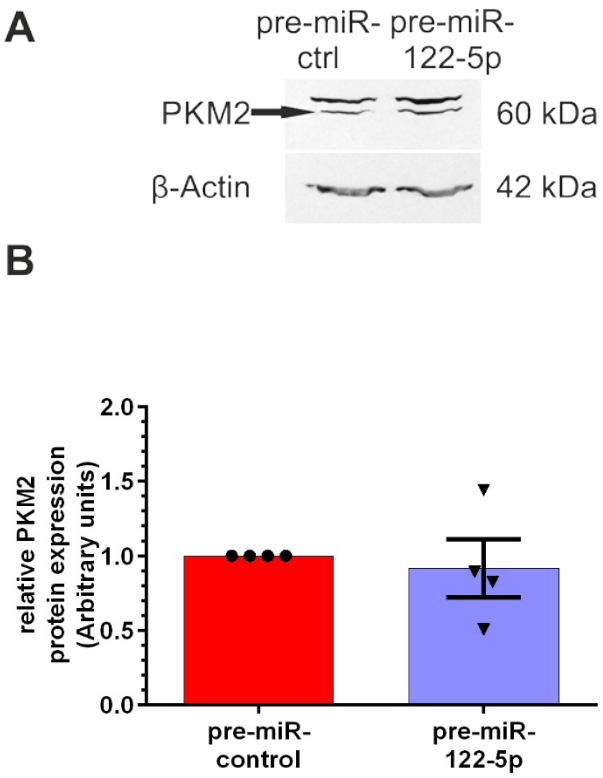

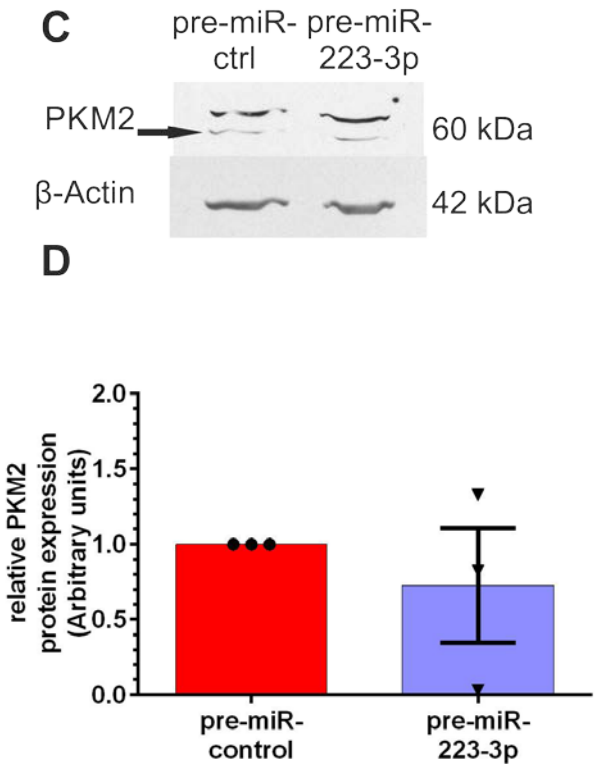

Figure 53: Transfection of either pre-miR-122-5p or pre-miR-223-3p has no effect on PKM2 protein levels in Shef3 hESCs

Representative PKM2 Western blot of Shef3 hESCs cultured at 5% oxygen and transfected with 200nM (A) pre-miR-122-5p or (C) pre-miR-223-3p compared to pre-miR-control. The PKM2 specific band is the lower band, indicated with the arrow. Cells were collected 48h post-transfection and protein isolated. Quantification of PKM2 expression (B and D). Protein expression was normalised to β-Actin and to 1 for pre-miR-control. Single points or triangles represent biological replicates and bars represent mean ±SEM. (n=4 for pre-miR-122-5p, n=3 for pre-miR-223-3p)

In conclusion, the protein expression data confirmed certain aspects of the bioinformatic data. As miR-122-5p was predicted to target PKM2, HIF1AN, SOX2 and NANOG, the transfection experiments with pre-miR-122-5p were able to support that SOX2 and NANOG protein expression were affected. The miRNA miR-223-3p was predicted to target HIF2A and NANOG of which NANOG was significantly down-regulated upon overexpression of miR-223-3p and therefore confirms that this miRNA is likely to directly affect NANOG protein expression. HIF2A protein expression was also investigated but quantification was not possible due to high levels of background signal obtained. However, preliminary observations suggest that pre-miR-122-5p but not miR-223-3p may slightly decrease HIF2A protein expression when compared to the pre-mir-control (Figure 54).

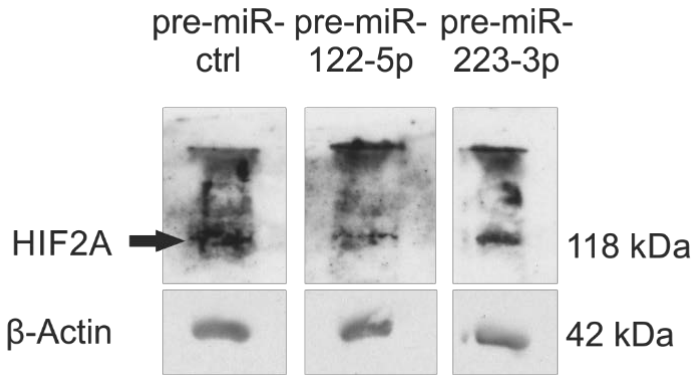

Figure 54: Effect of either pre-miR-122-5p or pre-miR-223-3p on HIF2A protein expression

HIF2A Western blot of Shef3 hESCs cultured at 5% oxygen and transfected with 200nM pre-miR-control, pre-miR-122-5p or pre-miR-223-3p. Cells were collected 48h post-transfection and protein isolated.

Taken together, miR-122-5p and miR-223-3p negatively regulate SOX2 and OCT4 protein expression respectively. Both miRNAs are not only predicted to target NANOG through bioinformatics but both miRNAs also negatively regulate NANOG protein expression.

4.4 Discussion

This chapter investigated the effects of miR-122-5p and miR-223-3p on hESCs cultured at 5% oxygen. The down-stream effects of these two miRNAs on target genes that are important for the maintenance of hESCs were analysed at the mRNA and protein level after increasing the expression of miR-122-5p and miR-223-3p using synthetic pre-miR RNA molecules.

While analysing qPCR data, the first challenge was to find a stable housekeeping gene (HKG) for hESCs that were cultured under hypoxia. Normalisation is an essential process to compare expression levels of different treatment groups to minimise errors that might occur in the preliminary material from sample collection such as RNA extraction, RNA quality and efficiency differences in the process of reverse transcribing RNA into cDNA. The most suitable HKG needs to be chosen carefully as it can vary depending on tissue, cell type and sample treatment (Tricarico *et al.*, 2002). For example, Glyceraldehyde 3-phosphate dehydrogenase (*GAPDH*), a frequently used HKG is not suitable for use when comparing hypoxia to normoxia due to a high level of variation when prostate cancer and human umbilical vein endothelia cell lines were investigated (Zhong and Simons, 1999). Furthermore, since hypoxia increases the rate of flux through glycolysis in hESCs and the expression of glycolytic proteins compared to normoxia (Forristal *et al.*, 2013; Christensen, Calder and Houghton, 2015) it is unsurprising that *GAPDH* is not a good HKG. Another HKG, *β-ACTIN* has been shown to be mostly stable in cardiosphere derived cells under hypoxia (Tan *et al.*, 2012). *UbiquitinC* (*UBC*) is a HGK frequently used primary chondrocytes and hESCs lines in hypoxic culture conditions (Foldager *et al.*, 2009; Forristal *et al.*, 2013; Petruzzelli *et al.*, 2014). The results of this chapter suggested that *UBC* was the best HKG when compared to *β-ACTIN* when cDNA was generated with random hexamers rather than with oligo-dT primers (Table 34). The use of random hexamer primers additionally increased accuracy since a smaller standard deviation was observed when compared to *β-ACTIN*. Latter observation may not be surprising as oligo-dT are biased towards the poly-A tail of the RNA. This may explain the big standard deviations observed when RNA was reverse transcribed using oligo-dT as the *UBC* and *β-ACTIN* TaqMan probes are both binding within the 5'UTR of the mRNA. In contrast, random hexamers can bind anywhere to the RNA and thus cover all regions of the RNA. Furthermore, using random hexamers enables the reverse transcribtion of RNA that might not be in perfect condition. This limitation down to RNA quality allows the utilisation of precious samples from hESCs. Additionally, random hexamers will better target regions in the 5' end of RNA which is of importance especially for long mRNA transcripts.

4.4.1 Effect of modulating miRNA expression in hESCs

There was no difference observed in the mRNA expression levels of *OCT4*, *SOX2* or *NANOG* between hESCs where the expression of miR-122-5p or miR-223-3p was increased relative to the control group. This suggests either that the transfection experiment of increasing the expression of miR-122-5p or miR-223-3p has failed, or that these miRNAs might have a post-translational effect (Bartel, 2004; He and Hannon, 2004). Indeed, increasing the expression of either miR-122-5p or miR-223-3p reduced NANOG expression significantly at the protein level. A similar significant reduction in SOX2 and OCT4 protein was obtained in hESCs cultured at 5% oxygen when the expression of miR-122-5p and miR-223-3p was increased respectively. Undoubtedly, the use of pre-miRNAs to overexpress either miR-122-5p or miR-223-3p can potentially confer with other effects that would not normally happen in the cell. However, since the expression of the miRNAs studied was already very low, further inhibition would have been much more difficult for determining differences at the target level. The effects seen for miR-122-5p and miR-223-3p on SOX2 and OCT4 expression respectively could indirectly regulate NANOG expression as NANOG is known to have binding sites for SOX2-OCT4 (Kuroda *et al.*, 2005; Rodda *et al.*, 2005). The uncorrelated results between mRNA expression and protein expression seem to be a commonly observed feature (Tian *et al.*, 2004; Tay *et al.*, 2008; Lundberg *et al.*, 2010; Vogel *et al.*, 2010; Schwanhäusser *et al.*, 2011). However, modifying the expression of miRNAs has a logical consequence that these miRNAs are either blocking mRNA translation or causing mRNA degradation according to the currently known mechanism of action (reviewed by Ha & Kim 2014). The latter scenario would be observed at mRNA and protein level whereas blockage of mRNA translation would not be measurable at the mRNA level and this likely explains the results obtained in this chapter. To date, the precise miRNA mechanism of action is still unclear as miRNA are able to promote mRNA degradation by recruiting other factors that are also used in the miRNA-unrelated break-down of mRNA, however this is not the case for all miRNA targeted mRNAs and remain to be investigated (Tat *et al.*, 2016). It is possible that miRNAs might inhibit the binding of ribosomes or polysomes, a cluster of ribosomes, which would block mRNA translation or miRNAs may stop the elongation of the amino-acid chain and therefore exert post-translational effects that would not be seen at the mRNA level. However, although it is likely that the miRNAs investigated might only block mRNA and not lead to degradation hence the lack of significant effects at the mRNA level, this effect could also be caused by the time point chosen in the experiment. RNA sample collections at a later time-point could omit a potential issue of mRNA/miRNA stability. This could result in capturing effects seen at later time points.

A similar phenomenon to the data presented was observed in the insulin resistant heart, when changes at the mRNA level were not detectable but the protein level for Glut4 was increased when miR-223-3p expression was increased (Lu, Buchan and Cook, 2010). miR-223-3p was also depicted to be highly expressed in specialised tissues such as spleen and lung but only moderately expressed in the heart (Lu, Buchan and Cook, 2010). This could be an indicator that this miRNA is usually expressed in differentiated tissues which is consistent with our findings where unspecialised hESCs express only low levels of miR-223-3p. Moreover, the expression of miR-223-3p is even lower in hESCs cultured at 5% compared to those maintained at 20% oxygen. It is tempting to speculate that miR-223-3p may be highly expressed in differentiated tissues because it might be required to constrain genes that are usually expressed in undifferentiated cells. To underpin this assumption, miR-223-3p was also found to have the majority of targets in the brain, demonstrating the role of this miRNA in the central nervous system (Harraz *et al.*, 2014). Overexpression of miR-223 caused a decrease in neuronal features such as dendritic length and branch number when differentiated from hESCs and inhibition of miR-223 up-regulated the calcium influx into human neurons that were differentiated from neural stem/progenitor cells causing immature neurons (Harraz *et al.*, 2014). The complement to our data was demonstrated by Harraz et al. (2014) where miR-223 was 2.8-fold up-regulated after human neural stem/progenitor cell differentiation. This suggests that miR-223-3p promotes differentiation by targeting genes important for maintaining the stem cell state of hESCs.

Furthermore, investigations in hESCs revealed that miR-223-3p acts as a regulator of the insulin-like growth factor receptor (IGF-1R) and fibroblast growth factor (FGF) where overexpression of miR-223-3p was found to induce differentiation whereas inhibition maintained the pluripotent state of hESCs (Yu *et al.*, 2013). These results are consistent with the findings in this work where miR-223-3p is significantly down-regulated in hESCs cultured at 5% oxygen compared to those maintained at 20% oxygen which may also underline the importance of physiological oxygen concentrations in culture. This suggests that a higher miR-223-3p expression in hESCs cultured at 20% oxygen could indicate a less pluripotent state when compared to those maintained at 5% oxygen. It remains to be investigated whether the effects observed were driven by the lower oxygen concentration or by the state of pluripotency in hESCs or both.

Forristal et al. (2010) measured mRNA levels of OCT4, SOX2 and NANOG that are significantly less expressed in hESCs cultured at 20% oxygen when compared to those cultured at 5% oxygen (Forristal *et al.*, 2010). miR-122-5p and miR-223-3p may play a part in this observation by negatively controlling OCT4, SOX2 and NANOG expression

in cells cultured at 20% oxygen. Consistently, recently published data for miR-223 showed that inhibition of this miRNA was found to maintain hESCs in an undifferentiated state (Yu *et al.*, 2013).

4.4.2 Possible role of miR-122-5p in energy metabolism

hESCs display a greater rate of flux through glycolysis at 5% oxygen than at 20% oxygen as they consume more glucose and produce more lactate and display a higher expression of the glucose transporter *GLUT1* (Forristal *et al.*, 2013). Increased glycolysis was observed with an up-regulation of PKM2 in rapidly proliferating cells such as cancer cells, hESCs or progenitor stem cells (Christofk *et al.*, 2008; Jung *et al.*, 2011). Recently, PKM2 expression was shown to be increased in hESCs in hypoxia compared to those maintained at 20% oxygen (Christensen, Calder and Houghton, 2015). It was found that PKM2 is playing a transcriptional role in regulating the expression of OCT4 rather than playing a direct role in hESCs metabolism (Christensen, Calder and Houghton, 2015). *In silico* investigations conducted in this thesis revealed, that miR-122-5p is the only miRNA from the category of "broadly conserved among vertebrates" that targets PKM2 (TargetScan6.2). Thus, overexpressing miR-122-5p in hESCs would be expected to cause a down-regulation of PKM2. This does not appear to be the case in the present data but further replicates are required to confirm whether miR-122-5p affects the expression of PKM2. However, cancer cells have many parallels with hESCs in view of their self-renewal capacity and proliferation. Cancer cells also use aerobic glycolysis for energy generation and hepatocellular carcinoma cells were shown to have a reduced miR-122-5p expression compared to healthy liver cells and overexpression of miR-122-5p reduced both mRNA and protein expression of PKM2 (Liu *et al.*, 2014). A regulatory mechanism between PKM2 and miR-122-5p has been observed when hESCs differentiate into hepatocytes (Jung *et al.*, 2011). By depleting PKM2 or overexpressing miR-122-5p proliferation was decreased and defects in self-renewal were observed in hESCs and hepatocellular carcinoma cells (HCCs) (Jung *et al.*, 2011). Furthermore, overexpression of miR-122-5p was shown to promote the expression of hepatocyte-specific genes of stem/progenitor cells (Doddapaneni *et al.*, 2013). These findings suggest that miR-122-5p promotes differentiation of stem/progenitor cells and might therefore explain why this miRNA is expressed at very low levels in undifferentiated hESCs.

In conclusion, this work suggests that miR-122-5p and miR-223-3p are both candidates that might affect the regulation of hESC pluripotency. Using RT-qPCR these two miRNAs were found to be significantly down-regulated under hypoxic conditions. The increased expression of miR-122-5p had an effect on SOX2 and increased miR-223-3p expression was affecting OCT4 protein expression. Strikingly, both miRNAs miR-122-5p and miR-223-3p were shown to inhibit NANOG expression at the protein level. However, the interaction-, targeting- and influential-network of miRNAs is far more complex than a

straightforward single-component action and outcome result. This means that although modulating the expression of a single miRNA at a time which in this case had an effect towards their target protein expression, this method will not show if the effects observed are due to a direct interaction. This issue will be addressed in the following chapter. Nonetheless, the data of this chapter are the first to report a differential altered miRNA expression in hESCs cultured under hypoxia when compared to atmospheric oxygen and indicate that miR-223-3p and miR-122-5p are involved in regulating hESC pluripotency.

Chapter 5

Evaluation of miR-122-5p and miR-223-3p binding sites in the NANOG 3'UTR

5.1 Introduction to evaluate miR-122-5p and miR-223-3p binding sites in the NANOG 3'UTR

5.1.1 Rational of miR-122-5p/miR-223-3p targeting the NANOG 3'UTR

The results from Chapter 4 showed that miR-122-5p and miR-223-3p regulate NANOG expression. NANOG is one of the core transcription factors of pluripotency and plays an important role in maintaining pluripotency, promoting self-renewal and in repressing differentiation (Boyer *et al.*, 2005; Wang *et al.*, 2006). Within the network of the core pluripotency transcription factors it is also NANOG that positively regulates SOX2 and OCT4 expression (Pan and Thomson, 2007).

Once hESCs begin to differentiate through decreased NANOG expression they will form derivates of early lineages such as extraembryonic endoderm and trophectoderm lineages (Hyslop *et al.*, 2005) or as more recently published neuroectoderm and/or neural crest (Z. Wang *et al.*, 2012b). Which exact lineage commitment seems to be variable due to different culture conditions, however, very early signs of differentiation can be measured through the expression of Brachyury, which is one of the earliest markers of mesodermal development as Brachyury is first expressed in the primitive streak during gastrulation (Wilkinson, Bhatt and Herrmann, 1990). The gene Brachyury encodes for the transcription factor T/Brachyury that is essential for mesoderm formation (Showell, Binder and Conlon, 2004; Papaioannou, 2014). A recent publication shed further light into the functional targets of human Brachyury and found that Brachyury is acting through SMAD which is essential for mesoderm but not for endoderm development (Faial *et al.*, 2015). In mice, Brachyury was also shown to regulate NANOG expression (Suzuki *et al.*, 2006). In terms of miRNA, miR-223 was shown to be involved in regulating hESC differentiation by directly targeting IGF-1R (Yu *et al.*, 2013). Inhibition of miR-223 increased both, NANOG and OCT4 protein expression but this related to a direct interaction of miR-223 with the 3'UTR of IGF-1R (Yu *et al.*, 2013).

MiR-122-5p and miR-223-3p were both more highly expressed in hESCs cultured at 20% oxygen when compared to 5% oxygen concentration. In addition, NANOG was predicted to be a target for both these miRNAs and Forristal et al. (2010) observed a higher rate of proliferation when hESCs were cultured at 5% and speculated that this could be due to the higher expression of NANOG which is able to directly bind to the kinases CDK6 and CDC25A (Neganova *et al.*, 2008; X. Zhang *et al.*, 2009; Forristal *et al.*, 2010). These kinases are both involved in cell-cycle regulations in the transition from G1 to S phase in hESCs (X. Zhang *et al.*, 2009).

Thus taking the results from the previous chapters forward, it is suggested that miR-122-5p and miR-223-3p might directly bind to the 3'UTR of NANOG. It was therefore of interest to investigate whether the down-regulation of NANOG was caused either indirectly or by a direct interaction with these miRNAs. This interaction can be investigated by performing a Dual-Luciferase-Reporter Assay which required exact knowledge of the location of where potential binding sites of miR-122-5p and miR-223-3p lay within the NANOG 3'UTR.

5.1.2 Prediction of exact miRNA target sites

Predicting the exact locations for miRNA-mRNA interactions is a challenging task because in contrast to plants, mammals do not have perfect miRNA-mRNA base pairing (Bartel, 2009). Additionally, it was thought for a long time that functional targets require at least 6nt matches within the seed-region with seed-pairing rules that follow canonical sites (Lim *et al.*, 2005; Grimson *et al.*, 2007; Bartel, 2009). These rules were sometimes supported by evolutionary conservation (Lewis, Burge and Bartel, 2005; Friedman *et al.*, 2009), secondary structure or neighbouring context information (Grimson *et al.*, 2007) as used by TargetScan6.2.

However, using canonical sites only as a "gold standard" for target prediction leaves out a huge possibility of other target sites such as non-canonical sites that cannot be identified using the seed-pairing rules. Non-canonical sites occur when the binding between the seed of the miRNA and mRNA does not entirely match. Non-canonical sites for example binding via centred base-pairing for miRNAs is only known for a few years which means that the interaction neither has the seed pairing nor do they have additional 3'pairing, instead they bind with 11 or 12 bp normal Watson-Crick from position 4-15 or 5-15 (Shin *et al.*, 2010). Transcriptome-wide identification of a miRNA called miR-155 showed that 40% of the targets occurred through non-canonical sites even though these sites seemed to be less effective than canonical ones (Loeb *et al.*, 2012).

Nevertheless, non-canonical sites were also shown to be functional and were functionally validated corroborating that perfect seed-matches are not always required (as reviewed by Brodersen & Voinnet 2009 and Seok et al. 2016). In humans, miR-196 was able to repress Hoxb8, a transcription factor that plays a role in development (Yekta, Shih and Bartel, 2004). This miR-196 and Hoxb8 3'UTR interaction comprised a GU wobble and had 3'compensatory Watson-Crick base pairing (Yekta, Shih and Bartel, 2004). Another non-canonical site in human was found for miR-124 targeting Mink1, a serine/threonine kinase. The binding of miR-124 and Mink1 was disturbed by a bulge in the seed sequence and only had marginal 3' compensatory base pairing despite being functional

to repress Mink1 expression (Chi, Hannon and Darnell, 2012). However, these functional non-canonical sites were also identified for murine Nanog where miR-296 bound with a GU wobble in the seed region and also contributed only marginally with 3'compensatory base pairing (Tay *et al.*, 2008).

Encouraged by these findings the prediction tool, SegalLab that allows single GU wobbles and mismatches was used to identify non-canonical binding sites of miR-122-5p and miR-223-3p within the NANOG 3'UTR (see Figure 55 for miRNA binding with GU wobble). SegalLab uses a x:y:z description of the seed, standing for seed size : mismatches : GU wobbles. GU wobbles are common base pair units in RNA and have similar thermodynamic stability to Watson-Crick base pairs but with their own unique properties that is specifically recognised by other RNAs and proteins (as reviewed by Varani & McClain 2000).

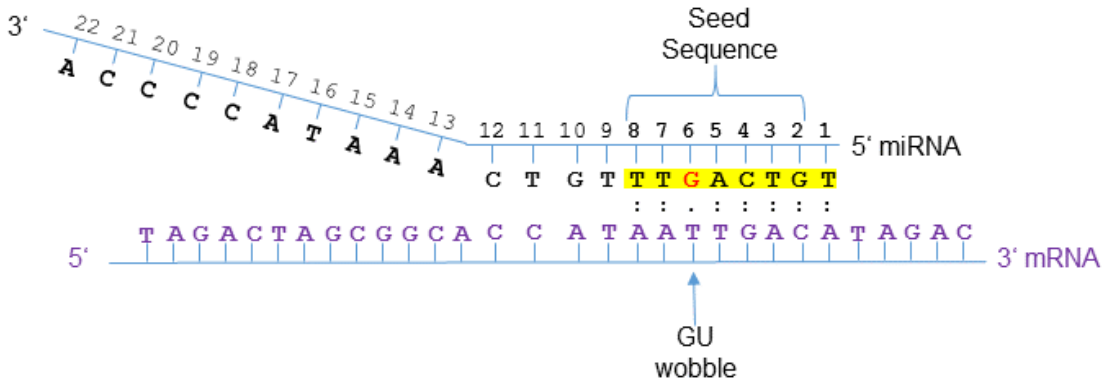

Figure 55: Schematic representation of miRNA-mRNA interaction with a GU wobble

Schematic demonstrating miRNA binding to mRNA with near perfect complementarity showing a GU wobble at position 6 of the miRNA. Note all RNA uracil bases are depicted as thymine. Colons depict Watson-Crick pairing, dots pairing for GU wobbles with base highlighted in red in miRNA sequence.

5.1.3 Study Aims

The aim of this chapter is to determine whether miR-122-5p and miR-223-3p directly regulate NANOG expression and to understand the down-stream effects and physiological relevance of this binding in hESCs.

Specific objectives:

- To elucidate potential binding sites of miR-122-5p and miR-223-3p in the NANOG 3'UTR.
- To clone a specific fragment of the NANOG 3'UTR containing the predicted miRNA binding sites into a pRL-TK vector and the two miRNAs miR-122-5p and miR-223-3p each into the pcDNA3.1(-) vector.
- To assess the specific interaction of miR-122-5p and miR-223-3p with the NANOG 3'UTR using Dual-Luciferase-Reporter assays.
- To investigate the functional impact of the miR-122-5p and miR-223-3p binding sites in hESCs.

5.2 Material and Methods

To investigate whether miR-122-5p and miR-223-3p have direct binding sites in the NANOG 3'UTR a Dual-Luciferase Reporter Assay was chosen. This assay required the NANOG 3'UTR as well as the sequences for each of the miRNAs investigated to be cloned into specific vectors.

5.2.1 Cloning Methods

5.2.1.1 Plasmid constructs

The strategy used to clone part of the NANOG 3'UTR, together with miR-122-5p and miR-223-3p is shown in Figure 56. These vectors were used to perform a Dual-Luciferase-Reporter Assay to investigate the direct binding sites of miR-122-5p and miR-223-3p in the NANOG 3'UTR.

Briefly, part of the NANOG 3'UTR, miR-122-5p and miR-223-3p were PCR amplified. Next, these fragments were TA cloned into the vector pCR2.1-TOPO (TOPO) (Figure 57). The resulting TOPO plasmids were digested and the fragments ligated into their digested destination vectors.The NANOG 3'UTR fragment was inserted into the renilla luciferase containing vector pRL-TK (Figure 58) and the two miRNAs, miR-122-5p and miR-223-3p were inserted into pcDNA3.1(-) (Figure 59). This resulted in three final plasmids pRL-TK-NANOG 3'UTR, pcDNA3.1(-)-miR-122-5p and pcDNA3.1(-)-miR-223-3p. The pGL2-control vector (Figure 60) was used to normalise all sample reactions as this vector expressed *firefly luciferase*.

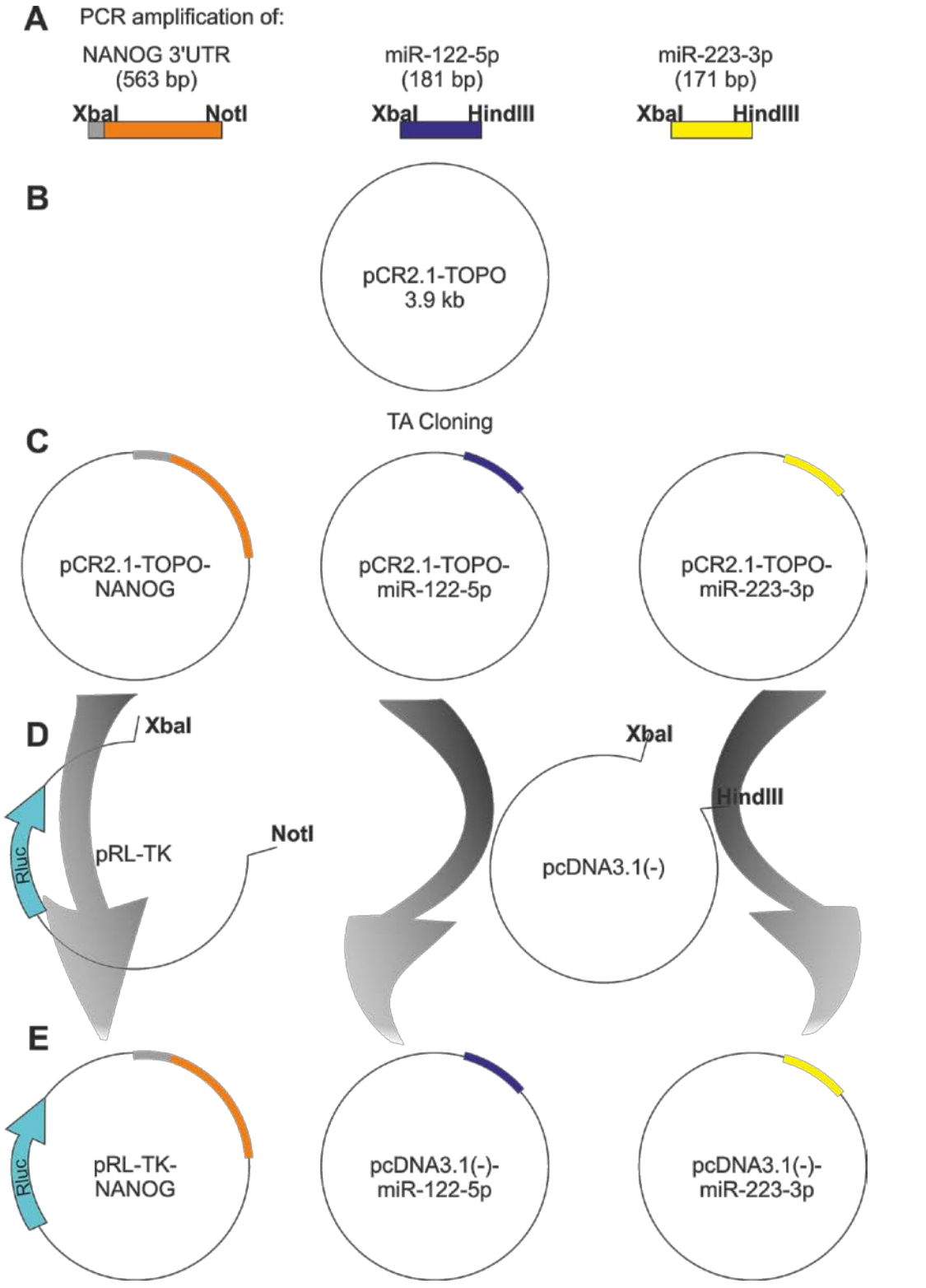

Figure 56: Schematics of Cloning strategy:

(A) PCR Amplification of NANOG 3'UTR, miR-122-5p and miR-223-3p. (B) The amplified products were sub-cloned into the pCR2.1-TOPO vector via TA cloning (C) TOPO vectors containing NANOG 3'UTR, miR-122-5p and miR-223-3p were digested with their appropriate restriction enzymes and (D) NANOG-3'UTR cloned into pRL-TK containing Renilla luciferase and miR-122-5p and miR-223-3p were cloned into pcDNA3.1(-). (E) Final vectors to be used for the Dual-Luciferase-Assay

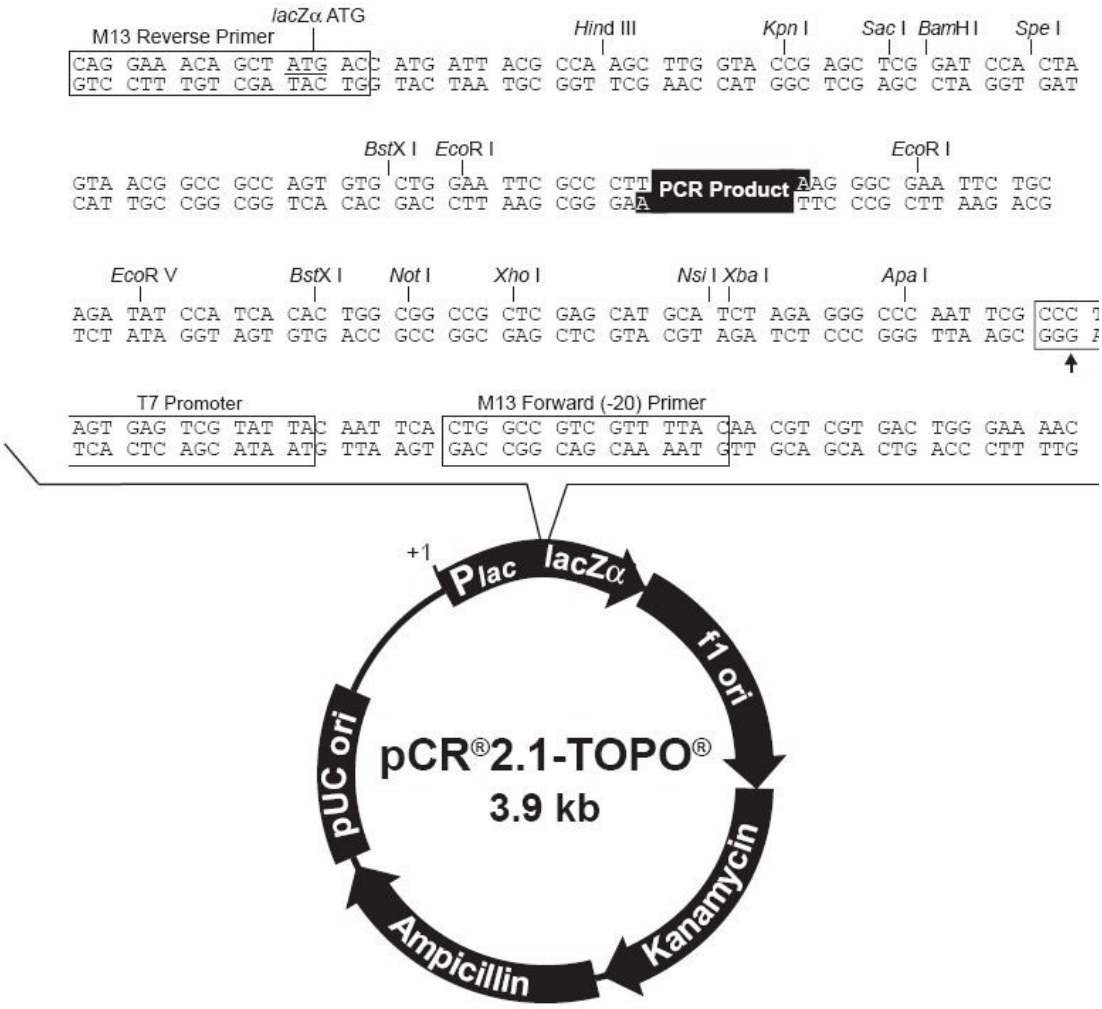

Figure 57: pCR2.1-TOPO vector

This vector was used to sub-clone the 3'UTR of NANOG, and the miRNAs miR-122-5p and miR-223-3p.

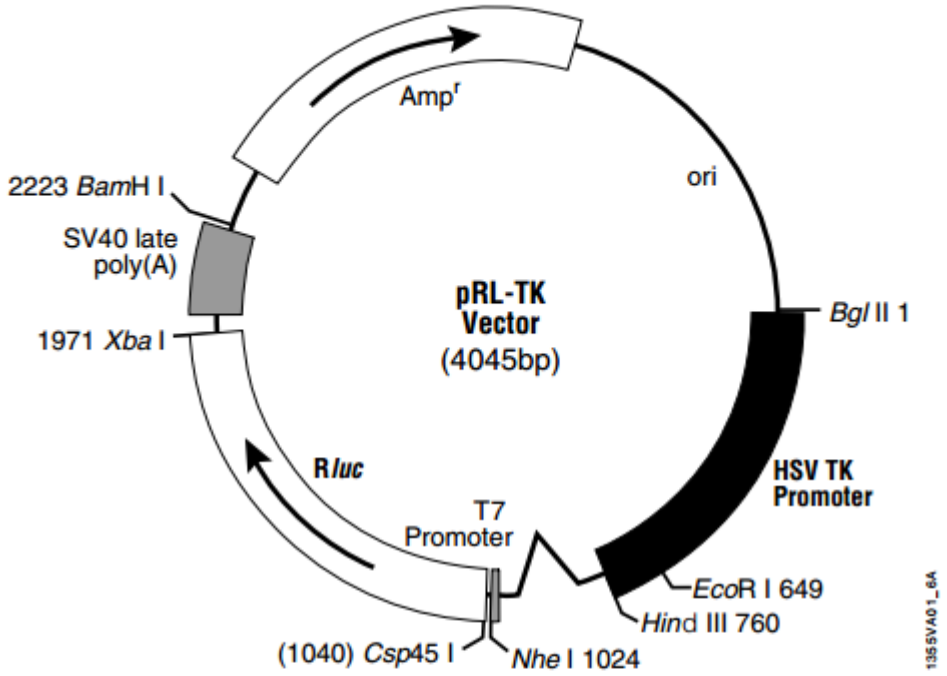

Sequence reference points:	
HSV-TK promoter	7–759
Chimeric intron	826–962
T7 RNA polymerase promoter (–17 to +2)	1006–1024
T7 RNA polymerase transcription initiation site	1023
R*luc* reporter gene	1034–1969
SV40 late polyadenylation signal	2011–2212
β-lactamase (Amp^r) coding region	2359–3219

Figure 58: pRL-TK vector

This vector was used to clone the 3'UTR of NANOG that contains the binding sites for miR-122-5p and miR-223-3p for further use in the Dual-Luciferase Assay as it contains the promotor and enhancer sequence for *renilla luciferase* expression.

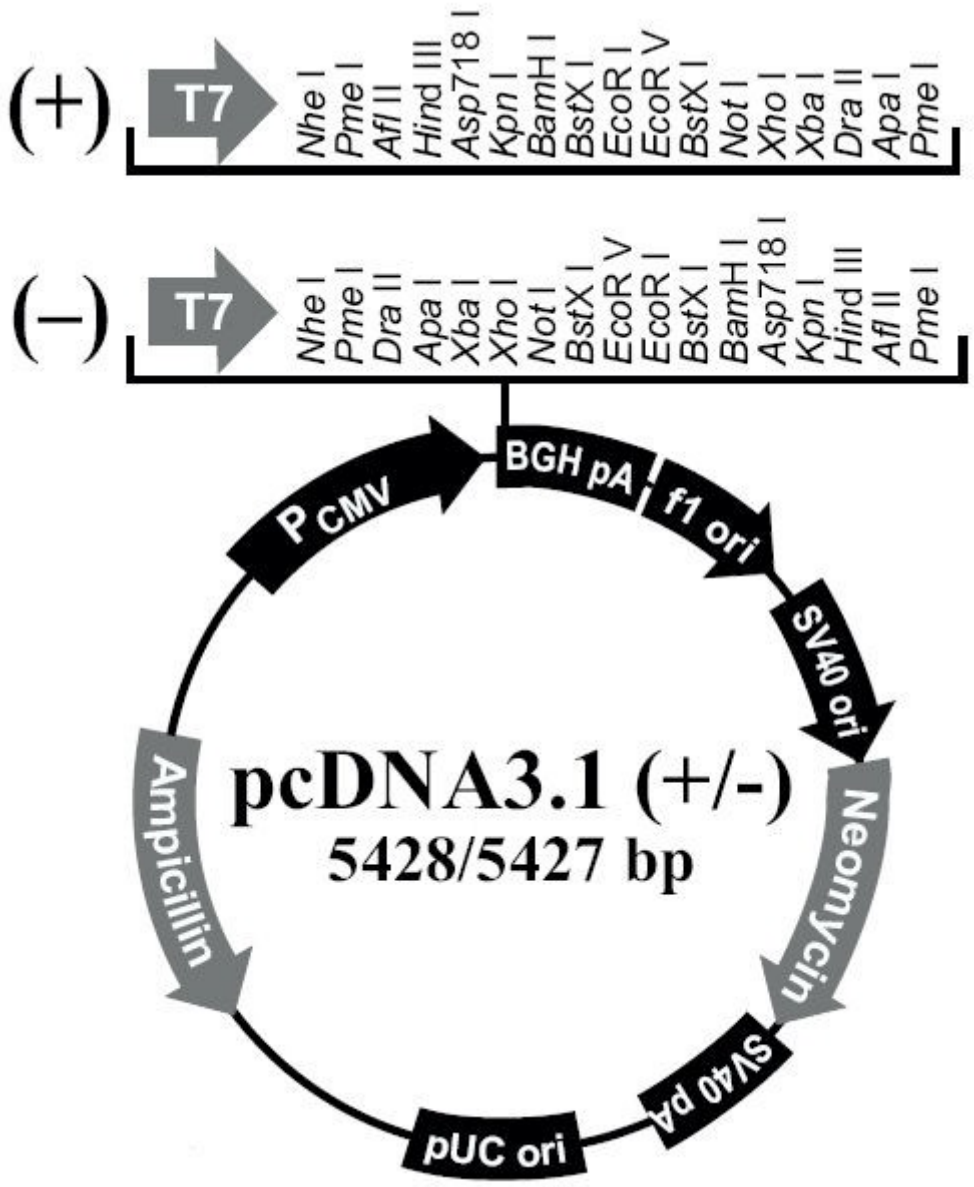

Figure 59: pcDNA3.1(-) vector

This vector was used to clone and overexpress the miRNAs miR-122-5p and miR-223-3p, to use in the Dual-Luciferase Assay.

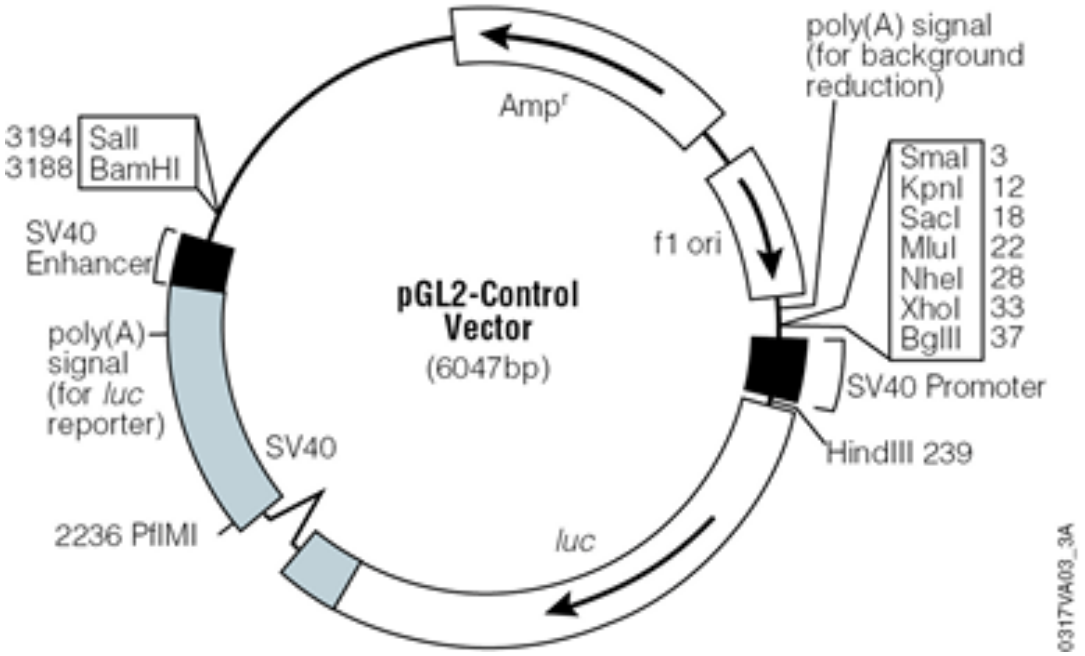

Reference points of the pGL2-control vector:

SV40 Promoter	42–244
Luciferase gene (*luc*)	268–1920
GLprimer2 binding site	269–291
SV40 late poly(A) signal	2710–2931
SV40 Enhancer	2940–3176
RVprimer4 binding site	3245–3264
ColE1-derived plasmid replication origin	3502
b-lactamase (Amp^r) gene	4264–5124
f1 origin	5256–5711
GLprimer1 binding site	6014–6036

Figure 60: pGL2-Control vector map (Promega)

This vector was used as control for the Dual-Luciferase Assay, containing the SV40 promotor and enhancer sequence for *firefly luciferase* expression.

5.2.1.2 Primer Design

Primers for PCR and DNA sequencing were designed with following main criteria: The length of the primer was chosen between 20-24 nt with a GC:AC ratio of 50:50. The ratio might be higher towards GC content for a higher melting temperature (Tm) to achieve an increased specificity. Primers were selected with up to three nucleotides of G/C at the 3'-end to avoid accumulation of As and Ts within the primer sequence. The Tm was calculated with the equation Tm=4x(G+C)+2x(A+T). Forward and reverse primer pairs were designed to have the same Tm. Restriction enzyme sites were added at the 5'-end of the primer suitable for insertion of the amplified product into the desired plasmid vectors. "Primer3" and/or "PrimerBlast" were used to design primer with the above mentioned criteria and to avoid primer self-complementation.

5.2.1.3 Polymerase Chain Reaction (PCR) for NANOG 3'UTR, miR-122-5p and miR-223-3p amplification

Genomic DNA from human articular chondrocytes was used as template, obtained from the Bone & Joint Research Group, Southampton UK (ethics number LREC 194/99/w, 27/10/10). The NANOG sequence was accessed from Ensembl (NANOG-001, ENST00000229307.8). A specific section of the NANOG 3'UTR (563bp total length) was generated with the primer pair 1 & 2 spanning a region from position 405-953 (relative to the start of the 4th exon) to amplify a product of 549bp which includes 13bp of the 4th and last exon of NANOG and 14bp in addition for the XbaI and NotI restriction enzyme sites. miR-122-5p was amplified using primer pair 3 & 4 and miR-223-3p was amplified using primer pair 5 & 6 (Table 35). For simplicity all sequences mentioned here will be denoted with thymine instead of uracil for mRNA and miRNA sequences.

Table 35: Primer and their sequences with highlighted restriction enzyme sites synthesised by Eurofins Genomics

	Primer	Sequence
1	NANOG 3'UTR XbaI For	5'-TCTAGATGAAGACGTGTGAAGATGAGTG-3'
2	NANOG 3'UTR NotI Rev	5'-GCGGCCGCGTCTTTTCTAGGCAGGGCGCGG-3'
3	122 XbaI For	5'-TCTAGAAGGTGAAGTTAACACCTTCGTGGC-3'
4	122 HindIII Rev	5'-AAGCTTCTTCTTGCTCAAAGCAAACGATGCC-3'
5	223 XbaI For	5'-TCTAGACTTCCCCACAGAAGCTCTTGGC-3'
6	223 HindIII Rev	5'-AAGCTTGTCATATCCCATCTGCCCTGGCC-3'
7	pRLTK for insert	5'-GAAGATGCACCTGATGAAATGGG-3'
8	miR122Mut For	5'-CGCGGTCTTGGCTCGAGGCAAGCTCCGTCTC-3'
9	miR122Mut Rev	5'-GAGACGGAGCTTGCCTCGAGCCAAGACCGCG-3'
10	miR223Mut For	5'-GTGTGAAGATGAGTGAAACTCGAGTTACTCAATTTCAG TCTGG-3'
11	miR223Mut Rev	5'-CCAGACTGAAATTGAGTAACTCGAGTTTCACTCATCTT CACAC-3'

The following PCR reaction was used for the amplification of the NANOG 3'UTR fragment and for amplifying the sequences of miR-122-5p and miR-223-3p (Table 36).

Table 36: PCR reaction for the amplification of NANOG 3'UTR, miR-122-5p and miR-223-3p

Total Volume	**25.00 µl**
5x GoTaqBuffer (green)	5.00 µl
10mM dNTPs	0.50 µl
5uM Forward Primer	2.50 µl
5uM Reverse Primer	2.50 µl
50ng DNA	1.30 µl
5U/ul GoTaqPol	0.25 µl
H_2O	12.95 µl

The PCR reaction was incubated at 95°C for 5 min followed by 35 cycles at 94°C for 1 min, 59.2°C for 1 min, 72°C for 45 sec. This was followed by 1 cycle at 72°C for 10 min.

The amplified product was subsequently loaded onto a Nancy (Sigma Aldrich) stained 1% Agarose Gel (30 min 120 V).

TCTAGATGAAGACGTGTGAAGATGAGTGAAACTGATATTACTCAATTTCAGTCTG
GACACTGGCTGAATCCTTCCTCTCCCCTCCTCCCATCCCTCATAGGATTTTTCTT
GTTTGGAAACCACGTGTTCTGGTTTCCATGATGCCCATCCAGTCAATCTCATGG
AGGGTGGAGTATGGTTGGAGCCTAATCAGCGAGGTTTCTTTTTTTTTTTTTTTCC
TATTGGATCTTCCTGGAGAAAATACTTTTTTTTTTTTTTTTTTGAAACGGAGTCT
TGCTCTGTCGCCCAGGCTGGAGTGCAGTGGCGCGGTCTTGGCTCACTGCAAG
CTCCGTCTCCCGGGTTCACGCCATTCTCCTGCCTCAGCCTCCCGAGCAGCTGG
GACTACAGGCGCCCGCCACCTCGCCCGGCTAATATTTTGTATTTTTAGTAGAGA
CGGGGTTTCACTGTGTTAGCCAGGATGGTCTCGATCTCCTGACCTTGTGATCCA
CCCGCCTCGGCCTCCCTAACAGCTGGGATTTACAGGCGTGAGCCACCGCGCC
CTGCCTAGAAAAGACGCGGCCGC

Figure 61: Part of NANOG 3'UTR sequence

(including 13bp of exon (green) plus 14bp for restriction enzyme site (red)), total length 563 bp (in yellow are shown two potential miRNA target sites investigated for miR-122-5p (ACT) and miR-223-3p (GATA) that were later mutated

TCTAGAAGGTGAAGTTAACACCTTCGTGGCTACAGAGTTTCCTTAGCAGAGCTG
TGGAGTGTGACAATGGTGTTTGTGTCTAAACTATCAAACGCCATTATCACACTAA
ATAGCTACTGCTAGGCAATCCTTCCCTCGATAAATGTCTTGGCATCGTTTGCTTT
GAGCAAGAAGAAGCTT

Figure 62: miR-122-5p sequence

(168bp plus 12bp for restriction enzyme sites (red)), 180bp

TCTAGActtccccacagaagctcttggCCTGGCCTCCTGCAGTGCCACGCTCCGTGTATTT
GACAAGCTGAGTTGGACACTCCATGTGGTAGAGTGTCAGTTTGTCAAATACCCC
AAGTGCGGCACATGCTTACCAGctctaggccagggcagatgggatatgacAAGCTT

Figure 63: miR-223-3p sequence

(159bp plus 12 bp for restriction enzyme sites (red)), 171bp, small letters indicate 5' upstream and 3' downstream sequence

5.2.1.4 Chemical Transformation

Amplified DNA (NANOG 3'UTR, miR-122-5p, miR-223-3p) was TA cloned into a TOPO vector and transformed into competent *E.coli* (DH5α, NEB C2987). 1.5 µl of each PCR product, 0.5 µl salt solution (1.2 M NaCl, 0.06 M $MgCl_2$) and 0.5 µl Topo Vector were incubated for 15 min at room temperature and then pre-chilled on ice before being added to 50 µl of *E.coli* and incubated for 30 min on ice. The reaction was then heat shocked for 1 min at 42°C and subsequently chilled on ice for further 2 min. 250 µl of S.O.C medium (2% tryptone, 0.5% yeast extract, 10 mM NaCl, 2.5 mM KCl, 10 mM $MgCl_2$, 10 mM $MgSO_4$, and 20 mM glucose) was added and incubated in a shaking incubator (300 rpm) for 1h at 37°C. The bacteria were then plated onto LB agar plates (Luria Bertani, 10 g/l Tryptone, 5 g/l yeast extract, 5 g/l NaCl, 15 g/l agar containing 100 µg/ml Ampicillin) in a sterile environment and incubated at 37°C overnight.

Up to 10 colonies were picked with a sterile pipette-tip and each of them inoculated in 5 ml of LB media containing 100 µg/ml Ampicillin and incubated overnight at 37°C in a shaking incubator (300 rpm).

5.2.1.5 QIAprep Spin Miniprep Kit

Isolation of plasmid DNA from overnight cultures of E.coli was performed using QIAprep Spin Miniprep Kit (Qiagen, Crawley, UK, see Appendix B.1)

To determine whether the selected colonies were successfully transformed, 5 µl DNA were subsequently digested for 1.5 h with the appropriate restriction enzyme pair (Table 37), loaded onto Nancy stained 1% agarose gel and the fragments separated with 120V for 20-30 min to visualise the presence and size of the plasmid and insert.

Table 37: Topo-Plasmid digestion for NANOG 3'UTR or miR-122-5p or miR-223-3p insert using EcoRI:

Total volume	**20.0 µl**
H_2O	12.5 µl
CutSmart(10x) Buffer, New England Biolabs	2.0 µl
EcoRI (GAATTC)	0.5 µl
Plasmid	5.0 µl

5.2.1.6 Restriction Enzyme Digest

After successful cloning of NANOG 3'UTR, miR-122-5p and miR-223-3p into the TOPO vector, the fragments were digested using the specifically designed restriction enzyme sites (Figure 56) for further cloning into pRLTK and pcDNA3.1 respectively (Table 38).

Table 38: Vectors with their desired restriction enzyme conditions

	pRLTK-SMAD2 (276 ng/µl)	TOPO-**NANOG 3'UTR** (315 ng/µl)	TOPO-**miR-122-5p** clone3 330ng/µl	TOPO-**miR-223-3p** clone 6 315 ng/µl	**pCDNA3.1(-) ON digest**
H2O	8.7 µl	2.0 µl	-	-	10.9 µl
Buffer	NEB 3.1 2.0 µl	NEB 3.1 2.0 µl	CutSmart Buffer 4.0 µl	CutSmart Buffer 2.0 µl	CutSmart Buffer
Enzyme1	XbaI (TCTAGA) 0.5 µl	XbaI (TCTAGA) 0.5 µl	XbaI (TCTAGA) 1.0 µl	XbaI (TCTAGA) 0.5 µl	XbaI (TCTAGA) 0.5 µl
Enzyme2	NotI (GCGGCCGC) 0.5 µl	NotI (GCGGCCGC) 0.5 µl	HindIII HF (AAGCTT) 1.0 µl	HindIII HF (AAGCTT) 0.5 µl	HindIII HF (AAGCTT) 0.5 µl
Plasmid	2 µg→7.3 µl	15-20ul → 15 µl (4.7 µg)	34 µl (11 µg)	15 µl (4.7 µg)	5.0 µl (2µg)
Total Volume	20 µl	20 µl	20 µl	20 µl	20 µl

The reactions were incubated for 3 h at 37°C except for pcDNA3.1 which was incubated overnight. The digests were loaded on a Nancy stained 1% agarose gel.

5.2.1.7 Agarose Gel Extraction

The Qiagen Gel Extraction Kit was used for the extraction of the specific bands of either, the plasmid-vector or the insert following the manufactures instructions (see Appendix B.2). The purified DNA was then measured using a NanoDrop (ND-1000, ThermoScientific) and centrifuged under speed vacuum to concentrate the sample according to the reading from the NanoDrop and the required concentrations used for the next step of the ligation reaction.

5.2.1.8 Ligation of Vector and Insert

These ligation reactions were required to obtain the final vector constructs, pRLTK-3'UTR NANOG, pcDNA3.1-miR-122-5p and pcDNA3.1-miR-223-3p. 200-300 ng of insert and 50-100 ng vector were used in following ligation reaction (Table 39):

Table 39: Ligation conditions for final vector constructs

	pRLTK-NANOG 3'UTR	pcDNA3.1-miR-122-5p	pcDNA3.1-miR-223-3p
Insert	3.5 µl of NANOG 3'UTR (260 ng)	4.5 µl of miR-122-5p (300 ng)	1 µl of miR-223-3p (210 ng)
Vector	1 µl pRLTK (82.2 ng)	1.5 µl pcDNA3.1(-) (75 ng)	1 µl pcDNA3.1(-) (50 ng)
Ligation Buffer (10x)	1 µl	1 µl	1 µl
T4 Enzyme (1 U/µl)	1 µl	1 µl	1 µl
H_2O	3.5 µl	2 µl	3.5 µl
Total Volume	10 µl	10 µl	10 µl

The ligation reactions were incubated at 16°C with shaking (300 rpm) overnight.

5.2.1.9 Transformation of final vector constructs into *E.coli*

Competent *E.coli* (DH5α, NEB C2987) were transformed using 5 µl of the ligation reaction and incubated for 30 min on ice. The transformed bacteria were then heat shocked for 1 min at 42°C and subsequently chilled on ice for further 2 min. Then, 250 µl of S.O.C media was added and incubated on a shaker (300 rpm) for 1 h at 37°C. The bacteria were then plated onto LB agar plates (LB Agar tablets (Sigma, USA) containing 100 µg/ml Ampicillin) in a sterile environment and incubated at 37°C overnight.

Up to 10 colonies were picked with a sterile pipette-tip and each of them inoculated in 5 ml of LB media containing 100 µg/ml Ampicillin and incubated overnight at 37°C in a shaking incubator (300 rpm). The plasmid DNA was extracted in the same manner as described in Chapter 5.2.1.5. To determine whether the selected colonies were successfully transformed, 5 µl DNA were subsequently digested for 1.5 h at 37°C with the appropriate restriction enzyme pair (Table 40) and loaded on a Nancy stained 1% agarose gel and the fragments separated with 120 V for 20-30 min.

Table 40: Restriction Enzyme Digest for constructs in their final vector pRLTK or pcDNA3.1(-)

	pRLTK- NANOG 3'UTR	pcDNA3.1(-) **miR-122-5p / miR-223-3p**
H_2O	12 µl	12 µl
Buffer	NEB 3.1 2.0 µl	CutSmart 2.0 µl
Enzyme1	XbaI (TCTAGA) 0.5 µl	XbaI (TCTAGA) 0.5 µl
Enzyme2	NotI (GCGGCCGC) 0.5 µl	HindIII HF (AAGCTT) 0.5 µl
Plasmid	5.0 µl	5.0 µl
Total Volume	20 µl	20 µl

5.2.1.10 Site-Directed Mutagenesis

Site-directed mutagenesis was used to change the miRNA binding sites in the fragment of NANOG 3'UTR. This was done in order to understand if the miRNA binding site was specific and analysed with a Dual-Luciferase-Reporter-Assay.

5.2.1.10.1 Primer Design for the site-directed mutagenesis

PrimerX (http://www.bioinformatics.org/primerx/cgi-bin/DNA_1.cgi) was used to design mutagenic primers for altering specific binding sites of miR-122-5p or miR-223-3p in the NANOG 3'UTR. Primers were designed in such a way that a XhoI restriction enzyme site (5' CTCGAG 3') was introduced in the 3'UTR region of NANOG where the miRNA binds to destroy their binding site and to be able to check the introduced mutation with a digest of the vector. Parameters were adjusted following the protocol for QuikChange Site-Directed Mutagenesis Kit by Stratagene (Table 41).

Table 41: Parameters for QuikChange site-directed mutagenesis

	Mutating miR-122-5p binding site with substitution of 3 bases	Mutating miR-223-3p binding site with substitution of 4 bases
Melting temperature:	77.6°C	74.0°C
GC content:	67.47%	41.86%
Length:	31 bp	43 bp
5' flanking region:	14 bp	20bp
3' flanking region:	14 bp	19bp
Terminates in G or C:	Yes	Yes
Mutation site at center:	Yes	Yes

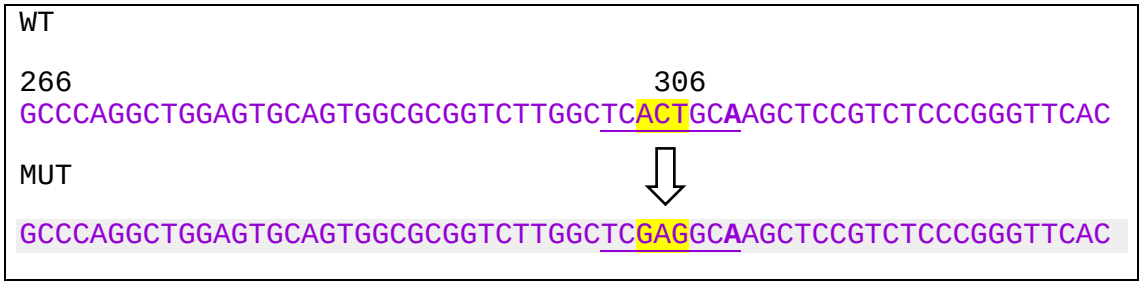

Figure 64: Schematic of site-directed mutagenesis of miR-122-5p binding site in NANOG 3'UTR at position 306

Site-directed mutagenesis was performed by introducing a XhoI (CTCGAG) binding site through substitution of three bases ACT301GAG (highlighted in yellow) to destroy the binding site of miR-122-5p at this position.

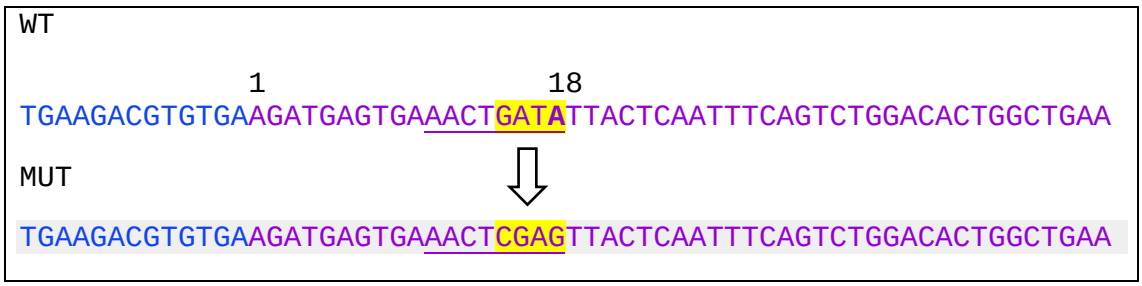

Figure 65: Schematics of site-directed mutagenesis of miR-223-3p binding site in NANOG 3'UTR at position 18

Site-directed mutagenesis was performed by introducing a XhoI (CTCGAG) binding site through substitution of four bases GATA15CGAG (highlighted in yellow) to destroy the binding site of miR-223-3p at this position. (bases in blue belong to the coding region of NANOG)

5.2.1.10.2 PCR Reaction for Site-Directed Mutagenesis

The substitution of 3 bases for the miR-122-5p binding site or 4 bases for the miR-223-3p binding site in the 3'UTR of NANOG was performed according to the Quick Change site-directed Mutagenesis Kit (Agilent Technologies).

The pRLTK-3'UTR NANOG vector was used for the site-directed mutagenesis as dsDNA template with the specific primers miR122MutFor/Rev and miR223MutFor/Rev (Table 35).

The reactions were prepared (Table 42) and incubated at 95°C for 30 sec followed by 12 cycles at 95°C for 30 sec, 77.8°C for miR-122-5p or 74.2°C for miR-223-3p for 1 min. This was followed by one cycle at 68°C for 4min 45 sec.

Table 42: Site-directed Mutagenesis PCR reaction

Reagent	Volume
10x Reaction Buffer	5.00 µl
25 or 50ng of dsDNA template (10ng/µl)	2.50 µl or 5.00 µl
125 ng Forward Primer (see Table 35 primer 8 or 10) (100ng/µl)	1.25 µl
125ng Reverse Primer (see Table 35 Primer 9 or 11) (100ng/µl)	1.25 µl
dNTPs (10 mM)	1.00 µl
PfuTurbo DNA Polymerase (Promega 3U/ µl)	1.00 µl
Total Volume	50.00 µl

The amplification product was subsequently digested with 1 µl DpnI (10 U/µl, Promega) for 1 h at 37°C to digest any parental DNA template that has not been mutated. Next, 1 µl of the DpnI treated DNA was transformed into *E.coli* as described in Chapter 5.2.1.9 and 4 clones were grown up to extract the plasmid DNA following the same procedure as described in Appendix B.1.

These clones were then subject to XhoI/BamHI digestion to determine positive clones, which results in a fragment of ~500bp for the mutated miR-122-5p binding site and ~800bp for the mutated miR-223-3p binding site next to the fragment size of the remaining plasmid. In contrast, digest of negative clones will result in a linearization of the plasmid.

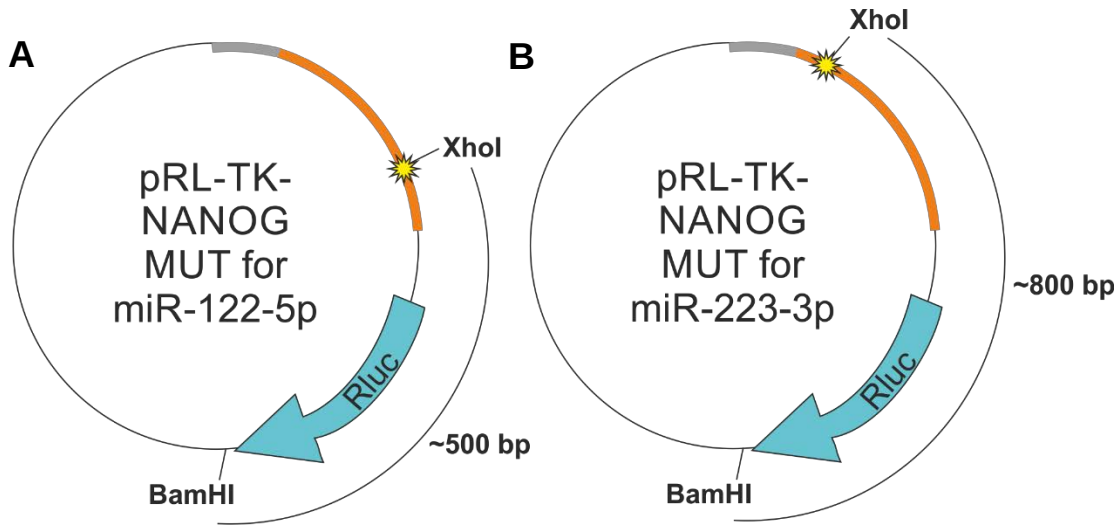

Figure 66: Schematic representation of the mutated pRL-TK vectors

Schematics of (A) pRL-TK vector with mutated miR-122-5p binding site and (B) for pRL-TK vector with mutated miR-223-3p binding site. Double-digest with the restriction enzymes XhoI and BamHI will result in either a ~500bp (A) or ~800bp (B) fragment as well as the bigger fragment of the remaining plasmid for positive clones.

5.2.1.11 Preparation of bacterial glycerol stocks

After the overnight culture of one *E.coli* colony in 5ml of LB media, 300 µl of bacterial cells were transferred into a screw top tube to 700 µl of 50% glycerol, mixed and stored at -80°C.

Without thawing the glycerol stock, frozen bacteria can be scraped onto LB agar plates (containing the appropriate antibiotics), grown overnight to isolate a single bacterial colony for an overnight culture in LB media.

5.2.1.12 Sequencing

Positive clones were sent for sequencing (BioSource or GATC) using M13F for the TOPO plasmid and T7 for pcDNA3.1 inserts and pimer7 “pRLTK for insert” (see Chapter 5.2.1.3, Table 35 on page 173) for pRLTK inserts.

Colonies of the correct sequence were expanded and DNA extracted the QIAgen plasmid maxiprep.

5.2.1.13 QIAgen Plasmid Maxiprep

To start the overnight culture for a maxiprep 200 µl of the previous mini-culture (5 ml) was added to 250 ml of LB media containing 100 µg/ml Ampicillin into a canonical flask. The culture was incubated at 37°C overnight with 300 rpm shaking and plasmid DNA extracted according to manufactures instructions (see Appendix B.3).

5.2.2 Dual-Luciferase Assay

5.2.2.1 Transfection of HeLa cells

For the luciferase assay HeLa cells, a human cervical cancer cell line, was cultured in DMEM medium containing 10% FBS and 1% Penicillin/Streptomycin (HeLa medium). HeLa cells were maintained in T175 flasks at 20% oxygen and 37°C. For passaging, HeLa cells were dissociated with 1x Trypsin (Invitrogen), collected and centrifuged at 1500 rpm for 4 min. The cell pellet was re-suspended in HeLa medium to a desired cell density ($2x10^4$ cells/well) and transferred into a 24-well-plate one day prior to transfection.

The transfection cocktail (Table 43) was incubated for 10 min at room temperature, before 350 µl/well of HeLa medium was added (see Figure 67).

Table 43: Dual-Luciferase transfection cocktail for each well of a 24-well-plate:

Component	Concentration
pGL2 control	2.5 ng/well
pRLTK-NANOG OR pRLTK-NANOG Mut at miR-223-3p binding site	0.5 ng/well
pcDNA3.1-empty OR pcDNA3-1-miR-122-5p OR pcDNA3.1-miR-223-3p	1 µg/well
Superfect (Lifetechnologies)	5 µl/well
DMEM (without FBS, without Penicillin/Steptomycin)	60 µl/well

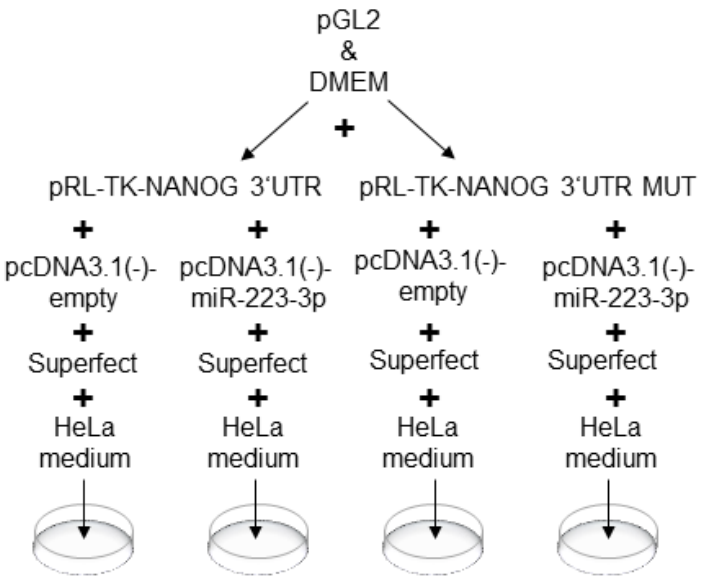

Figure 67: Schematics of applying the Dual-Luciferase transfection cocktail
Example of applying the transfection cocktail (Table 43) for each well to investigate the binding site of miR-223-3p in the NANOG 3'UTR. The same applied for miR-122-5p, using pcDNA-3.1(-)-miR-122-5p instead of pcDNA3.1(-)-miR-223-3p.

On day 1 post-passaging the cells were washed with 1xPBS and incubated with the complete transfection cocktail containing HeLa medium for 3 h at 37°C, before being washed once with 1xPBS and incubated for further 16 h at 37°C in 1 ml/well of HeLa medium. The transfections were carried out in duplicates for each condition and analysed.

5.2.2.2 Dual-Luciferase Reporter Assay

The dual-luciferase reporter assay was used to determine the direct interaction of two miRNAs, miR-122-5p and miR-223-3p with the 3'UTR of NANOG. The dual-luciferase reporter assay has two luciferase reporters; *firefly* (*Photinus pyralis*) and *renilla* (*Renilla reniformis*) *luciferase*. Each of the luciferase activities were measured with a luminometer (TD-20/20, Turner Designs).

The dual-luciferase reporter assay (Promega, #E1910) was utilised to measure the firefly and renilla luciferase activity of the transfected HeLa cells. 19 h post transfection, HeLa medium was removed and the cells washed with 1xPBS. Following the addition of 50 µl 1xPassive Lysis Buffer, cells were incubated for 20 min with shaking at room temperature. The cell lysate was transferred into an Eppendorf tube and centrifuged for 3 min at 13,000 rpm to separate cell debris. 20 µl of the cell lysate was added to 50 µl of Luciferase Assay Reagent II, thoroughly mixed by pipetting up and down several times and the *Firefly Luciferase* signal measured setting the luminometer to 70% sensitivity and performing a 2 s delay, followed by a 10 s measurement period. Immediately after the first measurement was taken 50 µl of Stop & Glo Reagent was added to quench the *Firefly Luciferase* activity, mixed and replaced into the luminometer to perform the second reading for the *Renilla Luciferase* signal with the same instrument settings.

The data were transferred into an Excel spread sheet calculating the normalised fold change in activity of luciferase activities (Firefly Luciferase activity)/(Renilla Luciferase activity) and then expressed as a percent activity. Each construct was compared to activity of the construct from the transfection with the empty pcDNA3.1 vector (pcDNA3.1(-)-Ø or control) to obtain a relative difference in activity between the tested constructs in each experimental group. The normalised fold changes in luciferase activities from each experiment were averaged and the statistical difference determined using a Students t-test.

5.2.3 Proliferation assay using Ki67

The Immunocytochemistry (ICC) for assessing proliferation was performed on hESCs cultured on Matrigel in 12-well plates on day three post-passage. These cells were also transfected with either synthetic pre-miRNAs or synthetic anti-miRNAs as described in Chapter 2.1.7. The cells were washed twice with 1xPBS and fixed in 4% paraformaldehyde for 20 min at 4°C. The cells were blocked and permeabilised in 3% donkey serum and 0.1% trition X-100 containing 1xPBS for 1 h at room temperature. The primary antibody Ki67 (Novocastra) was diluted 1:100 in the same block solution and added to the cells in the 12-well plate for 2 h at room temperature in a humidified box. After washing four times with 1xPBS the appropriate secondary antibody anti-mouse IgG-FITC was diluted 1:100 in the same block solution and added to the cells for 1h at room temperature in the dark. DAPI contained in the mounting solution was used to label nuclei (Vectashield, Vector Labs). Microscopy was performed using Zeiss microscope Observer.D1 and Observer.Z1 (Carl Zeisss MicroImaging GmbH, Jena).

5.2.3.1 Cell count

The cell count of Ki67 positively stained cells was done using Cellprofiler (Carpenter *et al.*, 2006; Lamprecht, Sabatini and Carpenter, 2007). Individual cells within any clump of cells were distinguished by drawing a line between them. Cellprofiler then counted the number of cells labelled for DAPI, the number of cells labelled for Ki67 and Ki67-positive-labelled-nuclei. With this information it was possible to calculate a percentage of Ki67-positive-stained-nuclei. Ki67-positive-stained-nuclei mean values from each group (pre/anti-miR-ctrl, pre/anti -miR-122-5p, pre/anti -miR-223-3p and pre/anti -miR-122-5p & pre/anti miR-223-3p) were analysed in GraphPad Prism and compared by a one-way ANOVA test followed by a Dunnett's multiple comparision test.

5.3 Results

5.3.1 Dual-Luciferase-Assay analysis of miR-122-5p and miR-223-3p in NANOG 3'UTR

5.3.1.1 Identification of distinct miRNA recognition elements in NANOG 3'UTR

In the previous chapter transfections with synthetic pre-miR-122-5p and pre-miR-223-3p were both able to decrease significantly NANOG protein expression ($p \leq 0.001$). In addition, pre-miR-122-5p decreased SOX2 protein expression ($p \leq 0.05$) and pre-miR-223-3p decreased OCT4 protein expression ($p \leq 0.05$). This could indicate a direct interaction between these miRNAs and the 3'UTR of these TFs. Since the effect of these miRNAs was strongest in repressing NANOG protein expression, these two miRNAs were investigated further. This chapter aims to determine whether miR-122-5p and miR-223-3p bind directly to the NANOG 3'UTR.

As shown from the bioinformatic investigations (Chapter 3.3.3), TargetScan (version 6.2) was unable to predict miRNA binding sites for miR-122-5p and miR-223-3p in the NANOG 3'UTR. However, the NANOG 3'UTR analysed with TargetScan only comprises 966 bp but according to ENSEMBLE it is more than 4000bp long. Hence, the online microRNA prediction tool from SegalLab (Kertesz *et al.*, 2007) was used to identify miRNA target sites which runs the PITA algorithm, available at: http://genie.weizmann.ac.il/pubs/mir07/mir07_prediction.html.
However, upon entering complete sequences for NANOG 3'UTR as well as for miR-122-5p and miR-223-3p the programme returned incompatible binding sites. This meant that the potential binding sites were checked manually and either sites with strong binding characteristics were chosen or alternatively, sites selected based on sequence complementarity alone (Figure 68).

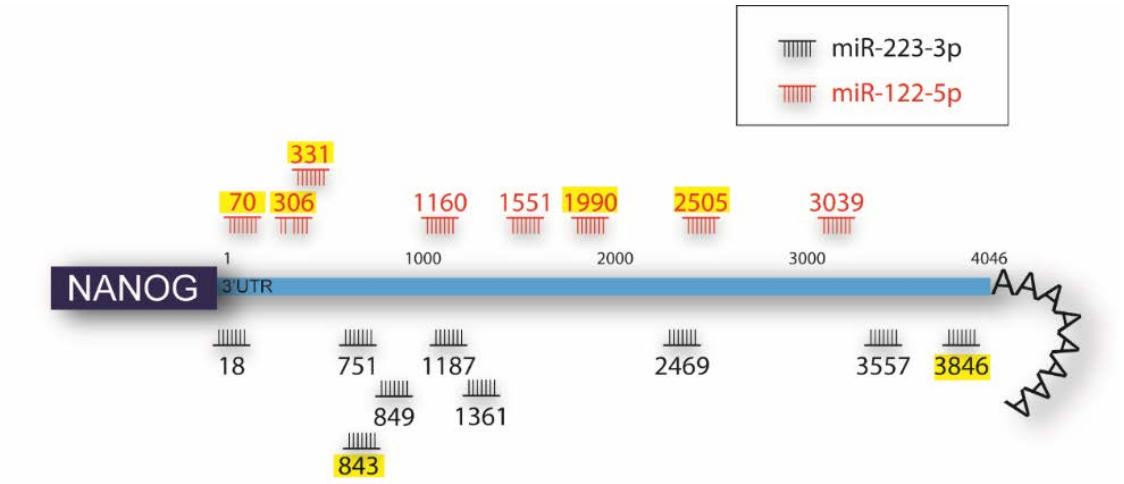

Figure 68: Predicted and annotated miRNA binding sites of miR-122-2p (red) and miR-223-3p (black) in the NANOG 3'UTR (highlighted binding positions were predicted by SegalLab).

The only predicted site from SegalLab within the first 500bp of the 3'UTR for the NANOG 3'UTR was at position 39 with a seed-match supposed to be 8:1:1 and a ddG value of +4.64 (Figure 69). Although not in our criteria of ddG≤-5, Figure 69 demonstrates that the position returned from Segal lab did not match with the sequence and returned a seed-match more like 8:3:2 which only left 3 bp with perfect complementarity. However, shifting this predicted binding site from position 39 to 40 improved the binding site merely towards a seed-match 8:3:1 returning 4 bp with perfect complementarity and thus looked at further binding sites with improved seed-matches.

```
(A)
1                                    87654321
2                      ACCCCATAAACTGTTTGACTGT 8:3:2 not 8:1:1
3                           :   :  ::. :::.
4    AGATGAGTGAAACTGATATTACTCAATTTCAGTCTGGACACTGGCTGAATCCTTCCT
   1                                        39
(B)
1                                    87654321
2                      ACCCCATAAACTGTTTGACTGT 8:3:1
3                      :     : ::   .  . ::::
4    AGATGAGTGAAACTGATATTACTCAATTTCAGTCTGGACACTGGCTGAATCCTTCCT
   1                                        40
```

Figure 69: miR-223-3p binding site for position 39 (and 40) in the NANOG 3'UTR as predicted by SegalLab

(A) Actual alignment of miRNA-mRNA as predicted by SegalLab and (B) one bp shifted and manually annotated alignment: showing (1) the position of the seed-match, (2) miRNA sequence from 3'-5' (using thymine instead of uracil), (3) sequence alignment, (4) mRNA sequence (using thymine instead of uracil). Red letters are indicating GU wobbles and highlighted in yellow are the matches between miRNA and mRNA

All other predicted sites by SegalLab were only 6mers (Table 33 in Chapter 3.3.3), with even worse sequential binding properties once manually checked. miR-223-3p however holds a promising binding site right in the beginning of the NANOG 3'UTR at position 18 (Figure 70). This binding site was manually identified, however delivered an almost perfect seed complementarity with a seed-match of 8:0:1 which means that it harbours only a single GU wobble at position 2 of the seed region. This binding site of miR-223-3p at position 18 in the NANOG 3'UTR was chosen for further analysis using the Dual-Luciferase-Reporter Assay.

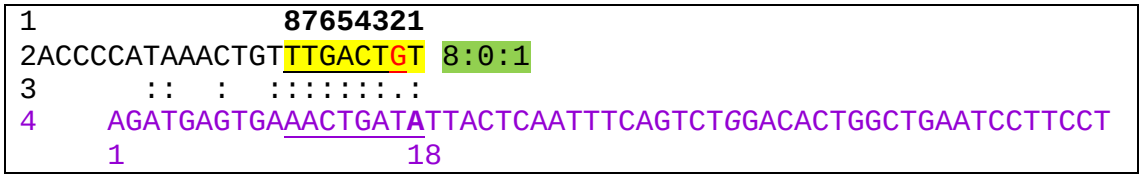

Figure 70: miR-223-3p binding site for position 18 in the NANOG 3'UTR

Manually annotated alignment: showing (1) the position of the seed-match, (2) miRNA sequence from 3'-5' (using thymine instead of uracil), (3) sequence alignment, (4) mRNA sequence (using thymine instead of uracil). Red letters are indicating GU wobbles and highlighted in yellow are the matches between miRNA and mRNA. This seed highlighted in green can be found in the schematics of Figure 68.

SegalLab was able to identify 16 miRNA binding sites of miR-122-5p within the NANOG 3'UTR (see table Table 31 in Chapter 3.3.3). However, following further analysis many of these sites were not as good as predicted by the SegalLab algorithm. Figure 71 illustrates seven binding sites of miR-122-5p in the first 500 bp of the NANOG 3'UTR and how their actual alignment appears. The first three alignments show very poor complementarity and not many consecutive and strong Watson-Crick pairing between the seed-sequence of the miRNA and the predicted binding position in the NANOG 3'UTR identified through SegalLab (Figure 71 A, B and C). Only the predicted binding site of miR-122-5p at positon 70 appeared to be exactly as SegalLab predicted (Figure 71 D). This binding site at position 70 is also reflected in Figure 68 because it has strong Watson-Crick pairing from seed position 2-5 followed by one mismatch and one GU wobble. One predicted binding site from SegalLab at position 325 turned out to have only a single Watson-Crick base pair which is unlikely to cause a miRNA-mRNA interaction (Figure 71 F). The binding sites for position 306 and 331 can also be seen in Figure 68 as these two sites correspond closely to the actual SegalLab prediction displaying an 8mer and two mismatches for both of them instead of an 8mer and one mismatch plus one GU wobble. However, although both binding sites have an A1 site the programme only allows a single mismatch and/or a single GU wobble which means that the binding at position 306 and 331 should be down-graded from an 8mer to a 6mer seed to 6:1:0 (Figure 71 E and G).

Figure 71: miR-122-5p binding sites in the the first 500bp of the NANOG 3'UTR as predicted by SegalLab

Alignments of miRNA-mRNA as predicted by SegalLab at position 56 (A), 61 (B), 64 (C), 70 (D), 306 (E), 325 (F) and 331 (G) of NANOG 3'UTR: showing (1) the position of the seed-match, (2) miRNA sequence from 3'-5' (using thymine instead of uracil), (3) sequence alignment, (4) mRNA sequence (using thymine instead of uracil). Red letters are indicating GU wobbles and highlighted in yellow are the matches between miRNA and mRNA. Seeds highlighted in green are those that can be found in the schematic of Figure 68.

5.3.1.2 Generation of plasmid-constructs for the Dual-Luciferase-Assay

5.3.1.2.1 Amplification of the NANOG 3'UTR, miR-122-5p and miR-223-3p

In order to utilise the Dual-Luciferase-Assay to test whether miR-122-5p and miR-223-3p are directly interacting with the NANOG 3'UTR and therefore supress NANOG translation, all specific regions were cloned into appropriate vectors.

First, the region of NANOG 3'UTR comprising 563bp starting at position 405 from the 4th exon and reaching up to position 536 of the 3'UTR and adding the 14 bp of the restriction enzyme sites (XbaI and NotI) was successfully amplified (Figure 72). The region of the NANOG 3'UTR was chosen as it contained the predicted binding sites for miR-122-5p and the discovered binding site for miR-223-3p (Chapter 5.3.1.1).

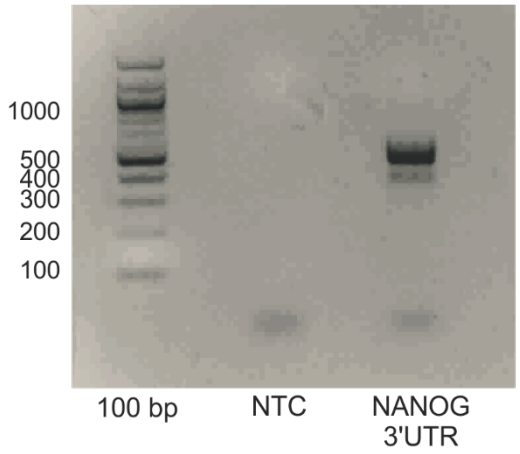

Figure 72: PCR amplified NANOG 3'UTR region

Nancy stained 1% agarose gel showing the expected 563 bp band of the amplified NANOG 3'UTR. Reference point is the QuickLoad 100bp DNA Ladder (NEB) on the left hand side. The middle lane is showing the no-template control (NTC).

Primers described in Table 35 were used to amplify miR-122 containing the 5p region and miR-223 containing the 3p region. Bands of the expected size 181 bp and 171 bp respectively were obtained (Figure 73).

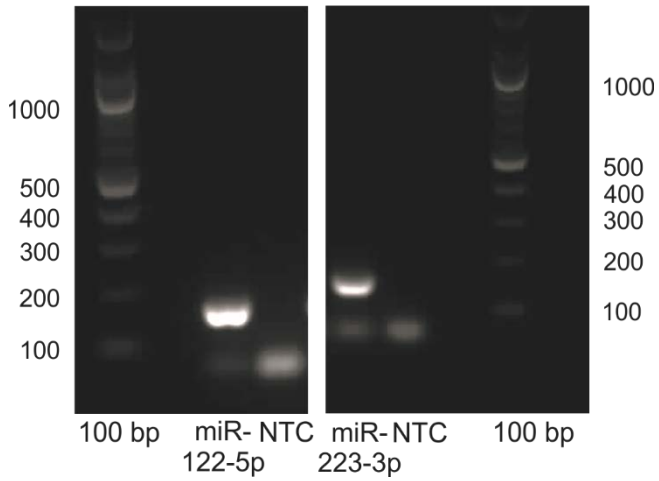

Figure 73: PCR amplified miR-122-5p and miR-223-3p

Nancy stained 1% agarose gel showing the expected size of the amplified miR-122-5p (181 bp) and miR-223-3p region (171bp). Reference point is the QuickLoad 100bp DNA Ladder (NEB) on the left and on the right hand side. NTC stands for no-template control.

5.3.1.2.2 Sub-cloning of desired inserts into the TOPO plasmid

Each of the three resulting amplified products were subsequently cloned into the TOPO-vector. Typically 10 clones were screened for the correct insert by digesting the plasmid-DNA with EcoRI. The NANOG-3'UTR was successfully integrated into the TOPO plasmid vector in 5 out of 10 clones as shown in Figure 74 generating a band of ~600bp.

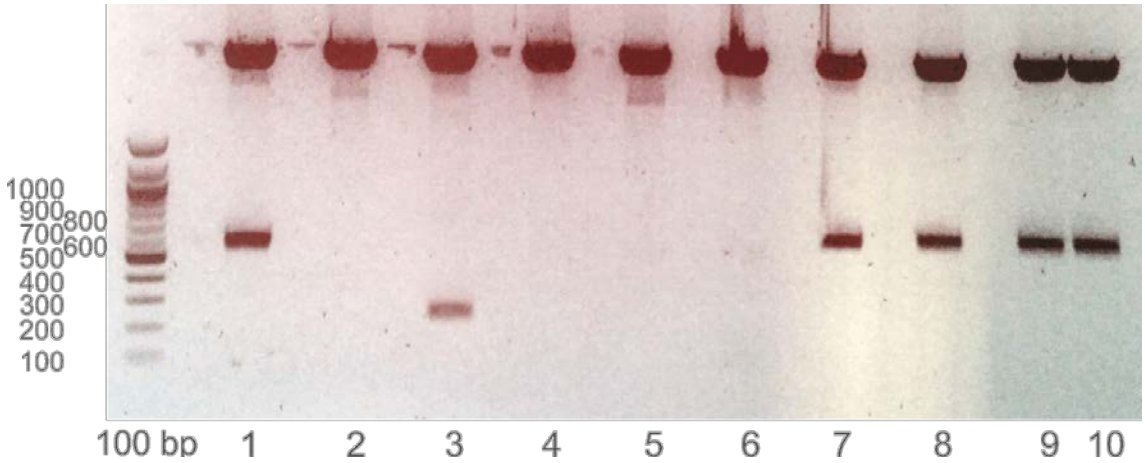

Figure 74: EcoRI digested TOPO-NANOG 3'UTR clones
Nancy stained 1% agarose gel with 10 clones of the vector TOPO-NANOG 3'UTR vector digested with EcoRI, showing 5 positive clones in lane 1, 7, 8, 9, 10. Reference point is the QuickLoad 100bp DNA Ladder (NEB) on the left hand side.

To further confirm the accuracy of the insert, the TOPO-NANOG 3'UTR was sequenced with the M13 forward primer provided by GATC Biotech (London) and aligned to see absolute complementarity to the sequence retrieved from ensemble (Figure 75).

```
>top sequence, NANOG 3UTR Clone10                    1205 nt vs.
>bottom sequence, NANOG 3UTR                         563 nt

            550       560       570       580       590       600
      CGACCTTAAGCGGGAAAGATCTACTTCTGCACACTTCTACTCACTTTGACTATAATGAGT
                              :::::::::::::::::::::::::::::::::::::
_     ----------------------ACTTCTGCACACTTCTACTCACTTTGACTATAATGAGT
                               10        20        30        40

            610       620       630       640       650       660
      TAAAGTCAGACCTGTGACCGACTTAGGAAGGAGAGGGGAGGAGGGTAGGGAGTATCCTAA
      ::::::::::::::::::::::::::::::::::::::::::::::::::::::::::::::
_     TAAAGTCAGACCTGTGACCGACTTAGGAAGGAGAGGGGAGGAGGGTAGGGAGTATCCTAA
          50        60        70        80        90       100

            670       680       690       700       710       720
      AAAGAACAAACCTTTGGTGCACAAGACCAAAGGTACTACGGGTAGGTCAGTTAGAGTACC
      ::::::::::::::::::::::::::::::::::::::::::::::::::::::::::::::
_     AAAGAACAAACCTTTGGTGCACAAGACCAAAGGTACTACGGGTAGGTCAGTTAGAGTACC
         110       120       130       140       150       160

            730       740       750       760       770       780
      TCCCACCTCATACCAACCTCGGATTAGTCGCTCCAAAGAAAAAAAAAAAAAAAGGATAAC
      ::::::::::::::::::::::::::::::::::::::::::::::::::::::::::::::
_     TCCCACCTCATACCAACCTCGGATTAGTCGCTCCAAAGAAAAAAAAAAAAAAAGGATAAC
         170       180       190       200       210       220

            790       800       810       820       830       840
      CTAGAAGGACCTCTTTTATGAAAAAAAAAAAAAAAAAAACTTTGCCTCAGAACGAGACAG
      ::::::::::::::::::::::::::::::::::::::::::::::::::::::::::::::
_     CTAGAAGGACCTCTTTTATGAAAAAAAAAAAAAAAAAAACTTTGCCTCAGAACGAGACAG
         230       240       250       260       270       280

            850       860       870       880       890       900
      CGGGTCCGACCTCACGTCACCGCGCCAGAACCGAGTGACGTTCGAGGCAGAGGGCCCAAG
      ::::::::::::::::::::::::::::::::::::::::::::::::::::::::::::::
_     CGGGTCCGACCTCACGTCACCGCGCCAGAACCGAGTGACGTTCGAGGCAGAGGGCCCAAG
         290       300       310       320       330       340

            910       920       930       940       950       960
      TGCGGTAAGAGGACGGAGTCGGAGGGCTCGTCGACCCTGATGTCCGCGGGCGGTGGAGCG
      ::::::::::::::::::::::::::::::::::::::::::::::::::::::::::::::
_     TGCGGTAAGAGGACGGAGTCGGAGGGCTCGTCGACCCTGATGTCCGCGGGCGGTGGAGCG
         350       360       370       380       390       400

            970       980       990      1000      1010      1020
      GGCCGATTATAAAACATAAAAATCATCTCTGCCCCAAAGTGACACAATCGGTCCTACCAG
      ::::::::::::::::::::::::::::::::::::::::::::::::::::::::::::::
_     GGCCGATTATAAAACATAAAAATCATCTCTGCCCCAAAGTGACACAATCGGTCCTACCAG
         410       420       430       440       450       460
```

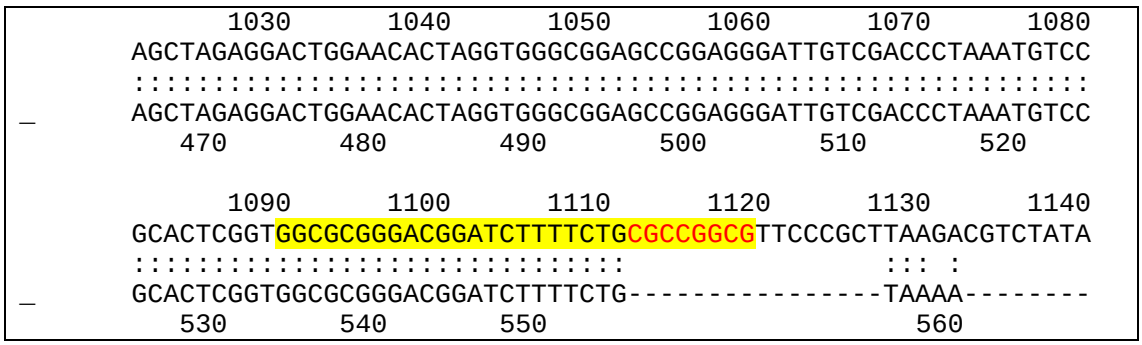

Figure 75: Sequence result from TOPO-NANOG 3'UTR clone 10

Sequencing performed by GATC. Alignment of sequence from NANOG 3'UTR in TOPO vector generated with GENESTREAM SEARCH network server IGH Montpellier, France (http://xylian.igh.cnrs.fr/bin/align-guess.cgi). Highlighted in yellow are the primer regions with restriction enzyme sites (red) important for cloning into pRL-TK.

Similarly, 10 clones were screened for the correct insert of the miRNAs by digesting the plasmid-DNA with EcoRI. miR-122-5p (Figure 76) and miR-223-3p (Figure 77) were successfully integrated into the TOPO plasmid vector generating a product of ~200 bp each.

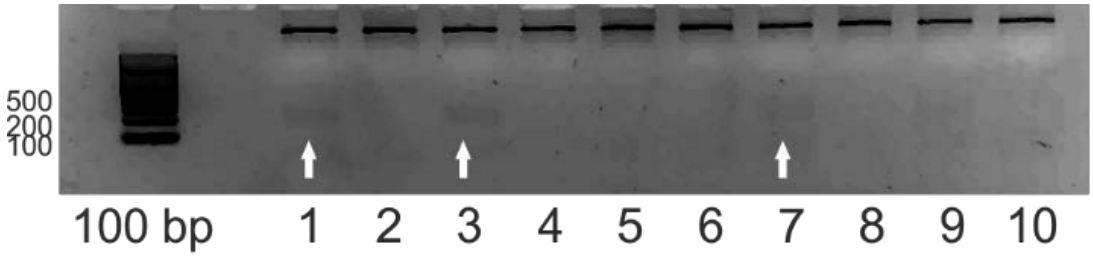

Figure 76: EcoRI digested TOPO-miR-122-5p clones

Nancy stained 1% agarose gel with 10 clones of the vector TOPO-NANOG 3'UTR vector digested with EcoRI, showing 3 positive clones in lane 1, 3 and 7. Reference point is the QuickLoad 100bp DNA Ladder (NEB) on the left hand side.

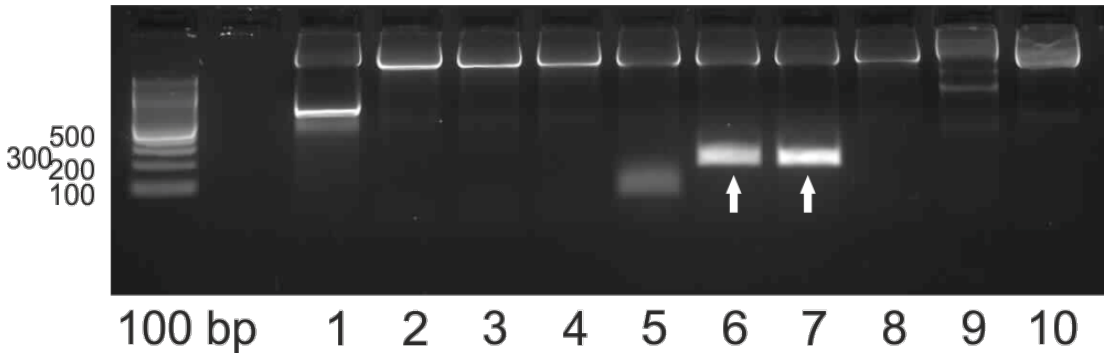

Figure 77: EcoRI digested TOPO-miR-223-3p clones

Nancy stained 1% agarose gel with 10 clones of the vector TOPO-NANOG 3'UTR vector digested with EcoRI, showing 2 positive clones in lane 6 and 7. Reference point is the QuickLoad 100bp DNA Ladder (NEB) on the left hand side.

To further confirm that these inserts were 100% complementarity with the sequence from Ensemble one clone of each, clone 3 of TOPO-miR-122-5p (Figure 78) and clone 6 TOPO-miR-223-3p (Figure 79) were sequenced with the M13 forward primer provided by GATC which is in close proximity to the insert of the TOPO vector (see Figure 57). This resulted in perfect alignments including restriction enzyme sites important for the next cloning step into pcDNA3.1(-).

```
>_ miR-122-5p clone 3                                  1089 nt vs.
>_ miR-122-5p                                           180 nt

               10        20        30        40        50        60
553292 GTAATATTCTTATAGGGCGAATTGGGCCCTCTAGATGCATGCTCGAGCGGCCGCCAGTGT
                                                 :::
_      ---------------------------------------ATG------------------


               70        80        90       100       110       120
553292 GATGGATATCTGCAGAAGTCGCCCTTTCTAGAAGGTGAAGTTAACACCTTCGTGGCTACA
         ::::                              ::::::::::::::::::::::::::
_      --TGGA--------------------------GGTGAAGTTAACACCTTCGTGGCTACA
                                         10        20        30

              130       140       150       160       170       180
553292 GAGTTTCCTTAGCAGAGCTGTGGAGTGTGACAATGGTGTTTGTGTCTAAACTATCAAACG
       ::::::::::::::::::::::::::::::::::::::::::::::::::::::::::::
_      GAGTTTCCTTAGCAGAGCTGTGGAGTGTGACAATGGTGTTTGTGTCTAAACTATCAAACG
           40        50        60        70        80        90

              190       200       210       220       230       240
553292 CCATTATCACACTAAATAGCTACTGCTAGGCAATCCTTCCCTCGATAAATGTCTTGGCAT
       ::::::::::::::::::::::::::::::::::::::::::::::::::::::::::::
_      CCATTATCACACTAAATAGCTACTGCTAGGCAATCCTTCCCTCGATAAATGTCTTGGCAT
          100       110       120       130       140       150

              250       260       270       280       290       300
553292 CGTTTGCTTTGAGCAAGAAGAAGCTTAAGGGCGAATTCCAGCACACTGGCGGCCGTTACT
       ::::::::::::::::::
_      CGTTTGCTTTGAGCAAGAAG----------------------------------------
```

Figure 78: Sequence result from TOPO-miR-122-5p clone 3

Sequencing performed by GATC. Alignment of sequence from miR-122-5p in TOPO vector generated with GENESTREAM SEARCH network server IGH Montpellier, France (http://xylian.igh.cnrs.fr/bin/align-guess.cgi). Highlighted in yellow are the primer regions with enzyme restriction sites (in red) important for cloning into pcDNA3.1(-).

```
>_ miR-223-3p clone 6                                  1164 nt vs.
>_ miR-223-3p                                           171 nt

               10        20        30        40        50        60
744525 AGTTAATCTATAGGGCGGATTGGGCCTCTAGATGCATGCTCGAGCGGCCGCCAGTGTGAT
       :     :::
_      A-----TCTC-------------------------------------------------


               70        80        90       100       110       120
744525 GGATATCTGCAGAAATCGCCCTTTCTAGACTTCCCCACAGAAGCTCTTGGCCTGGCCTCC
                                 ::::::::::::::::::::::::::::::
_      ---------------------------ACTTCCCCACAGAAGCTCTTGGCCTGGCCTCC
                                    10        20        30

              130       140       150       160       170       180
744525 TGCAGTGCCACGCTCCGTGTATTTGACAAGCTGAGTTGGACACTCCATGTGGTAGAGTGT
       ::::::::::::::::::::::::::::::::::::::::::::::::::::::::::::
_      TGCAGTGCCACGCTCCGTGTATTTGACAAGCTGAGTTGGACACTCCATGTGGTAGAGTGT
        40        50        60        70        80        90

              190       200       210       220       230       240
744525 CAGTTTGTCAAATACCCCAAGTGCGGCACATGCTTACCAGCTCTAGGCCAGGGCAGATGG
       ::::::::::::::::::::::::::::::::::::::::::::::::::::::::::::
_      CAGTTTGTCAAATACCCCAAGTGCGGCACATGCTTACCAGCTCTAGGCCAGGGCAGATGG
       100       110       120       130       140       150

              250       260       270       280       290       300
744525 GATATGACAAGCTTAAGGGCGAATTCCAGCACACTGGCGGCCGTTACTAGTGGATCCGAG
       ::::::::
_      GATATGAC-------------------------------------------------
       160
```

Figure 79: Sequence result from TOPO-miR-223-3p clone 6

Sequencing performed by GATC. Alignment of sequence from miR-223-3p in TOPO vector generated with GENESTREAM SEARCH network server IGH Montpellier, France (http://xylian.igh.cnrs.fr/bin/align-guess.cgi). Highlighted in yellow are the primer regions with enzyme restriction sites (in red) important for cloning into pcDNA3.1(-).

5.3.1.2.3 Final vector generation to use in Dual-Luciferase-Assay

After verification of the TOPO vector inserts, the inserts were digested and transformed into the final plasmid vectors appropriate for the Dual-Luciferase assay.

Figure 80 shows the XbaI/NotI digested TOPO-vector containing 563 bp of the NANOG 3'UTR (TOPO-NANOG) and the XbaI/NotI digested destination vector pRL-TK that is expressing the *Renilla luciferase* (pRLTK vector). Both these DNA fragments were extracted from the agarose gel, purified and ligated to form the final pRL-TK-NANOG 3'UTR vector.

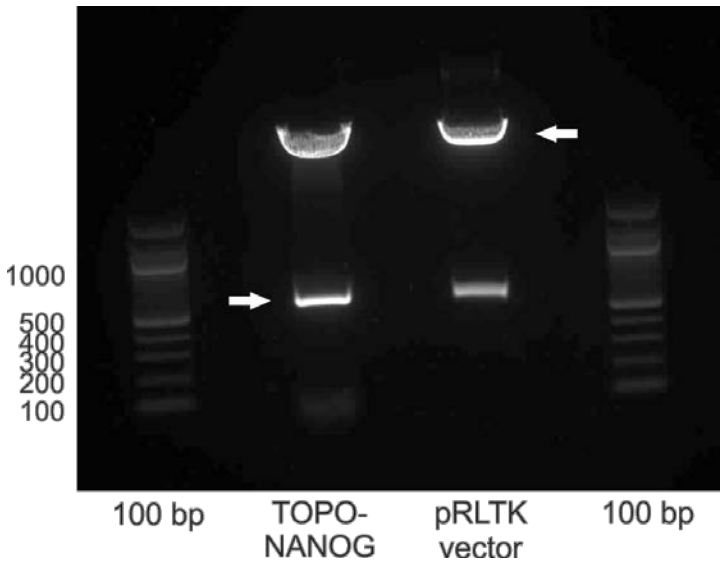

Figure 80: Vector digest of TOPO-NANOG and pRL-TK-vector with XbaI and NotI
Nancy stained 1% agarose gel showing the digested 563bp fragment of the NANOG 3'UTR and the digested individual pRL-TK vector, both depicted with a white arrow. Reference point is the QuickLoad 100bp DNA Ladder (NEB) on the left and right hand side.

10 colonies of pRL-TK-NANOG 3'UTR were purified, double digested with XbaI/NotI to confirm the presence of the expected 563 bp insert in 8 out of 10 clones (Figure 81).

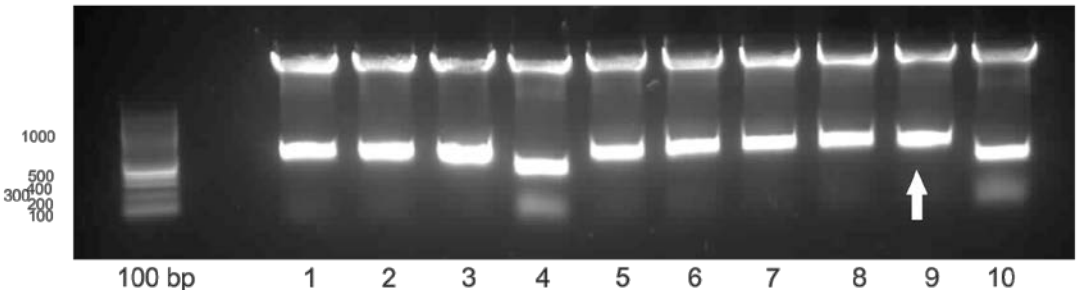

Figure 81: XbaI and NotI digested pRL-TK-NANOG 3'UTR clones

Nancy stained 1% agarose gel showing the digested 563bp fragment for NANOG 3'UTR and the digested pRL-TK vector with 8 positive clones (lanes 1, 2, 3, 4, 5, 6, 7, 8 and 9). Reference point is the QuickLoad 100bp DNA Ladder (NEB) on the left hand side. White arrow is indicating clone 9 that was further confirmed via sequencing (Data not shown).

TOPO-miR-122-5p was double digested with XbaI/HindIII and produced a band of the expected (181 bp) (Figure 82).

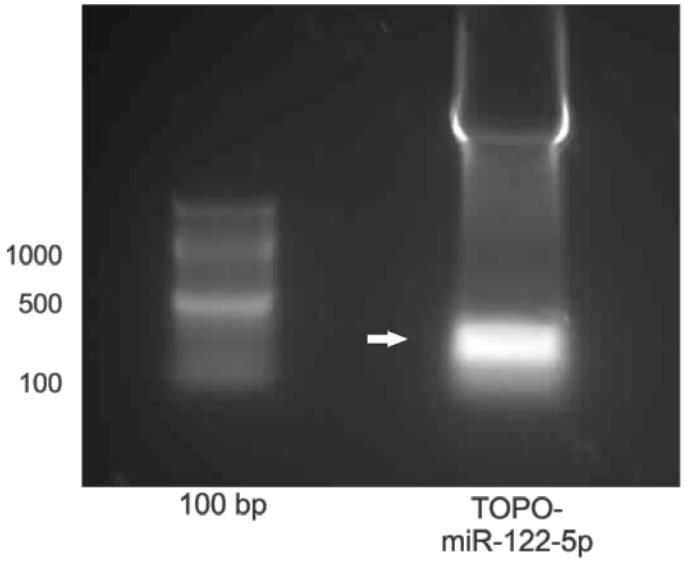

Figure 82: Vector digest of TOPO-miR-122-5p with XbaI and HindIII HF

Nancy stained 1% agarose gel showing the digested 181bp fragment for miR-122-5p and the digested pcDNA3.1(-) vector. Reference point is the QuickLoad 100bp DNA Ladder (NEB) on the left hand side.

TOPO-miR-223-3p and the destination vector pcDNA3.1(-) were double digested with XbaI/HindIII and produced a band of the expected size (171bp) which is 5.5kb big (Figure 83). pcDNA3.1(-) was 5.5 kb in size.

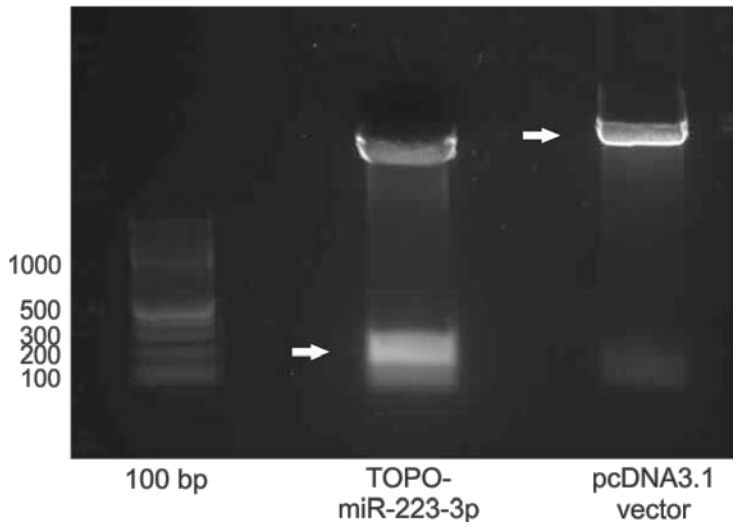

Figure 83: Vector digest of TOPO-miR-223-3p and pcDNA3.1(-)-vector with Xbal and HindIII HF

Nancy stained 1% agarose gel showing the digested 171bp fragment for miR-223-3p and the digested pcDNA3.1(-) vector. Reference point is the QuickLoad 100bp DNA Ladder (NEB) on the left hand side.

Each digested DNA fragment miR-122-5p, miR-223-3p and pcDNA3.1(-) was extracted from the agarose gel, purified and ligated to form the final pcDNA-3.1(-)-miR-122-5p and pcDNA-3.1(-)-miR-223-3p vectors.

10 individual colonies of both vectors were purified and double digested with XbaI/HindIII to confirm the presence of the expected insert sizes of 181 bp and 171 bp for miR-122-5p and miR-223-3p respectively. Figure 84 shows an agarose gel with 4 out of 10 positive clones for miR-122-5p after digest from which clone 5 was used in a Maxi-Prep.

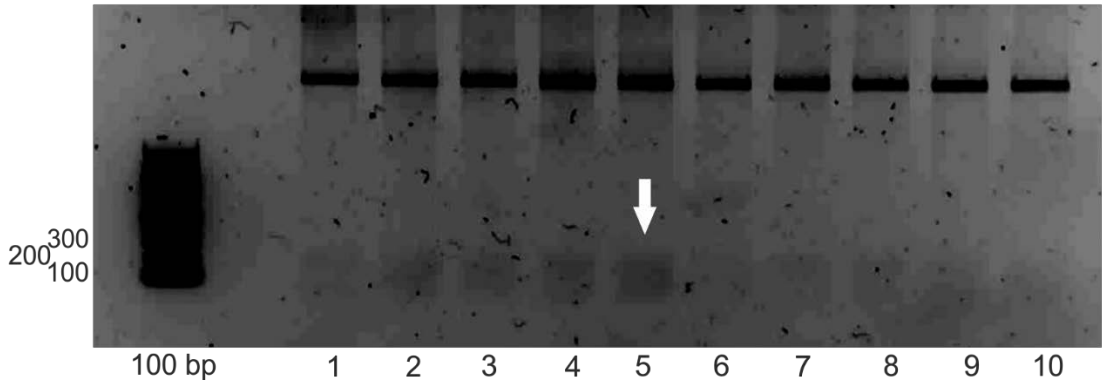

Figure 84: XbaI and HindIII HF digested pcDNA3.1(-)-miR-122-5p clones

Nancy stained 1% agarose gel showing the digested 181bp fragment for miR-122-5p and the digested pcDNA3.1(-) vector with 4 positive clones (lane 2, 3, 4, 5). Reference point is the QuickLoad 100bp DNA Ladder (NEB) on the left hand side. White arrow is indicating clone 5 that was used in a Maxi-Prep.

Figure 85 shows an agarose gel with 10 individual pcDNA-3.1(-)-miR-223-3p colonies double digested with XbaI/HindIII. Clone 3 and 8 did not show any unspecific bands. Therefore, clone 3 was used for amplification in a Maxi-Prep.

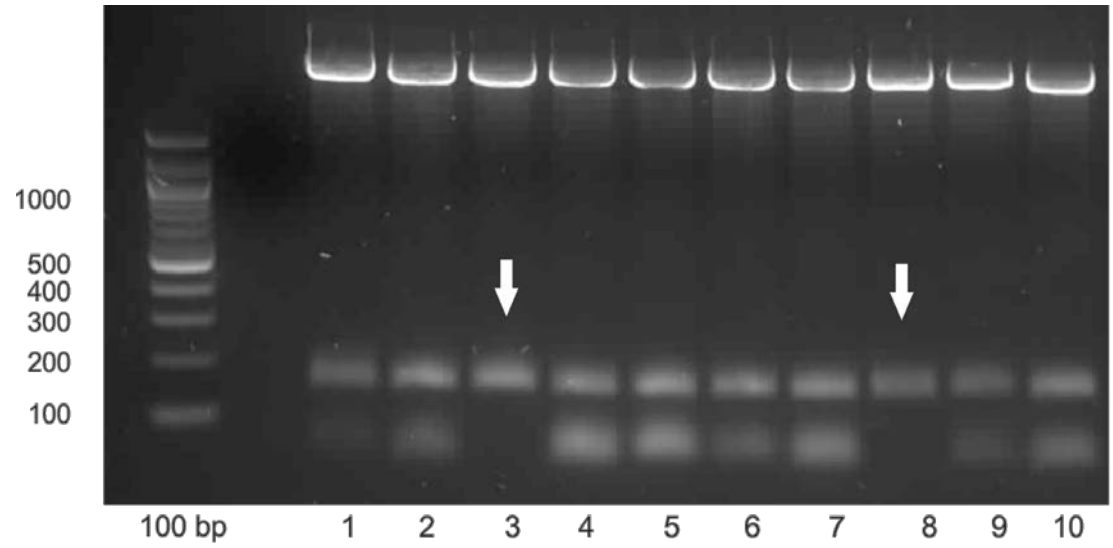

Figure 85: XbaI and HindIII HF digested pcDNA3.1(-)-miR-223-3p clones
Nancy stained 1% agarose gel showing the digested 171bp fragment for miR-223-3p and the digested pcDNA3.1(-) vector. Reference point is the QuickLoad 100bp DNA Ladder (NEB) on the left hand side. White arrows indicate clones without unspecifuc bands. Clone 3 was used in a Maxi-Prep.

In summary, the cloning procedure was successful, leading to the destination vectors pRL-TK-NANOG 3'UTR expressing Renilla luciferase, pcDNA3.1(-)-miR-122-5p and pcDNA3.1(-)-miR-223-3p which were used for the Dual-Luciferase-Assay.

5.3.1.2.4 Site-directed Mutagenesis of miRNA recognition elements in the NANOG 3'UTR

Site-directed mutagenesis was performed to prove the specific binding site of either miR-122-5p or miR-223-3p in the first ~500bp of NANOG 3'UTR. Plasmid DNA from pRL-TK-NANOG 3'UTR (wild-type (WT)) was used to successfully substitute either 3 bases for the binding site of miR-122-5p or 4 bases for the binding site of miR-223-3p. Figure 86 shows four clones for each mutated binding site after double digest with XhoI and BamHI. Positive clones appeared to have two fragments and therefore the site-directed mutagenesis procedure was successfully introducing the restriction enzyme site XhoI. Clones without successfully introduced XhoI binding sites were linearised only through the digestion with BamHI and can be seen for one clone in lane 11 of the miR-223-3p mutated binding site in NANOG 3'UTR (lane 10-13, Figure 86).

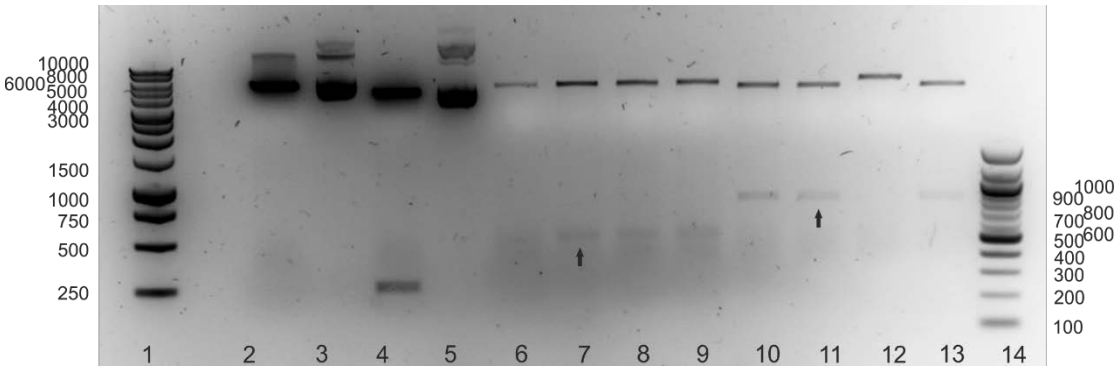

Figure 86: XhoI/BamHI digest of pRLTK-3'UTR NANOG miR-122-5p or miR-223-3p binding site mutant clones

Nancy stained 1% agarose gel showing: the 1 kb ladder (lane 1); digested WT vector (pRLTK-3'UTR NANOG) as negative control (lane 2); undigested WT vector (lane 3); digested TOPO-miR-223-3p vector as positive control (lane 4); undigested TOPO-miR-223-3p vector as negative control (lane 5); digested clones for pRLTK-3'UTR NANOG with mutated miR-122-5p binding site (lane 6 to 9); digested clones for pRLTK-3'UTR NANOG with mutated miR-223-3p binding site (lane 10 to 13); 100 bp ladder (lane 10). Black arrows indicate clones used for further investigation, expanding the clone in lane 7 and lane 11 of the mutated miR-122-5p and the mutated miR-223-3p binding site in pRLTK-3'UTR NANOG with a Maxi-Prep respectively.

To further confirm that the mutations were correct clone 2 of both the mutated miR-122-5p and miR-223-3p binding sites in pRLTK-NANOG 3'UTR were sequenced using the designed primer "pRLTK for insert" (Table 35). The aligned sequence of the mutated NANOG 3'UTR for the miR-122-5p binding site (Figure 87) and the miR-223-3p binding site (Figure 88) with the NANOG 3'UTR (WT) show that both contained the desired base substitutions. These vectors were suitable for the use in the Dual-Luciferase-Reporter Assays.

```
>_ NANOG 3UTR Mut122-5p site clone2                  723 nt vs.
>_ NANOG 3UTR WT                                       563 nt

               10        20        30        40        50        60
194152 TATCAAATCGTTCGTTGAGCGAGTTCTCAAAATGAACAATAATTCTAGATGAAGACGTGT
                         ::              :::            ::::::::::
_      ------------------GC--------------AACC-----------TGAAGACGTGT
                                                          10

               70        80        90       100       110       120
194152 GAAGATGAGTGAAACTGATATTACTCAATTTCAGTCTGGACACTGGCTGAATCCTTCCTC
       ::::::::::::::::::::::::::::::::::::::::::::::::::::::::::::
_      GAAGATGAGTGAAACTGATATTACTCAATTTCAGTCTGGACACTGGCTGAATCCTTCCTC
        20        30        40        50        60        70

              130       140       150       160       170       180
194152 TCCCCTCCTCCCATCCCTCATAGGATTTTTCTTGTTTGGAAACCACGTGTTCTGGTTTCC
       ::::::::::::::::::::::::::::::::::::::::::::::::::::::::::::
_      TCCCCTCCTCCCATCCCTCATAGGATTTTTCTTGTTTGGAAACCACGTGTTCTGGTTTCC
        80        90       100       110       120       130

              190       200       210       220       230       240
194152 ATGATGCCCATCCAGTCAATCTCATGGAGGGTGGAGTATGGTTGGAGCCTAATCAGCGAG
       ::::::::::::::::::::::::::::::::::::::::::::::::::::::::::::
_      ATGATGCCCATCCAGTCAATCTCATGGAGGGTGGAGTATGGTTGGAGCCTAATCAGCGAG
       140       150       160       170       180       190

              250       260       270       280       290       300
194152 GTTTCTTTTTTTTTTTTTTTCCTATTGGATCTTCCTGGAGAAAATACTTTTTTTTTTTT
       :::::::::::::::::::: ::::::::::::::::::::::::::::::::::::::
_      GTTTCTTTTTTTTTTTTTTT-CCTATTGGATCTTCCTGGAGAAAATACTTTTTTTTTTTT
       200       210       220       230       240       250

              310       320       330       340       350       360
194152 TTTTTTTGAAACGGAGTCTTGCTCTGTCGCCCAGGCTGGAGTGCAGTGGCGCGGTCTTGG
       ::::::::::::::::::::::::::::::::::::::::::::::::::::::::::::
_      TTTTTTTGAAACGGAGTCTTGCTCTGTCGCCCAGGCTGGAGTGCAGTGGCGCGGTCTTGG
        260       270       280       290       300       310

              370       380       390       400       410       420
194152 CTCGAGGCAAGCTCCGTCTCCCGGGTTCACGCCATTCTCCTGCCTCAGCCTCCCGAGCAG
       :::   ::::::::::::::::::::::::::::::::::::::::::::::::::::::
_      CTCACTGCAAGCTCCGTCTCCCGGGTTCACGCCATTCTCCTGCCTCAGCCTCCCGAGCAG
        320       330       340       350       360       370
```

```
               430        440        450        460        470        480
194152 CTGGGACTACAGGCGCCCGCCACCTCGCCCGGCTAATATTTTGTATTTTTAGTAGAAACG
       :::::::::::::::::::::::::::::::::::::::::::::::::::::::::: :::
_      CTGGGACTACAGGCGCCCGCCACCTCGCCCGGCTAATATTTTGTATTTTTAGTAGAGACG
        380        390        400        410        420        430

               490        500        510        520        530        540
194152 GGGTTTCACTGTGTTAGCCAGGATGGTCTCGATCTCCTGACCTTGTGATCCACCCGCCTC
       ::::::::::::::::::::::::::::::::::::::::::::::::::::::::::::::::
_      GGGTTTCACTGTGTTAGCCAGGATGGTCTCGATCTCCTGACCTTGTGATCCACCCGCCTC
        440        450        460        470        480        490

               550        560        570        580        590        600
194152 GGCCTCCCTAACAGCTGGGATTTACAGGCGTGAGCCACCGCGCCCTGCCTAAAAAAGACG
       :::::::::::::::::::::::::::::::::::::::::::::::::::: :::::::
_      GGCCTCCCTAACAGCTGGGATTTACAGGCGTGAGCCACCGCGCCCTGCCTAGAAAAGAC-
        500        510        520        530        540        550
```

Figure 87: Sequence result from pRL-TK-NANOG 3'UTR with mutated miR-122-5p binding site

Sequencing performed by GATC. Alignment of sequence from pRL-TK-NANOG 3'UTR with mutated miR-122-5p binding site with NANOG 3'UTR WT generated with GENESTREAM SEARCH network server IGH Montpellier, France (http://xylian.igh.cnrs.fr/bin/align-guess.cgi). Highlighted in yellow is the substitution of 3 bases from ACT301GAG (number is relative to starting point of NANOG 3'UTR).

```
>_ NANOG 3UTR Mut223-3p site clone2                  796 nt vs.
>_ NANOG 3UTR                                        563 nt

               10         20         30         40         50         60
137246 TTATCATCGTTCGTTGAGCGAGTTCTCAAAATGAACAATAATTCTAGATGAAGACGTGTG
                       ::               :::             ::::::::::::
_      -----------------GC--------------AACC-----------TGAAGACGTGTG
                                                          10

               70         80         90        100        110        120
137246 AAGATGAGTGAAACTCGAGTTACTCAATTTCAGTCTGGACACTGGCTGAATCCTTCCTCT
       ::::::::::::::    :::::::::::::::::::::::::::::::::::::::::
_      AAGATGAGTGAAACTGATATTACTCAATTTCAGTCTGGACACTGGCTGAATCCTTCCTCT
       20         30         40         50         60         70

               130        140        150        160        170        180
137246 CCCCTCCTCCCATCCCTCATAGGATTTTTCTTGTTTGGAAACCACGTGTTCTGGTTTCCA
       ::::::::::::::::::::::::::::::::::::::::::::::::::::::::::::::::
_      CCCCTCCTCCCATCCCTCATAGGATTTTTCTTGTTTGGAAACCACGTGTTCTGGTTTCCA
       80         90        100        110        120        130

               190        200        210        220        230        240
137246 TGATGCCCATCCAGTCAATCTCATGGAGGGTGGAGTATGGTTGGAGCCTAATCAGCGAGG
       ::::::::::::::::::::::::::::::::::::::::::::::::::::::::::::::::
_      TGATGCCCATCCAGTCAATCTCATGGAGGGTGGAGTATGGTTGGAGCCTAATCAGCGAGG
      140        150        160        170        180        190

               250        260        270        280        290        300
137246 TTTCTTTTTTTTTTTTTTTCCTATTGGATCTTCCTGGAGAAAATACTTTTTTTTTTTTTT
       ::::::::::::::::::::::::::::::::::::::::::::::::::::::::::::::::
_      TTTCTTTTTTTTTTTTTTTCCTATTGGATCTTCCTGGAGAAAATACTTTTTTTTTTTTTT
      200        210        220        230        240        250
```

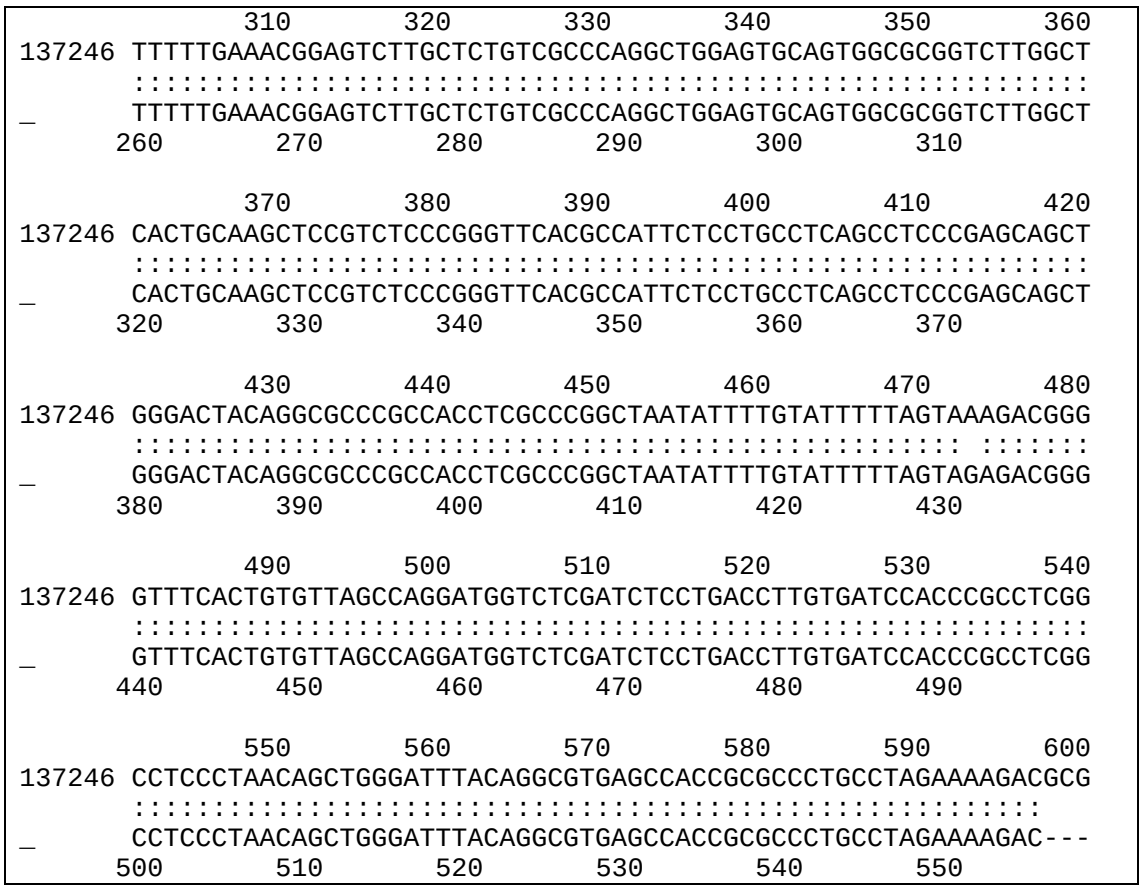

Figure 88: Sequence result from pRL-TK-NANOG 3'UTR with mutated miR-223-3p binding site

Sequencing performed by GATC. Alignment of sequence from pRL-TK-NANOG 3'UTR with mutated miR-223-3p binding site with NANOG 3'UTR WT generated with GENESTREAM SEARCH network server IGH Montpellier, France (http://xylian.igh.cnrs.fr/bin/align-guess.cgi). Highlighted in yellow is the substitution of 4 bases from GATA15CGAG (number is relative to starting point of NANOG 3'UTR).

5.3.1.3 Functional analysis of miR-122-5p binding site in the first ~500bp of the NANOG 3'UTR

The Dual-Luciferase-Assay (Promega) was performed in HeLa cells as they have low expression levels of mature miRNAs and fluorescence intensity measured from pRL-TK-NANOG 3'UTR (wild-type, WT) or pRL-TK-Mut-NANOG 3'UTR (Mutant, MUT). Both vector constructs were expressing *Renilla Luciferase* and contained the binding site for either miR-122-5p or miR-223-3p. Should miR-122-5p bind to the NANOG 3'UTR the fluorescence intensity produced by *Renilla Luciferase* would be reduced. The data were normalised to the fluorescent intensity of *Firefly Luciferase* which was expressed by the co-transfected pGL2 vector.

To determine whether miR-122-5p binds to the first ~500 bp of the NANOG 3'UTR Dual-Luciferase-Reporter Assays were used (Chapter 5.2.2). When pRL-TK-NANOG 3'UTR was transiently co-transfected into HeLa cells with pcDNA3.1(-)-miR-122-5p (WT+miR-122-5p) there was no difference in luciferase activity compared to the control which is the pRL-TK-NANOG 3'UTR vector that was transiently co-transfected with the empty pcDNA3.1(-) vector (WT +Ø) (Figure 89). This means that miR-122-5p has no target within the first ~500 bp of the NANOG 3'UTR. Consequently, this result shows that there is no binding site which necessitates further investigations with the mutated NANOG 3'UTR.

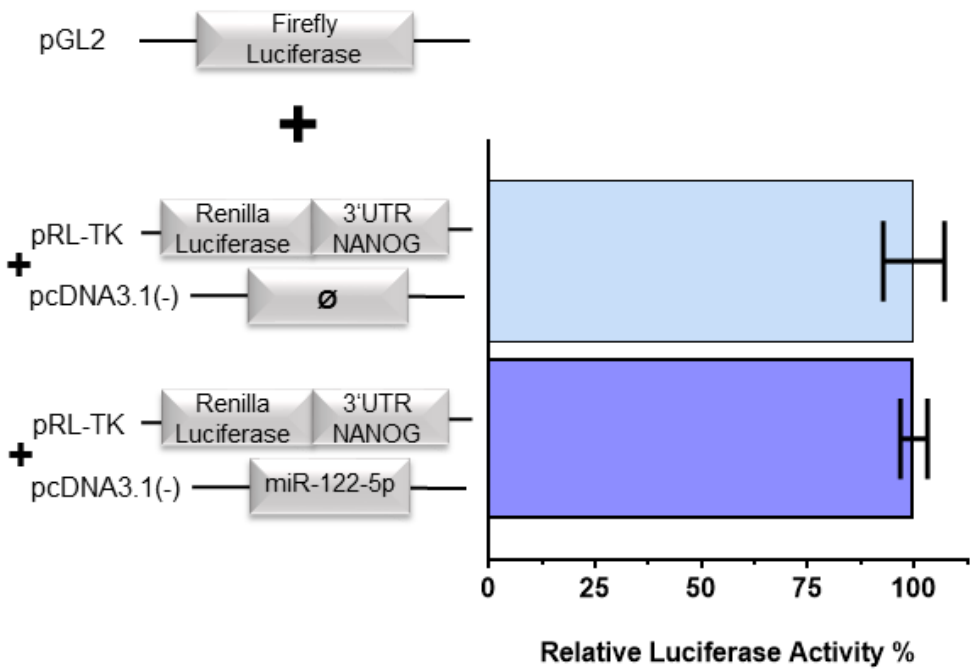

Figure 89: miR-122-5p has no miRNA binding site in the first ~500bp of the NANOG 3'UTR

Dual-Luciferase assay was performed on HeLa cells transfected with pGL2 (normalising control) and the pRL-TK vector containing the first ~500 bp of the NANOG 3'UTR. These plasmids were co-transfected with either pcDNA.3.(-)-Ø (control) or pcDNA3.1(-)-miR-122-5p. *Renilla Luciferase* values were normalised to *Firefly Luciferase* (pGL2) and were represented relative to the pRL-TK-NANOG 3'UTR with the control. Data represent mean ± SEM (error bars), n=3.

5.3.1.4 Functional analysis of miR-223-3p binding site in the first ~500bp of the NANOG 3'UTR

To determine whether miR-223-3 binds to the first ~500 bp of the NANOG 3'UTR Dual-Luciferase-Reporter Assays were used (Chapter 5.2.2). When pRL-TK-NANOG 3'UTR was transiently co-transfected into HeLa cells with pcDNA3.1(-)-miR-223-3p the luciferase activity was reduced to 82 % (p=0.0092) when compared to the control which is the pRL-TK-NANOG 3'UTR vector that was co-transfected with the empty pcDNA3.1(-)-Ø vector (Figure 90). This shows that miR-223-3p binds directly to the NANOG 3'UTR. In contrast, when the potential binding site at position 18 of the NANOG 3'UTR (as pictured in Figure 68 and 70) was mutated and HeLa cells were co-transfected with pRL-TK-NANOG 3'UTR Mut (GATA15CGAG) and pcDNA3.1(-)-miR-223-3p the luciferase activity was not significantly reduced compared to the control (Figure 90). The reduction in pRL-TK-NANOG 3'UTR only and not in the mutant vector showed the exact localisation of the binding region of miR-223-3p at position 18 of the NANOG 3'UTR because mutating this miR-223-3p binding site abrogated the down-regulation of luciferase activity exerted by miR-223-3p.

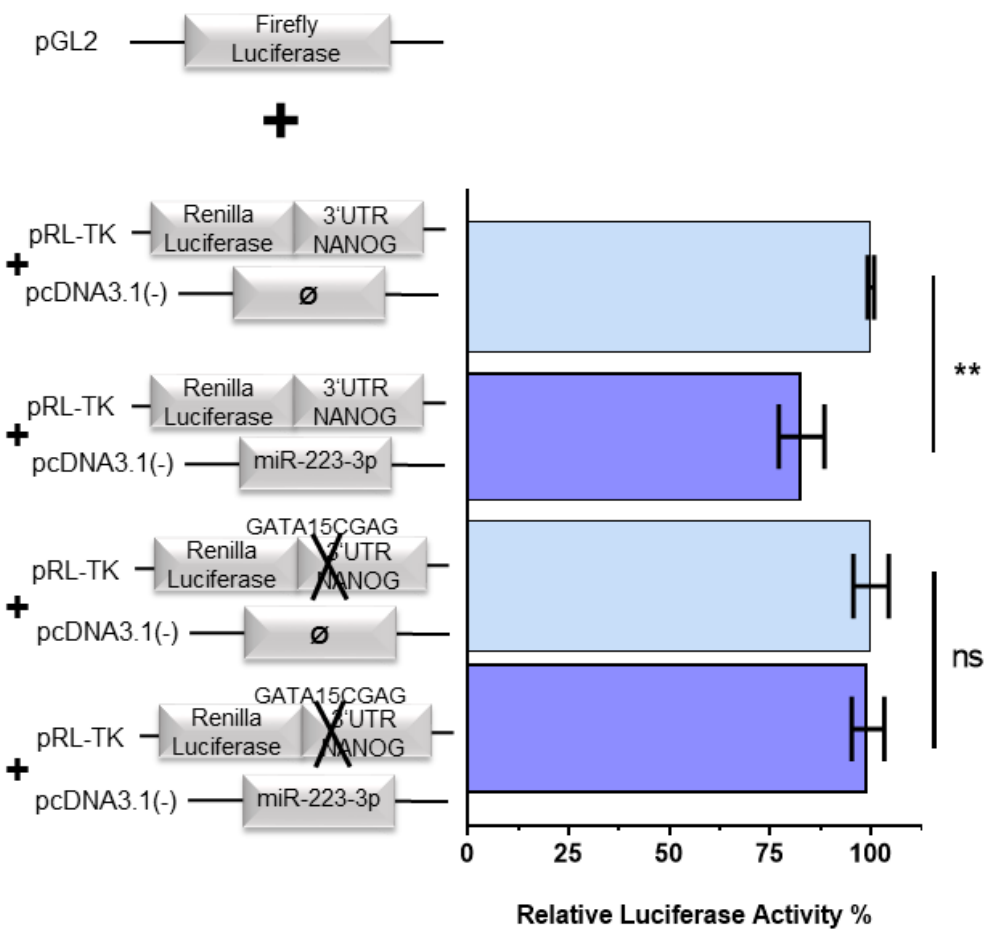

Figure 90: miR-223-3p targets NANOG 3'UTR

Dual-Luciferase assay was performed on HeLa cells transfected with pGL2 (normalising control) and the pRL-TK vector containing the first ~500 bp of the NANOG 3'UTR or the mutated pRL-TK-NANOG 3'UTR (GATA15CGAG). These plasmids were co-transfected with either pcDNA3.1(-)-Ø (control) or pcDNA3.1(-)-miR-223-3p. *Renilla Luciferase* values were normalised to *Firefly Luciferase* (pGL2) and were represented relative to the control for the pRL-TK-NANOG 3'UTR with the control or the mutated pRL-TK-NANOG 3'UTR with the control. Data represent mean ± SEM (error bars). Statistically significance **p≤0.01, not significant (ns), n=4.

5.3.2 Functional Analysis of down-stream effects of the miR-223-3p binding site in the NANOG 3'UTR of hESCs

The increased expression of miR-223-3p caused a significant reduction in NANOG protein expression in hESCs cultured at 5% oxygen. The Dual-Luciferase assay showed, that miR-223-3p binds directly to the NANOG 3'UTR. However, the functional significance of these results remain to be determined. Therefore, further down-stream effects were analysed that are likely to be affected by this functional miRNA-mRNA interaction.

5.3.2.1 Functional impact of increased expression of miR-223-3p on Brachyury expression in hESCs

NANOG is one of the main transcription factors in pluripotent hESCs and is of central importance for the maintenance of hESCs. Due to the significant down-regulatory effect of miR-223-3p on NANOG protein expression signs of early differentiation might occur. Therefore, Brachyury, an early mesodermal lineage marker was investigated. The overexpression of miR-223-3p showed a significant 2.2-fold increase ($p=0.041$) in Brachyury mRNA expression levels for Shef3 hESCs and a similar but not significant trend for Hues7 hESCs both cultured at 5% oxygen when compared to the transfection with pre-miR-control (Figure 91).

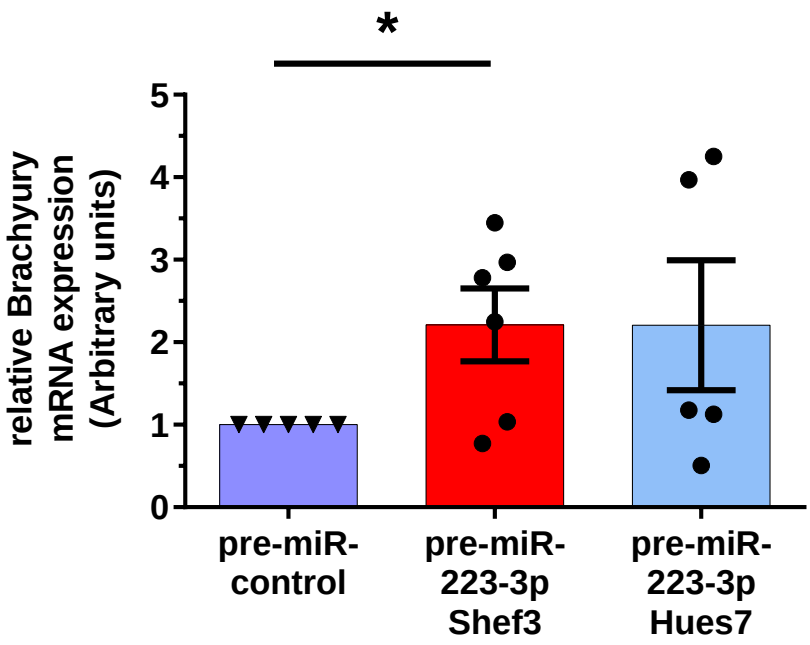

Figure 91: Relative Brachyury mRNA expression levels when either Shef3 or Hues7 hESCs were transfected with 200nM pre-miR-223-3p and cultured at 5% oxygen for 48h.

All data were normalised to UBC and to 1 for the pre-miR transfection control. Statistically significance *, p≤0.05. Bars represent mean ±SEM.

5.3.2.2 Functional impact of increased expression of miR-223-3p on CDK6 expression in hESCs

Since NANOG has been shown to bind CDK6, an important cell cycle regulator to increase proliferation (X. Zhang *et al.*, 2009) the effect of pre-miR-223-3p on the expression of CDK6 was investigated. When Shef3 hESCs cultured at 5% oxygen were transfected with pre-miR-233-3p a significant 20% reduction (p=0.0309) in CDK6 expression was observed compared to the transfection with pre-miR-control (Figure 92). A similar trend was also observed for Hues7 hESCs transfected with pre-miR-223 but did not reach significance (Figure 92).

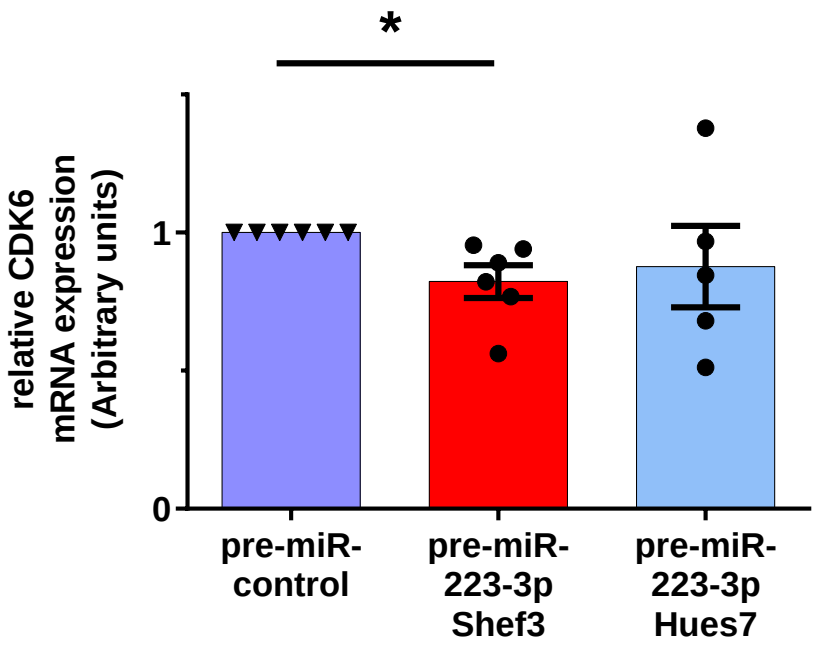

Figure 92: Relative CDK6 mRNA expression levels when either Shef3 or Hues7 hESCs were transfected with 200nM pre-miR-223-3p and cultured at 5% oxygen for 48h.

All data were normalised to UBC and to 1 for the pre-miR transfection control. Statistically significance *p≤0.05. Bars represent mean ±SEM.

5.3.2.3 Functional impact of increased expression of miR-122-5p and/or miR-223-3p on Ki67 expression in hESCs

In vitro, hESCs are known for their capacity of undifferentiated proliferation. This is sustained mainly through the expression of OCT4, SOX2 and NANOG. Increasing the expression of either miR-122-5p or miR-223-3p decreased NANOG expression. In addition, CDK6 mRNA expression was affected when miR-223-3p expression was increased. NANOG was also demonstrated to bind to CDK6 (X. Zhang *et al.*, 2009), which is involved in cell cycle regulation and increased proliferation. Since hESCs cultured at 5% oxygen display increased proliferation compared to those maintained at 20% oxygen (Forristal *et al.*, 2010), it was interesting to investigate if altered miR-122-5p or miR-223-3p expression had also an effect on hESCs proliferation. Ki67, a common proliferation marker, was used to determine differences in proliferation between the treatment groups. The addition of pre-miR-122-5p or pre-miR-223-3p would be expected to decrease hESCs proliferation compared to the transfection pre-miR-control. In contrast, the addition of anti-miR-122-5p or anti-miR-223-3p would be expected to increase hESCs proliferation compared to the transfection anti-miR-control. Hues7 hESCs were transfected with either anti-miR or pre-miRs 24h post-passaging, fixed and Ki67/DAPI labelled 48h post-passaging. After microscopy, images of Ki67 positive labelled cells were counted using Cellprofiler (Figure 93).

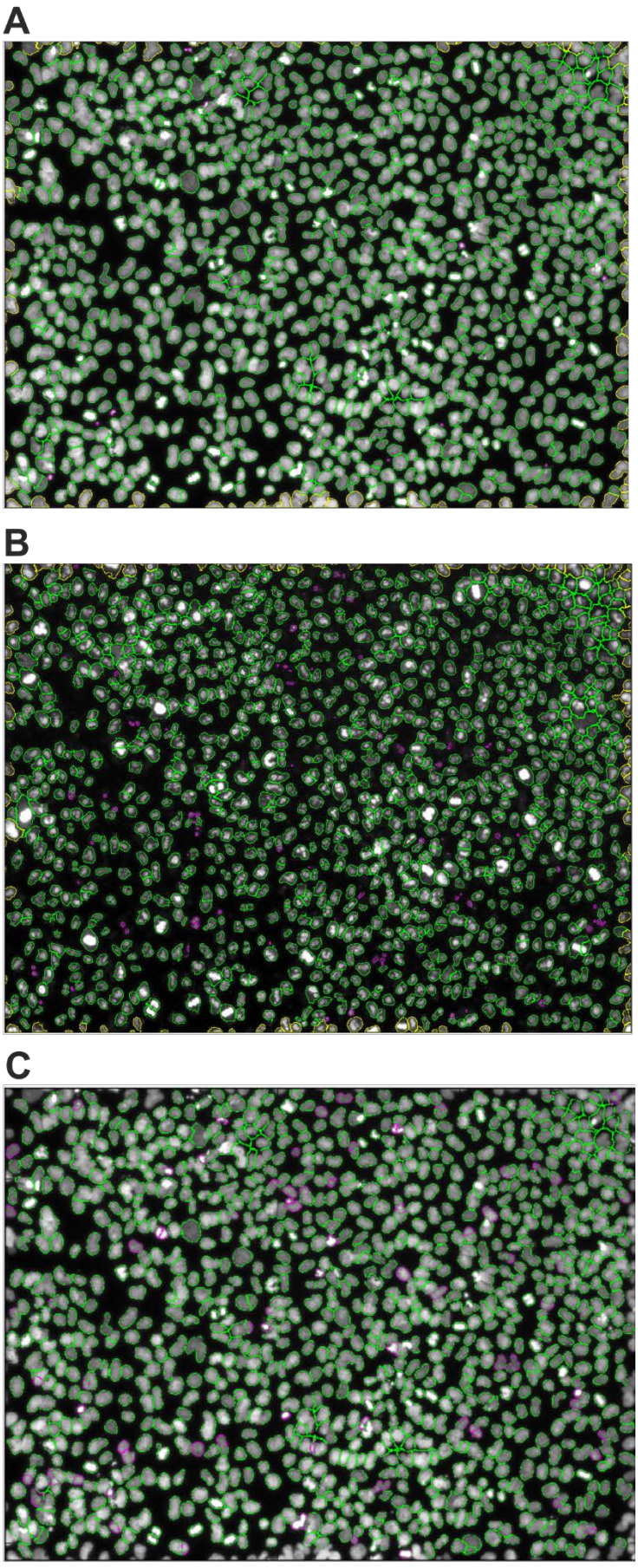
A
B
C

Figure 93: Cell count of Ki67 positive stained hESC nuclei using Cellprofiler

Representative immunocytochemistry pictures of Hues7 hESCs showing (A) identified cells with DAPI labelling (B) identified cells with Ki67 labelling (C) identified Ki67 positive nuclei (DAPI labelling). Cells were distinguished by drawing a line around them. Cells with a green outline were considered as positive labelled for either (A) DAPI or (B) Ki67 or (C) Ki67 positive nuclei but were not counted when to close or at the edge of the picture (yellow, A and B). Cells were not counted if there was no or weak labelling and appeared with a pink outline.

The data showed no significant changes between treatment groups of hESCs cultured at 5% oxygen when transfected with either pre-miR-122-5p or pre-miR-223-3p or when both pre-miRs were simultaneously transfected compared to the transfection pre-miR-control (Figure 94).

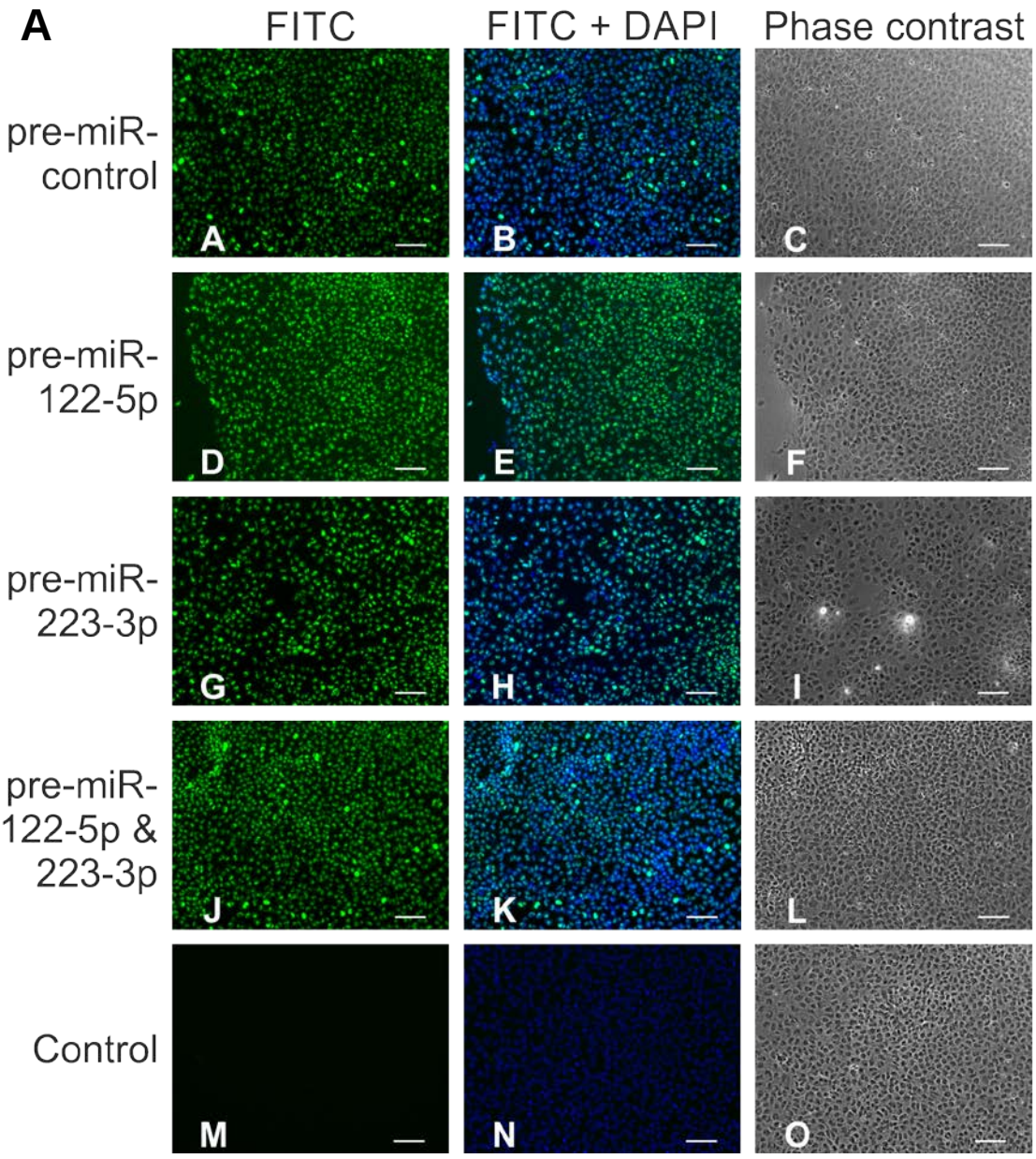

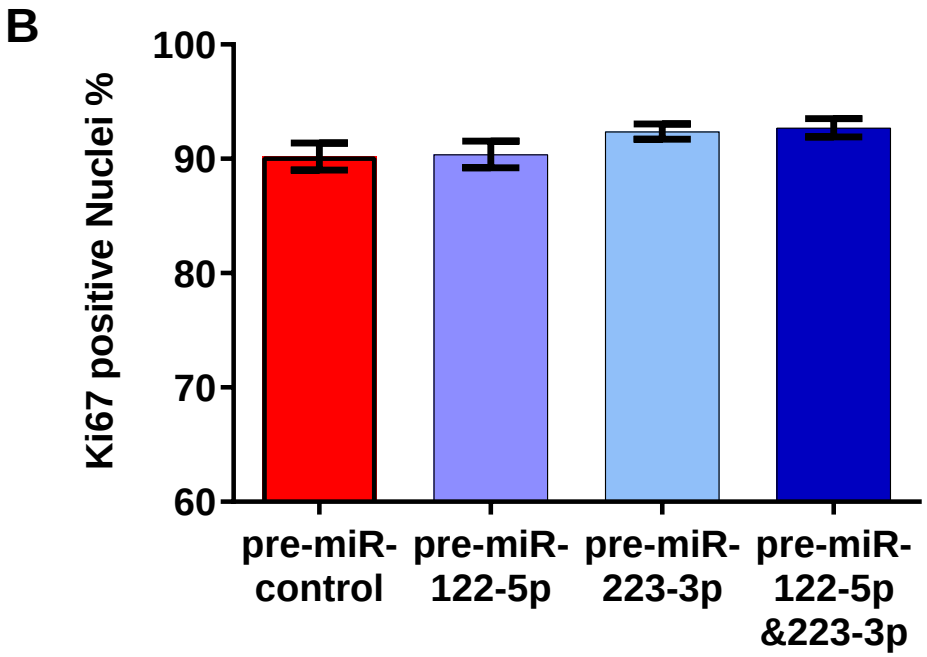

Figure 94: Ki67 expression in hESCs cultured at 5% oxygen and transfected with pre-miRs for 48h

(A) Immunocytochemistry showing representative Ki67 labelling (green; A-B, D-E, G-H, J-K) merged with DAPI (blue; B, E, H, K, N) of Hues7 hESCs at 5% oxygen on day 3 post-passage. Negative controls= FITC secondary antibody only (M-N) merged with DAPI (blue, N). Phase contrast images of colonies (C, F, I, L, O). Scale bar = 100 µm. hESCs were transfected 24h post-passaging with 200nM pre-miR-control (A-C), pre-miR-122-5p (D-F), pre-miR-223-3p (G-I) or pre-miR-122-3p & pre-miR-122-5p (J-L) and labelled 48h post-transfection.
(B) Bar graph represents percentage of Ki67 positive nuclei in each group. Means of the four groups were pre-miR-ctrl 90.2 ±1.19 (n=3), pre-miR-122-5p 90.4 ±1.2 (n=3), pre-miR-223 92.4 ±0.7 (n=3), pre-miR-122-5p & pre-miR-223-3p 92.7 ± 0.8 (n=3). Bars represent ±SEM (each biological replicate contains 3-4 investigated and counted regions of interest)

Similarly, no improvement in proliferation was observed by repressing these miRNAs when hESCs cultured at 5% oxygen where transfected with either anti-miR-122-5p or anti-miR-223-3p or when both anti-miRs were simultaneously transfected compared to the transfection anti-miR-control (Figure 95).

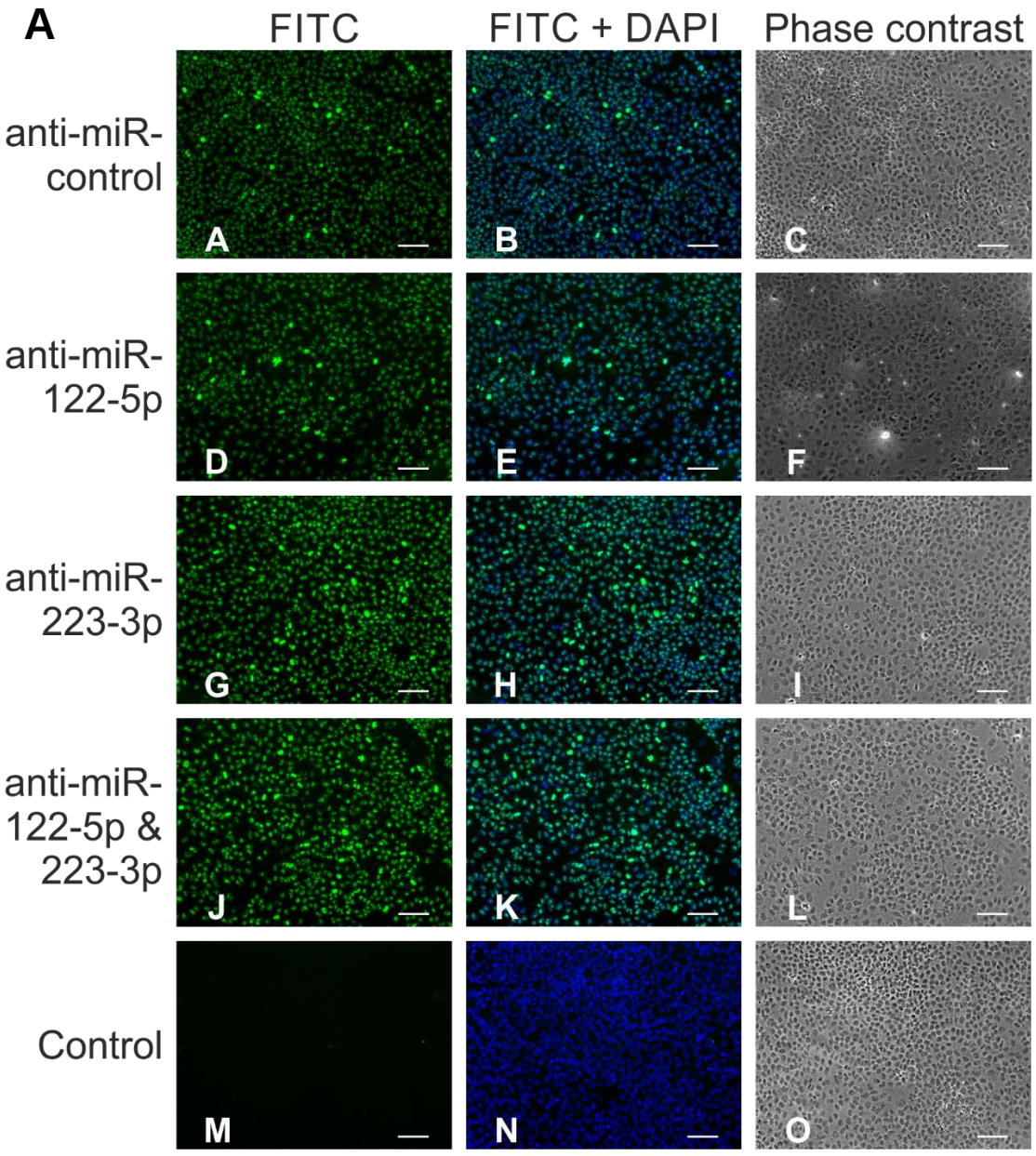

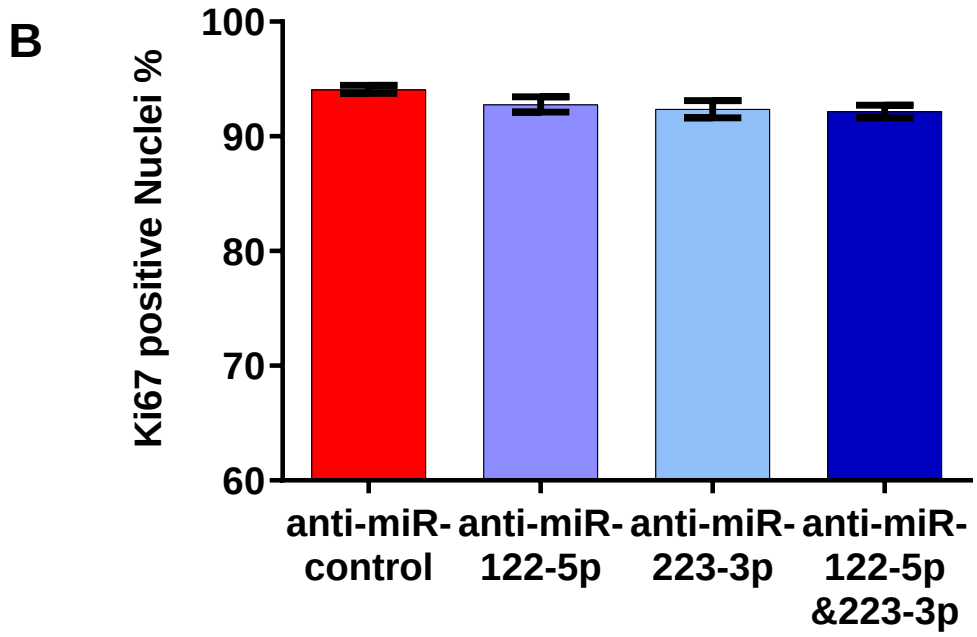

Figure 95: Ki67 expression in hESCs cultured at 5% oxygen and transfected with anti-miRs for 48h

(A) Immunocytochemistry showing representative Ki67 labelling (green; A-B, D-E, G-H, J-K) merged with DAPI (blue; B, E, H, K, N) of Hues7 hESCs at 5% oxygen on day 3 post-passage. Negative controls= FITC secondary antibody only (M-N) merged with DAPI (blue, N). Phase contrast images of colonies (C, F, I, L, O). Scale bar = 100 µm. hESCs were transfected 24h post-passaging with 200nM anti-miR-control (A-C), anti-miR-122-5p (D-F), anti-miR-223-3p (G-I) or anti-miR-122-3p & anti-miR-122-5p (J-L) and labelled 48h post-transfection.
(B) Bar graph represents percentage of Ki67 positive nuclei in each group. Means of the four groups were anti-miR-ctrl 93.7 ± 0.5 (n=3), anti-miR-122-5p 92.8 ± 0.7 (n=3), anti-miR-223 92.4 ± 0.7 (n=4), anti-miR-122-5p & anti-miR-223-3p 92.2 ± 0.5 (n=3). Bars represent ±SEM (each biological replicate contains 4 investigated and counted regions of interest).

5.4 Discussion

5.4.1 Challenges in miRNA-mRNA binding predictions

The first objective of this Chapter was to determine potential binding sites of the miRNAs miR-122-5p and miR-223-3p in the NANOG 3'UTR with the aim of identifying direct binding sites between these miRNAs and the mRNA of NANOG.

Initially, challenges in miRNA target prediction needed to be tackled to find distinct locations within the NANOG 3'UTR. The prediction algorithm used by TargetScan relies mainly on sequence complementarity, perfect seed-matches and includes non-canonical sites (only from v7.0 upwards, which was not the version used) when the binding sites have extensive additional 3' compensatory Watson-Crick base pairing. TargetScan is a useful tool for target-prediction as it is logic, frequently up-dated (v6.0 March 2012, v6.1 to v6.2 April 2012, v6.2 to v7.0 August 2015 and v.7.0 to v7.1 June 2016) and underpinned by published data. However, since TargetScan is relatively restricted to complementarity SegalLab was investigated which tolerates single GU wobbles as well as single mismatches within the seed-sequence thus allowing more binding possibilities but making it a more challenging approach to find functional binding sites. Additionally, there are some contradictory findings to whether miRNA binding leads to either up- or down-regulation of the target gene (as reviewed by Orang et al. 2014). The up-regulation of gene expression mediated through miRNAs is very cell type specific. KLF4 for example was shown to be up-regulated by miR-206 in confluent, non-tumour cells whereas miR-344 was down-regulating KLF4 expression in proliferating, normal cells (C.-C. Lin *et al.*, 2011). Although this is a valuable point, the data presented show in this thesis a clear decrease in NANOG protein expression when miR-122-5p or miR-223-3p were overexpressed. Thus, both these miRNAs follow the more conventional mechanisms of miRNA-mediated down-regulation of target genes.

This chapter demonstrates the difficulties encountered once the route was diverted from only looking at perfect complementarity within the seed-sequence. This was shown when SegalLab was interrogated returning exact positions for possible miRNA binding sites that did not match the actual sequence. A question arose as to why SegalLab was unable to identify the miR-223-3p binding site at position 18 in NANOG 3'UTR. This observation could be due to the close proximity of the coding region/start of the 3'UTR. Certainly, by focusing on the 3'UTR one aspect of the "gold standard" for miRNA-mRNA interaction was followed as approximately 60% of the actual binding sites of miRNAs are found in the 3'UTR in mammals (Friedman *et al.*, 2009). However, binding to the coding sequence has been observed not just in plants where miRNA binding sites outside the 3'UTR are

frequently found. miRNA recognition elements have been demonstrated throughout the genome including 5'UTR, coding sequence and 3'UTR (Tay *et al.*, 2008; Vogel *et al.*, 2010; Roberts, Lewis and Jopling, 2011). However, as the 3'UTR is the most investigated region it might bias the outcome of miRNA targets found so far. Strikingly, taking not just the 3'UTR into account but also including the 5'UTR and the coding region and different binding mechanisms it is difficult to predict functional miRNA binding sites. For example, miRNA targeting beyond the 3'UTR was demonstrated within the coding sequence of mouse pluripotent genes such as Nanog, Oct4 and Sox2 (Tay *et al.*, 2008). Thus, potential miRNA recognition sites in the work presented may have been missed but the 3'UTR is believed to contain more biologically functional sites. However, encouraged through published functional non-canonical miRNA target sites (as reviewed by Brodersen & Voinnet, 2009; Loeb et al. 2012) that did not follow 100% complementarity within the seed sequence as well as the existence of bulges (Chi, Hannon and Darnell, 2012; Martin *et al.*, 2014; Agarwal *et al.*, 2015), those non-100%-complementarity sides were considered and analysed with SegalLab and an approach using sequence complementarity only for target identification.

In this chapter numerous potential binding sites for miR-122-5p and miR-223-3p were found along the NANOG 3'UTR. It was decided to study the first ~500 bp of the NANOG 3'UTR as they contained promising binding sites for both miRNAs, miR-122-5p and miR-223-3p. Additionally, the first ~500 bp of the NANOG 3'UTR had only one discovered binding site for miR-223-3p and only three binding sites for miR-122-5p. Hence, miRNAs and the first ~500bp of the NANOG 3'UTR were cloned into vectors and transiently transfected in HeLa cells and a Dual-Luciferase-Reporter Assay performed. HeLa cells were used because they are optimal for miRNA studies as they have low expression levels of endogenous mature miRNAs (Obernosterer *et al.*, 2006; E. J. Lee *et al.*, 2008; Tomaselli *et al.*, 2015) and therefore allow the quantification of specific exogenous miRNA expression and interaction with their target mRNA. Hence, a novel binding site of miR-223-3p was identified at position 18 of the NANOG 3'UTR using a Dual-Luciferase-Reporter Assay with HeLa cells. The Dual-Luciferase-Reporter Assay is a much utilised method to assess the precise binding site and direct effect of one miRNA within a defined area of the target gene (Martinez-Nunez *et al.*, 2009, 2014; Jin *et al.*, 2013; Yu *et al.*, 2013). This study investigated the first ~500bp of the NANOG 3'UTR thus several other potential binding sites were not studied. It is possible there may be other binding sites which are functional. Thus a multidimensional analysis is needed to determine not only one miRNA binding site within the mRNA but also miRNA containing ribonucleoproteins and other related RNA-binding proteins that influence miRNA function. The significant 20% reduction in relative luciferase activity when miR-223-3p

was co-transfected with the NANOG 3'UTR is similar to that observed by other experiments (Yu *et al.*, 2013). Using site-directed mutagenesis was able to confirm the precise binding site for miR-223-3p at position 18 of the NANOG 3'UTR. It is tempting to speculate that the effect of miR-223 down-regulating IGF-1R seen by Yu et al. (2013) and the effect we have observed for miR-223-3p in the NANOG 3'UTR could regulate pluripotency in two stages by the same miRNA which demonstrates the complexity of gene expression, regulation and miRNA being multi-target regulators.

As miRNAs are able to target many genes, increasing the expression of a single miRNA is likely to influence a whole array of genes making the functional significance of a specific interaction difficult to interpret. This could explain the observation of the reduced NANOG expression when the expression of miR-122-5p was increased using pre-miRs and that no effect was observed when miR-122-5p was co-transfected with the NANOG 3'UTR using the Dual-Luciferase-Reporter Assay. Thus the reduced NANOG expression might be an indirect effect seen at the protein level. However, it is possible that miR-122-5p has its functional targets outside the first ~500 bp of the NANOG 3'UTR investigated as the first ~500 bp represent only one quarter of the entire NANOG 3'UTR length.

5.4.2 Functional impact of miR-223-3p in hESCs

The goal of the second part of this chapter was to study the functional impact of miR-223-3p targeting NANOG 3'UTR. hESCs were transfected with synthetic mature miRNAs to measure the effects at the mRNA and protein level of genes expected to be influenced by these miRNAs. Increasing the expression of miRNAs and analysing changes at their predicted targets is a common approach to discover and validate miRNA targets (Grimson *et al.*, 2007; Baek *et al.*, 2008). However, this might not be the ideal way of analysing the direct impact of a single miRNA as miRNAs are multipurpose gene regulators and could influence many other genes. As miR-223-3p was found to directly interact with NANOG causing its down-regulation at the protein-level this miRNA might initiate a cascade of down-stream effects. Therefore, the reduced expression of pluripotency markers observed in Chapter 4, especially NANOG, required further investigation as to whether these miRNAs have a functional impact on hESC maintenance.

Consequently, an early differentiation marker, Brachyury was investigated. Indeed, the transfection of synthetic miR-223-3p in hESCs caused an increase in Brachyury expression. This observation might be a consequence of miR-223-3p down-regulating NANOG protein expression. That miRNAs induce differentiation has been studied more intensively in mESCs. When differentiation occurs in mESCs, self-renewal is usually inhibited e.g. by the let-7 miRNA family. The let-7 miRNA family in turn is inhibited by the miR-290 cluster if self-renewal occurs (miR-290-295 in mouse is highly similar to miR-371 cluster in humans).

The miR-290 cluster has been also shown to play an important role in regulating the G1/S transition in ESCs by safeguarding proliferation (Wang *et al.*, 2008). CDK6, a kinase involved in cell cycle progression in the G1/S transition is positively correlated with NANOG (X. Zhang *et al.*, 2009) and could be indirectly regulated by miR-223-3p through the repression of NANOG. For hESC maintenance it is important that proliferation, pluripotency and self-renewal are all controlled. Differences in hESC proliferation were observed as hESCs were more proliferative under hypoxia than in normoxia (Ludwig et al. 2006; Forristal et al. 2010). This effect was thought to be related to increased levels of NANOG as CDK6 is a direct binding partner (X. Zhang *et al.*, 2009; Forristal *et al.*, 2010). Indeed, a decrease in CDK6 mRNA expression was observed when the expression of miR-223-3p was increased, therefore possible changes in proliferation in hESCs were investigated.

By investigating the proliferation marker Ki67 it was expected to see a decrease in the percentage of Ki67 positive hESCs when miR-122-5p or miR-223-3p expression was increased. Similarly, an increase in Ki67 positive cells was expected when the expression of miR-122-5p and/or miR-223-3p was inhibited by using anti-miRs. However, it seems that proliferation is unaffected by either miR-122-5p, miR-223 3p or both which is plausible if these miRNAs mainly regulate pluripotency and cells can be proliferative without being pluripotent. In contrast, Jung et al. (2011) found that either PKM2 knock-out or miR-122 overexpression displayed deficiencies in the proliferation of hESCs. We did not see any changes in PKM2 expression upon increasing the expression of miR-122-5p (Chapter 4.3.3) which may explain the lack of differences in proliferation. This lack could also be explained by the different cell line used for performing the proliferation assays, as Hues7 hESCs also did not reach statistical significance in the CDK6 mRNA expression, suggesting that an increased number of repeats may be needed. This is in agreement with observation of functional and molecular differences among hESCs lines which still need to be understood (Bock *et al.*, 2011). It was shown that miR-223 plays an important role in proliferation in other cell types such as granulocytes and smooth muscle cells (Johnnidis *et al.*, 2008; Song *et al.*, 2012). However, our findings are consistent with Yu et al. (2013) as they found that miR-223 is not required for proliferation in hESCs.

Overall, the results of this Chapter demonstrate a novel binding site for miR-223-3p in the 3'UTR of NANOG. The functional significance of this binding is evident from Dual-Luciferase-Reporter assays and miR-223-3p has a role in regulating early hESC differentiation but also in the regulation of CDK6. MiR-223-3p binding to the NANOG 3'UTR might be a reason why a decreased NANOG expression and a higher propensity towards spontaneous cell differentiation is seen in hESCs cultured at 20% oxygen when compared to those maintained at the more physiological 5% oxygen concentration.

Finally, this Chapter also highlights the current challenges surrounding miRNA research and the complexity of determining functional miRNA targets.

Chapter 6
General Discussion and Future Work

6.1 General Discussion

Environmental oxygen tension is known to regulate the expression of pluripotency markers OCT4, SOX2 and NANOG but the mechanisms involved are not fully understood. The investigations of this thesis provide information about miRNAs, considered as master gene regulators that are differentially expressed in hESCs when two different culture conditions are compared, 5% and 20% oxygen. Thus confirming that miRNAs are important in gene regulation and are involved in the hypoxic regulation of hESCs.

Data from TaqMan miRNA arrays showed the expression profile of miRNAs in hESCs cultured under 5% and 20% oxygen concentration. Not all miRNAs tested were expressed in hESCs, probably due to their early developmental stage. However, the two oxygen concentrations orchestrate two different pools of miRNAs. These two pools consists of miRNAs that are either down-regulated or up-regulated under hypoxia. MiRNAs most commonly repress their target gene expression and it is known that the pluripotency genes are up-regulated under hypoxia. Thus, the data of the miRNA arrays indicate that miRNAs up-regulated under hypoxia lead to inhibition of genes responsible for differentiation and that miRNAs down-regulated under hypoxia support the maintenance of the pluripotent state of hESCs. To the best of our knowledge, this is the first report to show that miRNAs are differentially regulated by environmental oxygen tension in hESCs.

This thesis also presents a large amount of *in silico* work. Thus revealing possible miRNAs-mRNA interactions which were focussed on miRNA targets that might be involved in regulating the pluripotent stem cell state directly through the core pluripotency unit and HIFs. MiRNAs that are down-regulated under hypoxia and target pluripotency genes will facilitate the expression of these genes in hESCs cultured at 5% oxygen. In contrast, these genes will show decreased expression in hESCs maintained at atmospheric oxygen conditions. The data presented show also the importance of biological validation. One advantage of the data-mining undertaken in this thesis was the combined approach of using TaqMan miRNA arrays together with two different bioinformatic prediction tools. Each of them alone is not comprehensive enough but combining them can deliver knowledge about the expression profile within the cell-type investigated. In addition, combining current knowledge with mRNA target prediction for each single miRNA of the array can lead to successful target identification. This approach allowed the results obtained from the arrays to be validated using RT-qPCR. During this study miR-122-5p and miR-223-3p were selected as miRNAs of interest for further

investigations. Both miRNAs were down-regulated under hypoxia across two array-sets with predicted targets such as HIF2A for miR-223-3p and HIF3A and an inhibitor of HIF1A for miR-122-5p. Additional investigations showed that these two miRNAs had further targets such as PKM2, SOX2 and NANOG but miRNAs mutually down-regulated by all three arrays were not predicted to target these additional genes, hence not considered for investigations at this time but interesting to further investigate in the future. In detail, miR-122-5p was additionally predicted to target PKM2, SOX2 and NANOG; miR-223-3p was predicted to target NANOG. The process of revealing targets through bioinformatic predictions is an emerging and quickly advancing field and enormously helpful for finding possible miRNA-mRNA interactions. Undoubtedly some important targets have been missed as databases are up-dating constantly and algorithms could be further improved. However, this study highlights the importance of cross-disciplinary research as it would have been unlikely to discover these miRNA binding sites without current advances in bioinformatics.

The data contained in this thesis shows the mechanism of how miR-122-5p and miR-223-3p regulate gene expression in hESCs by exerting post-translational inhibition of their target genes rather than destabilising mRNA. This is due to no changes being observed at the mRNA level suggesting a blockage rather than a degradation of mRNA. However, a significant reduction at the protein level was seen upon overexpression of miR-122-5p or miR-223-3p in hESCs which underpins the importance of studying target gene expression at the protein level. In addition, by utilising miRNAs that are either derived from the guide- or passenger strand highlights how both strands are utilised and functional. This is in contrast to outdated views of miRNA-processing that described one strand, usually the passenger-strand, as degraded or non-functional for mRNA targeting (Zhang *et al.*, 2013). This serves to highlight the speed of discovery in the miRNA field.

One of the main results of this thesis is the identification of a direct binding site of miR-223-3p at position 18 at the NANOG 3'UTR which was successfully validated by site-directed mutagenesis of this binding site to corroborate the direct interaction. This finding indicates that this direct binding site of miR-223-3p in the NANOG 3'UTR is causing the reduction in NANOG protein expression that was seen when miR-223-3p was overexpressed in hESCs. This is the first time, that miR-223-3p has been shown to directly bind to NANOG 3'UTR. Indeed, previous findings were correlating miR-223-3p also with a role in pluripotency but demonstrating these effects related to the binding to IGF-1R (Yu *et al.*, 2013). The data presented in this thesis propose that miR-223-3p is involved in the hypoxic regulation of pluripotency in hESCs directly via NANOG protein

expression as depicted by Figure 96. This finding could potentially work in cooperation with the direct target of miR-223-3p in the IGF-IR (Yu *et al.*, 2013).

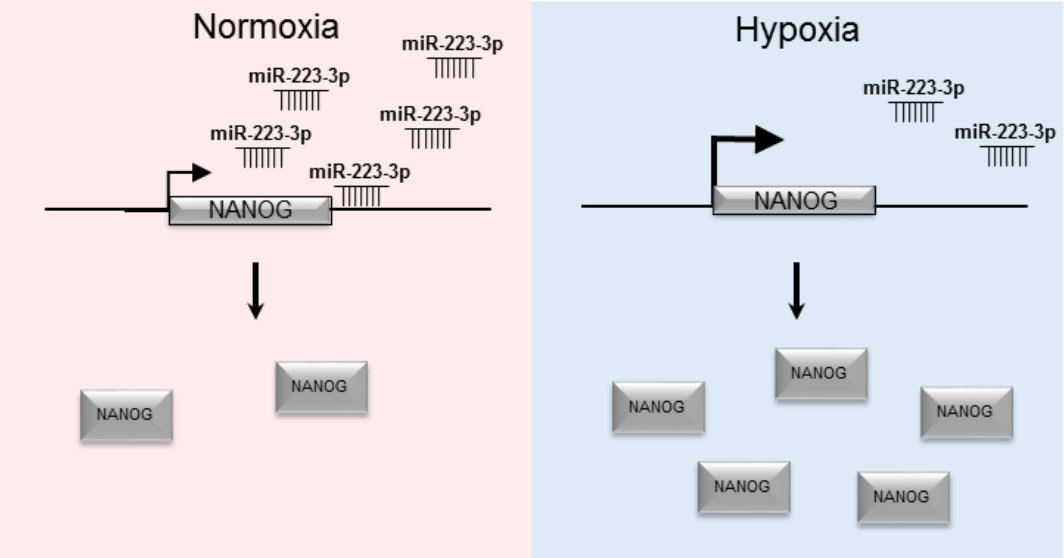

Figure 96: Schematic representation of miR-223-3p regulating NANOG expression in hESCs

miR-223-3p is up-regulated in normoxia and therefore causing the reduction in NANOG protein expression. Under hypoxic oxygen concentrations, less miR-233-3p is expressed and therefore more NANOG protein expression is present.

A lack of data demonstrating a physiological role of miRNAs has been recently criticised (Reviewed by Y. J. Lee et al. 2016). This has been addressed in this thesis. Given the important role of NANOG in hESCs maintenance, especially in regulating the S-phase entry it is not surprising that one of the down-stream effectors of NANOG and important cell-cycle regulators CDK6 (X. Zhang *et al.*, 2009) was affected by overexpressing miR-223-3p. Equally important, this thesis shows that the effect of overexpressing miR-223-3p, which is acting via NANOG induces differentiation as one of the earliest mesendodermal lineage markers, Brachyury, was more highly expressed in these hESCs compared to the control. Despite the improvements in understanding the role of hypoxia in hESCs, little is known how the whole interactome is communicating. The data of this thesis show, that miR-223-3p represses NANOG protein expression at 20% oxygen but without influencing hESCs proliferation, highlighting the role of miRNAs in fine-tuning gene expression rather than inducing drastic changes. Taken the advances in *in silico* miRNA-mRNA predictions together with those in molecular biology more effort is needed for validating these interactions and evaluating further functional roles for

miRNAs. This thesis gives some insight into the physiological role of miR-233-3p in regulating the pluripotent stage of hESCs. Moreover, hypoxia and the down-regulated miR-223 expression might suggest that the cells maintained at low oxygen levels comprise a more pluripotent/naïve like state than those maintained at 20% oxygen concentration.

Differences in miRNA expression that occur between the culture of hESCs at 5% or 20% oxygen might not just have implications towards the maintenance of hESCs but also for the generation of iPSCs. Indeed, the miRNA cluster miR-302/367 alone was used to reprogramme mouse and human somatic cells (Anokye-Danso *et al.*, 2011b). Repressing miR-223-3p expression with miR-223-3p anti-miRNAs for example in the process of reprogramming cells could further enhance NANOG expression and therefore pluripotency and self-renewal. Another interesting aspect of the miRNA expression profile in hESCs between the two different oxygen concentrations is, that this information could help to determine the pluripotent state of hESCs and consequently induce the expression of miRNAs that are beneficial for a pluripotent stem cell state or repress miRNAs that cause differentiation. Recently, miRNA profiles were used for non-invasively determining the pluripotent state of stem cells by measuring the miRNA-expression profile specifically the expression of miR-292-3p and miR-294 in the cell culture medium (Zhang *et al.*, 2016). This could be used in future to simultaneously determine changes of pluripotency in any experiments undertaken which could further help explain differences in experimental outcomes as the pluripotent stem cell state is not static due to spontaneous differentiation occurring in culture systems. The advanced knowledge about specific miRNAs and their targets such as miR-223-3p targeting NANOG 3'UTR could further enhance our understanding of how to preserve certain cell-states, to support the transition into a specialised cell or to reverse cellular processes.

Another important aspect to mention is that this thesis is also demonstrating that the target prediction algorithms are not yet perfect to concisely represent true miRNA targets because they are not yet capable to adequately calculate the complexity of miRNA-mediated gene regulation. This has been addressed in the last result chapter, mentioning only the main result where miR-223-3p has a functional binding site at position 18 of the NANOG 3'UTR which was identified manually rather than solely relying on prediction algorithms. A possible reason that this site was not detected by SegalLab is likely due to the close proximity to the coding region. Although there are many algorithms available there is a desire for new methods that can universally consider all known aspects of miRNA-mRNA interaction. Biologically validated targets, such as the ones validated in this thesis, miR-223-3p for NANOG 3'UTR but also the investigated miR-122-5p site that

did not function as direct binding site in NANOG 3'UTR can contribute to improve prediction algorithms as these results can be used for algorithms that learn or train from these data, a process called machine learning.

The data provided here not only contribute to the basic understanding of how pluripotency in hESCs is regulated, they also underpin the importance of physiological culture conditions and that miRNAs could potentially be used to better maintain hESCs *in vitro* (e.g. miR-223-3p inhibitors) but they also provide further information which could benefit the generation of iPSCs. The difference in miRNA expression observed between the two different oxygen concentrations in this thesis emphasises that miRNAs are tightly regulated and that their regulation is organised in a complex network. Further understanding of this complex network could provide a very specific fine-tuning-switch. This may allow the manipulation of hESCs such as for distinct lineage commitment which could have an enormous potential in personalised and regenerative medicine as well as for drug testing on human tissue, thus bringing the therapeutic potential of miRNAs further forward. Additionally, this knowledge may help to further develop current techniques to derive or reprogram cells into a naïve or primed human PSC state as the data provided here show the functional role of miR-223-3p in regulating NANOG expression. Unveiling more and more questions of how the pluripotent stem cell network is regulated will enable us to achieve a better understanding of hESCs that will ultimately lead to improved efficiencies for the generation of iPSCs and to defined and more standardised culture conditions that will help to achieve more reproducible results across different cell lines and laboratories.

These investigations contribute towards a better understanding of how hypoxia is regulating hESCs and show that miRNAs play an important role in the multifaceted regulatory network of pluripotency towards enhanced stemness. This study also contributes to investigations made outside the transcriptional level as the functions of the core-pluripotency factors are not well studied when they are post-translational modified.

6.2 Future Work

To further understand the impact of miRNAs in the hypoxic regulation of hESCs when compared to normoxia the following experiments could be investigated:

-To investigate miR-223-3p and miR-122-5p in the NANOG 3'UTR beyond the first 500bp. Dual-Luciferase-Reporter assay could be performed.

-To further investigate the impact of miR-122-5p and miR-223-3p in hESCs at 5% oxygen with the addition of pre-miRs for miR-122-5p and miR-223-3p. This could be undertaken in conjunction with measuring the expression of miR-292-3p and miR-294 in the cell culture medium to validate and utilise the findings from Zhang et al. (2016) who was showing that these miRNAs are determinants of the pluripotent state of hESCs.

-To further investigate if miR-223-3p promotes differentiation towards a specific lineage by performing qPCR and Western-blots for SOX7, SOX17 or GATA6 early endodermal lineage markers and TBX6 or SNAIL for early mesodermal lineage markers.

-To determine whether the protein levels of HIF3A and HIF2A are affected by miR-122-5p and miR-223-3p respectively under hypoxia, as they are predicted targets. Western-blot or FACS could be used to quantify HIF2A or HIF3A. And subsequently investigating potential miRNA binding sites for HIF2A performing Dual-Luciferase-Reporter assays.

-To investigate potential binding sites in the 5'UTR and CDS of miR-122-5p and miR-223-3p in NANOG/HIF2A/HIF3A using bioinformatics followed by performing Dual-Luciferase-Reporter assay.

-To determine further targets of either miR-122-5p or miR-223-3p using other methods than miRNA overexpression/inhibition only. This could be performed using tagged miRNA pull-downs or immunoprecipitations of miRISC. Briefly, for tagged miRNA pull-downs usually synthetic miRNA duplexes are used that contain e.g. one biotin group. Once these tagged miRNAs are incorporated into miRISC the complex can be affinity-purified and analysed (e.g. miR-TRAP). For immunoprecipitation of miRISC, cells are transfected with synthetic miRNAs versus a control. The synthetic miRNAs are enriching the miRNA-mRNA-miRISC pool versus control which can be immunoprecipitated with antibodies against one of the miRISC members such as AGO2 and any mRNA bound can be isolated and analysed with microarray analysis or RNA-sequencing techniques (e.g. RIP-ChIP, RIP-Seq or PAR/HITS-CLIP).

-To determine if any up-regulated miRNAs under hypoxia are targeting genes responsible for differentiation and therefore supressing them using bioinformatics as a

first step and then validating miRNA expression in hESCs cultured in hypoxia when compared to normoxia.

-To determine metabolic changes in hESCs cultured at 5% oxygen concentration with the addition of pre-miRs, since PKM2 is a potential target for miR-122-5p.

-Re-mining array data, as algorithms improve using the classical software TargetScan v7.1 (June 2016) but also others such as miRDB that uses machine learning methods to predict targets based on high-throughput sequence data. Or other databases could be explored such as miRTar that incorporates alternative splice variants of miRNA targets and target sites outside the 3'UTR.

VII. Apendices

Appendix A Supplementary Data

Table 44: List of miRNAs targeting KLF4 which are down-regulated under hypoxia compared to normoxia in hESCs

	KLF4
ABC	
AB	1x hsa-miR-145-5p 1x hsa-miR-152-3p 1x hsa-miR-26b-5p 1x hsa-miR-29a-3p
BC	1x hsa-miR-520f-3p 1x hsa-miR-103a-3p
AC	2x hsa-miR-32-5p

Appendix B Supplementary Methods

B.1 QIAprep Spin Miniprep Kit

1. 3 ml of the overnight culture was harvested by centrifuging at 13,000 rpm for 3 min.
2. The bacterial pellet was subsequently resuspended in 250 µl Buffer P1 (with lyse blue and RNAse A added) by vortexing.
3. Followed by the addition of 250 µl Buffer P2 (Lysis Buffer), inverting the tubes 4-6 times until homogeneously coloured in blue and incubating the tubes for no longer than 5min.
4. 350 µl of Buffer N3 were added and tubes inverted 4-6 times until the blue colour disappeared.
5. The suspension was then centrifuged for 10 min at 13,000 rpm.
6. After centrifugation, the supernatant was applied to the QIAprep spin column, followed by centrifuging for 1 min at 13,000 rpm.
7. Subsequently, the column was washed with 0.75 ml Buffer PE, followed by centrifuging for 1 min at 13,000 rpm.
8. The flow through was discarded followed by one additional centrifugation step to remove residual buffer.
9. The column was then transferred to a clean 1.5 ml Eppendorf tube, 50µl of RNAse free water was applied to the centre of the column and incubated for 1 min at room temperature. The DNA was subsequently eluted by centrifuging for 2 min at 13,000 rpm.

B.2 Qiagen Gel Extraction Kit

1. The DNA fragments were cut from the agarose gel using a clean scalpel.
2. The gel fragments were weighed and 3 times the volume of Buffer QG added to 1 volume of gel (100 mg gel ~ 100 µl) and incubated at 50°C for 10 min or until dissolved.
3. Then, 1 volume of isopropanol was added and mixed.
4. The sample was then applied to a QIAquick spin column and centrifuged for 1 min at 13,000 rpm to bind the DNA.
5. The flow through was discarded followed by a washing step with 500 µl buffer QG and a washing step with 750 µl Buffer PE, each washing step followed by centrifugation of 1 min with 13,000 rpm.
6. The QIAquick column was then transferred into a fresh Eppendorf tube and the DNA eluted with 30 µl H_2O.

B.3 QIAgen Plasmid Maxiprep Kit

1) The overnight culture was harvested by centrifuging at 6,000 x g for 15 min at 4°C.
2) The bacterial pellet was subsequently resuspended in 10 ml Buffer P1.
3) After the addition of 10 ml Buffer P2 (Lysis Buffer) tubes were inverted 4-6 times until homogeneously coloured in blue and incubated for no longer than 5 min.
4) After the addition of 10 ml pre-chilled Buffer P3 (Neutralisation Buffer) tubes were inverted 4-6 times until colourless and incubated on ice fore 20 min.
5) The solution mix was then transferred into a smaller tube and centrifuged at 20,000 x g for 30 min.
6) After equilibration of the QIAgen tip with 10 ml Buffer QBT, the supernatant of the solution mix was applied to the QIAgen tip moving through by gravity flow.
7) The QIAgen tip was subsequently washed by applying 2x 30 ml Buffer QC.
8) The DNA was eluted by adding 15 ml Buffer QF into a 50 ml falcon tube and DNA precipitated by adding 10.5 ml (0.7 volumes) room-temperature isopropanol, followed by centrifuging at 15,000 x g for 30 min.
9) The supernatant was discarded and the DNA pellet resuspended in 0.5 ml RNAse free water, transferred into a 2 ml tube followed by adding 50 µl NaAc (3M) and 1.125 ml 100% ethanol and centrifuged at 13,000 rpm for 15 min at room temperature.
10) The supernatant was carefully discarded and the DNA pellet air-dried and re-dissolved in 0.5 ml RNAse free water.

VIII. List of References

Agarwal, V., Bell, G. W., Nam, J.-W. and Bartel, D. P. (2015) 'Predicting effective microRNA target sites in mammalian mRNAs', *eLife*, 4(AUGUST2015), pp. 1–38. doi: 10.7554/eLife.05005.

Alexiou, P., Maragkakis, M., Papadopoulos, G. L., Reczko, M. and Hatzigeorgiou, A. G. (2009) 'Lost in translation: an assessment and perspective for computational microRNA target identification.', *Bioinformatics (Oxford, England)*, 25(23), pp. 3049–55. doi: 10.1093/bioinformatics/btp565.

Ambros, V. (2004) 'The functions of animal microRNAs.', *Nature*, 431(7006), pp. 350–5. doi: 10.1038/nature02871.

Ambrosetti, D. C., Basilico, C., Dailey, L., Ambrosetti, D., Basilico, C. and Dailey, L. (1997) 'Synergistic activation of the fibroblast growth factor 4 enhancer by Sox2 and Oct-3 depends on protein-protein interactions facilitated by a specific spatial arrangement of factor binding sites . Synergistic Activation of the Fibroblast Growth Factor 4 En', *Molecular and cellular biology*, 17(11), pp. 6321–6329.

Ambrosetti, D. C., Schöler, H. R., Dailey, L. and Basilico, C. (2000) 'Modulation of the activity of multiple transcriptional activation domains by the DNA binding domains mediates the synergistic action of Sox2 and Oct-3 on the fibroblast growth factor-4 enhancer.', *The Journal of biological chemistry*, 275(30), pp. 23387–97. doi: 10.1074/jbc.M000932200.

Amit, M., Carpenter, M. K., Inokuma, M. S., Chiu, C.-P., Harris, C. P., Waknitz, M. A., Itskovitz-Eldor, J. and Thomson, J. A. (2000) 'Clonally derived human embryonic stem cell lines maintain pluripotency and proliferative potential for prolonged periods of culture.', *Developmental biology*, 227(2), pp. 271–8. doi: 10.1006/dbio.2000.9912.

Amit, M. and Itskovitz-Eldor, J. (2006) 'Feeder-free culture of human embryonic stem cells.', *Methods in enzymology*, 420, pp. 37–49. doi: 10.1016/S0076-6879(06)20003-X.

Amit, M., Margulets, V., Segev, H., Shariki, K., Laevsky, I., Coleman, R. and Itskovitz-Eldor, J. (2003) 'Human feeder layers for human embryonic stem cells.', *Biology of reproduction*, 68(6), pp. 2150–6. doi: 10.1095/biolreprod.102.012583.

Amit, M., Shariki, C., Margulets, V. and Itskovitz-Eldor, J. (2004) 'Feeder Layer- and Serum-Free Culture of Human Embryonic Stem Cells', *Biology of Reproduction*, 70(3), pp. 837–845. doi: 10.1095/biolreprod.103.021147.

Andrews, P. W. (1998) 'Teratocarcinomas and human embryology: Pluripotent human EC cell lines', *APMIS*. Blackwell Publishing Ltd, 106(1–6), pp. 158–168. doi: 10.1111/j.1699-0463.1998.tb01331.x.

Anokye-Danso, F., Trivedi, C. M., Juhr, D., Gupta, M., Cui, Z., Tian, Y., Zhang, Y., Yang, W., Gruber, P. J., Epstein, J. a and Morrisey, E. E. (2011a) 'Highly efficient miRNA-mediated reprogramming of mouse and human somatic cells to pluripotency.', *Cell stem cell*. Elsevier Inc., 8(4), pp. 376–88. doi: 10.1016/j.stem.2011.03.001.

Anokye-Danso, F., Trivedi, C. M., Juhr, D., Gupta, M., Cui, Z., Tian, Y., Zhang, Y., Yang, W., Gruber, P. J., Epstein, J. a and Morrisey, E. E. (2011b) 'Highly efficient miRNA-mediated reprogramming of mouse and human somatic cells to pluripotency.', *Cell stem cell*. Elsevier Inc., 8(4), pp. 376–88. doi: 10.1016/j.stem.2011.03.001.

Arvey, A., Larsson, E., Sander, C., Leslie, C. S. and Marks, D. S. (2010) 'Target mRNA abundance dilutes microRNA and siRNA activity.', *Mol. Syst. Biol.* Nature Publishing Group, 6(363), p. 363. doi: 10.1038/msb.2010.24.

Attisano, L., Wrana, J. L., Moustakas, A., Souchelnytskyi, S., Heldin, C.-H., Wrana, J. L., Massagué, J., Blain, S. W., Lo, R. S., Caestecker, M. P. de, Piek, E., Roberts, A. B.,

Wan, M., Podos, S. D., Hanson, K. K., Wang, Y. C., Ferguson, E. L., Stroschein, S. L., Bonni, S., Wrana, J. L., Luo, K., Wan, Y., Liu, X. and Kirschner, M. W. (2002) 'Signal transduction by the TGF-beta superfamily.', *Science (New York, N.Y.)*. American Association for the Advancement of Science, 296(5573), pp. 1646–7. doi: 10.1126/science.1071809.

Auerbach, S. and Brinster, R. L. (1968) 'Effect of Oxygen Concentration on the Development of Two-cell Mouse Embryos', *Nature*, 217(5127), pp. 465–466. doi: 10.1038/217465a0.

Avery, S., Inniss, K. and Moore, H. (2006) 'The Regulation of Self-Renewal in Human Embryonic Stem Cells', *Stem cells and development*, 15, pp. 729–740.

Avilion, A. a, Nicolis, S. K., Pevny, L. H., Perez, L., Vivian, N. and Lovell-Badge, R. (2003) 'Multipotent cell lineages in early mouse development depend on SOX2 function.', *Genes & development*, 17(1), pp. 126–40. doi: 10.1101/gad.224503.

Babiarz, J. E., Ruby, J. G., Wang, Y., Bartel, D. P. and Blelloch, R. (2008) 'Mouse ES cells express endogenous shRNAs, siRNAs, and other Microprocessor-independent, Dicer-dependent small RNAs.', *Genes & development*, 22(20), pp. 2773–85. doi: 10.1101/gad.1705308.

Badcock, G., Pigott, C., Goepel, J. and Andrews, P. W. (1999) 'The Human Embryonal Carcinoma Marker Antigen TRA-1-60 Is a Sialylated Keratan Sulfate Proteoglycan', *Cancer Res.*, 59(18), pp. 4715–4719.

Baek, D., Villén, J., Shin, C., Camargo, F. D., Gygi, S. P. and Bartel, D. P. (2008) 'The impact of microRNAs on protein output.', *Nature*, 455(7209), pp. 64–71. doi: 10.1038/nature07242.

Bagga, S., Bracht, J., Hunter, S., Massirer, K., Holtz, J., Eachus, R. and Pasquinelli, A. E. (2005) 'Regulation by let-7 and lin-4 miRNAs results in target mRNA degradation.', *Cell*, 122(4), pp. 553–63. doi: 10.1016/j.cell.2005.07.031.

Bar, M., Wyman, S. K., Fritz, B. R., Qi, J., Garg, K. S., Parkin, R. K., Kroh, E. M., Bendoraite, A., Mitchell, P. S., Nelson, A. M., Ruzzo, W. L., Ware, C., Radich, J. P., Gentleman, R., Ruohola-Baker, H. and Tewari, M. (2008) 'MicroRNA discovery and profiling in human embryonic stem cells by deep sequencing of small RNA libraries.', *Stem cells (Dayton, Ohio)*, 26(10), pp. 2496–505. doi: 10.1634/stemcells.2008-0356.

Bartel, D. P. (2004) 'MicroRNAs : Genomics , Biogenesis , Mechanism , and Function Genomics : The miRNA Genes', *Cell*, 116, pp. 281–297.

Bartel, D. P. (2009) 'MicroRNAs: target recognition and regulatory functions.', *Cell*, 136(2), pp. 215–33. doi: 10.1016/j.cell.2009.01.002.

Beattie, G. M., Lopez, A. D., Bucay, N., Hinton, A., Firpo, M. T., King, C. C. and Hayek, A. (2005) 'Activin A maintains pluripotency of human embryonic stem cells in the absence of feeder layers.', *Stem cells*, 23(4), pp. 489–495. doi: 10.1634/stemcells.2004-0279.

Becker, A. J., McCulloch, E. A. and Till, J. E. (1963) 'CYTOLOGICAL DEMONSTRATION OF THE CLONAL NATURE OF SPLEEN COLONIES DERIVED FROM TRANS-PLANTED MOUSE MARROW CELLS', *Nature*, 197(4866), pp. 452–454.

Becker, K. A., Ghule, P. N., Therrien, J. A., Lian, J. B., Stein, J. L., van Wijnen, A. J. and Stein, G. S. (2006) 'Self-renewal of human embryonic stem cells is supported by a shortened G1 cell cycle phase', *Journal of Cellular Physiology*. Wiley Subscription Services, Inc., A Wiley Company, 209(3), pp. 883–893. doi: 10.1002/jcp.20776.

Bertero, A., Madrigal, P., Galli, A., Hubner, N. C., Moreno, I., Burks, D., Brown, S., Pedersen, R. A., Gaffney, D., Mendjan, S., Pauklin, S. and Vallier, L. (2015) 'Activin/Nodal signaling and NANOG orchestrate human embryonic stem cell fate decisions by controlling the H3K4me3 chromatin mark', *Genes and Development*, 29(7),

pp. 702–717. doi: 10.1101/gad.255984.114.

Bertero, T., Robbe-Sermesant, K., Le Brigand, K., Ponzio, G., Pottier, N., Rezzonico, R., Mazure, N. M., Barbry, P. and Mari, B. (2013) 'MicroRNA Target Identification: Lessons from HypoxamiRs', *Antioxidants & Redox Signaling*, 0(0).

Bock, C., Kiskinis, E., Verstappen, G., Gu, H., Boulting, G., Smith, Z. D., Ziller, M., Croft, G. F., Amoroso, M. W., Oakley, D. H., Gnirke, A., Eggan, K. and Meissner, A. (2011) 'Reference maps of human ES and iPS cell variation enable high-throughput characterization of pluripotent cell lines', *Cell*. Elsevier Inc., 144(3), pp. 439–452. doi: 10.1016/j.cell.2010.12.032.

Bohnsack, M. T., Czaplinski, K. and Gorlich, D. (2004) 'Exportin 5 is a RanGTP-dependent dsRNA-binding protein that mediates nuclear export of pre-miRNAs.', *RNA (New York, N.Y.)*, 10(2), pp. 185–91.

Boissart, C., Nissan, X., Giraud-Triboult, K., Peschanski, M. and Benchoua, A. (2012) 'miR-125 potentiates early neural specification of human embryonic stem cells', *Development*, 139(7), pp. 1247–1257. doi: 10.1242/dev.073627.

Bone, H. K., Nelson, A. S., Goldring, C. E., Tosh, D. and Welham, M. J. (2011) 'A novel chemically directed route for the generation of definitive endoderm from human embryonic stem cells based on inhibition of GSK-3.', *Journal of cell science*, 124(Pt 12), pp. 1992–2000. doi: 10.1242/jcs.081679.

Bowles, J., Schepers, G. and Koopman, P. (2000) 'Phylogeny of the SOX family of developmental transcription factors based on sequence and structural indicators.', *Developmental biology*, 227(2), pp. 239–55. doi: 10.1006/dbio.2000.9883.

Boyer, L. A., Lee, T. I., Cole, M. F., Johnstone, S. E., Levine, S. S., Zucker, J. P., Guenther, M. G., Kumar, R. M., Murray, H. L., Jenner, R. G., Gifford, D. K., Melton, D. A., Jaenisch, R. and Young, R. A. (2005) 'Core transcriptional regulatory circuitry in human embryonic stem cells.', *Cell*, 122(6), pp. 947–56. doi: 10.1016/j.cell.2005.08.020.

Braam, S. R., Zeinstra, L., Litjens, S., Ward-van Oostwaard, D., van den Brink, S., van Laake, L., Lebrin, F., Kats, P., Hochstenbach, R., Passier, R., Sonnenberg, A. and Mummery, C. L. (2008) 'Recombinant vitronectin is a functionally defined substrate that supports human embryonic stem cell self-renewal via alphavbeta5 integrin.', *Stem cells*, 26(9), pp. 2257–2265. doi: 10.1634/stemcells.2008-0291.

Braillard, P.-A. and Malaterre, C. (2015) *Explanation in biology : an enquiry into the diversity of explanatory patterns in the life sciences*. Springer.

Brandenberger, R., Wei, H., Zhang, S., Lei, S., Murage, J., Fisk, G. J., Li, Y., Xu, C., Fang, R., Guegler, K., Rao, M. S., Mandalam, R., Lebkowski, J. and Stanton, L. W. (2004) 'Transcriptome characterization elucidates signaling networks that control human ES cell growth and differentiation.', *Nature biotechnology*, 22(6), pp. 707–16. doi: 10.1038/nbt971.

Braun, J. E., Huntzinger, E. and Izaurralde, E. (2012) 'A molecular link between miRISCs and deadenylases provides new insight into the mechanism of gene silencing by microRNAs', *Cold Spring Harbor Perspectives in Biology*, 4(12). doi: 10.1101/cshperspect.a012328.

Braun, J. E., Huntzinger, E. and Izaurralde, E. (2013) 'The Role of GW182 Proteins in miRNA-Mediated Gene Silencing', in Chan, E. K. L. and Fritzler, M. J. (eds) *Ten Years of Progressin GW/P Body Research*. Springer New York, pp. 147–163. doi: 10.1007/978-1-4614-5107-5_9.

Brennecke, J., Stark, A., Russell, R. B. and Cohen, S. M. (2005) 'Principles of microRNA-target recognition.', *PLoS biology*, 3(3), p. e85. doi: 10.1371/journal.pbio.0030085.

Brodersen, P. and Voinnet, O. (2009) 'Revisiting the principles of microRNA target recognition and mode of action', *Nature Reviews Molecular Cell Biology*. Nature

Publishing Group, 10(2), pp. 141–148. doi: 10.1038/nrm2619.

Brons, I. G. M., Smithers, L. E., Trotter, M. W. B., Rugg-Gunn, P., Sun, B., Chuva de Sousa Lopes, S. M., Howlett, S. K., Clarkson, A., Ahrlund-Richter, L., Pedersen, R. A. and Vallier, L. (2007) 'Derivation of pluripotent epiblast stem cells from mammalian embryos.', *Nature*, 448(7150), pp. 191–5. doi: 10.1038/nature05950.

Brook, F. A. and Gardner, R. L. (1997) 'The origin and efficient derivation of embryonic stem cells in the mouse', *National Academy of Scienes*, 94(11), pp. 5709–5712.

Burdon, T., Smith, A. and Savatier, P. (2002) 'Signalling, cell cycle and pluripotency in embryonic stem cells', *Trends in Cell Biology*, 12(9), pp. 432–438. doi: 10.1016/S0962-8924(02)02352-8.

Calabrese, J. M., Seila, A. C., Yeo, G. W. and Sharp, P. a (2007) 'RNA sequence analysis defines Dicer's role in mouse embryonic stem cells', *Proc Natl Acad Sci U S A*, 104(46), pp. 18097–18102. doi: 10.1073/pnas.0709193104.

Calder, A., Roth-Albin, I., Bhatia, S., Pilquil, C., Lee, J. H., Bhatia, M., Levadoux-Martin, M., McNicol, J., Russell, J., Collins, T. and Draper, J. S. (2012) 'Lengthened G1 Phase Indicates Differentiation Status in Human Embryonic Stem Cells', *Stem Cells and Development*, 22(2), p. 120829080827006. doi: 10.1089/scd.2012.0168.

Camps, C., Buffa, F. M., Colella, S., Moore, J., Sotiriou, C., Sheldon, H., Harris, A. L., Gleadle, J. M. and Ragoussis, J. (2008) 'hsa-miR-210 Is induced by hypoxia and is an independent prognostic factor in breast cancer.', *Clinical cancer research : an official journal of the American Association for Cancer Research*, 14(5), pp. 1340–8. doi: 10.1158/1078-0432.CCR-07-1755.

Card, D. A. G., Hebbar, P. B., Li, L., Trotter, K. W., Komatsu, Y., Mishina, Y. and Archer, T. K. (2008) 'Oct4/Sox2-regulated miR-302 targets cyclin D1 in human embryonic stem cells.', *Molecular and cellular biology*, 28(20), pp. 6426–38. doi: 10.1128/MCB.00359-08.

Carpenter, A. E., Jones, T. R., Lamprecht, M. R., Clarke, C., Kang, I. H., Friman, O., Guertin, D. A., Chang, J. H., Lindquist, R. A., Moffat, J., Golland, P. and Sabatini, D. M. (2006) 'CellProfiler: image analysis software for identifying and quantifying cell phenotypes.', *Genome biology*, 7(10), p. R100. doi: 10.1186/gb-2006-7-10-r100.

Cartwright, P., McLean, C., Sheppard, A., Rivett, D., Jones, K. and Dalton, S. (2005) 'LIF/STAT3 controls ES cell self-renewal and pluripotency by a Myc-dependent mechanism.', *Development (Cambridge, England)*, 132(5), pp. 885–96. doi: 10.1242/dev.01670.

Chambers, I., Colby, D., Robertson, M., Nichols, J., Lee, S., Tweedie, S. and Smith, A. (2003a) 'Functional expression cloning of Nanog, a pluripotency sustaining factor in embryonic stem cells.', *Cell*, 113(5), pp. 643–55.

Chambers, I., Colby, D., Robertson, M., Nichols, J., Lee, S., Tweedie, S. and Smith, A. (2003b) 'Functional expression cloning of Nanog, a pluripotency sustaining factor in embryonic stem cells.', *Cell*, 113(5), pp. 643–55.

Chambers, I., Silva, J., Colby, D., Nichols, J., Nijmeijer, B., Robertson, M., Vrana, J., Jones, K., Grotewold, L. and Smith, A. (2007) 'Nanog safeguards pluripotency and mediates germline development.', *Nature*, 450(7173), pp. 1230–4. doi: 10.1038/nature06403.

Chan, S. Y. and Loscalzo, J. (2010) 'MicroRNA-210 A unique and pleiotropic hypoxamir', *Cell Cycle*, 9(6), pp. 1072–1083.

Chan, S. Y., Zhang, Y.-Y., Hemann, C., Mahoney, C. E., Jay, L. and Loscalzo, J. (2009) 'MicroRNA-210 Controls Mitochondrial Metabolism during Hypoxia by Repressing the Iron-Sulfur Cluster Assembly Proteins ISCU1/2', *October*, 10(4), pp. 273–284. doi: 10.1016/j.cmet.2009.08.015.MicroRNA-210.

Chan, Y. C., Banerjee, J., Choi, S. Y. and Sen, C. K. (2012) 'miR-210: the master hypoxamir.', *Microcirculation (New York, N.Y.: 1994)*, 19(3), pp. 215–23. doi: 10.1111/j.1549-8719.2011.00154.x.

Chen, A. E. and Melton, D. A. (2007) 'Derivation of human embryonic stem cells by immunosurgery.', *Journal of visualized experiments*, (10), p. 574. doi: 10.3791/574.

Chen, H.-F., Kuo, H.-C., Chen, W., Wu, F.-C., Yang, Y.-S. and Ho, H.-N. (2009) 'A reduced oxygen tension (5%) is not beneficial for maintaining human embryonic stem cells in the undifferentiated state with short splitting intervals.', *Human reproduction (Oxford, England)*, 24(1), pp. 71–80. doi: 10.1093/humrep/den345.

Chen, Y., Gelfond, J. A. L., McManus, L. M. and Shireman, P. K. (2009) 'Reproducibility of quantitative RT-PCR array in miRNA expression profiling and comparison with microarray analysis', *BMC Genomics*, 10(1), p. 407. doi: 10.1186/1471-2164-10-407.

Chew, J., Loh, Y., Zhang, W., Chen, X., Tam, W., Yeap, L., Li, P., Ang, Y., Robson, P., Ng, H. and Lim, B. (2005) 'Reciprocal Transcriptional Regulation of Complex in Embryonic Stem Cells Reciprocal Transcriptional Regulation of Pou5f1 and Sox2 via the Oct4 / Sox2 Complex in Embryonic Stem Cells'. doi: 10.1128/MCB.25.14.6031.

Chi, S. W., Hannon, G. J. and Darnell, R. B. (2012) 'Supplementary data: An alternative mode of microRNA target recognition.', *Nature structural & molecular biology*. NIH Public Access, 19(3), pp. 321–7. doi: 10.1038/nsmb.2230.

Choi, E., Choi, E. and Hwang, K.-C. (2013) 'MicroRNAs as novel regulators of stem cell fate.', *World journal of stem cells*, 5(4), pp. 172–187. doi: 10.4252/wjsc.v5.i4.172.

Chow, D. C., Wenning, L. A., Miller, W. M. and Papoutsakis, E. T. (2001) 'Modeling pO(2) distributions in the bone marrow hematopoietic compartment. II. Modified Kroghian models.', *Biophysical journal*, 81(2), pp. 685–96. doi: 10.1016/S0006-3495(01)75733-5.

Christensen, D. R., Calder, P. C. and Houghton, F. D. (2015) 'GLUT3 and PKM2 regulate OCT4 expression and support the hypoxic culture of human embryonic stem cells.', *Scientific reports*. Nature Publishing Group, 5(October), p. 17500. doi: 10.1038/srep17500.

Christofk, H. R., Vander Heiden, M. G., Harris, M. H., Ramanathan, A., Gerszten, R. E., Wei, R., Fleming, M. D., Schreiber, S. L. and Cantley, L. C. (2008) 'The M2 splice isoform of pyruvate kinase is important for cancer metabolism and tumour growth.', *Nature*, 452(7184), pp. 230–3. doi: 10.1038/nature06734.

Cloonan, N., Brown, M. K., Steptoe, A. L., Wani, S., Chan, W. L., Forrest, A. R. R., Kolle, G., Gabrielli, B. and Grimmond, S. M. (2008) 'The miR-17-5p microRNA is a key regulator of the G1/S phase cell cycle transition.', *Genome Biology*, 9(8), p. R127. doi: 10.1186/gb-2008-9-8-r127.

Condic, M. L. (2014) 'Totipotency: What It Is and What It Is Not', *Stem cells and development*, 23(8), pp. 796–812. doi: 10.1089/scd.2013.0364.

Cook, G. A. and Lauer, C. M. (1968) *The Encyclopedia of Chemical Elements*. PediaPress.

Coulouarn, C., Factor, V. M., Andersen, J. B., Durkin, M. E. and Thorgeirsson, S. S. (2009) 'Loss of miR-122 expression in liver cancer correlates with suppression of the hepatic phenotype and gain of metastatic properties.', *Oncogene*. Nature Publishing Group, 28(40), pp. 3526–36. doi: 10.1038/onc.2009.211.

Covello, K. L., Kehler, J., Yu, H., Gordan, J. D., Arsham, A. M., Hu, C.-J., Labosky, P. a, Simon, M. C. and Keith, B. (2006) 'HIF-2alpha regulates Oct-4: effects of hypoxia on stem cell function, embryonic development, and tumor growth.', *Genes & development*, 20(5), pp. 557–70. doi: 10.1101/gad.1399906.

Cowan, C. a, Klimanskaya, I., McMahon, J., Atienza, J., Witmyer, J., Zucker, J. P., Wang, S., Morton, C. C., McMahon, A. P., Powers, D. and Melton, D. A. (2004) 'Derivation of

embryonic stem-cell lines from human blastocysts.', *The New England journal of medicine*, 350(13), pp. 1353–6. doi: 10.1056/NEJMsr040330.

Crosby, M. E., Kulshreshtha, R., Ivan, M. and Glazer, P. M. (2009) 'MicroRNA regulation of DNA repair gene expression in hypoxic stress.', *Cancer research*, 69(3), pp. 1221–9. doi: 10.1158/0008-5472.CAN-08-2516.

Csak, T., Bala, S., Lippai, D., Satishchandran, A., Catalano, D., Kodys, K. and Szabo, G. (2015) 'microRNA-122 regulates hypoxia-inducible factor-1 and vimentin in hepatocytes and correlates with fibrosis in diet-induced steatohepatitis', *Liver international : official journal of the International Association for the Study of the Liver*, 35(2), pp. 532–541. doi: 10.1111/liv.12633.microRNA-122.

Dalton, S. (2013) 'Signaling networks in human pluripotent stem cells', *Current Opinion in Cell Biology*, 25(2), pp. 241–246. doi: 10.1126/scisignal.2001449.Engineering.

Dani, C., Chambers, I., Johnstone, S., Robertson, M., Ebrahimi, B., Saito, M., Taga, T., Li, M., Burdon, T., Nichols, J. and Smith, A. (1998) 'Paracrine induction of stem cell renewal by LIF-deficient cells: a new ES cell regulatory pathway.', *Developmental biology*, 203(1), pp. 149–62. doi: 10.1006/dbio.1998.9026.

Davidson, K. C., Adams, A. M., Goodson, J. M., McDonald, C. E., Potter, J. C., Berndt, J. D., Biechele, T. L., Taylor, R. J. and Moon, R. T. (2012) 'Wnt/b-catenin signaling promotes differentiation, not self-renewal, of human embryonic stem cells and is repressed by Oct4', *Proceedings of the National Academy of Sciences*, 109(12), pp. 4485–4490. doi: 10.1073/pnas.1118777109.

Ding, S., Wu, T. Y. H., Brinker, A., Peters, E. C., Hur, W., Gray, N. S. and Schultz, P. G. (2003) 'Synthetic small molecules that control stem cell fate.', *Proceedings of the National Academy of Sciences of the United States of America*, 100(13), pp. 7632–7. doi: 10.1073/pnas.0732087100.

Doble, B. W. (2003) 'GSK-3: tricks of the trade for a multi-tasking kinase', *Journal of Cell Science*, 116(7), pp. 1175–1186. doi: 10.1242/jcs.00384.

Doble, B. W., Patel, S., Wood, G. A., Kockeritz, L. K. and Woodgett, J. R. (2007) 'Functional redundancy of GSK-3alpha and GSK-3beta in Wnt/beta-catenin signaling shown by using an allelic series of embryonic stem cell lines.', *Developmental cell*, 12(6), pp. 957–71. doi: 10.1016/j.devcel.2007.04.001.

Doddapaneni, R., Chawla, Y. K., Das, A., Kalra, J. K., Ghosh, S. and Chakraborti, A. (2013) 'Overexpression of microRNA-122 enhances in vitro hepatic differentiation of fetal liver-derived stem/progenitor cells.', *Journal of cellular biochemistry*, 114(7), pp. 1575–83. doi: 10.1002/jcb.24499.

Doench, J. G., Petersen, C. P. and Sharp, P. a (2003) 'siRNAs can function as miRNAs.', *Genes & development*, 17(4), pp. 438–42. doi: 10.1101/gad.1064703.

Dumoulin, J. C. M., Meijers, C. J. J., Bras, M., Coonen, E., Geraedts, J. P. M. and Evers, J. L. H. (1999) 'Effect of oxygen concentration on human in-vitro fertilization and embryo culture.', *Human reproduction (Oxford, England)*, 14(2), pp. 465–9.

Ebert, M. S. and Sharp, P. A. (2012) 'Roles for MicroRNAs in conferring robustness to biological processes', *Cell*. Elsevier Inc., 149(3), pp. 505–524. doi: 10.1016/j.cell.2012.04.005.

Eiselleova, L., Peterkova, I., Neradil, J., Slaninova, I., Hampl, A. and Dvorak, P. (2008) 'Comparative study of mouse and human feeder cells for human embryonic stem cells', *International Journal of Developmental Biology*, 52(4), pp. 353–363. doi: 10.1387/ijdb.082590le.

Ellerström, C., Strehl, R. and Moya, K. (2006) 'Derivation of a xeno-free human embryonic stem cell line', *Stem Cells*, 24(10), pp. 2170–2176.

Esau, C., Davis, S., Murray, S. F., Yu, X. X., Pandey, S. K., Pear, M., Watts, L., Booten,

S. L., Graham, M., McKay, R., Subramaniam, A., Propp, S., Lollo, B. a, Freier, S., Bennett, C. F., Bhanot, S. and Monia, B. P. (2006) 'miR-122 regulation of lipid metabolism revealed by in vivo antisense targeting.', *Cell metabolism*, 3(2), pp. 87–98. doi: 10.1016/j.cmet.2006.01.005.

Evans, M. J. and Kaufman, M. H. (1981) 'Establishment in culture of pluripotential cells from mouse embryos', *Nature*, 292 (58, pp. 154–156.

Ezashi, T., Das, P. and Roberts, R. M. (2005) 'Low O2 tensions and the prevention of differentiation of hES cells.', *Proceedings of the National Academy of Sciences of the United States of America*, 102(13), pp. 4783–8. doi: 10.1073/pnas.0501283102.

Faial, T., Bernardo, A. S., Mendjan, S., Diamanti, E., Ortmann, D., Gentsch, G. E., Mascetti, V. L., Trotter, M. W. B., Smith, J. C. and Pedersen, R. A. (2015) 'Brachyury and SMAD signalling collaboratively orchestrate distinct mesoderm and endoderm gene regulatory networks in differentiating human embryonic stem cells.', *Development*, 142(12), pp. 2121–35. doi: 10.1242/dev.117838.

Favaro, E., Ramachandran, A., McCormick, R., Gee, H., Blancher, C., Crosby, M., Devlin, C., Blick, C., Buffa, F., Li, J. L., Vojnovic, B., das Neves, R. P., Glazer, P., Iborra, F., Ivan, M., Ragoussis, J. and Harris, A. L. (2010) 'MicroRNA-210 regulates mitochondrial free radical response to hypoxia and krebs cycle in cancer cells by targeting iron sulfur cluster protein ISCU', *PLoS ONE*, 5(4). doi: 10.1371/journal.pone.0010345.

Filipczyk, A. A., Laslett, A. L., Mummery, C. L. and Pera, M. F. (2007) 'Differentiation is coupled to changes in the cell cycle regulatory apparatus of human embryonic stem cells', *Stem Cell Research*, 1(1), pp. 45–60. doi: 10.1016/j.scr.2007.09.002.

Fischer, B. and Bavister, B. D. (1993) 'Oxygen tension in the oviduct and uterus of rhesus monkeys, hamsters and rabbits.', *Journal of reproduction and fertility*, 99(2), pp. 673–679.

Foldager, C. B., Munir, S., Ulrik-Vinther, M., Søballe, K., Bünger, C. and Lind, M. (2009) 'Validation of suitable house keeping genes for hypoxia-cultured human chondrocytes.', *BMC molecular biology*, 10, p. 94. doi: 10.1186/1471-2199-10-94.

Folmes, C. D. L., Nelson, T. J., Martinez-Fernandez, A., Arrell, D. K., Lindor, J. Z., Dzeja, P. P., Ikeda, Y., Perez-Terzic, C. and Terzic, A. (2011) 'Somatic oxidative bioenergetics transitions into pluripotency-dependent glycolysis to facilitate nuclear reprogramming.', *Cell metabolism*, 14(2), pp. 264–71. doi: 10.1016/j.cmet.2011.06.011.

Forristal, C. E., Christensen, D. R., Chinnery, F. E., Petruzzelli, R., Parry, K. L., Sanchez-Elsner, T. and Houghton, F. D. (2013) 'Environmental oxygen tension regulates the energy metabolism and self-renewal of human embryonic stem cells.', *PloS one*, 8(5), p. e62507. doi: 10.1371/journal.pone.0062507.

Forristal, C. E., Wright, K. L., Hanley, N. a, Oreffo, R. O. C. and Houghton, F. D. (2010) 'Hypoxia inducible factors regulate pluripotency and proliferation in human embryonic stem cells cultured at reduced oxygen tensions.', *Reproduction (Cambridge, England)*, 139(1), pp. 85–97. doi: 10.1530/REP-09-0300.

Forsyth, N. R., Musio, A., Vezzoni, P., Simpson, A. H. R. W., Noble, B. S. and McWhir, J. (2006) 'Physiologic oxygen enhances human embryonic stem cell clonal recovery and reduces chromosomal abnormalities.', *Cloning and stem cells*, 8(1), pp. 16–23. doi: 10.1089/clo.2006.8.16.

Friedman, R. C., Farh, K. K.-H., Burge, C. B. and Bartel, D. P. (2009) 'Most mammalian mRNAs are conserved targets of microRNAs.', *Genome research*, 19(1), pp. 92–105. doi: 10.1101/gr.082701.108.

Fusaki, N., Ban, H., Nishiyama, A., Saeki, K. and Hasegawa, M. (2009) 'Efficient induction of transgene-free human pluripotent stem cells using a vector based on Sendai

virus, an RNA virus that does not integrate into the host genome.', *Proceedings of the Japan Academy. Series B, Physical and biological sciences*, 85(8), pp. 348–62. doi: 10.2183/pjab.85.348.

Gafni, O., Weinberger, L., Mansour, A. A., Manor, Y. S., Chomsky, E., Ben-Yosef, D., Kalma, Y., Viukov, S., Maza, I., Zviran, A., Rais, Y., Shipony, Z., Mukamel, Z., Krupalnik, V., Zerbib, M., Geula, S., Caspi, I., Schneir, D., Shwartz, T., Gilad, S., Amann-Zalcenstein, D., Benjamin, S., Amit, I., Tanay, A., Massarwa, R., Novershtern, N. and Hanna, J. H. (2013) 'Derivation of novel human ground state naive pluripotent stem cells.', *Nature*. Nature Publishing Group, 504(7479), pp. 282–6. doi: 10.1038/nature12745.

Gangaraju, V. K. and Lin, H. (2009) 'MicroRNAs: key regulators of stem cells.', *Nature reviews. Molecular cell biology*, 10(2), pp. 116–25. doi: 10.1038/nrm2621.

Garcia, D. M., Baek, D., Shin, C., Bell, G. W., Grimson, A. and Bartel, D. P. (2011) 'Weak seed-pairing stability and high target-site abundance decrease the proficiency of lsy-6 and other microRNAs.', *Nature structural & molecular biology*. Nature Publishing Group, a division of Macmillan Publishers Limited. All Rights Reserved., 18(10), pp. 1139–46. doi: 10.1038/nsmb.2115.

Ghosal, S., Saha, S., Das, S., Sen, R., Goswami, S., Jana, S. S. and Chakrabarti, J. (2016) 'miRepress: modelling gene expression regulation by microRNA with non-conventional binding sites.', *Scientific reports*. Nature Publishing Group, 6(February), p. 22334. doi: 10.1038/srep22334.

Goto, Y., Noda, Y., Mori, T. and Nakano, M. (1993) 'Increased generation of reactive oxygen species in embryos cultured in vitro', *Free Radical Biology and Medicine*, 15(1), pp. 69–75. doi: 10.1016/0891-5849(93)90126-F.

Greber, B., Wu, G., Bernemann, C., Joo, J. Y., Han, D. W., Ko, K., Tapia, N., Sabour, D., Sterneckert, J., Tesar, P. and Schöler, H. R. (2010) 'Conserved and Divergent Roles of FGF Signaling in Mouse Epiblast Stem Cells and Human Embryonic Stem Cells', *Cell Stem Cell*, 6(3), pp. 215–226. doi: 10.1016/j.stem.2010.01.003.

Greer, S. N., Metcalf, J. L., Wang, Y. and Ohh, M. (2012) 'The updated biology of hypoxia-inducible factor.', *The EMBO journal*. Nature Publishing Group, 31(11), pp. 2448–60. doi: 10.1038/emboj.2012.125.

Greve, T. S., Judson, R. L. and Blelloch, R. (2013) 'microRNA Control of Mouse and Human Pluripotent Stem Cell Behavior.', *Annual review of cell and developmental biology*. doi: 10.1146/annurev-cellbio-101512-122343.

Grimson, A., Farh, K. K.-H., Johnston, W. K., Garrett-Engele, P., Lim, L. P. and Bartel, D. P. (2007) 'MicroRNA targeting specificity in mammals: determinants beyond seed pairing.', *Molecular cell*, 27(1), pp. 91–105. doi: 10.1016/j.molcel.2007.06.017.

Gruber, A. J., Grandy, W. a, Balwierz, P. J., Dimitrova, Y. a, Pachkov, M., Ciaudo, C., van Nimwegen, E. and Zavolan, M. (2014) 'Embryonic stem cell-specific microRNAs contribute to pluripotency by inhibiting regulators of multiple differentiation pathways.', *Nucleic acids research*, pp. 1–14. doi: 10.1093/nar/gku544.

Gu, Y. Z., Moran, S. M., Hogenesch, J. B., Wartman, L. and Bradfield, C. A. (1998) 'Molecular characterization and chromosomal localization of a third alpha-class hypoxia inducible factor subunit, HIF3alpha.', *Gene expression*, 7(3), pp. 205–13.

Guérin, P., Mouatassim, S. El and Ménézo, Y. (2001) 'Oxidative stress and protection against reactive oxygen species in the pre-implantation embryo and its surroundings', *Human Reproduction*, 7(2), pp. 175–189.

Guo, C.-W., Kawakatsu, M., Idemitsu, M., Urata, Y., Goto, S., Ono, Y., Hamano, K. and Li, T.-S. (2013) 'Culture under low physiological oxygen conditions improves the stemness and quality of induced pluripotent stem cells.', *Journal of cellular physiology*,

228(11), pp. 2159–66. doi: 10.1002/jcp.24389.

Guo, G., Von Meyenn, F., Santos, F., Chen, Y., Reik, W., Bertone, P., Smith, A. and Nichols, J. (2016) 'Naive Pluripotent Stem Cells Derived Directly from Isolated Cells of the Human Inner Cell Mass', *Stem Cell Reports*. The Authors, 6(4), pp. 437–446. doi: 10.1016/j.stemcr.2016.02.005.

Guo, W.-T., Wang, X.-W. and Wang, Y. (2014) 'Micro-management of pluripotent stem cells.', *Protein & cell*. doi: 10.1007/s13238-013-0014-z.

Gupta, V. and Bamezai, R. N. K. (2010) 'Human pyruvate kinase M2: a multifunctional protein.', *Protein science : a publication of the Protein Society*, 19(11), pp. 2031–44. doi: 10.1002/pro.505.

Ha, M. and Kim, V. N. (2014) 'Regulation of microRNA biogenesis.', *Nature reviews. Molecular cell biology*. Nature Publishing Group, 15(8), pp. 509–524. doi: 10.1038/nrm3838.

Haeckel, E. (1868) *Natürliche Schöpfungsgeschichte*. Berlin: Georg Reimer.

Hanna, L. A., Foreman, R. K., Tarasenko, I. A., Kessler, D. S. and Labosky, P. A. (2002) 'Requirement for Foxd3 in maintaining pluripotent cells of the early mouse embryo.', *Genes & development*, 16(20), pp. 2650–61. doi: 10.1101/gad.1020502.

Harley, C. B. (1991) 'Telomere loss: mitotic clock or genetic time bomb?', *Mutation Research/DNAging*, 256(2–6), pp. 271–282. doi: 10.1016/0921-8734(91)90018-7.

Harley, C. B., Vaziri, H., Counter, C. M. and Allsopp, R. C. (1992) 'The telomere hypothesis of cellular aging.', *Experimental gerontology*, 27(4), pp. 375–82.

Harraz, M. M., Xu, J.-C., Guiberson, N., Dawson, T. M. and Dawson, V. L. (2014) 'MiR-223 regulates the differentiation of immature neurons', *Molecular and Cellular Therapies*, 2(1), p. 18. doi: 10.1186/2052-8426-2-18.

He, L. and Hannon, G. J. (2004) 'MicroRNAs: small RNAs with a big role in gene regulation.', *Nature reviews. Genetics*, 5(7), pp. 522–31. doi: 10.1038/nrg1379.

Henderson, J., Draper, J. and Baillie, H. (2002) 'Preimplantation human embryos and embryonic stem cells show comparable expression of stage-specific embryonic antigens', *Stem …*, (20), pp. 329–337.

Hewitson, L. C. and Leese, H. J. (1993) 'Energy metabolism of the trophectoderm and inner cell mass of the mouse blastocyst.', *The Journal of experimental zoology*, 267(3), pp. 337–43. doi: 10.1002/jez.1402670310.

Houbaviy, H. B., Dennis, L., Jaenisch, R. and Sharp, P. A. (2005) 'Characterization of a highly variable eutherian microRNA gene Characterization of a highly variable eutherian microRNA gene', *RNA*, 11(1), pp. 1245–1257. doi: 10.1261/rna.2890305.Ambros.

Houbaviy, H. B., Murray, M. F. and Sharp, P. a (2003) 'Embryonic Stem Cell-Specific MicroRNAs', *Developmental Cell*, 5(2), pp. 351–358. doi: 10.1016/S1534-5807(03)00227-2.

Houghton, F. D. (2006) 'Energy metabolism of the inner cell mass and trophectoderm of the mouse blastocyst.', *Differentiation; research in biological diversity*, 74(1), pp. 11–8. doi: 10.1111/j.1432-0436.2006.00052.x.

Houghton, F. D., Hawkhead, J. A., Humpherson, P. G., Hogg, J. E., Balen, A. H., Rutherford, A. J. and Leese, H. J. (2002) 'Non-invasive amino acid turnover predicts human embryo developmental capacity', 17(4), pp. 999–1005.

Hu, C., Wang, L., Chodosh, L. a, Keith, B. and Simon, M. C. (2003) 'Differential Roles of Hypoxia-Inducible Factor 1 alpha (HIF-1 alpha) and HIF-2 alpha in Hypoxic Gene Regulation.', *Molecular and Cellular Biology*, 23(24), pp. 9361–9374. doi: 10.1128/MCB.23.24.9361.

Huang, X., Ding, L., Bennewith, K. L., Tong, R. T., Welford, S. M., Ang, K. K., Story, M., Le, Q.-T. and Giaccia, A. J. (2009) 'Hypoxia-inducible mir-210 regulates normoxic gene expression involved in tumor initiation.', *Molecular cell*. Elsevier Ltd, 35(6), pp. 856–67. doi: 10.1016/j.molcel.2009.09.006.

Huang, X., Le, Q.-T. and Giaccia, A. J. (2010) 'MiR-210, micromanager of the hypoxia pathway', *Cell Trends in Molecular Medicine*, 16(5), pp. 230–237. doi: 10.1016/j.molmed.2010.03.004.MiR-210.

Huo, J. S. and Zambidis, E. T. (2013) 'Pivots of pluripotency: The roles of non-coding RNA in regulating embryonic and induced pluripotent stem cells', *Biochimica et Biophysica Acta - General Subjects*. Elsevier B.V., 1830(2), pp. 2385–2394. doi: 10.1016/j.bbagen.2012.10.014.

Hyslop, L., Stojkovic, M., Armstrong, L., Walter, T., Stojkovic, P., Przyborski, S., Herbert, M., Murdoch, A., Strachan, T. and Lako, M. (2005) 'Downregulation of NANOG induces differentiation of human embryonic stem cells to extraembryonic lineages.', *Stem cells (Dayton, Ohio)*, 23(8), pp. 1035–43. doi: 10.1634/stemcells.2005-0080.

Ilic, D., Stephenson, E., Wood, V., Jacquet, L., Stevenson, D., Petrova, A., Kadeva, N., Codognotto, S., Patel, H., Semple, M., Cornwell, G., Ogilvie, C. and Braude, P. (2012) 'Derivation and feeder-free propagation of human embryonic stem cells under xeno-free conditions.', *Cytotherapy*. Elsevier, 14(1), pp. 122–8. doi: 10.3109/14653249.2011.623692.

Itskovitz-Eldor, J., Schuldiner, M., Karsenti, D., Eden, A., Yanuka, O., Amit, M., Soreq, H. and Benvenisty, N. (2000) 'Differentiation of human embryonic stem cells into embryoid bodies compromising the three embryonic germ layers.', *Molecular medicine (Cambridge, Mass.)*, 6(2), pp. 88–95. doi: 10859025.

Ivan, M., Harris, A. L., Martelli, F. and Kulshreshtha, R. (2008) 'Hypoxia response and microRNAs: no longer two separate worlds.', *Journal of cellular and molecular medicine*, 12(5A), pp. 1426–31. doi: 10.1111/j.1582-4934.2008.00398.x.

Ivanova, N., Dobrin, R., Lu, R., Kotenko, I., Levorse, J., DeCoste, C., Schafer, X., Lun, Y. and Lemischka, I. R. (2006) 'Dissecting self-renewal in stem cells with RNA interference', *Nature*, 442(7102), pp. 533–538. doi: 10.1038/nature04915.

Iyer, N. V, Kotch, L. E., Agani, F., Leung, S. W., Laughner, E., Wenger, R. H., Gassmann, M., Gearhart, J. D., Lawler, A. M., Yu, A. Y. and Semenza, G. L. (1998) 'Cellular and developmental control of O2 homeostasis by hypoxia-inducible factor 1alpha', *Genes & Development*, 12(2), pp. 149–162. doi: 10.1101/gad.12.2.149.

Jaenisch, R. and Young, R. (2008) 'Stem cells, the molecular circuitry of pluripotency and nuclear reprogramming.', *Cell*, 132(4), pp. 567–82. doi: 10.1016/j.cell.2008.01.015.

Jang, Y.-Y. and Sharkis, S. J. (2007) 'A low level of reactive oxygen species selects for primitive hematopoietic stem cells that may reside in the low-oxygenic niche', *Blood Journal*, 110(8), pp. 3056–3064. doi: 10.1182/blood-2007-05-087759.An.

Jiang, B.-H., Zheng, J. Z., Leung, S. W., Roe, R. and Semenza, G. L. (1997) 'Transactivation and Inhibitory Domains of Hypoxia-inducible Factor 1 : Modulation of transcriptional activity by oxygen tension', *Journal of Biological Chemistry*, 272(31), pp. 19253–19260. doi: 10.1074/jbc.272.31.19253.

Jin, Y., Chen, Z., Liu, X. and Zhou, X. (2013) 'Evaluating the microRNA targeting sites by luciferase reporter gene assay.', *Methods in molecular biology (Clifton, N.J.)*. NIH Public Access, 936, pp. 117–27. doi: 10.1007/978-1-62703-083-0_10.

Johnnidis, J. B., Harris, M. H., Wheeler, R. T., Stehling-Sun, S., Lam, M. H., Kirak, O., Brummelkamp, T. R., Fleming, M. D. and Camargo, F. D. (2008) 'Regulation of progenitor cell proliferation and granulocyte function by microRNA-223', *Nature*. Nature Publishing Group, 451(7182), pp. 1125–1129. doi: 10.1038/nature06607.

Jones-Rhoades, M. W., Bartel, D. P. and Bartel, B. (2006) 'MicroRNAS and their regulatory roles in plants.', *Annual review of plant biology*, 57, pp. 19–53. doi: 10.1146/annurev.arplant.57.032905.105218.

Jopling, C. L., Schütz, S. and Sarnow, P. (2008) 'Position-dependent function for a tandem microRNA miR-122-binding site located in the hepatitis C virus RNA genome.', *Cell host & microbe*, 4(1), pp. 77–85. doi: 10.1016/j.chom.2008.05.013.

Jørgensen, N., Rajpert-De Meyts, E., Graem, N., Müller, J., Giwercman, A. and Skakkebaek, N. E. (1995) 'Expression of immunohistochemical markers for testicular carcinoma in situ by normal human fetal germ cells.', *Laboratory investigation; a journal of technical methods and pathology*, 72(2), pp. 223–31.

Josephson, R., Ording, C. J., Liu, Y., Shin, S., Lakshmipathy, U., Toumadje, A., Love, B., Chesnut, J. D., Andrews, P. W., Rao, M. S. and Auerbach, J. M. (2007) 'Qualification of embryonal carcinoma 2102Ep as a reference for human embryonic stem cell research.', *Stem cells*, 25(2), pp. 437–446. doi: 10.1634/stemcells.2006-0236.

Jouneau, A., Ciaudo, C., Sismeiro, O., Brochard, V., Jouneau, L., Vandormael-Pournin, S., Coppée, J.-Y., Zhou, Q., Heard, E., Antoniewski, C. and Cohen-Tannoudji, M. (2012) 'Naive and primed murine pluripotent stem cells have distinct miRNA expression profiles.', *RNA (New York, N.Y.)*, 18(2), pp. 253–64. doi: 10.1261/rna.028878.111.

Judson, R. L., Babiarz, J. E., Venere, M. and Blelloch, R. (2009) 'Embryonic stem cell-specific microRNAs promote induced pluripotency.', *Nature biotechnology*, 27(5), pp. 459–61. doi: 10.1038/nbt.1535.

Jung, C. J., Iyengar, S., Blahnik, K. R., Ajuha, T. P., Jiang, J. X., Farnham, P. J. and Zern, M. (2011) 'Epigenetic modulation of miR-122 facilitates human embryonic stem cell self-renewal and hepatocellular carcinoma proliferation.', *PloS one*, 6(11), p. e27740. doi: 10.1371/journal.pone.0027740.

Kallio, P. J., Okamoto, K., O'Brien, S., Carrero, P., Makino, Y., Tanaka, H. and Poellinger, L. (1998) 'Signal transduction in hypoxic cells: inducible nuclear translocation and recruitment of the CBP/p300 coactivator by the hypoxia-inducible factor-1alpha.', *The EMBO journal*, 17(22), pp. 6573–86. doi: 10.1093/emboj/17.22.6573.

Kapinas, K., Grandy, R., Ghule, P., Medina, R., Becker, K., Pardee, A., Zaidi, S. K., Lian, J., Stein, J., van Wijnen, A. and Stein, G. S. (2013) 'The abbreviated pluripotent cell cycle', *Journal of Cellular Physiology*, 228(1), pp. 9–20. doi: 10.1002/jcp.24104.

Kasterstein, E., Strassburger, D., Komarovsky, D., Bern, O., Komsky, A., Raziel, A., Friedler, S. and Ron-El, R. (2013) 'The effect of two distinct levels of oxygen concentration on embryo development in a sibling oocyte study.', *Journal of assisted reproduction and genetics*. Springer, 30(8), pp. 1073–1079. doi: 10.1007/s10815-013-0032-z.

Keller, G. M. (1995) 'In vitro differentiation of embryonic stem cells', *Current Opinion in Cell Biology*. Elsevier Current Trends, 7(6), pp. 862–869. doi: 10.1016/0955-0674(95)80071-9.

Kelly, T. J., Souza, A. L., Clish, C. B. and Puigserver, P. (2011) 'A Hypoxia-Induced Positive Feedback Loop Promotes Hypoxia-Inducible Factor 1α Stability through miR-210 Suppression of Glycerol-3-Phosphate Dehydrogenase 1-Like', *Mol Cell Biol*, 31(13), pp. 2696–2706. doi: 10.1128/MCB.01242-10.

Kertesz, M., Iovino, N., Unnerstall, U., Gaul, U. and Segal, E. (2007) 'The role of site accessibility in microRNA target recognition.', *Nature genetics*, 39(10), pp. 1278–84. doi: 10.1038/ng2135.

Kiezun, A., Artzi, S., Modai, S., Volk, N., Isakov, O. and Shomron, N. (2012) 'miRviewer: a multispecies microRNA homologous viewer', *BMC Research Notes*, 5(1), p. 92. doi: 10.1186/1756-0500-5-92.

Kim, J. B., Sebastiano, V., Wu, G., Araúzo-Bravo, M. J., Sasse, P., Gentile, L., Ko, K., Ruau, D., Ehrich, M., van den Boom, D., Meyer, J., Hübner, K., Bernemann, C., Ortmeier, C., Zenke, M., Fleischmann, B. K., Zaehres, H. and Schöler, H. R. (2009) 'Oct4-induced pluripotency in adult neural stem cells.', *Cell*, 136(3), pp. 411–9. doi: 10.1016/j.cell.2009.01.023.

Kim, J. B., Zaehres, H., Wu, G., Gentile, L., Ko, K., Sebastiano, V., Araúzo-Bravo, M. J., Ruau, D., Han, D. W., Zenke, M. and Schöler, H. R. (2008) 'Pluripotent stem cells induced from adult neural stem cells by reprogramming with two factors.', *Nature*, 454(7204), pp. 646–50. doi: 10.1038/nature07061.

Kim, J. W., Tchernyshyov, I., Semenza, G. L. and Dang, C. V. (2006) 'HIF-1-mediated expression of pyruvate dehydrogenase kinase: A metabolic switch required for cellular adaptation to hypoxia', *Cell Metabolism*, 3(3), pp. 177–185. doi: 10.1016/j.cmet.2006.02.002.

Kleinman, H. K. and Martin, G. R. (2005) 'Matrigel: Basement membrane matrix with biological activity', *Seminars in Cancer Biology*, 15(5), pp. 378–386. doi: 10.1016/j.semcancer.2005.05.004.

Klemm, J. D. and Pabo, C. O. (1996) 'Oct-1 POU domain-DNA interactions: cooperative binding of isolated subdomains and effects of covalent linkage.', *Genes & Development*, 10(1), pp. 27–36. doi: 10.1101/gad.10.1.27.

Kozomara, A. and Griffiths-Jones, S. (2014) 'miRBase: annotating high confidence microRNAs using deep sequencing data.', *Nucleic acids research*, 42(1), pp. D68-73. doi: 10.1093/nar/gkt1181.

Krek, A., Grün, D., Poy, M. N., Wolf, R., Rosenberg, L., Epstein, E. J., MacMenamin, P., da Piedade, I., Gunsalus, K. C., Stoffel, M. and Rajewsky, N. (2005) 'Combinatorial microRNA target predictions.', *Nature genetics*, 37(5), pp. 495–500. doi: 10.1038/ng1536.

Kulshreshtha, R., Davuluri, R., Calin, G. A. and Ivan, M. (2008) 'A microRNA component of the hypoxic response.', *Cell death and differentiation*, 15(4), pp. 667–71. doi: 10.1038/sj.cdd.4402310.

Kulshreshtha, R., Ferracin, M., Wojcik, S. E., Garzon, R., Alder, H., Agosto-Perez, F. J., Davuluri, R., Liu, C.-G., Croce, C. M., Negrini, M., Calin, G. a and Ivan, M. (2007) 'A microRNA signature of hypoxia.', *Molecular and cellular biology*, 27(5), pp. 1859–67. doi: 10.1128/MCB.01395-06.

Kunarso, G., Chia, N.-Y., Jeyakani, J., Hwang, C., Lu, X., Chan, Y.-S., Ng, H.-H. and Bourque, G. (2010) 'Transposable elements have rewired the core regulatory network of human embryonic stem cells', *Nat. Genet.*, 42(7), pp. 631–634. doi: 10.1038/ng.600.

Kuroda, T., Tada, M., Kubota, H., Hatano, S., Suemori, H., Nakatsuji, N., Kimura, H. and Tada, T. (2005) 'Octamer and Sox Elements Are Required for Transcriptional cis Regulation of Nanog Gene Expression', *Mol. Cell. Biol.*, 25(6), pp. 2475–2485. doi: 10.1128/MCB.25.6.2475.

Lagos-Quintana, M., Rauhut, R., Lendeckel, W. and Tuschl, T. (2001) 'Identification of novel genes coding for small expressed RNAs.', *Science (New York, N.Y.)*, 294(5543), pp. 853–8. doi: 10.1126/science.1064921.

Lai, E. C., Tam, B. and Rubin, G. M. (2005) 'Pervasive regulation of Drosophila Notch target genes by GY-box-, Brd-box-, and K-box-class microRNAs', *Genes and Development*, 19(9), pp. 1067–1080. doi: 10.1101/gad.1291905.

Lakshmipathy, U., Davila, J. and Hart, R. P. (2011) 'MicroRNA in pluripotent stem cells', *Regenerative Medicine*, 5(4), pp. 545–555. doi: 10.2217/rme.10.34.MicroRNA.

Lamprecht, M. R., Sabatini, D. M. and Carpenter, A. E. (2007) 'CellProfiler TM: free, versatile software for automated biological image analysis', *BioTechniques*, 42(1), pp.

71–75. doi: 10.2144/000112257.

Landgraf, P., Rusu, M., Sheridan, R., Sewer, A., Iovino, N., Aravin, A., Pfeffer, S., Rice, A., Kamphorst, A. O., Landthaler, M., Lin, C., Socci, N. D., Hermida, L., Fulci, V., Chiaretti, S., Foà, R., Schliwka, J., Fuchs, U., Novosel, A., Müller, R.-U., Schermer, B., Bissels, U., Inman, J., Phan, Q., Chien, M., Weir, D. B., Choksi, R., De Vita, G., Frezzetti, D., Trompeter, H.-I., Hornung, V., Teng, G., Hartmann, G., Palkovits, M., Di Lauro, R., Wernet, P., Macino, G., Rogler, C. E., Nagle, J. W., Ju, J., Papavasiliou, F. N., Benzing, T., Lichter, P., Tam, W., Brownstein, M. J., Bosio, A., Borkhardt, A., Russo, J. J., Sander, C., Zavolan, M. and Tuschl, T. (2007) 'A mammalian microRNA expression atlas based on small RNA library sequencing.', *Cell*, 129(7), pp. 1401–14. doi: 10.1016/j.cell.2007.04.040.

Lando, D., Peet, D. J., Gorman, J. J., Whelan, D. A., Whitelaw, M. L. and Bruick, R. K. (2002) 'FIH-1 is an asparaginyl hydroxylase enzyme that regulates the transcriptional activity of hypoxia-inducible factor', *Genes and Development*, 16(12), pp. 1466–1471. doi: 10.1101/gad.991402.

Lannon, C., Moody, J., King, D., Thomas, T., Eaves, A. and Miller, C. (2008) 'A defined, feeder-independent medium for human embryonic stem cell culture', *Cell Research*, 18(August), pp. S34–S34. doi: 10.1038/cr.2008.124.

Laurent, L. C., Chen, J., Ulitsky, I., Mueller, F.-J., Lu, C., Shamir, R., Fan, J.-B. and Loring, J. F. (2008) 'Comprehensive microRNA profiling reveals a unique human embryonic stem cell signature dominated by a single seed sequence.', *Stem cells (Dayton, Ohio)*, 26(6), pp. 1506–16. doi: 10.1634/stemcells.2007-1081.

Lee, E. J., Baek, M., Gusev, Y., Brackett, D. J., Nuovo, G. J. and Schmittgen, T. D. (2008) 'Systematic evaluation of microRNA processing patterns in tissues, cell lines, and tumors.', *RNA (New York, N.Y.)*, 14(1), pp. 35–42. doi: 10.1261/rna.804508.

Lee, J., Kim, H. K., Han, Y.-M. and Kim, J. (2008) 'Pyruvate kinase isozyme type M2 (PKM2) interacts and cooperates with Oct-4 in regulating transcription.', *The international journal of biochemistry & cell biology*, 40(5), pp. 1043–54. doi: 10.1016/j.biocel.2007.11.009.

Lee, M., Kim, Y., Ryu, J. H., Kim, K., Han, Y. M. and Lee, H. (2016) 'Long-term, feeder-free maintenance of human embryonic stem cells by mussel-inspired adhesive heparin and collagen type I', *Acta Biomaterialia*, 32(August), pp. 138–148. doi: 10.1016/j.actbio.2016.01.008.

Lee, R. C., Feinbaum, R. L. and Ambros, V. (1993) 'The C. elegans heterochronic gene lin-4 encodes small RNAs with antisense complementarity to lin-14', *Cell*, 75(5), pp. 843–854. doi: 10.1016/0092-8674(93)90529-Y.

Lee, Y. J., Ramakrishna, S., Chauhan, H., Park, W. S., Hong, S.-H. and Kim, K.-S. (2016) 'Dissecting microRNA-mediated regulation of stemness, reprogramming, and pluripotency', *Cell Regeneration*. Cell Regeneration, 5(1), p. 2. doi: 10.1186/s13619-016-0028-0.

Lengner, C. J., Gimelbrant, A. A., Erwin, J. a, Cheng, A. W., Guenther, M. G., Welstead, G. G., Alagappan, R., Frampton, G. M., Xu, P., Muffat, J., Santagata, S., Powers, D., Barrett, C. B., Young, R. a, Lee, J. T., Jaenisch, R. and Mitalipova, M. (2010) 'Derivation of pre-X inactivation human embryonic stem cells under physiological oxygen concentrations.', *Cell*. Elsevier Ltd, 141(5), pp. 872–83. doi: 10.1016/j.cell.2010.04.010.

Lewis, B. P., Burge, C. B. and Bartel, D. P. (2005) 'Conserved seed pairing, often flanked by adenosines, indicates that thousands of human genes are microRNA targets.', *Cell*, 120(1), pp. 15–20. doi: 10.1016/j.cell.2004.12.035.

Lewis, B. P., Shih, I., Jones-Rhoades, M. W., Bartel, D. P. and Burge, C. B. (2003) 'Prediction of mammalian microRNA targets.', *Cell*, 115(7), pp. 787–98. doi: 10.1016/S0092-8674(03)01018-3.

Li, M. A. and He, L. (2012) 'microRNAs as novel regulators of stem cell pluripotency and somatic cell reprogramming.', *BioEssays : news and reviews in molecular, cellular and developmental biology*, 34(8), pp. 670–80. doi: 10.1002/bies.201200019.

Li, Q. F., Wang, X. R., Yang, Y. W. and Lin, H. (2006) 'Hypoxia upregulates hypoxia inducible factor (HIF)-3alpha expression in lung epithelial cells: characterization and comparison with HIF-1alpha.', *Cell research*, 16(6), pp. 548–58. doi: 10.1038/sj.cr.7310072.

Lichner, Z., Páll, E., Kerekes, A., Pállinger, E., Maraghechi, P., Bosze, Z. and Gócza, E. (2011) 'The miR-290-295 cluster promotes pluripotency maintenance by regulating cell cycle phase distribution in mouse embryonic stem cells.', *Differentiation; research in biological diversity*, 81(1), pp. 11–24. doi: 10.1016/j.diff.2010.08.002.

Lim, L. P., Lau, N. C., Garrett-Engele, P., Grimson, A., Schelter, J. M., Castle, J., Bartel, D. P., Linsley, P. S. and Johnson, J. M. (2005) 'Microarray analysis shows that some microRNAs downregulate large numbers of target mRNAs.', *Nature*, 433(7027), pp. 769–73. doi: 10.1038/nature03315.

Lin, C.-C., Liu, L.-Z., Addison, J. B., Wonderlin, W. F., Ivanov, A. V and Ruppert, J. M. (2011) 'A KLF4-miRNA-206 Autoregulatory Feedback Loop Can Promote or Inhibit Protein Translation Depending upon Cell Context', *Molecular and cellular biology*. American Society for Microbiology (ASM), 31(12), pp. 2513–27. doi: 10.1128/MCB.01189-10.

Lin, S.-L., Chang, D. C., Lin, C.-H., Ying, S.-Y., Leu, D. and Wu, D. T. S. (2011) 'Regulation of somatic cell reprogramming through inducible mir-302 expression', *Nucleic Acids Research*, 39(3), pp. 1054–1065. doi: 10.1093/nar/gkq850.

Liu, A. M., Xu, Z., Shek, F. H., Wong, K.-F., Lee, N. P., Poon, R. T., Chen, J. and Luk, J. M. (2014) 'miR-122 Targets Pyruvate Kinase M2 and Affects Metabolism of Hepatocellular Carcinoma.', *PloS one*, 9(1), p. e86872. doi: 10.1371/journal.pone.0086872.

Liu, S., Liu, H., Pan, Y., Tang, S., Xiong, J., Hui, N., Wang, S., Qi, Z. and Li, L. (2004) 'Human embryonic germ cells isolation from early stages of post-implantation embryos', *Cell and Tissue Research*. Springer-Verlag, 318(3), pp. 525–531. doi: 10.1007/s00441-004-0990-7.

Livak, K. J. and Schmittgen, T. D. (2001) 'Analysis of relative gene expression data using real-time quantitative PCR and the 2(-Delta Delta C(T)) Method.', *Methods San Diego Calif*. Elsevier, 25(4), pp. 402–408.

Loeb, G. B., Khan, A. A., Canner, D., Hiatt, J. B., Shendure, J., Darnell, R. B., Leslie, C. S. and Rudensky, A. Y. (2012) 'Transcriptome-wide miR-155 Binding Map Reveals Widespread Noncanonical MicroRNA Targeting', *Molecular Cell*. Elsevier Inc., 48(5), pp. 760–770. doi: 10.1016/j.molcel.2012.10.002.

Loh, K. M. and Lim, B. (2011) 'A precarious balance: pluripotency factors as lineage specifiers.', *Cell stem cell*. Elsevier Inc., 8(4), pp. 363–9. doi: 10.1016/j.stem.2011.03.013.

Loh, Y.-H., Wu, Q., Chew, J.-L., Vega, V. B., Zhang, W., Chen, X., Bourque, G., George, J., Leong, B., Liu, J., Wong, K.-Y., Sung, K. W., Lee, C. W. H., Zhao, X.-D., Chiu, K.-P., Lipovich, L., Kuznetsov, V. a, Robson, P., Stanton, L. W., Wei, C.-L., Ruan, Y., Lim, B. and Ng, H.-H. (2006) 'The Oct4 and Nanog transcription network regulates pluripotency in mouse embryonic stem cells.', *Nature genetics*, 38(4), pp. 431–40. doi: 10.1038/ng1760.

Long, D., Lee, R. C., Williams, P., Chan, C. Y., Ambros, V. and Ding, Y. (2007) 'Potent effect of target structure on microRNA function.', *Nature structural & molecular biology*, 14(4), pp. 287–94. doi: 10.1038/nsmb1226.

Loscalzo, J. (2010) ‘The cellular response to hypoxia : tuning the system with microRNAs’, *Journal of Clinical Investigation*, 120(11), pp. 3815–3817. doi: 10.1172/JCI45105.translation.

Louafi, F., Martinez-Nunez, R. T. and Sanchez-Elsner, T. (2010) ‘MicroRNA-155 targets SMAD2 and modulates the response of macrophages to transforming growth factor-{beta}.’, *The Journal of biological chemistry*, 285(53), pp. 41328–36. doi: 10.1074/jbc.M110.146852.

Lu, H., Buchan, R. J. and Cook, S. a (2010) ‘MicroRNA-223 regulates Glut4 expression and cardiomyocyte glucose metabolism.’, *Cardiovascular research*, 86(3), pp. 410–20. doi: 10.1093/cvr/cvq010.

Ludwig, T. E., Bergendahl, V., Levenstein, M. E., Yu, J., Probasco, M. D. and Thomson, J. A. (2006) ‘Feeder-independent culture of human embryonic stem cells’, *Nature Methods*, 3(August 2016), pp. 637–646. doi: 10.1038/nmeth902.

Ludwig, T. E., Levenstein, M. E., Jones, J. M., Berggren, W. T., Mitchen, E. R., Frane, J. L., Crandall, L. J., Daigh, C. a, Conard, K. R., Piekarczyk, M. S., Llanas, R. a and Thomson, J. a (2006) ‘Derivation of human embryonic stem cells in defined conditions.’, *Nature biotechnology*, 24(2), pp. 185–7. doi: 10.1038/nbt1177.

Ludwig, T. E. and Thomson, J. A. (2007) ‘Defined, feeder-independent medium for human embryonic stem cell culture.’, *Current protocols in stem cell biology*, Chapter 1, p. Unit 1C.2. doi: 10.1002/9780470151808.sc01c02s2.

Lundberg, E., Fagerberg, L., Klevebring, D., Matic, I., Geiger, T., Cox, J., Älgenäs, C., Lundeberg, J., Mann, M. and Uhlen, M. (2010) ‘Defining the transcriptome and proteome in three functionally different human cell lines’, *Molecular Systems Biology*. EMBO Press, 6(1), pp. 25–29. doi: 10.1038/msb.2010.106.

Lüningschrör, P., Hauser, S., Kaltschmidt, B. and Kaltschmidt, C. (2013) ‘MicroRNAs in pluripotency, reprogramming and cell fate induction.’, *Biochimica et biophysica acta*. Elsevier B.V., 1833(8), pp. 1894–903. doi: 10.1016/j.bbamcr.2013.03.025.

MacArthur, B. D., Sevilla, A., Lenz, M., Müller, F.-J., Schuldt, B. M., Schuppert, A. a, Ridden, S. J., Stumpf, P. S., Fidalgo, M., Ma’ayan, A., Wang, J. and Lemischka, I. R. (2012) ‘Nanog-dependent feedback loops regulate murine embryonic stem cell heterogeneity.’, *Nature cell biology*. Nature Publishing Group, 14(11), pp. 1139–47. doi: 10.1038/ncb2603.

Maherali, N., Sridharan, R., Xie, W., Utikal, J., Eminli, S., Arnold, K., Stadtfeld, M., Yachechko, R., Tchieu, J., Jaenisch, R., Plath, K. and Hochedlinger, K. (2007) ‘Directly reprogrammed fibroblasts show global epigenetic remodeling and widespread tissue contribution.’, *Cell stem cell*, 1(1), pp. 55–70. doi: 10.1016/j.stem.2007.05.014.

Mahon, P. C., Hirota, K. and Semenza, G. L. (2001) ‘FIH-1: A novel protein that interacts with HIF-1α and VHL to mediate repression of HIF-1 transcriptional activity’, *Genes and Development*, 15(20), pp. 2675–2686. doi: 10.1101/gad.924501.

Makino, Y., Cao, R., Svensson, K. and Bertilsson, G. (2001) ‘Inhibitory PAS domain protein is a negative regulator of hypoxia-inducible gene expression’, *Nature*, 414(November), pp. 550–554.

Makino, Y., Kanopka, A., Wilson, W. J., Tanaka, H. and Poellinger, L. (2002) ‘Inhibitory PAS domain protein (IPAS) is a hypoxia-inducible splicing variant of the hypoxia-inducible factor-3alpha locus.’, *The Journal of biological chemistry*, 277(36), pp. 32405–8. doi: 10.1074/jbc.C200328200.

Marson, A., Levine, S. S., Cole, M. F., Frampton, G. M., Brambrink, T., Johnstone, S. E., Guenther, M. G., Johnston, W. K., Wernig, M., Newman, J., Calabrese, J. M., Dennis, L. M., Volkert, T. L., Gupta, S., Love, J., Hannett, N., Sharp, P. a, Bartel, D. P., Jaenisch, R. and Young, R. a (2008) ‘Connecting microRNA genes to the core transcriptional

regulatory circuitry of embryonic stem cells.', *Cell*, 134(3), pp. 521–33. doi: 10.1016/j.cell.2008.07.020.

Martin, G. R. (1981) 'Isolation of a pluripotent cell line from early mouse embryos cultured in medium conditioned by teratocarcinoma stem cells', *Proceedings of the National Academy of …*, 78(12), pp. 7634–7638.

Martin, H. C., Wani, S., Steptoe, A. L., Krishnan, K., Nones, K., Nourbakhsh, E., Vlassov, A., Grimmond, S. M. and Cloonan, N. (2014) 'Imperfect centered miRNA binding sites are common and can mediate repression of target mRNAs.', *Genome biology*, 15(3), p. R51. doi: 10.1186/gb-2014-15-3-r51.

Martinez-Nunez, R. T., Bondanese, V. P., Louafi, F., Francisco-Garcia, A. S., Rupani, H., Bedke, N., Holgate, S., Howarth, P. H., Davies, D. E. and Sanchez-Elsner, T. (2014) 'A microRNA network dysregulated in asthma controls IL-6 production in bronchial epithelial cells.', *PloS one*, 9(10), p. e111659. doi: 10.1371/journal.pone.0111659.

Martinez-Nunez, R. T., Louafi, F., Friedmann, P. S. and Sanchez-Elsner, T. (2009) 'MicroRNA-155 modulates the pathogen binding ability of dendritic cells (DCs) by down-regulation of DC-specific intercellular adhesion molecule-3 grabbing non-integrin (DC-SIGN).', *The Journal of biological chemistry*, 284(24), pp. 16334–42. doi: 10.1074/jbc.M109.011601.

Martinez, N. J. and Gregory, R. I. (2010) 'MicroRNA gene regulatory pathways in the establishment and maintenance of ESC identity.', *Cell stem cell*. Elsevier Inc., 7(1), pp. 31–5. doi: 10.1016/j.stem.2010.06.011.

Mathieu, J., Zhang, Z., Zhou, W., Wang, A. J., Heddleston, J. M., Pinna, C. M. a, Hubaud, A., Stadler, B., Choi, M., Bar, M., Tewari, M., Liu, A., Vessella, R., Rostomily, R., Born, D., Horwitz, M., Ware, C., Blau, C. A., Cleary, M. a, Rich, J. N. and Ruohola-Baker, H. (2011) 'HIF Induces Human Embryonic Stem Cell Markers in Cancer Cells', *Cancer research*, 71(13), pp. 4640–52. doi: 10.1158/0008-5472.CAN-10-3320.

Matsui, Y., Toksoz, D., Nishikawa, S., Nishikawa, S.-I., Williams, D., Zsebo, K. and Hogan, B. L. M. (1991) 'Effect of Steel factor and leukaemia inhibitory factor on murine primordial germ cells in culture', *Nature*. Nature Publishing Group, 353(6346), pp. 750–752. doi: 10.1038/353750a0.

Melton, C. and Blelloch, R. (2010) 'Microrna regulation of embryonic stem cell self-renewal and differentiation', *Advances in Experimental Medicine and Biology*, 695, pp. 105–117. doi: 10.1007/978-1-4419-7037-4_8.

Melton, C., Judson, R. L. and Blelloch, R. (2010) 'Opposing microRNA families regulate self-renewal in mouse embryonic stem cells.', *Nature*. Macmillan Publishers Limited. All rights reserved, 463(7281), pp. 621–6. doi: 10.1038/nature08725.

Miranda, K. C., Huynh, T., Tay, Y., Ang, Y.-S., Tam, W.-L., Thomson, A. M., Lim, B. and Rigoutsos, I. (2006) 'A pattern-based method for the identification of MicroRNA binding sites and their corresponding heteroduplexes.', *Cell*, 126(6), pp. 1203–17. doi: 10.1016/j.cell.2006.07.031.

Mitalipov, S. and Wolf, D. (2009) 'Totipotency, pluripotency and nuclear reprogramming.', *Advances in biochemical engineering/biotechnology*, 114, pp. 185–99. doi: 10.1007/10_2008_45.

Mitchell, J. A. and Yochim, J. M. (1968) 'Measurement of Intrauterine Oxygen Tension in the Rat and Its Regulation by Ovarian Steroid Hormones', *Endocrinology*. The Endocrine Society, 80(2).

Mitsui, K., Tokuzawa, Y., Itoh, H., Segawa, K., Murakami, M., Takahashi, K., Maruyama, M., Maeda, M. and Yamanaka, S. (2003) 'The homeoprotein Nanog is required for maintenance of pluripotency in mouse epiblast and ES cells.', *Cell*, 113(5), pp. 631–42.

Miyazaki, T., Futaki, S., Hasegawa, K., Kawasaki, M., Sanzen, N., Hayashi, M., Kawase,

E., Sekiguchi, K., Nakatsuji, N. and Suemori, H. (2008) 'Recombinant human laminin isoforms can support the undifferentiated growth of human embryonic stem cells', *Biochemical and Biophysical Research Communications*, 375(1), pp. 27–32. doi: 10.1016/j.bbrc.2008.07.111.

Miyoshi, N., Ishii, H., Nagano, H., Haraguchi, N., Dewi, D. L., Kano, Y., Nishikawa, S., Tanemura, M., Mimori, K., Tanaka, F., Saito, T., Nishimura, J., Takemasa, I., Mizushima, T., Ikeda, M., Yamamoto, H., Sekimoto, M., Doki, Y. and Mori, M. (2011) 'Reprogramming of mouse and human cells to pluripotency using mature microRNAs.', *Cell stem cell*. Elsevier Inc., 8(6), pp. 633–8. doi: 10.1016/j.stem.2011.05.001.

Mohyeldin, A., Garzón-Muvdi, T. and Quiñones-Hinojosa, A. (2010) 'Oxygen in stem cell biology: a critical component of the stem cell niche.', *Cell stem cell*, 7(2), pp. 150–61. doi: 10.1016/j.stem.2010.07.007.

Mourelatos, Z. (2008) 'Small RNAs: The seeds of silence', *Nature*. Nature Publishing Group, 455(7209), pp. 44–45. doi: 10.1038/455044a.

Mourelatos, Z., Dostie, J., Paushkin, S., Sharma, A., Charroux, B., Abel, L., Rappsilber, J., Mann, M. and Dreyfuss, G. (2002) 'miRNPs: a novel class of ribonucleoproteins containing numerous microRNAs.', *Genes & development*, 16(6), pp. 720–8. doi: 10.1101/gad.974702.

Murry, C. E. and Keller, G. M. (2008) 'Differentiation of Embryonic Stem Cells to Clinically Relevant Populations: Lessons from Embryonic Development', *Cell*, 132(4), pp. 661–680. doi: 10.1016/j.cell.2008.02.008.

Nallamshetty, S., Chan, S. Y. and Loscalzo, J. (2013) 'Hypoxia: a master regulator of microRNA biogenesis and activity.', *Free radical biology & medicine*. Elsevier, 64, pp. 20–30. doi: 10.1016/j.freeradbiomed.2013.05.022.

Neganova, I., Zhang, X., Atkinson, S. P. and Lako, M. (2008) 'Expression and functional analysis of G1 to S regulatory components reveals an important role for CDK2 in cell cycle regulation in human embryonic stem cells.', *Oncogene*, 28(10), pp. 1–11. doi: 10.1038/onc.2008.358.

Nelson, D. L. and Cox, M. M. (2000) *Lehninger Principles of Biochemistry, Third Edition*.

Nichols, J. and Smith, A. (2009a) 'Naive and primed pluripotent states.', *Cell stem cell*. Elsevier Inc., 4(6), pp. 487–92. doi: 10.1016/j.stem.2009.05.015.

Nichols, J. and Smith, A. (2009b) 'Naive and primed pluripotent states.', *Cell stem cell*. Elsevier Inc., 4(6), pp. 487–92. doi: 10.1016/j.stem.2009.05.015.

Nichols, J. and Smith, A. (2011) 'The origin and identity of embryonic stem cells.', *Development (Cambridge, England)*, 138(1), pp. 3–8. doi: 10.1242/dev.050831.

Nichols, J., Zevnik, B., Anastassiadis, K., Niwa, H., Klewe-Nebenius, D., Chambers, I., Schöler, H. R. and Smith, A. (1998) 'Formation of pluripotent stem cells in the mammalian embryo depends on the POU transcription factor Oct4.', *Cell*, 95(3), pp. 379–91.

Niwa, H., Burdon, T., Chambers, I. and Smith, A. (1998) 'Self-renewal of pluripotent embryonic stem cells is mediated via activation of STAT3.', *Genes & development*, 12(13), pp. 2048–60.

Niwa, H., Miyazaki, J. and Smith, A. (2000) 'Quantitative expression of Oct-3/4 defines differentiation, dedifferentiation or self-renewal of ES cells.', *Nature genetics*, 24(4), pp. 372–6. doi: 10.1038/74199.

Noguchi, T., Inoue, H. and Tanaka, T. (1986) 'The M1- and M2-type isozymes of rat pyruvate kinase are produced from the same gene by alternative RNA splicing.', *The Journal of biological chemistry*, 261(29), pp. 13807–12.

Obernosterer, G., Leuschner, P. J. F., Alenius, M. and Martinez, J. (2006) 'Post-

transcriptional regulation of microRNA expression', *Cold Spring Harbor Laboratory Press*, (Pillai 2005), pp. 1161–1167. doi: 10.1261/rna.2322506.Bentwich.

Ohanian, M., Humphreys, D. T., Anderson, E., Preiss, T. and Fatkin, D. (2013) 'A heterozygous variant in the human cardiac miR-133 gene, MIR133A2, alters miRNA duplex processing and strand abundance.', *BMC genetics*, 14(1), p. 18. doi: 10.1186/1471-2156-14-18.

Ohtsuka, S. and Dalton, S. (2008) 'Molecular and biological properties of pluripotent embryonic stem cells.', *Gene therapy*, 15(2), pp. 74–81. doi: 10.1038/sj.gt.3303065.

Okita, K., Ichisaka, T. and Yamanaka, S. (2007) 'Generation of germline-competent induced pluripotent stem cells.', *Nature*, 448(7151), pp. 313–7. doi: 10.1038/nature05934.

Oliver, J. A., Maarouf, O., Cheema, F. H., Martens, T. P. and Al-Awqati, Q. (2004) 'The renal papilla is a niche for adult kidney stem cells.', *The Journal of clinical investigation*. American Society for Clinical Investigation, 114(6), pp. 795–804. doi: 10.1172/JCI20921.

Onyango, P., Jiang, S., Uejima, H., Shamblott, M. J., Gearhart, J. D., Cui, H. and Feinberg, A. P. (2002) 'Monoallelic expression and methylation of imprinted genes in human and mouse embryonic germ cell lineages.', *Proceedings of the National Academy of Sciences of the United States of America*, 99(16), pp. 10599–10604. doi: 10.1073/pnas.152327599.

Orang, A. V., Safaralizadeh, R. and Kazemzadeh-Bavili, M. (2014) 'Mechanisms of miRNA-Mediated Gene Regulation from Common Downregulation to mRNA-Specific Upregulation', *International Journal of Genomics*, pp. 1–15. doi: 10.1155/2014/970607.

Pan, G., Li, J., Zhou, Y., Zheng, H. and Pei, D. (2006) 'A negative feedback loop of transcription factors that controls stem cell pluripotency and self-renewal.', *FASEB journal : official publication of the Federation of American Societies for Experimental Biology*, 20(10), pp. 1730–2. doi: 10.1096/fj.05-5543fje.

Pan, G. and Thomson, J. a (2007) 'Nanog and transcriptional networks in embryonic stem cell pluripotency.', *Cell research*, 17(1), pp. 42–9. doi: 10.1038/sj.cr.7310125.

Papaioannou, V. E. (2014) 'The T-box gene family: emerging roles in development, stem cells and cancer.', *Development (Cambridge, England)*, 141(20), pp. 3819–33. doi: 10.1242/dev.104471.

Park, S., Dadak, A. M., Haase, V. H., Giaccia, A. J., Johnson, R. S. and Fontana, L. (2003) 'Hypoxia-Induced Gene Expression Occurs Solely through the Action of Hypoxia-Inducible Factor 1 α (HIF-1 α): Role of Cytoplasmic Trapping of HIF-2 α Hypoxia-Induced Gene Expression Occurs Solely through the Action of Hypoxia-Inducible Factor 1 ⎵ (HIF-1 '. doi: 10.1128/MCB.23.14.4959.

Pasquinelli, A. E. and Ruvkun, G. (2002) 'Control of developmental timing by micrornas and their targets.', *Annual review of cell and developmental biology*. Annual Reviews 4139 El Camino Way, P.O. Box 10139, Palo Alto, CA 94303-0139, USA, 18, pp. 495–513. doi: 10.1146/annurev.cellbio.18.012502.105832.

Pauklin, S. and Vallier, L. (2013) 'The cell cycle state of stem cells determines cell fate propensity', *Cell*. Elsevier, 155(1), pp. 135–147. doi: 10.1016/j.cell.2013.08.031.

Peerani, R., Onishi, K., Mahdavi, A., Kumacheva, E. and Zandstra, P. W. (2009) 'Manipulation of signaling thresholds in "engineered stem cell niches" identifies design criteria for pluripotent stem cell screens', *PLoS ONE*, 4(7). doi: 10.1371/journal.pone.0006438.

Pera, M. F., Reubinoff, B. E. and Trounson, A. (2000) 'Human embryonic stem cells.', *Journal of Cell Science*, 113, pp. 5–10.

Petruzzelli, R., Christensen, D. R., Parry, K. L., Sanchez-Elsner, T. and Houghton, F. D. (2014) 'HIF-2α regulates NANOG expression in human embryonic stem cells following

hypoxia and reoxygenation through the interaction with an Oct-Sox cis regulatory element.', *PloS one*, 9(10), p. e108309. doi: 10.1371/journal.pone.0108309.

Petryniak, B., Staudt, L. M., Postema, C. E., Mccormack, W. T. and Thompson, C. B. (1989) 'Characterization of chicken octamer-binding proteins demonstrate that POU domain-containing homeobox transcription factors have been highly conserved during vertebrate evolution', *Proceedings of the National Academy of Sciences of the United States of America*, 87, pp. 1099–1103.

Prigione, A., Fauler, B., Lurz, R., Lehrach, H. and Adjaye, J. (2010) 'The senescence-related mitochondrial/oxidative stress pathway is repressed in human induced pluripotent stem cells.', *Stem cells (Dayton, Ohio)*, 28(4), pp. 721–33. doi: 10.1002/stem.404.

Prigione, A., Rohwer, N., Hoffmann, S., Mlody, B., Drews, K., Bukowiecki, R., Blümlein, K., Wanker, E. E., Ralser, M., Cramer, T. and Adjaye, J. (2014) 'HIF1α modulates cell fate reprogramming through early glycolytic shift and upregulation of PDK1-3 and PKM2.', *Stem cells (Dayton, Ohio)*, 32(2), pp. 364–76. doi: 10.1002/stem.1552.

Radzisheuskaya, A., Chia, G. L. Bin, dos Santos, R. L., Theunissen, T. W., Castro, L. F. C., Nichols, J. and Silva, J. (2013) 'A defined Oct4 level governs cell state transitions of pluripotency entry and differentiation into all embryonic lineages.', *Nature cell biology*, 15(6), pp. 579–90. doi: 10.1038/ncb2742.

Rane, S., He, M., Sayed, D., Vashistha, H., Malhotra, A., Sadoshima, J., Vatner, D. E., Vatner, S. F. and Abdellatif, M. (2009) 'Downregulation of miR-199a derepresses hypoxia-inducible factor-1alpha and Sirtuin 1 and recapitulates hypoxia preconditioning in cardiac myocytes.', *Circulation research*, 104(7), pp. 879–86. doi: 10.1161/CIRCRESAHA.108.193102.

Ren, J., Jin, P., Wang, E., Marincola, F. M. and Stroncek, D. F. (2009) 'MicroRNA and gene expression patterns in the differentiation of human embryonic stem cells', *Journal of Translational Medicine*, 7, p. 20. doi: 10.1186/1479-5876-7-20.

Resnick, J. L., Bixler, L. S., Cheng, L. and Donovan, P. J. (1992) 'Long-term proliferation of mouse primordial germ cells in culture', *Nature*. Nature Publishing Group, 359(6395), pp. 550–551. doi: 10.1038/359550a0.

Reubinoff, B. E., Pera, M. F., Fong, C. Y., Trounson, A. and Bongso, A. (2000) 'Embryonic stem cell lines from human blastocysts: somatic differentiation in vitro.', *Nature biotechnology*, 18(4), pp. 399–404. doi: 10.1038/74447.

Revel, A., Achache, H., Stevens, J., Smith, Y. and Reich, R. (2011) 'MicroRNAs are associated with human embryo implantation defects', *Human Reproduction*, 26(10), pp. 2830–2840. doi: 10.1093/humrep/der255.

Rinaudo, P. F., Giritharan, G., Talbi, S., Dobson, A. T. and Schultz, R. M. (2006) 'Effects of oxygen tension on gene expression in preimplantation mouse embryos', *Fertility and Sterility*, 86. doi: 10.1016/j.fertnstert.2006.05.017.

Rizzino, A. (2009) 'Sox2 and Oct-3/4: A Versatile Pair of Master Regulators that Orchestrate the Self-renewal and Pluripotency of Embryonic Stem Cells by Functioning as Molecular Rheostats', *Wiley Interdiciplinary Reviews: System Biology and Medicine*, 1(2), pp. 228–236. doi: 10.1002/wsbm.12.Sox2.

Roberts, A. P. E., Lewis, A. P. and Jopling, C. L. (2011) 'miR-122 activates hepatitis C virus translation by a specialized mechanism requiring particular RNA components.', *Nucleic acids research*, 39(17), pp. 7716–29. doi: 10.1093/nar/gkr426.

Rodda, D. J., Chew, J.-L., Lim, L.-H., Loh, Y.-H., Wang, B., Ng, H.-H. and Robson, P. (2005) 'Transcriptional regulation of nanog by OCT4 and SOX2.', *The Journal of biological chemistry*, 280(26), pp. 24731–7. doi: 10.1074/jbc.M502573200.

Rosner, M. H., Vigano, M. A., Ozato, K., Timmons, P. M., Poirier, F., Rigby, P. W. J. and

Staudt, L. M. (1990) ‘A POU-domain transcription factor in early stem cells and germ cells of the mammalian embryo’, *Nature*, 345, pp. 686–692.

Ryskov, A. P., Ivanov, P. L., Kramerov, D. A. and Georgiev, G. P. (1983) ‘Mouse ubiquitous B2 repeat in polysomal and cytoplasmic poly(A)+RNAs: uniderectional orientation and 3’-end localization’, *Nucleic acids research*, 11(18), pp. 6541–6558.

Sathananthan, A. H. and Trounson, A. O. (2000) ‘Mitochondrial morphology during preimplantational human embryogenesis’, *Human Reproduction*, 15(suppl 2), pp. 148–159. doi: 10.1093/humrep/15.suppl_2.148.

Sato, N., Meijer, L., Skaltsounis, L., Greengard, P. and Brivanlou, A. H. (2004) ‘Maintenance of pluripotency in human and mouse embryonic stem cells through activation of Wnt signaling by a pharmacological GSK-3-specific inhibitor.’, *Nature medicine*, 10(1), pp. 55–63. doi: 10.1038/nm979.

Schöler, H. R. (2004) ‘The potential of stem cells. An Inventory’, *Bundesgesundheitsblatt, Gesundheitsforschung, Gesundheitsschutz*, 47(6), pp. 565–77. doi: 10.1007/s00103-004-0818-3.

Schöler, H. R., Dressler, G. R., Balling, R., Rohdewohld, H. and Gruss, P. (1990) ‘Oct-4: a germline-specific transcription factor mapping to the mouse t-complex’, *The EMBO journal*, 9(7), pp. 2185–2195.

Schwanhäusser, B., Busse, D., Li, N., Dittmar, G., Schuchhardt, J., Wolf, J., Chen, W. and Selbach, M. (2011) ‘Global quantification of mammalian gene expression control’, *Nature*. Nature Publishing Group, 473(7347), pp. 337–342. doi: 10.1038/nature10098.

Seagroves, T. N., Ryan, H. E., Lu, H. A. N., Wouters, B. G., Knapp, M., Thibault, P., Laderoute, K. and Johnson, R. S. (2001) ‘Transcription Factor HIF-1 Is a Necessary Mediator of the Pasteur Effect in Mammalian Cells’, 21(10), pp. 3436–3444. doi: 10.1128/MCB.21.10.3436.

Segev, H., Fishman, B., Ziskind, A., Shulman, M. and Itskovitz-Eldor, J. (2004) ‘Differentiation of human embryonic stem cells into insulin-producing clusters.’, *Stem cells*, 22, pp. 265–274. doi: 10.1634/stemcells.22-3-265.

Seki, T., Yuasa, S., Oda, M., Egashira, T., Yae, K., Kusumoto, D., Nakata, H., Tohyama, S., Hashimoto, H., Kodaira, M., Okada, Y., Seimiya, H., Fusaki, N., Hasegawa, M. and Fukuda, K. (2010) ‘Generation of induced pluripotent stem cells from human terminally differentiated circulating t cells’, *Cell Stem Cell*. Elsevier Ltd, 7(1), pp. 11–13. doi: 10.1016/j.stem.2010.06.003.

Sela, Y., Molotski, N., Golan, S., Itskovitz-Eldor, J. and Soen, Y. (2012) ‘Human embryonic stem cells exhibit increased propensity to differentiate during the G1 phase prior to phosphorylation of retinoblastoma protein’, *Stem Cells*, 30(6), pp. 1097–1108. doi: 10.1002/stem.1078.

Semenza, G. L. (2004) ‘Hydroxylation of HIF-1: oxygen sensing at the molecular level.’, *Physiology (Bethesda, Md.)*, 19, pp. 176–82. doi: 10.1152/physiol.00001.2004.

Semenza, G. L. (2012) ‘Hypoxia-inducible factors in physiology and medicine’, *Cell*. Elsevier Inc., 148(3), pp. 399–408. doi: 10.1016/j.cell.2012.01.021.

Semenza, G. L., Jiang, B., Leung, S. W., Passantino, R., Concordet, J., Maire, P. and Giallongo, A. (1996) ‘Hypoxia Response Elements in the Aldolase A , Enolase 1 , and Lactate Dehydrogenase A Gene Promoters Contain Essential Binding Sites for Hypoxia-inducible Factor 1 *’, 271(51), pp. 32529–32537.

Semenza, G. L. and Wang, G. L. (1992) ‘A nuclear factor induced by hypoxia via de novo protein synthesis binds to the human erythropoietin gene enhancer at a site required for transcriptional activation.’, *Molecular and cellular biology*, 12(12), pp. 5447–54.

Seok, H., Ham, J., Jang, E.-S. and Chi, S. W. (2016) ‘MicroRNA Target Recognition: Insights from Transcriptome-Wide Non-Canonical Interactions’, *Mol Cells*, 39(5), pp.

375–381. doi: 10.14348/molcells.2016.0013.

Shamblott, M. J., Axelman, J., Wang, S., Bugg, E. M., Littlefield, J. W., Donovan, P. J., Blumenthal, P. D., Huggins, G. R. and Gearhart, J. D. (1998) 'Derivation of pluripotent stem cells from cultured human primordial germ cells.', *Proceedings of the National Academy of Sciences of the United States of America*, 95(23), pp. 13726–31.

Shin, C., Nam, J., Farh, K. K., Rosaria, H., Shkumatava, A. and Bartel, D. P. (2010) 'Expanding the MicroRNA Targeting Code: Functional Sites with Centered Pairing', *Molecular Cell*, 38(6), pp. 789–802. doi: 10.1016/j.molcel.2010.06.005.Expanding.

Showell, C., Binder, O. and Conlon, F. L. (2004) 'T-box Genes in Early Embryogenesis', *Developmental Dynamics*, 229(1), pp. 201–218. doi: 10.1002/dvdy.10480.

Silva, J., Barrandon, O., Nichols, J., Kawaguchi, J., Theunissen, T. W. and Smith, A. (2008) 'Promotion of reprogramming to ground state pluripotency by signal inhibition.', *PLoS biology*, 6(10), p. e253. doi: 10.1371/journal.pbio.0060253.

Silva, J. and Smith, A. (2008) 'Capturing Pluripotency', *Cell*, 132(4), pp. 532–536. doi: 10.1016/j.cell.2008.02.006.

Singh, A. M., Bechard, M., Smith, K. and Dalton, S. (2012) 'Reconciling the different roles of Gsk3β in "naïve" and "primed" pluripotent stem cells', *Cell Cycle*, 11(16), pp. 2991–2996. doi: 10.4161/cc.21110.

Singh, A. M., Hamazaki, T., Hankowski, K. E. and Terada, N. (2007) 'A heterogeneous expression pattern for Nanog in embryonic stem cells.', *Stem cells (Dayton, Ohio)*, 25(10), pp. 2534–42. doi: 10.1634/stemcells.2007-0126.

Singh, A. M., Reynolds, D., Cliff, T., Ohtsuka, S., Mathyses, A., Sun, Y., Menendez, L., Kulik, M. and Dalton, S. (2012) 'Signaling network cross-talk in human pluripotent cells: a Smad2/3-regulated switch that controls the balance between self-renewal and differentiation', *Cell stem cell*, 10(3), pp. 312–326. doi: 10.1016/j.stem.2012.01.014.Signaling.

Sinkkonen, L., Hugenschmidt, T., Berninger, P., Gaidatzis, D., Mohn, F., Artus-Revel, C. G., Zavolan, M., Svoboda, P. and Filipowicz, W. (2008) 'MicroRNAs control de novo DNA methylation through regulation of transcriptional repressors in mouse embryonic stem cells.', *Nature structural & molecular biology*, 15(3), pp. 259–67. doi: 10.1038/nsmb.1391.

Smith, A. (2001) 'Embryo-derived stem cells: of mice and men', *Annual review of cell and developmental biology*, 17, pp. 435–462.

Smith, T. G., Robbins, P. A. and Ratcliffe, P. J. (2008) 'The human side of hypoxia-inducible factor.', *British journal of haematology*, 141(3), pp. 325–34. doi: 10.1111/j.1365-2141.2008.07029.x.

Solter, D. and Knowles, B. B. (1975) 'Immunosurgery of mouse blastocyst.', *Proceedings of the National Academy of Sciences*, 72(12), pp. 5099–5102. doi: 10.1073/pnas.72.12.5099.

Song, L., Duan, P., Guo, P., Li, D., Li, S., Xu, Y. and Zhou, Q. (2012) 'Downregulation of miR-223 and miR-153 mediates mechanical stretch-stimulated proliferation of venous smooth muscle cells via activation of the insulin-like growth factor-1 receptor', *Archives of Biochemistry and Biophysics*, 528(2), pp. 204–211. doi: 10.1016/j.abb.2012.08.015.

Spitz, F. and Furlong, E. E. M. (2012) 'Transcription factors: from enhancer binding to developmental control', *Nature Reviews Genetics*. Nature Publishing Group, 13(9), pp. 613–626. doi: 10.1038/nrg3207.

Stadler, B., Ivanovska, I., Mehta, K., Song, S., Nelson, A. M., Tan, Y., Mathieu, J., Darby, C., Blau, C. A., Ware, C., Peters, G., Miller, D. G., Shen, L., Cleary, M. a and Ruohola-Baker, H. (2010) 'Characterization of microRNAs involved in embryonic stem cell states.', *Stem cells and development*, 19(7), pp. 935–50. doi: 10.1089/scd.2009.0426.

Stadtfeld, M., Nagaya, M., Utikal, J., Weir, G. and Hochedlinger, K. (2008) 'Induced pluripotent stem cells generated without viral integration.', *Science (New York, N.Y.)*, 322(5903), pp. 945–9. doi: 10.1126/science.1162494.

Stark, A., Bushati, N., Jan, C. H., Kheradpour, P., Hodges, E., Brennecke, J., Bartel, D. P., Cohen, S. M. and Kellis, M. (2008) 'A single Hox locus in Drosophila produces functional microRNAs from opposite DNA strands', *Genes and Development*, 22(1), pp. 8–13. doi: 10.1101/gad.1613108.

Sturm, R. A., Das, G. and Herr, W. (1988) 'The ubiquitous octamer-binding protein Oct-1 contains a POU domain with a homeo box subdomain.', *Genes & Development*, 2(12a), pp. 1582–1599. doi: 10.1101/gad.2.12a.1582.

Sturm, R. A. and Herr, W. (1988) 'The POU domain is a bipartite DNA-binding structure', *Nature*, 336(8), pp. 601–604.

Subramanyam, D., Lamouille, S., Judson, R. L., Liu, J. Y., Bucay, N., Derynck, R. and Blelloch, R. (2011) 'Multiple targets of miR-302 and miR-372 promote reprogramming of human fibroblasts to induced pluripotent stem cells.', *Nature biotechnology*, 29(5), pp. 443–8. doi: 10.1038/nbt.1862.

Suh, M.-R., Lee, Y., Kim, J. Y., Kim, S.-K., Moon, S.-H. S. Y., Lee, J. Y., Cha, K.-Y., Chung, H. M., Yoon, H. S., Moon, S. Y., Kim, V. N. and Kim, K.-S. (2004) 'Human embryonic stem cells express a unique set of microRNAs', *Developmental biology*, 270(2), pp. 488–98. doi: 10.1016/j.ydbio.2004.02.019.

Sun, B. K., Deaton, A. M. and Lee, J. T. (2006) 'A transient heterochromatic state in Xist preempts X inactivation choice without RNA stabilization', *Molecular Cell*, 21(5), pp. 617–628. doi: 10.1016/j.molcel.2006.01.028.

Suzuki, A., Raya, A., Kawakami, Y., Morita, M., Matsui, T., Nakashima, K., Gage, F. H., Rodriguez-Esteban, C. and Belmonte, J. C. (2006) 'Maintenance of embryonic stem cell pluripotency by Nanog-mediated reversal of mesoderm specification', *Nat Clin Pract Cardiovasc Med*, 3 Suppl 1(March), pp. S114–S122. doi: 10.1038/ncpcardio0442.

Takahashi, K., Tanabe, K., Ohnuki, M., Narita, M., Ichisaka, T., Tomoda, K. and Yamanaka, S. (2007) 'Induction of pluripotent stem cells from adult human fibroblasts by defined factors.', *Cell*, 131(5), pp. 861–72. doi: 10.1016/j.cell.2007.11.019.

Takahashi, K. and Yamanaka, S. (2006) 'Induction of pluripotent stem cells from mouse embryonic and adult fibroblast cultures by defined factors.', *Cell*, 126(4), pp. 663–76. doi: 10.1016/j.cell.2006.07.024.

Takashima, Y., Guo, G., Loos, R., Nichols, J., Ficz, G., Krueger, F., Oxley, D., Santos, F., Clarke, J., Mansfield, W., Reik, W., Bertone, P. and Smith, A. (2014) 'Resetting Transcription Factor Control Circuitry toward Ground-State Pluripotency in Human', *Cell*. Elsevier, 158(6), pp. 1254–69. doi: 10.1016/j.cell.2014.08.029.

Takubo, K., Goda, N., Yamada, W., Iriuchishima, H., Ikeda, E., Kubota, Y., Shima, H., Johnson, R. S., Hirao, A., Suematsu, M. and Suda, T. (2010) 'Regulation of the HIF-1alpha level is essential for hematopoietic stem cells.', *Cell stem cell*, 7(3), pp. 391–402. doi: 10.1016/j.stem.2010.06.020.

Tan, S. C., Carr, C. a, Yeoh, K. K., Schofield, C. J., Davies, K. E. and Clarke, K. (2012) 'Identification of valid housekeeping genes for quantitative RT-PCR analysis of cardiosphere-derived cells preconditioned under hypoxia or with prolyl-4-hydroxylase inhibitors.', *Molecular biology reports*, 39(4), pp. 4857–67. doi: 10.1007/s11033-011-1281-5.

Tanaka, T., Wiesener, M., Bernhardt, W., Eckardt, K.-U. and Warnecke, C. (2009) 'The human HIF (hypoxia-inducible factor)-3alpha gene is a HIF-1 target gene and may modulate hypoxic gene induction.', *The Biochemical journal*, 424(1), pp. 143–51. doi: 10.1042/BJ20090120.

Tang, K., Yang, J., Gao, X., Wang, C., Liu, L., Kitani, H., Atsumi, T. and Jing, N. (2002) 'Wnt-1 promotes neuronal differentiation and inhibits gliogenesis in P19 cells.', *Biochemical and biophysical research communications*, 293(1), pp. 167–73. doi: 10.1016/S0006-291X(02)00215-2.

Tat, T. T., Maroney, P. A., Chamnongpol, S., Coller, J. and Nilsen, T. W. (2016) 'Cotranslational microRNA mediated messenger RNA destabilization', *eLife*. eLife Sciences Publications Limited, 5, pp. 8–15. doi: 10.7554/eLife.12880.

Tay, Y., Zhang, J., Thomson, A. M., Lim, B. and Rigoutsos, I. (2008) 'MicroRNAs to Nanog, Oct4 and Sox2 coding regions modulate embryonic stem cell differentiation.', *Nature*, 455(7216), pp. 1124–8. doi: 10.1038/nature07299.

Teo, A. K. K., Arnold, S. J., Trotter, M. W. B., Brown, S., Ang, L. T., Chng, Z., Robertson, E. J., Dunn, N. R. and Vallier, L. (2011) 'Pluripotency factors regulate definitive endoderm specification through eomesodermin', *Genes and Development*, 25(3), pp. 238–250. doi: 10.1101/gad.607311.

Tesar, P. J., Chenoweth, J. G., Brook, F. a, Davies, T. J., Evans, E. P., Mack, D. L., Gardner, R. L. and McKay, R. D. G. (2007) 'New cell lines from mouse epiblast share defining features with human embryonic stem cells.', *Nature*, 448(7150), pp. 196–9. doi: 10.1038/nature05972.

Theunissen, T. W., Powell, B. E., Wang, H., Mitalipova, M., Faddah, D. A., Reddy, J., Fan, Z. P., Maetzel, D., Ganz, K., Shi, L., Lungjangwa, T., Imsoonthornruksa, S., Stelzer, Y., Rangarajan, S., D'Alessio, A., Zhang, J., Gao, Q., Dawlaty, M. M., Young, R. A., Gray, N. S. and Jaenisch, R. (2014) 'Systematic identification of culture conditions for induction and maintenance of naive human pluripotency.', *Cell stem cell*. Elsevier, 15(4), pp. 471–87. doi: 10.1016/j.stem.2014.07.002.

Thomson, J. A., Itskovitz-Eldor, J., Shapiro, S. S., Waknitz, M. A., Swiergiel, J. J., Marshall, V. S. and Jones, J. M. (1998) 'Embryonic Stem Cell Lines Derived from Human Blastocysts', *Science*, 282(5391), pp. 1145–1147. doi: 10.1126/science.282.5391.1145.

Thomson, M., Liu, S. J., Zou, L. N., Smith, Z., Meissner, A. and Ramanathan, S. (2011) 'Pluripotency factors in embryonic stem cells regulate differentiation into germ layers', *Cell*, 145(6), pp. 875–889. doi: 10.1016/j.cell.2011.05.017.

Tian, H., McKnight, S. L. and Russell, D. W. (1997) 'Endothelial PAS domain protein 1 (EPAS1), a transcription factor selectively expressed in endothelial cells.', *Genes & Development*, 11(1), pp. 72–82. doi: 10.1101/gad.11.1.72.

Tian, Q., Stepaniants, S. B., Mao, M., Weng, L., Feetham, M. C., Doyle, M. J., Yi, E. C., Dai, H., Thorsson, V., Eng, J., Goodlett, D., Berger, J. P., Gunter, B., Linsley, P. S., Stoughton, R. B., Aebersold, R., Collins, S. J., Hanlon, W. A. and Hood, L. E. (2004) 'Integrated Genomic and Proteomic Analyses of Gene Expression in Mammalian Cells', *Molecular & Cellular Proteomics*. American Society for Biochemistry and Molecular Biology, 3(10), pp. 960–969. doi: 10.1074/mcp.M400055-MCP200.

Till, J. E. and McCulloch, E. a (1961) 'A direct measurement of the radiation sensitivity of normal mouse bone marrow cells. 1961.', *Radiation research*, 14(2), pp. 213–222.

Till, J. E., McCulloch, E. A. and Siminovitch, L. (1963) 'A STOCHASTIC MODEL OF STEM CELL PROLIFERATION, BASED ON THE GROWTH OF SPLEEN COLONY-FORMING CELLS*', *Proc Natl Acad Sci U S A*, pp. 29–36.

Tomaselli, S., Galeano, F., Alon, S., Raho, S., Galardi, S., Polito, V., Presutti, C., Vincenti, S., Eisenberg, E., Locatelli, F. and Gallo, A. (2015) 'Modulation of microRNA editing, expression and processing by ADAR2 deaminase in glioblastoma', *Genome Biology*, 16(1), p. 5. doi: 10.1186/s13059-014-0575-z.

Tricarico, C., Pinzani, P., Bianchi, S., Paglierani, M., Distante, V., Pazzagli, M., Bustin, S. a and Orlando, C. (2002) 'Quantitative real-time reverse transcription polymerase

chain reaction: normalization to rRNA or single housekeeping genes is inappropriate for human tissue biopsies', *Analytical Biochemistry*, 309(2), pp. 293–300. doi: 10.1016/S0003-2697(02)00311-1.

Trompouki, E., Bowman, T. V, Lawton, L. N., Fan, Z. P., Wu, D. C., Dibiase, A., Martin, C. S., Cech, J. N., Sessa, A. K., Leblanc, J. L., Li, P., Durand, E. M., Mosimann, C., Heffner, G. C., Daley, G. Q., Paulson, R. F., Young, R. A. and Zon, L. I. (2011) 'Lineage regulators direct BMP and Wnt pathways to cell-specific programs during differentiation and regeneration', *Cell*, 147(3), pp. 577–589. doi: 10.1016/j.cell.2011.09.044.

Trounson, A. (2006) 'The production and directed differentiation of human embryonic stem cells.', *Endocrine reviews*, 27(2), pp. 208–19. doi: 10.1210/er.2005-0016.

Tsankov, A. M., Gu, H., Akopian, V., Ziller, M. J., Donaghey, J., Amit, I., Gnirke, A. and Meissner, A. (2015) 'Transcription factor binding dynamics during human ES cell differentiation.', *Nature*. Nature Publishing Group, 518(7539), pp. 344–9. doi: 10.1038/nature14233.

Tsutsui, H., Valamehr, B., Hindoyan, A., Qiao, R., Ding, X., Guo, S., Witte, O. N., Liu, X., Ho, C.-M. and Wu, H. (2011) 'AN OPTIMIZED SMALL MOLECULE INHIBITOR COCKTAIL SUPPORTS LONG-TERM MAINTENANCE OF HUMAN EMBRYONIC STEM CELLS', *Nature Communications*, 2(167), pp. 1–18. doi: 10.1038/ncomms1165.AN.

Turnpenny, L., Brickwood, S., Spalluto, Cosma, M., Piper, K., Cameron, I. T., Wilson, D. I. and Hanley, N. a. (2003) 'Derivation of Human Embryonic Germ Cells: An Alternative Source of Pluripotent Stem Cells', *Stem Cells*, 21(Mp 808), pp. 598–609. doi: 10.1634/stemcells.21-5-598.

Turnpenny, L., Spalluto, C. M., Perrett, R. M., O'Shea, M., Hanley, K. P., Cameron, I. T., Wilson, D. I. and Hanley, N. a (2006) 'Evaluating human embryonic germ cells: concord and conflict as pluripotent stem cells.', *Stem cells (Dayton, Ohio)*, 24(2), pp. 212–20. doi: 10.1634/stemcells.2005-0255.

Uckac, P. U., Gul, D. T. and Kocabas, F. (2014) 'Hypoxic Niche of Glycolytic Stem and Progenitor Cells', *Arch Stem Cell Res*, 1(1), pp. 1–8.

Valencia-Sanchez, M. A., Liu, J., Hannon, G. J. and Parker, R. (2006) 'Control of translation and mRNA degradation by miRNAs and siRNAs', *Genes & Development*, 20, pp. 515–524. doi: 10.1101/gad.1399806.miRNAs.

Vallier, L., Mendjan, S., Brown, S., Chng, Z., Teo, A., Smithers, L. E., Trotter, M. W. B., Cho, C. H.-H., Martinez, A., Rugg-Gunn, P., Brons, G. and Pedersen, R. A. (2009) 'Activin/Nodal signalling maintains pluripotency by controlling Nanog expression.', *Development (Cambridge, England)*, 136(8), pp. 1339–49. doi: 10.1242/dev.033951.

Varani, G. and McClain, W. H. (2000) 'The G x U wobble base pair. A fundamental building block of RNA structure crucial to RNA function in diverse biological systems.', *EMBO reports*, 1(1), pp. 18–23. doi: 10.1093/embo-reports/kvd001.

Varum, S., Momcilović, O., Castro, C., Ben-Yehudah, A., Ramalho-Santos, J. and Navara, C. S. (2009) 'Enhancement of human embryonic stem cell pluripotency through inhibition of the mitochondrial respiratory chain.', *Stem cell research*, 3(2–3), pp. 142–56. doi: 10.1016/j.scr.2009.07.002.

Varum, S., Rodrigues, A. S., Moura, M. B., Momcilovic, O., Easley, C. a, Ramalho-Santos, J., Van Houten, B. and Schatten, G. (2011) 'Energy metabolism in human pluripotent stem cells and their differentiated counterparts.', *PloS one*, 6(6), p. e20914. doi: 10.1371/journal.pone.0020914.

Vella, M. C., Choi, E.-Y., Lin, S.-Y., Reinert, K. and Slack, F. J. (2004) 'The C. elegans microRNA let-7 binds to imperfect let-7 complementary sites from the lin-41 3'UTR', *Genes & Development*, pp. 132–137. doi: 10.1101/gad.1165404.for.

Vernay, B. (2005) 'Otx2 Regulates Subtype Specification and Neurogenesis in the Midbrain', *Journal of Neuroscience*, 25(19), pp. 4856–4867. doi: 10.1523/JNEUROSCI.5158-04.2005.

Vogel, C. and Marcotte, E. M. (2012) 'Insights into the regulation of protein abundance from proteomic and transcriptomic analyses.', *Nature reviews. Genetics*. Nature Publishing Group, 13(4), pp. 227–32. doi: 10.1038/nrg3185.

Vogel, C., de Sousa Abreu, R., Ko, D., Le, S.-Y., Shapiro, B. A., Burns, S. C., Sandhu, D., Boutz, D. R., Marcotte, E. M. and Penalva, L. O. (2010) 'Sequence signatures and mRNA concentration can explain two-thirds of protein abundance variation in a human cell line', *Molecular Systems Biology*. EMBO Press, 6(400), pp. 2860–2870. doi: 10.1038/msb.2010.59.

Voss, T. C. and Hager, G. L. (2013) 'Dynamic regulation of transcriptional states by chromatin and transcription factors', *Nature Reviews Genetics*. Nature Research, 15(2), pp. 69–81. doi: 10.1038/nrg3623.

Wang, F., Thirumangalathu, S. and Loeken, M. R. (2006) 'Establishment of new mouse embryonic stem cell lines is improved by physiological glucose and oxygen.', *Cloning and stem cells*. Mary Ann Liebert, Inc. 2 Madison Avenue Larchmont, NY 10538 USA, 8(2), pp. 108–16. doi: 10.1089/clo.2006.8.108.

Wang, G. L., Jiang, B.-H., Rue, E. A. and Semenza, G. L. (1995) 'Hypoxia-inducible factor 1 is a basic-helix-loop-helix-PAS heterodimer regulated by cellular O2 tension.', *Proceedings of the National Academy of Sciences of the United States of America*, 92(12), pp. 5510–4.

Wang, J., Rao, S., Chu, J., Shen, X., Levasseur, D. N., Theunissen, T. W. and Orkin, S. H. (2006) 'A protein interaction network for pluripotency of embryonic stem cells', *Nature*, 444(7117), pp. 364–8. doi: 10.1038/nature05284.

Wang, L., Menendez, P., Cerdan, C. and Bhatia, M. (2005) 'Hematopoietic development from human embryonic stem cell lines.', *Experimental hematology*, 33(9), pp. 987–96. doi: 10.1016/j.exphem.2005.06.002.

Wang, W., Wilfred, B. R., Xie, K., Jennings, M. H., Hu, Y., Arnold, J. and Nelson, P. T. (2010) 'Individual microRNAs (miRNAs) display distinct mRNA targeting "rules"', *RNA Biology*, 7(3), pp. 373–380.

Wang, Y., Baskerville, S., Shenoy, A., Babiarz, J. E., Baehner, L. and Blelloch, R. (2008) 'Embryonic stem cell-specific microRNAs regulate the G1-S transition and promote rapid proliferation.', *Nature genetics*, 40(12), pp. 1478–83. doi: 10.1038/ng.250.

Wang, Y., Keys, D. N., Au-Young, J. K. and Chen, C. (2009) 'MicroRNAs in embryonic stem cells.', *Journal of cellular physiology*, 218(2), pp. 251–5. doi: 10.1002/jcp.21607.

Wang, Y., Li, L., Moore, B. T., Peng, X. H., Fang, X., Lappe, J. M., Recker, R. R. and Xiao, P. (2012) 'Mir-133a in human circulating monocytes: A potential biomarker associated with postmenopausal osteoporosis', *PLoS ONE*, 7(4), pp. 1–7. doi: 10.1371/journal.pone.0034641.

Wang, Z., Oron, E., Nelson, B., Razis, S. and Ivanova, N. (2012a) 'Distinct lineage specification roles for NANOG, OCT4, and SOX2 in human embryonic stem cells', *Cell Stem Cell*. Elsevier Inc., 10(4), pp. 440–454. doi: 10.1016/j.stem.2012.02.016.

Wang, Z., Oron, E., Nelson, B., Razis, S. and Ivanova, N. (2012b) 'Distinct lineage specification roles for NANOG, OCT4, and SOX2 in human embryonic stem cells, Suppl DATA', *Cell Stem Cell*, 10(4), pp. 440–454. doi: 10.1016/j.stem.2012.02.016.

Ward, J. H. (1963) 'Hierarchical Grouping to Optimize Objective Function', *Journal of the American Statistical Association*, 58(301), pp. 236–244.

Ware, C., Nelson, A. M., Mecham, B., Hesson, J., Zhou, W., Jonlin, E. C., Jimenez-Caliani, A. J., Deng, X., Cavanaugh, C., Cook, S., Tesar, P. J., Okada, J., Margaretha,

L., Sperber, H., Choi, M., Blau, C. A., Treuting, P. M., Hawkins, R. D., Cirulli, V. and Ruohola-Baker, H. (2014) 'Derivation of naive human embryonic stem cells.', *Proceedings of the National Academy of Sciences of the United States of America*, 111(12), pp. 4484–9. doi: 10.1073/pnas.1319738111.

Warren, L., Manos, P. D., Ahfeldt, T., Loh, Y. H., Li, H., Lau, F., Ebina, W., Mandal, P. K., Smith, Z. D., Meissner, A., Daley, G. Q., Brack, A. S., Collins, J. J., Cowan, C., Schlaeger, T. M. and Rossi, D. J. (2010) 'Highly efficient reprogramming to pluripotency and directed differentiation of human cells with synthetic modified mRNA', *Cell Stem Cell*, 7(5), pp. 618–630. doi: 10.1016/j.stem.2010.08.012.

Wellner, U., Schubert, J., Burk, U. C., Schmalhofer, O., Zhu, F., Sonntag, A., Waldvogel, B., Vannier, C., Darling, D., zur Hausen, A., Brunton, V. G., Morton, J., Sansom, O., Schüler, J., Stemmler, M. P., Herzberger, C., Hopt, U., Keck, T., Brabletz, S. and Brabletz, T. (2009) 'The EMT-activator ZEB1 promotes tumorigenicity by repressing stemness-inhibiting microRNAs.', *Nature cell biology*. Nature Publishing Group, 11(12), pp. 1487–95. doi: 10.1038/ncb1998.

Wernig, M., Meissner, A., Foreman, R., Brambrink, T., Ku, M., Hochedlinger, K., Bernstein, B. E. and Jaenisch, R. (2007) 'In vitro reprogramming of fibroblasts into a pluripotent ES-cell-like state.', *Nature*, 448(7151), pp. 318–24. doi: 10.1038/nature05944.

Westfall, S. D., Sachdev, S., Das, P., Hearne, L. B., Hannink, M., Roberts, R. M. and Ezashi, T. (2008) 'Identification of oxygen-sensitive transcriptional programs in human embryonic stem cells.', *Stem cells and development*, 17(5), pp. 869–81. doi: 10.1089/scd.2007.0240.

White, J. and Dalton, S. (2005) 'Cell Cycle Control of Embryonic Stem Cells', *Stem Cell Reviews*. Humana Press, 1(2), pp. 131–138. doi: 10.1385/SCR:1:2:131.

Wilkinson, D. G., Bhatt, S. and Herrmann, B. G. (1990) 'Expression pattern of the mouse T gene and its role in mesoderm formation', *Nature*. Nature Publishing Group, 343(6259), pp. 657–659. doi: 10.1038/343657a0.

Wilson, E. B. (1896) *The Cell in Development and Inheritance*. New York: Macmillan Publishers Limited. All rights reserved.

Witkos, T. M., Koscianska, E. and Krzyzosiak, W. J. (2011) 'Practical Aspects of microRNA Target Prediction', *Current Molecular Medicine*, 11(2), pp. 93–109. doi: 10.2174/156652411794859250.

Wray, J., Kalkan, T. and Smith, A. (2010) 'The ground state of pluripotency.', *Biochemical Society transactions*, 38(4), pp. 1027–32. doi: 10.1042/BST0381027.

Xiao, L., Yuan, X. and Sharkis, S. J. (2006) 'Activin A maintains self-renewal and regulates fibroblast growth factor, Wnt, and bone morphogenic protein pathways in human embryonic stem cells.', *Stem cells*, 24(6), pp. 1476–1486. doi: 10.1634/stemcells.2005-0299.

Xu, C., Inokuma, M. S., Denham, J., Golds, K., Kundu, P., Gold, J. D. and Carpenter, M. K. (2001) 'Feeder-free growth of undifferentiated human embryonic stem cells.', *Nature biotechnology*, 19(10), pp. 971–4. doi: 10.1038/nbt1001-971.

Xu, C., Police, S., Rao, N. and Carpenter, M. K. (2002) 'Characterization and enrichment of cardiomyocytes derived from human embryonic stem cells', *Circulation Research*, 91(6), pp. 501–508. doi: 10.1161/01.RES.0000035254.80718.91.

Xu, N., Papagiannakopoulos, T., Pan, G., Thomson, J. a and Kosik, K. S. (2009) 'MicroRNA-145 regulates OCT4, SOX2, and KLF4 and represses pluripotency in human embryonic stem cells.', *Cell*. Elsevier Ltd, 137(4), pp. 647–58. doi: 10.1016/j.cell.2009.02.038.

Xu, R. H., Sampsell-Barron, T. L., Gu, F., Root, S., Peck, R. M., Pan, G., Yu, J.,

Antosiewicz-Bourget, J., Tian, S., Stewart, R. and Thomson, J. A. (2008) 'NANOG Is a Direct Target of TGFβ/Activin-Mediated SMAD Signaling in Human ESCs', *Cell Stem Cell*, 3(2), pp. 196–206. doi: 10.1016/j.stem.2008.07.001.

Yang, H. W., Hwang, K. J., Kwon, H. C., Kim, H. S., Choi, K. W. and Oh, K. S. (1998) 'Detection of reactive oxygen species (ROS) and apoptosis in human fragmented embryos', *Human Reproduction*, 13(4), pp. 998–1002. doi: 10.1093/humrep/13.4.998.

Yang, J.-S., Phillips, M. D., Betel, D., Mu, P., Ventura, A., Siepel, A. C., Chen, K. C. and Lai, E. C. (2011) 'Widespread regulatory activity of vertebrate microRNA* species.', *RNA (New York, N.Y.)*, 17(2), pp. 312–326. doi: 10.1261/rna.2537911.

Yekta, S., Shih, I.-H. and Bartel, D. P. (2004) 'MicroRNA-directed cleavage of HOXB8 mRNA.', *Science (New York, N.Y.)*. American Association for the Advancement of Science, 304(5670), pp. 594–6. doi: 10.1126/science.1097434.

Yeom, Y. I., Ha, H. S., Balling, R., Schöler, H. R. and Artzt, K. (1991) 'Structure, expression and chromosomal location of the Oct-4 gene.', *Mechanisms of development*, 35(3), pp. 171–179. doi: 10.1016/0925-4773(91)90016-Y.

Ying, Q.-L., Nichols, J., Chambers, I. and Smith, A. (2003) 'BMP Induction of Id Proteins Suppresses Differentiation and Sustains Embryonic Stem Cell Self-Renewal in Collaboration with STAT3', *Cell*, 115(3), pp. 281–292. doi: 10.1016/S0092-8674(03)00847-X.

Ying, Q.-L., Wray, J., Nichols, J., Batlle-Morera, L., Doble, B., Woodgett, J., Cohen, P. and Smith, A. (2008) 'The ground state of embryonic stem cell self-renewal.', *Nature*, 453(7194), pp. 519–23. doi: 10.1038/nature06968.

Young, R. A. (2011) 'Control of the Embryonic Stem Cell State', *Cell*. Elsevier Inc., 144(6), pp. 940–54. doi: 10.1016/j.cell.2011.01.032.

Yu, J., Vodyanik, M. a, Smuga-Otto, K., Antosiewicz-Bourget, J., Frane, J. L., Tian, S., Nie, J., Jonsdottir, G. a, Ruotti, V., Stewart, R., Slukvin, I. I. and Thomson, J. a (2007) 'Induced pluripotent stem cell lines derived from human somatic cells.', *Science (New York, N.Y.)*, 318(5858), pp. 1917–20. doi: 10.1126/science.1151526.

Yu, P., Pan, G., Yu, J. and Thomson, J. A. (2011) 'FGF2 sustains NANOG and switches the outcome of BMP4-induced human embryonic stem cell differentiation', *Cell Stem Cell*. Elsevier Inc., 8(3), pp. 326–334. doi: 10.1016/j.stem.2011.01.001.

Yu, Y.-H., Zhang, L., Wu, D.-S., Zhang, Z., Huang, F.-F., Zhang, J., Chen, X.-P., Liang, D.-S., Zeng, H. and Chen, F.-P. (2013) 'MiR-223 regulates human embryonic stem cell differentiation by targeting the IGF-1R/Akt signaling pathway.', *PloS one*, 8(11), p. e78769. doi: 10.1371/journal.pone.0078769.

Zachar, V., Prasad, S. M., Weli, S. C., Gabrielsen, A., Petersen, K., Petersen, M. B. and Fink, T. (2010) 'The effect of human embryonic stem cells (hESCs) long-term normoxic and hypoxic cultures on the maintenance of pluripotency.', *In vitro cellular & developmental biology. Animal*, 46(3–4), pp. 276–83. doi: 10.1007/s11626-010-9305-3.

Zeng, Y., Yi, R. and Cullen, B. R. (2003) 'MicroRNAs and small interfering RNAs can inhibit mRNA expression by similar mechanisms.', *Proceedings of the National Academy of Sciences of the United States of America*, 100(17), pp. 9779–84. doi: 10.1073/pnas.1630797100.

Zeng, Y., Zhang, X., Kang, K., Chen, J., Wu, Z., Huang, J., Lu, W., Chen, Y., Zhang, J., Wang, Z., Zhai, Y., Qu, J., Ramchandran, R., Raj, J. U., Wang, J. and Gou, D. (2016) 'MicroRNA-223 Attenuates Hypoxia-induced Vascular Remodeling by Targeting RhoB/MLC2 in Pulmonary Arterial Smooth Muscle Cells.', *Scientific reports*. Nature Publishing Group, 6(October 2015), p. 24900. doi: 10.1038/srep24900.

Zhang, J., Khvorostov, I., Hong, J. S., Oktay, Y., Vergnes, L., Nuebel, E., Wahjudi, P. N., Setoguchi, K., Wang, G., Do, A., Jung, H.-J., McCaffery, J. M., Kurland, I. J., Reue, K.,

Lee, W.-N. P., Koehler, C. M. and Teitell, M. A. (2011) 'UCP2 regulates energy metabolism and differentiation potential of human pluripotent stem cells.', *The EMBO journal*. EMBO Press, 30(24), pp. 4860–73. doi: 10.1038/emboj.2011.401.

Zhang, S. G., Liu, C. Y., Li, L., Sun, T. W., Luo, Y. G., Yun, W. J. and Zhang, J. Y. (2013) 'Examination of Artificial MiRNA Mimics with Centered-Site Complementarity for Gene Targeting', *PLoS ONE*, 8(8). doi: 10.1371/journal.pone.0072062.

Zhang, X., Neganova, I., Przyborski, S., Yang, C., Cooke, M., Atkinson, S. P., Anyfantis, G., Fenyk, S., Keith, W. N., Hoare, S. F., Hughes, O., Strachan, T., Stojkovic, M., Hinds, P. W., Armstrong, L. and Lako, M. (2009) 'A role for NANOG in G1 to S transition in human embryonic stem cells through direct binding of CDK6 and CDC25A.', *The Journal of cell biology*, 184(1), pp. 67–82. doi: 10.1083/jcb.200801009.

Zhang, Y., Feng, G.-H., Xu, K., Wang, L., Cui, P., Li, Y., Wang, C., Teng, F., Hao, J., Wan, H.-F., Tan, Y., Wang, X.-J. and Zhou, Q. (2016) 'A non-invasive method to determine the pluripotent status of stem cells by culture medium microRNA expression detection', *Scientific Reports*. Nature Publishing Group, 6(22380). doi: 10.1038/srep22380.

Zhang, Z., Sun, H., Dai, H., Walsh, R., Imakura, M., Schelter, J. M., Burchard, J., Dai, X., Chang, A. N., Diaz, R. L., Marszalek, J. R., Bartz, S. R., Carleton, M., Cleary, M. A., Linsley, P. S. and Grandori, C. (2009) 'MicroRNA miR-210 modulates cellular response to hypoxia through the MYC antagonist MNT', *Cell Cycle*, 8(17), pp. 2756–2768. doi: 10.4161/cc.8.17.9387.

Zhong, H. and Simons, J. W. (1999) 'Direct Comparison of GAPDH , ␣ -Actin , Cyclophilin , and 28S rRNA as Internal Standards for Quantifying RNA Levels under Hypoxia', 526, pp. 523–526.

Zhou, W., Choi, M., Margineantu, D., Margaretha, L., Hesson, J., Cavanaugh, C., Blau, C. A., Horwitz, M. S., Hockenbery, D., Ware, C. and Ruohola-Baker, H. (2012) 'HIF1α induced switch from bivalent to exclusively glycolytic metabolism during ESC-to-EpiSC/hESC transition.', *The EMBO journal*. EMBO Press, 31(9), pp. 2103–16. doi: 10.1038/emboj.2012.71.

Zhou, W. and Freed, C. R. (2009) 'Adenoviral gene delivery can reprogram human fibroblasts to induced pluripotent stem cells', *Stem Cells*, 27(11), pp. 2667–2674. doi: 10.1002/stem.201.